cis-Dihydroxylation and Epoxidation of Alkenes by Manganese Catalysts - Selectivity, Reactivity and Mechanism

Boer, Johannes Wietse de

cis-Dihydroxylation and Epoxidation of Alkenes by Manganese Catalysts
Selectivity, Reactivity and Mechanism

Johannes W. de Boer

Printed by PrintPartners Ipskamp BV, Enschede, the Netherlands.

university of groningen

The work described in this thesis was carried out at the Stratingh Institute for Chemistry, University of Groningen, the Netherlands.

The work described in this thesis was financially supported by the Dutch Economy, Ecology, Technology (EET) programme (EETK01106), a joint programme of the Ministry of Economic Affairs, the Ministry of Education, Culture and Science, and the Ministry of Housing, Spatial Planning and the Environment.

ISBN 978-90-367-3335-9 (printed version)
ISBN 978-90-367-3336-6 (electronic version)

RIJKSUNIVERSITEIT GRONINGEN

cis-Dihydroxylation and Epoxidation of Alkenes by Manganese Catalysts
Selectivity, Reactivity and Mechanism

Proefschrift

ter verkrijging van het doctoraat in de
Wiskunde en Natuurwetenschappen
aan de Rijksuniversiteit Groningen
op gezag van de
Rector Magnificus, dr. F. Zwarts,
in het openbaar te verdedigen op
vrijdag 22 februari 2008
om 16.15 uur

door

Johannes Wietse de Boer

geboren op 28 april 1979
te Dokkum

Promotor :	Prof. dr. B.L. Feringa
Copromotor :	Dr. R. Hage
Beoordelingscommissie :	Prof. dr. J.B.F.N. Engberts Prof. dr. L. Que, Jr. Prof. dr. J. Reedijk

Contents

Preface

Oxidation reactions are among the most elementary of organic transformations and are essential in chemical industry.[1] Whereas complete oxidation of hydrocarbons with (atmospheric) oxygen yields carbon dioxide and water (*i.e.* combustion), partial and selective oxidation of hydrocarbons introduces functional groups and yields useful products and intermediates.[2,3] Even if the (initial) product of such an oxidation is not of immediate use, the formation of, for example, an alcohol from an alkane or epoxide from an alkene offers a handle to introduce selectively other functional groups and/or attach other building blocks and in doing so, quickly build up molecular complexity.

Oxidative transformations include the oxidation of alkenes to their corresponding epoxides and diols (or into dicarbonyl compounds via C=C bond cleavage), selective C-H bond activation and the oxidation of alcohols to aldehydes, ketones or carboxylic acids (Figure 1).[4,5] Stain removal from cloths and the bleaching of paper pulp are also examples of important oxidation processes, which operate by oxidizing the staining compounds by oxygen or via electron transfer and thereby reducing their absorption of visible light.[6]

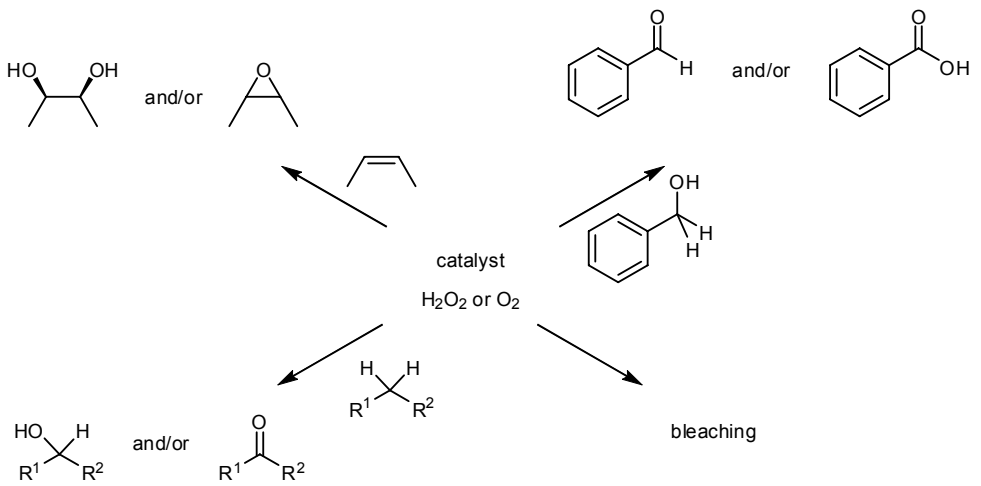

Figure 1 Examples of oxidative transformations.

Despite considerable advances in recent years, major challenges remain in oxidation chemistry. The need for increased atom efficiency demands the use of oxidants, which do not generate stoichiometric amounts of by-products. From an environmental and atom economy perspective, the two most desirable oxidants to use are molecular oxygen (O_2) and hydrogen peroxide (H_2O_2).[1a] Selectivity is another key issue. In order to develop a useful process, the introduction of oxygen atom(s) to the substrate should occur only at the desired position(s) in the molecule, otherwise a complex mixture of (by)products is obtained. Furthermore, the product formed should not be oxidised further (*i.e.* overoxidation should not happen).

Although catalysts are needed to activate O_2 or H_2O_2, their role is not simply to allow the use of these oxidants under ambient conditions. The most important role of these catalysts is to activate the oxidants in such a way as to ensure that only the desired oxidative transformation will occur. This holds for the chemoselectivity (*e.g.* alkene vs. alkane

oxidation), regioselectivity (*e.g.* internal vs. external alkenes) and enantioselectivity of the reaction. Moreover, the catalyst should be cheap, (potentially) available at large scale and be non-toxic. Furthermore, the catalyst should show high activity and be robust, to enable its application at low concentration and give constant performance over prolonged periods.

The research described in this thesis focusses on the development of new protocols for the clean and selective *cis*-dihydroxylation and epoxidation of alkenes and on the mechanistic understanding of these processes. Complexes based on Mn-tmtacn (where tmtacn = *N*,*N'*,*N''*-trimethyl-1,4,7-triazacyclononane, see Figure 3.1, Chapter 3) have proven to be effective in both bleaching applications and for the activation of H_2O_2 towards the oxidation of alkenes.[7] As a first-row transition metal manganese is relatively non-toxic (in fact it is an essential trace element). However, as for many manganese based complexes, catalase-type activity is usually observed when employing Mn-tmtacn. Many groups have therefore used additives to suppress this wasteful decomposition of H_2O_2. However, the precise role of these additives and the mechanism by which the Mn-tmtacn based catalysts operate was understood only poorly.

The approach taken during the research described in this thesis is to combine the information gathered from varying reaction conditions systematically (*e.g.* catalyst precursor, pretreatment procedures, solvent) and their influence on the performance of the catalyst (substrate conversion, product formation and selectivity in time) with the intriguing solution chemistry of Mn-tmtacn, which was explored with a broad range of spectroscopic techniques. The key for the optimisation of catalytic performance and the fundamental improvements made in understanding the mode of action of these manganese-based catalysts is the interaction and feedback between those two approaches.

Chapter 1 provides a broad overview of the more synthetically useful enantioselective catalytic systems for both the epoxidation and *cis*-dihydroxylation of alkenes reported to date. Although many enantioselective epoxidation catalysts have been developed, the terminal oxidants used are generally not atom-efficient. Regarding enantioselective *cis*-dihydroxylation, the only synthetically useful catalysts are based on Os, which is both expensive and toxic.

Since active oxygen causes oxidative stress *in vivo*, enzymes, called catalases, are involved in the safe decomposition of H_2O_2, affording cellular protection. In Chapter 2 the relationship between the dinuclear manganese-containing catalase enzymes and oxidation catalysts is reviewed and discussed.

Chapter 3 starts with an overview of the additives used in Mn-tmtacn based catalysis. The discovery of the suppression of the catalase-type activity of the Mn-tmtacn catalyst by the use of carboxylic acid additives at co-catalytic level is described. The factors controlling the activity and selectivity of this newly developed catalytic system are explored. By judicious choice of the carboxylic acid additive, the selectivity towards either *cis*-dihydroxylation or epoxidation can be tuned under otherwise similar reaction conditions.

Chapter 4 describes the solution chemistry of the Mn-tmtacn family of complexes. The focus is on the various μ-oxo and/or μ-carboxylato[i] bridged manganese dimers and their interconversion. A range of physical techniques (including NMR, ESR, UV-Vis and FT-IR spectroscopy, mass spectrometry and electrochemistry) has been applied to determine the dependence of the nature of the non-carboxylato bridging ligands of the manganese dimers on the redox state of the manganese centers and presence or absence of carboxylic acids and/or water in the reaction medium.

Chapter 5 explores both the factors responsible for the lag period and the species present in solution during the catalytic *cis*-dihydroxylation and epoxidation of alkenes by the catalytic system described in Chapter 3. Analysis of the effects of variation in reaction parameters on both the behavior and stability of Mn-tmtacn complexes and on the catalytic performance, together with isotopic labeling studies, led to new insights into the mechanism by which this powerful catalyst operates.

In Chapter 6 the generality of the mechanism proposed for the Mn-tmtacn catalysed oxidation of alkenes in the presence of carboxylic acid additives is discussed in relation with the systems and additives used by other groups. The results suggest strongly that again dinuclear carboxylato bridged complexes are key to catalytic activity.

Chapter 7 describes the development of the first catalytic enantioselective *cis*-dihydroxylation catalyst based on manganese using H_2O_2 as oxidant.

In Chapter 8 the results of the research described in this thesis are discussed in relation to the requirements for new oxidation catalysts discussed above. Focus is on the major issues encountered, solutions and possibilities for future developments.

References

[1] a) Beller, M. *Adv. Synth. Catal.* **2004**, *346*, 107-108. b) Lenoir, D. *Angew. Chem. Int. Ed.* **2006**, *45*, 3206-3210.
[2] Caron, S.; Dugger, R. W.; Gut Ruggeri, S.; Ragan, J. A.; Brown Ripin, D. H. *Chem. Rev.* **2006**, *106*, 2943-2989.
[3] Chang, D.; Zhang, J.; Witholt, B.; Li, Z. *Biocatal. Biotrans.* **2004**, *22*, 113-130.
[4] a) Sheldon, R. A.; Kochi, J. K. *Metal-Catalyzed Oxidations of Organic Compounds*, Academic Press, New York, **1981**. b) Bäckvall, J.-E. (ed.) *Modern Oxidation Methods*, Wiley VCH, Weinheim, **2004**.
[5] Sharpless, K. B. *Angew. Chem. Int. Ed.* **2002**, *41*, 2024-2032.
[6] Hage, R.; Lienke, A. *Angew. Chem. Int. Ed.* **2006**, *45*¸ 206-222.
[7] Hage, R.; Iburg, J. E.; Kerschner, J.; Koek, J. H.; Lempers E. L. M.; Martens R. J.; Racherla, U. S.; Russell S. W.; Swarthoff, T.; van Vliet M. R. P.; Warnaar, J. B.; van der Wolf, L.; Krijnen, B. *Nature* **1994**, *369*, 637-639.

[i] Although IUPAC recommends to use names such as acetato, carboxylato, oxido and hydroxido for anionic ligands, in this thesis the more prevalent and older trivial names such as 'oxo' and 'hydroxo' are used.

Chapter 1
Enantioselective epoxidation and *cis*-dihydroxylation catalysts

The metal-catalysed enantioselective epoxidation and cis-dihydroxylation of alkenes is discussed. Special attention is given to typical reaction conditions employed, selectivities achieved, terminal oxidants used and the synthetic utility of these catalytic systems.

Sections 1.1.2-1.1.4 of this chapter have been adapted from: J. Brinksma, J. W. de Boer, R. Hage, B. L. Feringa, *Manganese-based Oxidation with Hydrogen Peroxide*, in: *Modern Oxidation Methods*, J.-E. Bäckvall (ed.), Wiley-VCH, Weinheim, **2004**, pp. 295-326.

An overview of the more synthetically useful enantioselective catalytic systems for both the epoxidation and *cis*-dihydroxylation of alkenes reported to date, is provided in this chapter. Typical reaction conditions, enantioselectivities achieved, terminal oxidants used and their synthetic utility are discussed briefly for each catalytic system. This chapter is not intended to afford a detailed and comprehensive overview of all aspects of the oxidation catalysts discussed, for this the reader is referred to the various excellent reviews mentioned in the individual sections. For epoxidation, the focus is mainly on first row transition-metal catalysts and as a consequence catalysts based on Re[1], Ru[2] and W[3,4] are not discussed. For *cis*-dihydroxylation both the Os- and Fe-based catalysts are discussed. The non-heme iron catalysts developed by Que *et al.*[5] are discussed in more detail, due to their relevance to the Mn-tmtacn catalysts described in this thesis.

1.1 Epoxidation

1.1.1 Titanium

The Ti-catalysed asymmetric epoxidation of allylic alcohols was first reported by Sharpless *et al.*[6] in 1980 (for V-catalysed epoxidations, see ref. [7]). Treatment of an allylic alcohol with ^{t}BuOOH in the presence of catalytic amounts of $Ti^{IV}(O^iPr)_4$ and (*S,S*)- or (*R,R*)-dialkyltartrate affords the corresponding epoxides in high yield (50-90%) and with high *ee* (>90 %, Scheme 1.1).[8,9] The most commonly used dialkyl tartrate ligands are diethyl- and diisopropyl tartrate, (*S,S*)- or (*R,R*)-DET and -DIPT, respectively. The catalyst is sensitive to H_2O and anhydrous reagents and conditions should be used.[10] The presence of molecular sieves generally enhances both the yield and *ee* of the reaction.[11]

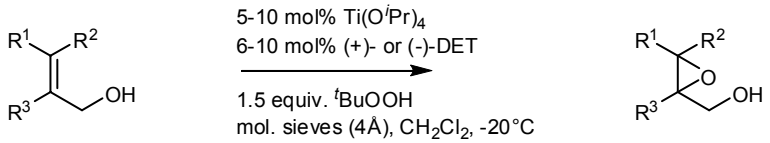

Scheme 1.1 Epoxidation of allylic alcohols mediated by $Ti^{IV}(O^iPr)_4$ and (*S,S*)- or (*R,R*)-diethyltartrate.[8]

The catalytically active species is believed to be a Ti^{IV}_2 dimer containing two dialkyl tartrate ligands (Figure 1.1) and both the oxidant ^{t}BuOOH and the allylic alcohol coordinate to one of the Ti^{IV} centres.[8] The coordination of the allylic alcohol positions the substrate in such a way that the oxygen is delivered to one enantiotopic face of the alkene and this is key to the high *ee*'s observed for this reaction. A large number of both allylic and homoallylic alcohols have been used as substrates, showing the versatility of this epoxidation catalyst for (natural product) synthesis.[8,12] The necessity for the presence of this alcohol functionality, however, limits this catalyst to this class of substrates.

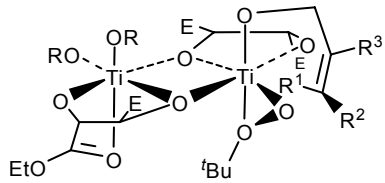

Figure 1.1 Active complex for Ti-tartrate catalysed epoxidation.[8]

Recently, Katsuki and coworkers reported a series of Ti-based catalysts which are not sensitive to H_2O and which can use H_2O_2 as oxidant.[13,14,15] The ligands used were derived from the well-known salen ligands where either one or both of the imine functionalities are reduced (*i.e.* salalen or salan ligands, respectively, Figure 1.2).

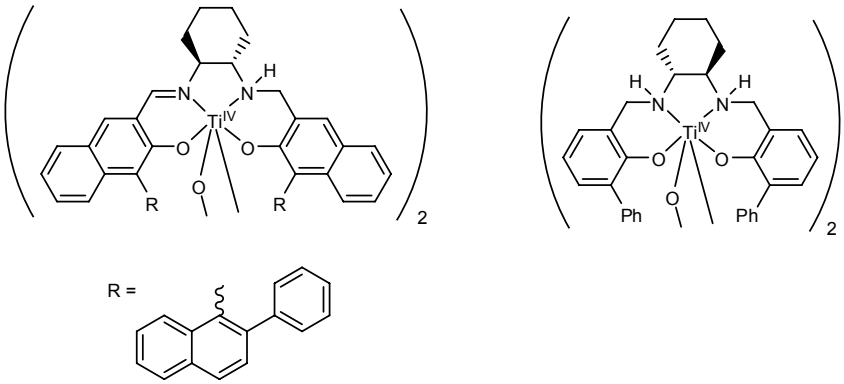

Figure 1.2 $(Ti^{IV}(\mu\text{-}O)(salalen))_2$ and $(Ti^{IV}(\mu\text{-}O)(salan))_2$ complexes.[14,15]

Typical reaction conditions employ 2-5 mol% of the Ti-dimer and a slight excess of H_2O_2 (30%) (1.01-1.5 equiv.) in CH_2Cl_2 at room temperature (Scheme 1.2).[14,15] The yields are moderate to good (50-99%) and *ee*'s are typically between 75 and 99%. Substrates reported so far include aryl-substituted alkenes, such as styrene and 1,2-dihydronaphthalene, and aliphatic *cis*-alkenes.[14,15] It is worth noting that several terminal alkenes could be converted to their corresponding epoxides with 70-85% *ee*. The active species is proposed to be a mononuclear Ti^{IV}-η^2-OOH species based on CSI-MS (cold-spray ionisation mass-spectrometry) alone, where the Ti^{IV} centre acts as a Lewis acid to activate the peroxide.[14]

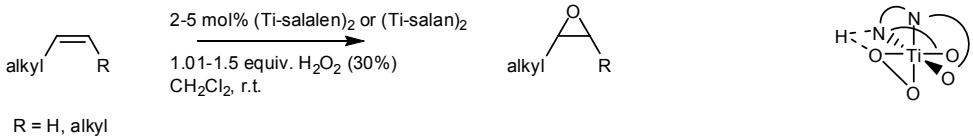

Scheme 1.2 Catalytic epoxidation by $(Ti^{IV}(\mu\text{-}O)(salalen))_2$ and $(Ti^{IV}(\mu\text{-}O)(salan))_2$ (left) and proposed catalytic active species (right).[14,15]

1.1.2 Mn-porphyrins

Both Fe^{III}- and Mn^{III}-porphyrins have been employed for the epoxidation of alkenes.[16] These complexes are converted to their respective high-valent metal-oxo species by terminal oxidants such as iodosylbenzene and sodium hypochlorite (NaClO). Many chiral porphyrin derivatives have been prepared and moderate to good *ee*'s (up to 96%) have been obtained in several cases.[17,18,19] The substrate scope tested is usually limited to styrene and a few derivatives thereof and best results are generally obtained with *cis*-alkenes such as *cis*-β-methylstyrene. However, while for high asymmetric induction during the interaction of the approaching alkene to the high-valent metal-oxo intermediate the chiral groups should be close to the metal-oxo moiety to afford a (rigid) chiral pocket, at the same time these groups should not be too close, since intramolecular oxidation (and finally inactivation) of the catalyst occurs.[18] Catalyst stability is a serious issue with porphyrin-based oxidation catalysts, especially when the often tedious syntheses of the (chiral) porphyrin ligands are considered.

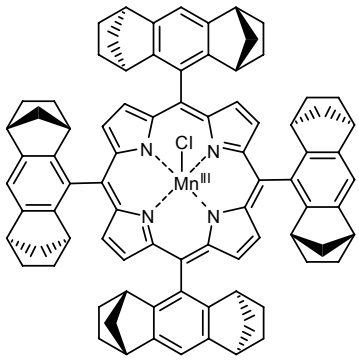

Figure 1.3 Example of chiral porphyrin epoxidation catalyst.[20]

Without additives, the use of H_2O_2 as oxidant leads to homolytic cleavage of the O-O bond of the intermediate hydroperoxo complex, resulting in the formation of hydroxyl radicals and as a consequence non-selective oxidation of the substrate occurs.[16] However, when a nitrogen containing heteroarene such as imidazole coordinates axially to the Mn^{III}-porphyrin, heterolytic cleavage of the O-O bond is promoted, yielding the catalytically active Mn^{V}=O intermediate.[21] Although excess H_2O_2 (3-5 equiv.) was required, good yields (85-99%) have been obtained for the epoxidation of several alkenes using [Mn^{III}(TDCPP)]Cl **1.1** (TDCPP: *tetra*-2,6-dichlorophenylporphyrin, Figure 1.4).[22] The amount of imidazole used can be lowered to 1 equiv. with respect to (w.r.t.) the manganese porphyrin when also a small amount (1 equiv. w.r.t. catalyst) of carboxylic acid is used.[23] When both the imidazole and carboxylic acid were attached to the manganese porphyrin (**1.2**) (Figure 1.4 and 1.5) up to 1000 t.o.n.'s have been obtained for several substrates, including cyclooctene and *p*-chlorostyrene, using 2 equiv. of H_2O_2 w.r.t. substrate (Figure 1.5).[24,25] A few examples of chiral porphyrins employing H_2O_2 are known, however, the *ee*'s obtained are low (ca. 30%).[26,27]

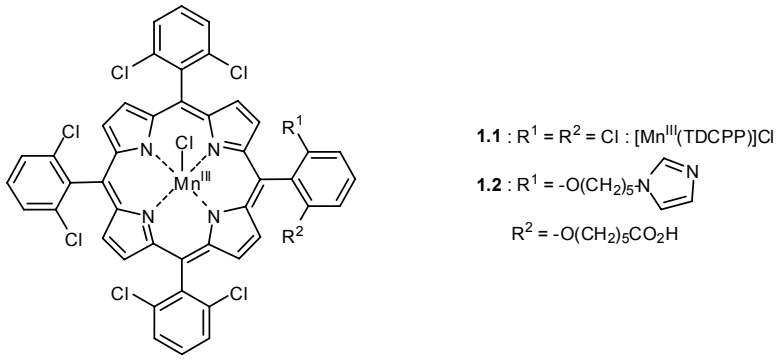

Figure 1.4 Mn-porphyrins used for the catalytic epoxidation of alkenes employing H_2O_2 as terminal oxidant.[22,24]

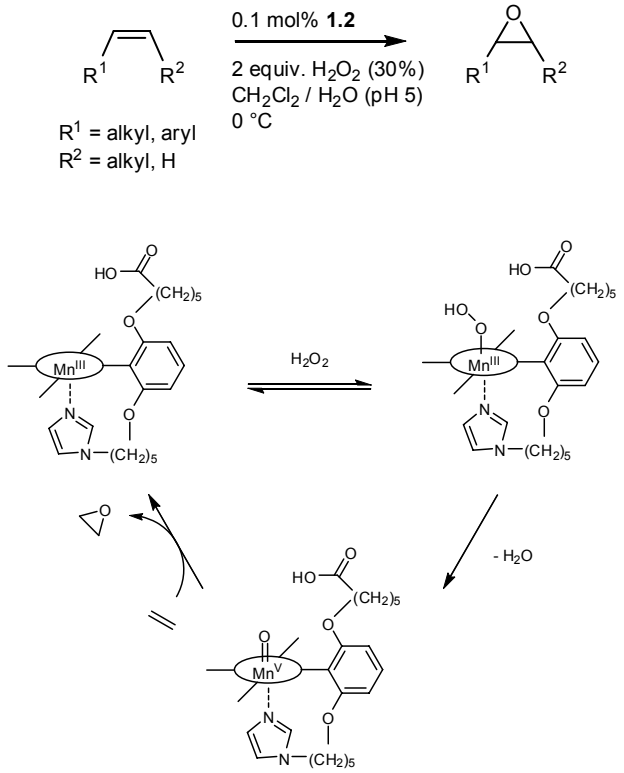

Figure 1.5 Epoxidation of alkenes catalysed by Mn-porphyrin **1.2** (see Figure 1.4).[23,24,25]

As structural and functional mimicks for porphyrin containing enzymes, such as cytochrome P450, both Fe- and Mn-containing metalloporphyrins are useful models to gain insight into the intriguing chemistry exhibited by these biologically relevant systems.

However, despite progress made, the tedious synthesis and purification of the (chiral) porphyrin ligands and the (generally) high catalyst loadings required, render these Fe- and Mn-porphyrins less practical as epoxidation catalysts for (asymmetric) chemical synthesis.

1.1.3 Mn-salen

Following the initial report by Kochi on the use of Mn-salen complexes as epoxidation catalysts,[28] the groups of Jacobsen[29] and Katsuki[30] reported the incorporation of a chiral diamine functionality in the salen ligand (Figure 1.6) affording enantioselective epoxidation catalysts. The use of the Mn-salen catalysts results generally in good to exellent *ee*'s (>90%) and yields (>80%) for the epoxidation of *cis*-disubstituted and trisubstituted alkenes employing iodosylbenzene as oxidant.[31,32] *Trans*-alkenes give, generally, lower *ee*'s, although several Mn-salen derivatives are known to give good *ee*'s (up to 80%) for a number of *trans*-alkenes also.[31] Although high *ee*'s can be obtained, the stability of the Mn-salen complexes is often a problem and t.o.n.'s are usually in the range of 40-200. A robust Mn-salen catalyst was introduced by Katsuki *et al.*[33] based on ligand **1.5** with a carboxylic acid functionality attached to the diamine bridge (Figure 1.6) and up to 9200 t.o.n.'s have been obtained using iodosylbenzene as oxidant.

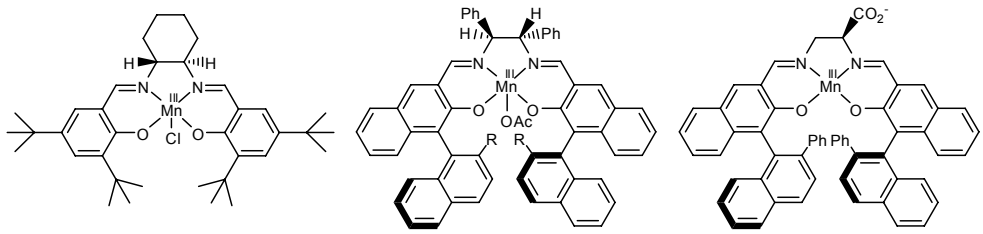

1.3 **1.4** **1.5**

Figure 1.6 Chiral Mn-salen complexes introduced by Jacobsen (**1.3**) and Katsuki (**1.4** and **1.5**) for asymmetric epoxidation of alkenes.[31]

The catalytically active species is proposed to be a Mn^{V}=O intermediate,[31,36] as was confirmed by electrospray ionisation mass spectrometry.[34] An extensive discussion of the stereoselectivity, mechanism and scope of this asymmetric epoxidation[31] is beyond the scope of this chapter. Despite the fact that there is consensus on the nature of the active species (*i.e.* a Mn^{V}-oxo intermediate), some controversy remains on the exact way the enantioselection takes place. Three key issues can be distinguished: i) the catalyst structure (*i.e.* if the salen ligand is planar, bent or twisted), ii) the trajectory of the approach of the reacting alkene, and iii) the mode of oxygen transfer from the Mn^{V}=O intermediate to the alkene (involving a concerted pathway, a stepwise radical pathway or a metallaoxetane intermediate).[31,32,35]

Cumulative experimental evidence indicates that the substituents at the C_2-symmetric diimine bridge and bulky substituents at the 3,3'-positions play an important role in governing the trajectory of side-on approach of the olefin, and thus in the asymmetric induction. With the five-membered chelate ring (comprising the ethylenediamine and the

Mn^V-ion) being non-planar, the approach of the alkene over the downwardly bent benzene ring of the Mn-salen along one of the Mn-N bonds can be envisioned (Figure 1.7). The largest substituent of the alkene (R_L) is then pointing away from the 3,3'-substituents and this governs the stereochemical outcome of the reaction between the Mn^V=O intermediate and the alkene.[31,32,35]

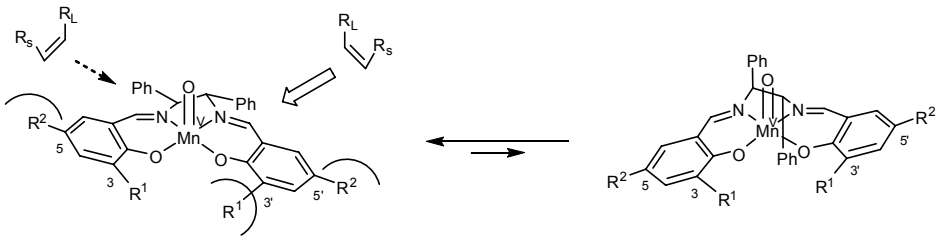

Figure 1.7 Model rationalizing the stereocontrol in Mn-salen epoxidation.[31c]

The typical oxidants used are hypochlorite (ClO^-), iodosylbenzene or *m*-chloroperbenzoic acid (*m*CPBA).[31,36] However, considerable effort has been devoted to the use of H_2O_2 in combination with Mn-salen catalysts. Promising results have been reported for certain substrates, although low turnover numbers (generally around 20-50) were obtained with H_2O_2 as terminal oxidant. When employing H_2O_2, the presence of additives such as imidazole (derivatives) or carboxylates is required.[37,38,39,40] The role of these additives is attributed to preventing O-O bond homolysis leading to non-selective oxidation pathways and destruction of the catalyst.

Berkessel and coworkers developed a chiral dihydrosalen ligand with a covalently attached imidazole group.[37,38] With the corresponding Mn-salen complex **1.6**, 1,2-dihydronaphthalene was converted to the corresponding epoxide with moderate *ee* (up to 64%) using a dilute (1%) aqueous solution of H_2O_2 as oxidant.

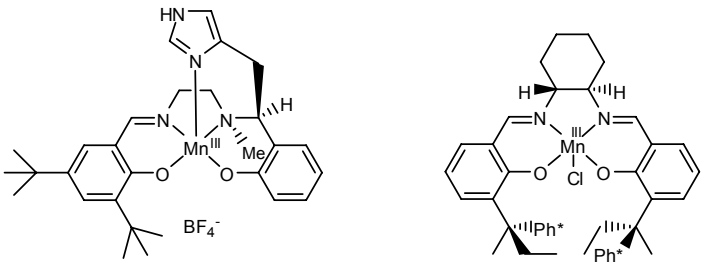

1.6 **1.7** Ph* = 4-*t*-butylphenyl

Figure 1.8 Chiral Mn-salen catalysts.[37,38,39]

Using Mn-salen **1.7** together with *N*-methylimidazole as an axial ligand, Katsuki and coworkers obtained up to 95% *ee* for the epoxidation of substituted chromenes with 10 equiv. of H_2O_2 (30% aq.) as oxidant.[39] It should be noted, however, that only a very limited number of substrates were reported (*ee*'s ranging from 88-98%). With carboxylate salts or carboxylic anhydrides in combination with either aqueous H_2O_2 or UHP (urea-H_2O_2), respectively, moderate to excellent *ee*'s (55-99%) have been obtained for the epoxidation of several *cis*-alkenes.[40,41,42]

1.1.4 Mn-salts

Burgess and coworkers have reported a very simple, yet effective, system for the epoxidation of alkenes employing H_2O_2 as oxidant mediated by a Mn^{II}-salt in the presence of $NaHCO_3$ buffer.[43,44,45] Although HCO_3^- is known to activate H_2O_2 for the epoxidation of various alkenes,[46] the presence of a Mn-salt strongly increases both the yield and the rate of the reaction.[44] Peroxycarbonate (HCO_4^-) is formed *in situ* under reaction conditions from $NaHCO_3^-$ and H_2O_2 as observed by ^{13}C NMR (Figure 1.9). It is believed that a manganese η^2-peroxycarbonate ($[Mn^{II}\text{-}\eta^2\text{-}HCO_4]^+$) species is formed.[44] Whether the manganese ion acts as a Lewis acid to activate HCO_4^- or a Mn^{IV}=O intermediate is formed, is not known and neither is the nuclearity of the active species.

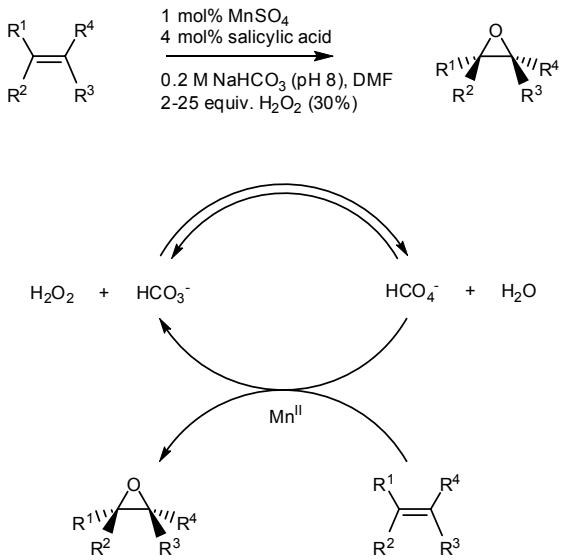

Figure 1.9 Typical reaction conditions (top) and proposed mechanism for the epoxidation of alkenes by $Mn^{II}/NaHCO_3$ (bottom).[43,44,45]

Typical conditions employ $MnSO_4$ (1 mol%), 0.2 M $NaHCO_3$ buffer (pH 8.0) and 10 equiv. of H_2O_2 (30%) and either DMF or ^{t}BuOH is used as an organic co-solvent (Figure 1.9).[44] In the presence of various additives the excess of H_2O_2 used can be lowered and at the same time, the yields of the epoxide product are increased. The screening of a large number of

additives indicated that CH_3CO_2Na (6 mol%) was the best additive when ^{t}BuOH was used as co-solvent and salicylic acid (4 mol%) with DMF as co-solvent. In the latter case the amount of H_2O_2 required for near quantitative conversion of the substrate could be lowered to 2-5 equiv., depending on the substrate. The yield of epoxide product is typically between 55-99% and a wide range of alkenes can be employed as substrate, although terminal aliphatic alkenes are not reactive and *cis*-alkenes yield a mixture of *cis*- and *trans*-products. Since no (chiral) ligands are involved, only racemic products are obtained in the case of prochiral substrates.

1.1.5 Metal-free epoxidation catalysts

Enantioselective epoxidation of alkenes can also be accomplished using metal free catalysts. Both oligopeptides (Juliá-Colonna epoxidation) and chiral ketones (forming chiral dioxiranes as the oxygen transferring species) have been used as organocatalysts for epoxidation.

In the Juliá-Colonna enantioselective epoxidation oligopeptides are used as catalyst, usually polyleucine or polyalanine, for the epoxidation of α,β-unsaturated ketones and -esters employing H_2O_2 as terminal oxidant under basic conditions.[47] Although high *ee*'s have been obtained (up to 99%), the very basic conditions used and the limited substrate scope are drawbacks of this system.

The combination of catalytic amounts of (chiral) ketones and potassium peroxomonosulfate (*i.e.* Oxone: $2KHSO_5.KHSO_4.K_2SO_4$) results in the formation of (chiral) dioxiranes, which in turn are capable of enantioselective epoxidation of alkenes.[48] Many chiral ketones have been used successfully by Shi and coworkers, including binaphtyl derivatives and carbohydrate derived ketones as depicted in Figure 1.10.[49,50]

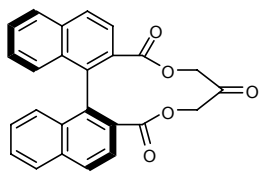

1.8

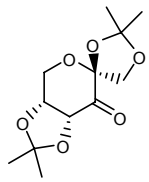

1.9

Figure 1.10 Chiral ketones.[49,50]

The ketone interacts with potassium peroxomonosulfate forming a dioxirane (Figure 1.11). This dioxirane subsequently oxidizes the alkene to the corresponding epoxide, regenerating the free ketone.[50] The oxidant used most often is $KHSO_5$. The substrates most commonly employed are both *trans*- and trisubstituted alkenes, however, good results with *cis*- and terminal alkenes have been obtained also.[49,50,51] Both yields (>70%) and *ee*'s (>90%) obtained are usually good. The catalyst loading is typically high (10-30 mol%) and excess $KHSO_5$ is used (1.1-5 equiv.). Especially the latter is a major drawback for large scale applications since Oxone is far from being an atom-efficient oxidant, even in cases where only 1 equiv. is needed.

Recently, H_2O_2 has been successfully applied as terminal oxidant in the presence of a nitrile (CH_3CN is then often used as (co-)solvent).[52] It is believed that H_2O_2 and CH_3CN form a peroxyimidic acid *in situ*,[53] which is in turn responsible for the regeneration of the dioxirane from the ketone.[52]

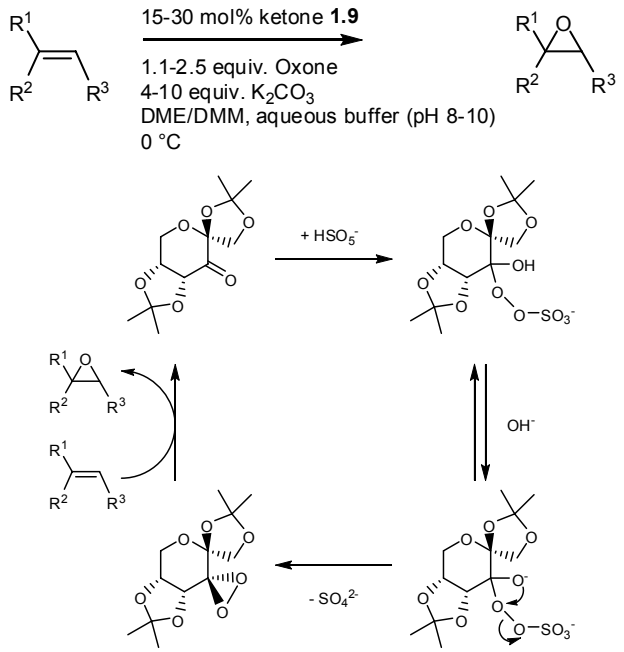

Figure 1.11 Typical reaction conditions (top) and proposed catalytic cycle (bottom) for dioxirane-based epoxidation.[49,50,51]

1.2 *Cis*-dihydroxylation

The two textbook[54] examples of stoichiometric reagents for the *cis*-dihydroxylation of alkenes are OsO_4 and $KMnO_4$. Although OsO_4 is the most reliable reagent and affords the highest yields and selectivities of the *cis*-diol, its (large-scale) application is limited since it is an expensive and very toxic reagent.[55] Various methods that are catalytic in OsO_4 have been developed and employ secondary oxidants such as H_2O_2, chlorates (ClO_3^-), or *N*-methylmorpholine *N*-oxide (NMO) in stoichiometric amounts, although the use of H_2O_2 often results in lower chemoselectivity.[55] The use of $KMnO_4$ often partially results in C-C bond cleavage as side reaction, and yields of the desired *cis*-diol product usually do not exceed 50%.[56]

1.2.1 Os-catalyzed *cis*-dihydroxylation

The best known and well-established catalysts for the enantioselective *cis*-dihydroxylation of alkenes were developed by Sharpless and coworkers. They reported the first catalytic asymmetric dihydroxylation (AD) reaction in 1988.[57] Using catalytic amounts of OsO_4 and

ligands based on the cinchona alkaloids dihydroquinine (DHQ) or dihydroquinidine (DHQD), enantioselective *cis*-dihydroxylation of virtually all classes of alkenes can be accomplished.[58,59,60] Over the years many cinchona-based alkaloids have been tested and it is apparent that the nature of the substituent at the C9 position of the ligand is the most important factor for attaining high *ee*.[58] The three ligand classes depicted in Figure 1.12 are complementary and together serve all substitution patterns of alkenes (*i.e.* primary, 1,1'-disubstituted, *cis*-1,2-disubstituted, *trans*-1,2-disubstituted, tri- and tetra-substituted alkenes). Yields are usually high (>75 %) and *ee*'s are good to excellent (80-99%).[58]

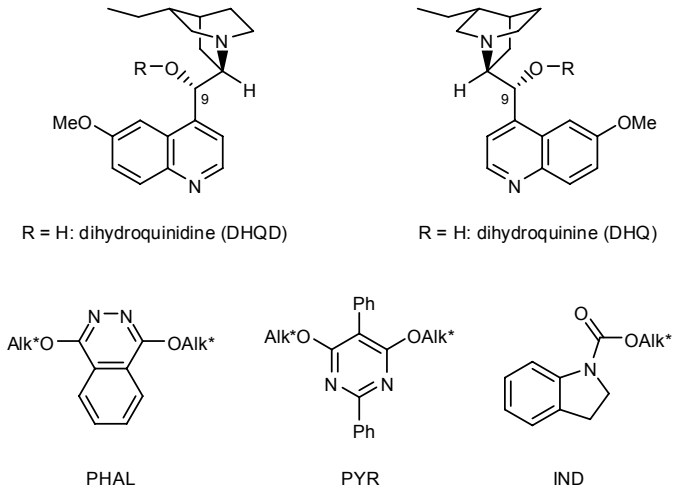

Figure 1.12 Cinchona alkaloid derived ligands used in the Os-catalyzed *cis*-dihydroxylation (Alk* = cinchona alkaloid).[59]

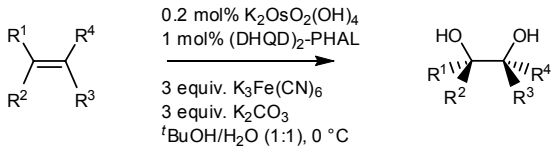

Scheme 1.3 Typicall reaction conditions employing AD-mix-α.[61]

Several reoxidants of the Os catalyst have been employed, *e.g.* NMO or potassium ferricyanide ($K_3Fe(CN)_6$). Premixes are commercially available[62] at present, making this Os-based catalytic method a convenient procedure for lab-scale enantioselective *cis*-dihydroxylation. The commercial premixes, known as AD-mix-α and AD-mix-β, contain the non-volatile Os source $K_2OsO_2(OH)_4$, $K_3Fe(CN)_6$, K_2CO_3 and the ligand $(DHQ)_2$PHAL or $(DHQD)_2$PHAL, respectively (Scheme 1.3).[58,61]

Recent developments include the use of more environmentally benign reoxidants for the Os catalyst, such as H_2O_2[63] or O_2,[64] and efforts to attach the Os catalyst to a solid support.[65] However, despite the fact that the Os-catalyzed *cis*-dihydroxylation of alkenes affords

excellent enantioselectivities and yields for a wide range of alkenes, the practical utility, particularly on a large-scale, is severely hampered by the cost and, especially, the high toxicity associated with Os.

1.2.2 Fe-catalyzed *cis*-dihydroxylation and epoxidation

Iron based complexes have been employed successfully for the oxidation of alkenes employing H_2O_2 as oxidant.[66,67,68] In a series of papers, Que and coworkers have reported on their extensive investigations of a family of non-heme Fe complexes containing tri- and tetradentate ligands such as TPA, BPMEN and Ph-DPAH (Figure 1.13). These complexes both catalyze the hydroxylation of alkanes[69,70] and the epoxidation and/or *cis*-dihydroxylation of alkenes, and they are functional models for non-heme iron containing enzymes such as Rieske dioxygenases. This is a class of enzymes involved in the biodegradation of arenes by catalysing the *cis*-dihydroxylation of an arene double bond and contain the 2-His-1-carboxylato facial triad motif, a common feature for many dioxygen activating mononuclear non-heme Fe containing enzymes.[71]

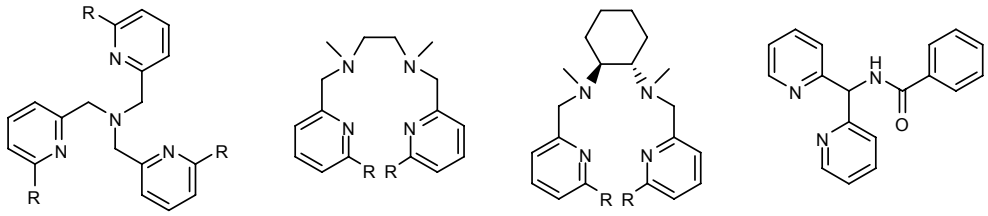

Figure 1.13 TPA, BPMEN and Ph-DPAH (derived) ligands.

While investigating the reactivity of a series of Fe^{II} containing complexes based on the TPA family[72] of ligands, Que and coworkers found that these complexes are capable of *cis*-dihydroxylation of alkenes, in addition to epoxidation, albeit with low t.o.n.'s (Scheme 1.4). Comparison with the reactivity of related Fe-complexes showed that the presence of two labile sites *cis* to one another is a prerequisite for *cis*-dihydroxylation activity of these Fe complexes. That is, if the two labile sites are *trans* or if only one labile site is present, only epoxidation is observed.[73,74,75] While the catalyst based on the ligand TPA favors *cis*-dihydroxylation over epoxidation only slightly (Table 1.1, entry 3), the introduction of two or more Me substituents at the 6-position of the ligand results in catalysts which strongly favors *cis*-dihydroxylation over epoxidation. Differences between both catalysts are also observed when comparing the results of ^{18}O labelling experiments. While for Fe-TPA one of the oxygens in the *cis*-diol product originates from H_2O_2 (and the other from H_2O), both oxygens of the *cis*-diol product of the Fe-(6-Me_3TPA) catalyzed reaction originate from H_2O_2.[76]

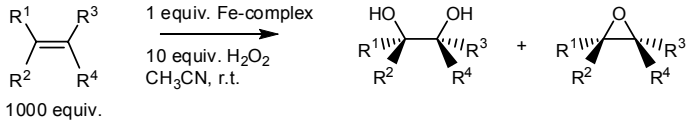

Scheme 1.4 *Cis*-dihydroxylation and epoxidation of alkenes by Fe-based catalysts employing H_2O_2 as oxidant.[77]

Table 1.1 Selected examples for catalytic oxidation of cyclooctene by Fe catalysts.[a]

Entry	Catalyst	t.o.n. *cis*-diol	epoxide	*cis*-diol/epoxide	Ref.
1	$[Fe^{II}(BPMEN)(CH_3CN)_2]^{2+}$	0.9(2)	7.5(6)	1:8	[77]
2	$[Fe^{II}(6\text{-}Me_2\text{-}BPMEN)(OTf)_2]^{2+}$	6.2(1)[b]	1.5(1)	4:1	[77]
3	$[Fe^{II}(TPA)(CH_3CN)_2]^{2+}$	4.0(2)	3.4(1)	1.2:1	[77]
4	$[Fe^{II}(6\text{-}Me_3\text{-}TPA)(CH_3CN)_2]^{2+}$	4.9(6)	0.7(6)	7:1	[77]
5	$[Fe^{II}(6\text{-}Me_3\text{-}TPA)(4\text{-}Me\text{-}benzoato)]^{+}$	5.0(6)	0.5(1)	10:1	[77]
6	$[Fe^{II}(6\text{-}Me_3\text{-}TPA)(benzoato)]^{+}$	6.1(4)	0.5(1)	12:1	[77]
7	$[Fe^{II}(6\text{-}Me_3\text{-}TPA)(3\text{-}NO_2\text{-}benzoato)]^{+}$	6.7(3)	0.4(1)	17:1	[77]
8	$[Fe^{II}(Ph\text{-}DPAH)_2]^{2+}$	7.0(6)	0.5(1)	14:1	[78]
9	$[Fe^{II}(TPA)(OTf)_2]^{2+}$ [c]	5.9	4.3	1.4:1	[89]
10	$[Fe^{II}(TPA)(OTf)_2]^{2+}$ [c,d]	0.8	13.1	1:16	[89]

a) Conditions: catalyst:H_2O_2:cyclooctene 1:10:1000 in CH_3CN. b) Also 0.2(1) turnover number *trans*-diol observed. c) Conditions: catalyst:H_2O_2:cyclooctene 1:14.5:500 in CH_3CN. d) In the presence of CH_3CO_2H (100 equiv. w.r.t. to catalyst).

When either $Fe^{II}(TPA)$ or $Fe^{II}(6\text{-}Me_3TPA)$ were used as a catalyst in the oxidation of a series of electron-deficient alkenes, only *cis*-dihydroxylation and not epoxidation of these electron-deficient alkenes was observed.[80] Competition experiments between electron-rich (cyclooctene and 1-octene) and electron-deficient alkenes (*tert*-butyl acrylate and dimethyl fumarate) showed that class A catalysts (represented by Fe-TPA) form an electrophilic oxidant, while class B catalysts (represented by Fe-6-Me_3-TPA) form a nucleophilic oxidant.[80] Another promising system is based on the ligand Ph-DPAH (Figure 1.13).[78] Excellent selectivities for *cis*-dihydroxylation were obtained for a range of both electron-rich and electron-deficient alkenes under limiting oxidant conditions (catalyst:oxidant:alkene 1:10:1000) (see, for example, entry 8, Table 1.1).

The species $[Fe^{III}(TPA)(\eta^1\text{-}OOH)]^{2+}$ has been observed at -40 °C when $[Fe^{II}(TPA)]^{2+}$ was treated with H_2O_2 in CH_3CN.[69] It should be noted, however, that species observed at low temperatures do not necessarily relate to the intermediates effecting oxidation catalysis at room temperature.[79] Careful analysis of both product distribution, ^{18}O labelling studies[77,73,76,80,81,82] and DFT calculations[83,84] has led to the proposed mechanisms for *cis*-dihydroxylation and epoxidation catalysed by the Fe-TPA and Fe-BPMEN family of complexes depicted in Figure 1.14. The most extensively studied and best representative for the 'class A' catalysts is $[Fe^{II}(TPA)]^{2+}$ (water-assisted pathway, *wa*, Figure 1.14, upper part) (other examples of this class include catalysts based upon the ligands TPA, 6-Me-TPA and BPMEN).[85] The low-spin Fe^{III} centre in $[Fe^{III}(\eta^1\text{-}OOH)(TPA)]^{2+}$ weakens the O-O bond. Water coordinates to the site *cis* to the end-on bound hydroperoxo ligand and forms a hydrogen bond with the non-bonded oxygen atom of the η^1-OOH ligand. This results in the

proposed formation of a {Fe^{V}=O(OH)} intermediate via heterolytic cleavage of the O-O bond and loss of water. If this {Fe^{V}=O(OH)} species reacts quickly with the alkene to afford the *cis*-diol product, this fits well with the labelling results,[77,85] provided that no oxygen exchange with solvent H_2O and the Fe^{V} intermediate occurs. The oxygen incorporated in the epoxide product originates mainly from H_2O_2 (90 %), with a minor percentage originating from H_2O (9 %).[77] In order to fit with the observed ^{18}O incorporation in the epoxide product, it is required that oxygen exchange between solvent H_2O and the {Fe^{V}=O(OH)} is much slower than reaction with the alkene. The limited oxo-hydroxo tautomerisation, required for the only partial incorporation of H_2O in the epoxide product, is rationalised by the different *trans* ligands to the oxo and hydroxo ligands, respectively, resulting in non-equivalent coordination sites.[85]

The complexes that show the highest selectivity for *cis*-dihydroxylation, 'class B' catalysts containing more than one Me substituent at the 6-position of the ligand (*e.g.* 6-Me_2-TPA, 6-Me_3-TPA and 6-Me_2-BPMEN), are best represented by $[Fe^{II}(6\text{-}Me_3\text{-TPA})]^{2+}$.[77] This catalyst is proposed to react via a non-water-assisted (*nwa*) pathway (Figure 1.14, lower part).[73] The Fe^{III}-η^1-OOH intermediate formed initially is proposed to convert to the species Fe^{III}-η^2-OOH containing a side-on bound hydroperoxo group. The latter species is proposed to either react with the alkene directly or the O-O bond is cleaved first, to afford a Fe^{V}(=O)(OH) intermediate, which then reacts with the alkene.[77,76] It should be noted that neither the proposed Fe^{III}-η^2-OOH, nor the Fe^{V}(=O)(OH) intermediate have been observed spectroscopically and their involvement is inferred solely from ^{18}O labelling studies.[76,85] The spin-state of the intermediate Fe^{III}-η^1-OOH species, low-spin for class A and high-spin for class B catalysts, respectively, is proposed to be key to the differences observed between both classes of catalyst by controlling the mode of O-O bond cleavage in the Fe^{III}-η^1-OOH intermediate.[76]

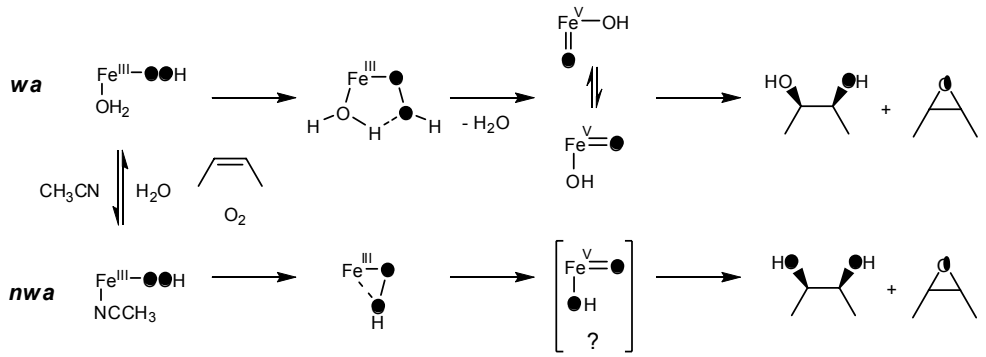

Figure 1.14 Proposed mechanism for Fe-catalyzed oxidation of alkenes.[77,76,80,85]

In the majority of reports on the Fe-TPA and Fe-BPMEN family of catalyst so-called limiting oxidant conditions are used. That is, the catalyst:oxidant:substrate ratio is typically 1:10:1000 and the oxidant H_2O_2 added slowly over time. This favors the study of the chemistry and reactivity of these complexes since both catalyst and oxidant decomposition are limited. However, these limiting oxidant conditions hamper the practical utility of this

fascinating family of catalysts severely, since maximum turnover numbers are only 10 (up to 30 t.o.n. for a few selected examples, see *e.g.* ref. [77] and [78]) and as a consequence substrate conversion is usually limited to 1-3 %.

There are, however, two studies reported where limiting substrate conditions are used, *i.e.* where excess H_2O_2 is used and thus full conversion of substrate is possible. Jacobsen and coworkers employed 3 mol% of the complex $[Fe^{II}(BPMEN)(CH_3CN)_2](SbF_6)_2$ as catalyst for the epoxidation of several mono- and di-alkyl substituted alkenes in CH_3CN (Scheme 1.5).[86] In the presence of 30 mol% of CH_3CO_2H (*vide infra*) overoxidation was suppressed and the amount of H_2O_2 used could be lowered to 1.5 equiv. w.r.t. substrate. Under these conditions (catalyst:oxidant:substrate 1:50:33) full conversion of the alkene was obtained and the corresponding epoxides were isolated in 61-90%. Around the same time, Que *et al.* reported the use of Fe-catalysed oxidation of alkenes under limiting substrate conditions also (catalyst:oxidant:substrate 1:137:34) (Scheme 1.5).[87] Interestingly, in addition to epoxidation, *cis*-dihydroxylation was observed as the dominant process, as under the limiting oxidant conditions reported earlier. Employing the complex $[Fe^{II}(5\text{-}Me_3\text{-}TPA)(CH_3CN)_2]^{2+}$ *cis*-diol/epoxide ratios in the range of 1.5-4.3 were obtained for several alkyl substituted alkenes and the *cis*-diols were obtained with 45-67% yield. Unfortunately, however, the catalysts affording the highest *cis*-diol/epoxide ratios (4-7:1)[77] under limiting oxidant conditions (*i.e.* 6-Me_2-TPA, 6-Me_3-TPA and 6-Me_2-BPMEN) were not very active under these limiting substrate conditions and less then 6 % combined yield of products was obtained. It should be noted that even under these limiting substrate conditions the catalyst loading is still high (3 mol%) and the t.o.n.'s that can be achieved is thus limited to 34.

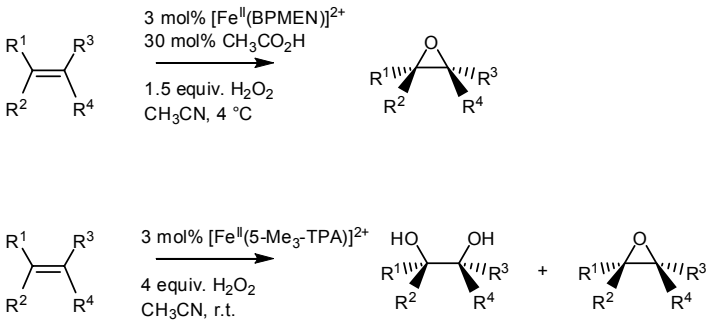

Scheme 1.5 Conditions used by Jacobsen *et al.*[86] and Que *et al.*[87] employing limiting substrate conditions.

As mentioned above, Jacobsen *et al.* employed complex $[Fe^{II}(BPMEN)(CH_3CN)_2]^{2+}$ (3 mol%) as catalyst for the epoxidation of alkenes employing H_2O_2 as oxidant and the presence of the additive CH_3CO_2H (30 mol%) suppressed overoxidation of the epoxide product and allowed for an increased addition rate of H_2O_2.[86] When the mononuclear complex $[Fe^{II}(BPMEN)(CH_3CN)_2]^{2+}$ was treated with H_2O_2 in the presence of CH_3CO_2H in CH_3CN the carboxylato bridged dinuclear complex $[Fe^{III}_2(\mu\text{-}O)(\mu\text{-}CH_3CO_2)(BPMEN)_2]^{3+}$ was isolated. Although in the presence of CH_3CO_2H the latter dinuclear Fe^{III}_2 complex

exhibited the same catalytic activity as the mononuclear complex,[i] (spectroscopic) evidence was not provided as to whether this dinuclear complex or a mononuclear complex is present during catalysis.

Stack and coworkers reported on the epoxidation activity of the μ-oxo bridged dinuclear complex $[Fe^{III}_2(\mu\text{-}O)(H_2O)_2(phen)_4]^{4+}$ employing peracetic acid (PAA) as oxidant.[88] Good conversions (87-100%) and high isolated yields (86-90%) were reported for a range of alkenes, however, PAA and not H_2O_2 is used as oxidant, limiting the atom-efficiency of this reaction.

Que and coworkers reported the *in situ* formation of PAA from CH_3CO_2H and H_2O_2 catalysed by either Fe(TPA) or Fe(BPMEN) complexes during the catalytic epoxidation and *cis*-dihydroxylation of alkenes.[89] That is, these Fe-based catalysts both catalyse the formation of PAA (from CH_3CO_2H and H_2O_2) and subsequently catalyse the oxidation of the alkene by activating PAA. The *in situ* formation of PAA was inferred from an extensive range of control reactions and comparison of t.o.n. and *cis*-diol/epoxide ratios using either PAA or H_2O_2 in the presence or absence of CH_3CO_2H and/or H_2O. With increasing CH_3CO_2H concentration the selectivity towards epoxidation is improved at the expense of *cis*-dihydroxylation (Table 1.1, entries 9 and 10), in line with the results reported by Jacobsen *et al.*[86] (*vide supra*).

Thus, Que *et al.*[89] proposed that the role of CH_3CO_2H is in the *in situ* formation of PAA. However, Jacobsen *et al.*[86] reported that the carboxylato-bridged dinuclear complex $[Fe^{III}_2(\mu\text{-}O)(\mu\text{-}CH_3CO_2)(BPMEN)_2]^{3+}$ is an active catalyst for the epoxidation of alkenes employing H_2O_2. On the other hand, Que *et al.*[87] have reported that this same complex is not active. It should be noted, however, that the conditions used by Jacobsen employed (excess) CH_3CO_2H, while Que *et al.* employed otherwise similar conditions, however, CH_3CO_2H was absent. Furthermore, Que *et al.* have found small, yet significant, effects of the carboxylato anion (4-methylbenzoato, benzoato or 3-nitrobenzoato) on the observed selectivity for the *cis*-dihydroxylation and epoxidation activity of the complex $[Fe^{II}(6\text{-}Me_3\text{-}TPA)(RCO_2)]^+$ (Table 1.1, entries 5-7).[77] Also, upon treatment with H_2O_2 the complex $[Fe^{II}(BPMEN)(CH_3CN)_2]^{2+}$ has been reported to hydroxylate benzoic acid, forming the complex $[Fe^{III}(BPMEN)(salicylato)]^+$.[90] The role of carboxylic acid in the catalytic epoxidation and *cis*-dihydroxylation of alkenes by this series of Fe-based catalysts is intriguing and deserves further exploration.

The introduction of a chiral backbone in the BPMEN ligand afforded the chiral catalysts $[Fe^{II}(BPMCN)(CH_3CN)_2]^{2+}$ and $[Fe^{II}(6\text{-}Me_2\text{-}BPMCN)(CH_3CN)_2]^{2+}$ (Figure 1.13).[91] These complexes constitute the first enantioselective *cis*-dihydroxylation catalysts based on Fe and *ee*'s up to 82% were obtained. Interestingly, the *ee* increases upon raising the temperature (for *trans*-2-heptene 40, 79 and 88% *ee* at 0, 30 and 50°C, respectively), suggesting that two active species are present, probably with two different BPMCN conformations, and one of them is favoured at increased temperature.[91] Despite being a promising alternative for the Os based *cis*-dihydroxylation catalysts (see section 1.2.1), the substrate scope reported so far is rather limited and, moreover, only catalysis under limiting

[i] That is selective epoxide formation under limiting substrate conditions.

oxidant conditions (catalyst:oxidant:alkene 1:20:1000) has been reported (up to 11 t.o.n.'s for *cis*-diol).

1.3 Summary and conclusions

Although many enantioselective epoxidation catalysts have been developed, the terminal oxidants used are generally not atom-efficient (*e.g.* ^{t}BuOOH, NaClO or iodosylbenzene). The catalytic systems employing H_2O_2 either do not show enantioselectivity or have only a limited substrate scope when H_2O_2 is used as oxidant. Furthermore, catalyst loadings are generally high and catalyst stability is often limited, especially when H_2O_2 is used as oxidant.

Regarding (enantioselective) *cis*-dihydroxylation, the only synthetically useful catalysts are based on Os, which is both expensive and toxic. Moreover, these Os-based catalysts generally employ oxidants such as NMO or $K_3Fe(CN)_6$, and not H_2O_2. Que and coworkers developed a promising family of catalysts based on Fe. However, here turnover numbers are low (often under oxidant limiting conditions) and these systems are not synthetically useful yet. It is therefore desirable to develop robust catalytic systems that show high enantioselectivity and employ H_2O_2 as oxidant.

1.4 References

[1] a) Herrmann, W. A.; Fischer, R. W.; Scherer, W.; Rauch, M. U. *Angew. Chem. Int. Ed.* **1993**, *32*, 1157-1160. b) Rudolph, J.; Reddy, K. L.; Chiang, J. P.; Sharpless, K. B. *J. Am. Chem. Soc.* **1997**, *119*, 6189-6190.
[2] a) Tse, M. K.; Bohor, S.; Klawonn, M.; Anilkumar, G.; Jiao, H.; Döbler, C.; Spannenberg, A.; Mägerlein, W.; Hugl, H.; Beller, M. *Chem. Eur. J.* **2006**, *12*, 1855-1874. b) Tse, M. K.; Bohor, S.; Klawonn, M.; Anilkumar, G.; Jiao, H.; Spannenberg, A.; Döbler, C.; Mägerlein, W.; Hugl, H.; Beller, M. *Chem. Eur. J.* **2006**, *12*, 1875-1888.
[3] Noyori, R.; Aoki, M.; Sato, K. *Chem. Commun.* **2003**, 1977-1986.
[4] a) Neumann, R. *Prog. Inorg. Chem.* **1998**, *47*, 317-370. b) Nardello, V.; Aubry, J.-M.; De Vos, D. E.; Neumann, R.; Adam, W.; Zhang, R.; ten Elshof, J. E.; Witte, P. T.; Alsters, P. L. *J. Molec. Catal. A: Chem.* **2006**, *251*, 185-193. c) Maheswari, P. U.; Tang, X.; Hage, R.; Gamez, P.; Reedijk, J. *J. Molec. Catal. A: Chem.* **2006**, *258*, 295-301.
[5] See section 1.2.2 for relevant references.
[6] Katsuki, T.; Sharpless, K. B. *J. Am. Chem. Soc.* **1980**, *102*, 5974-5976.
[7] See for example: a) Michaelson, R. C.; Palermo, R. E.; Sharpless, K. B. *J. Am. Chem. Soc.* **1977**, *99*, 1990-1992. b) Bolm, C. *Coord. Chem. Rev.* **2003**, *237*, 245-256.
[8] Katsuki, T. in: *Comprehensive Asymmetric Catalysis*, Jacobsen, E. N.; Pfaltz, A. and Yamamoto, H. (eds.), Springer, Berlin, **1999**, pp. 621-648.
[9] Johnson, R. A.; Sharpless, K. B., in: *Catalytic Asymmetric Synthesis*, Ojima, I. (ed.), VCH Publishers, New York, **1993**, pp.103-158.
[10] Hill, G. J.; Rossiter, B. E.; Sharpless, K. B. *J. Org. Chem.* **1983**, *48*, 3607-3608.
[11] a) Hanson, R. M.; Sharpless, K. B. *J. Org. Chem.* **1986**, *51*, 1922-1925. b) Gao, Y.; Hanson, R. M.; Klunder, J. M.; Ko, S. Y.; Masamune, H.; Sharpless, K. B. *J. Am. Chem. Soc.* **1987**, *109*, 5765-5780.

[12] Pfenninger, A. *Synthesis* **1986**, 89-116.
[13] Matsumoto, K.; Sawada, Y.; Saito, B.; Sakai, K.; Katsuki, T. *Angew. Chem. Int. Ed.* **2005**, *44*, 4935-4939.
[14] Sawada, Y.; Matsumoto, K.; Kondo, S.; Watanabe, H.; Ozawa, T.; Suzuki, K.; Saito, B. Katsuki, T. *Angew. Chem. Int. Ed.* **2006**, *45*, 3478-3480.
[15] Sawada, Y.; Matsumoto, K.; Katsuki, T. *Angew. Chem. Int. Ed.* **2007**, *46*, 4559-4561.
[16] Meunier, B. *Chem. Rev.* **1992**, *92*, 1411-1456.
[17] Collman, J. P.; Zhang, X.; Lee, V. J.; Uffelman, E. S.; Brauman, J. I. *Science* **1993**, *261*, 1404-1411.
[18] Campbell, L. A.; Kodadek, T. *J. Mol. Catal. A: Chem.* B **1996**, *113*, 293-310.
[19] Rose, E.; Andrioletti, B.; Zrig, S.; Quelquejeu-Ethève, M. *Chem. Soc. Rev.* **2005**, *34*, 573-583.
[20] Halterman, R. L.; Jan, S.-T. *J. Org. Chem.* **1991,** *56*, 5253-5254.
[21] Battioni, P.; Renaud, J. P.; Bartoli, J. F.; Reina-Artiles, M.; Fort, M.; Mansuy, D. *J. Am. Chem. Soc.* **1988**, *110*, 8462-8470.
[22] Renaud, J.-P.; Battioni, P.; Bartoli, J. F.; Mansuy, D. *J. Chem. Soc., Chem. Commun.* **1985**, 888-889.
[23] Anelli, P. L.; Banfi, S.; Montanari, F.; Quici, S. *J. Chem. Soc., Chem. Commun.* **1989**, 779-781.
[24] Banfi, S.; Legramandi, F.; Montanari, F.; Pozzi, G.; Quici, S. *J. Chem. Soc., Chem. Commun.* **1991**, 1285-1287.
[25] Anelli, P. L.; Banfi, S.; Legramandi, F.; Montanari, F.; Pozzi, G.; Quici, S. *J. Chem. Soc., Perkin Trans. 1* **1993**, 1345-1357.
[26] Collman, J. P.; Lee, V. J.; Kellen-Yuen, C. J.; Zhang, X.; Ibers, J. A.; Brauman, J. I. *J. Am. Chem. Soc.* **1995**, *117*, 692-703.
[27] Vilain, S.; Maillard, P.; Momenteau, M. *J. Chem. Soc., Chem. Commun.* **1994**, 1697-1698.
[28] Srinivasan, K.; Michaud, P.; Kochi, J. K. *J. Am. Chem. Soc.* **1986**, *108*, 2309-2320.
[29] Zhang, W.; Loebach, J. L.; Wilson, S. R.; Jacobsen, E. N. *J. Am. Chem. Soc.* **1990**, *112*, 2801-2803.
[30] Irie, R.; Nodda, K.; Ito, Y.; Matsumoto, N.; Katsuki, T. *Tetrahedron Lett.* **1990**, *31*, 7345-7348.
[31] a) Jacobsen, E. N.; Wu, M. H. in: *Comprehensive Asymmetric Catalysis*, Jacobsen, E. N.; Pfaltz, A. and Yamamoto, H. (eds.), Springer, Berlin, **1999**, pp. 649-677. b) Katsuki, T. *J. Mol. Catal. A: Chem.* **1996**, *113*, 87-107. c) Katsuki, T. *Adv. Synth. Catal.* **2002**, *344*, 131-147. d) Katsuki, T. *Synlett* **2003**, 281-297.
[32] Katsuki, T. *Coord. Chem. Rev.* **1995**, *140*, 189-214.
[33] Ito, Y. N.; Katsuki, T. *Tetrahedron Lett.* **1998**, *39*, 4325 - 4328.
[34] Feichtinger, D.; Plattner, D. A. *Angew. Chem. Int. Ed.* **1997**, *36*, 1718 - 1719.
[35] a) Dalton, C. T.; Ryan, K. M.; Wall, V. M.; Bousquet, C.; Gilheany, D. G. *Top. Catal.* **1998**, *5*, 75-91. b) Canali, L: Sherrington, D. C. *Chem. Soc. Rev.* **1999**, *28*, 85-93.
[36] a) Palucki, M.; Pospisil, P. J.; Zhang, W.; Jacobsen, E. N. *J. Am. Chem. Soc.* **1994**, *116*, 9333-9334. b) Palucki, M.; McCormick, G. J.; Jacobsen, E. N. *Tetrahedron Lett.* **1995**, *36*, 5457-5460. c) Jacobsen, E. N.; Deng, L.; Furukawa, Y.; Martinez, L. E. *Tetrahedron* **1994**, *50*, 4323-4334. d) Hughes, D. L.; Smith, G. B.; Liu, J.; Dezeny, G. C.; Senanayake, C. H.; Larsen, R. D.; Verhoeven, T. R.; Reider, P. J. *J. Org. Chem.* **1997**, *62*, 2222-2229.
[37] Berkessel, A.; Frauenkron, M.; Schwenkreis, T.; Steinmetz, A. *J. Mol. Catal. A: Chem.* **1997**, *117*, 339-346.
[38] a) Schwenkreis, T.; Berkessel, A. *Tetrahedron Lett.* **1993**, *34*, 4785-4788. b) Berkessel, A.; Frauenkron, M.; Schwenkreis, T.; Steinmetz, A.; Baum, G.; Fenske, D. *J. Mol. Catal. A: Chem.* **1996**, *113*, 321-342.
[39] Irie, R.; Hosoya, N.; Katsuki, T. *Synlett* **1994**, 255 - 256.

[40] a) Pietikäinen, P. *Tetrahedron Lett.* **1994**, *35*, 941-944. b) Pietikäinen, P. *Tetrahedron* **1998**, *54*, 4319-4326.
[41] Pietikäinen, P. *J. Mol. Catal. A: Chem.* **2001**, *165*, 73-79.
[42] a) Kureshy, R. I.; Khan, N. H.; Abdi, S. H. R.; Patel, S. T.; Jasra, R. V. *Tetrahedron: Asymmetry* **2001**, *12*, 433-437. b) Kureshy, R. I.; Khan, N. H.; Abdi, S. H. R.; Singh, S.; Ahmed, I.; Shukla, R. S.; Jasra, R. V. *J. Catal.* **2003**, *219*, 1-7.
[43] Lane, B. S.; Burgess, K. *J. Am. Chem. Soc.* **2001**, *123*, 2933-2934.
[44] Lane, B. S.; Vogt, M.; DeRose, V. J.; Burgess, K. *J. Am. Chem. Soc.* **2002**, *124*, 11946-11954.
[45] Lane, B. S.; Burgess, K. *Chem. Rev.* **2003**, *103*, 2457-2473.
[46] Yao, H.; Richardson, D. E. *J. Am. Chem. Soc.* **2000**, *122*, 3220-3221.
[47] Kelly, D. R.; Roberts, S. M. *Biopolymers* **2006**, *84*, 74-89.
[48] Curci, R.; Fiorentino, M.; Serio, M. R. *J. Chem. Soc., Chem. Commun.* **1984**, 155-156.
[49] Denmark, S. E.; Wu, Z. *Synlett.* **1999**, 847-859.
[50] Shi, Y. *Organocatalytic Oxidation. Ketone-catalyzed Asymmetric Epoxidation of Olefins*, in: *Modern Oxidation Methods*, Bäckvall, J.-E. (ed.), Wiley-VCH, Weinheim, **2004**, pp.51-82.
[51] a) Tian, H.; She, X.; Shu, L.; Yu, H.; Shi, Y. *J. Am. Chem. Soc.* **2000**, *122*, 11551-11552. b) Tian, H.; She, X.; Xu, J.; Shi, Y. *Org. Lett.* **2001**, *3*, 1929-1931. c) Wong, O. A.; Shi, Y. *J. Org. Chem.* **2006**, *71*, 3973-3976.
[52] a) Shu, L.; Shi, Y. *Tetrahedron Lett.* **1999**, *40*, 8721-8724. b) Shu, L.; Shi, Y. *Tetrahedron* **2001**, *57*, 5213-5218. c) Wang, Z.-X.; Shu, L.; Frohn, M.; Tu, Y.; Shi. Y. *Org. Synth.* **2003**, *80*, 9-13.
[53] Payne, G. B.; Deming, P. H.; Williams, P. H. *J. Org. Chem.* **1961**, *26*, 659-663.
[54] a) March, J. *Advanced Organic Chemistry: Reactions, Mechanisms and Structure* (fourth edition), **1992**, Wiley, New York. b) Fox, M. A.; Whitesell, J. K. *Organic Chemistry* (second edition), **1997**, Jones and Bartlett, Sudbury.
[55] Schröder, M. *Chem. Rev.* **1980**, *80*, 187-213.
[56] Fatiadi, A. J. *Synthesis* **1987**, 85-127.
[57] Jacobsen, E. N.; Markó, I.; Mungall, W. S.; Schröder, M.; Sharpless, K. B. *J. Am. Chem. Soc.* **1988**, *110*, 1968-1970.
[58] Kolb, H. C.; VanNieuwenhze, M. S.; Sharpless, K. B. *Chem. Rev.* **1994**, *94*, 2483-2547.
[59] Beller, M.; Sharpless, K. B. *Diols via Catalytic Dihydroxylation*, in: *Applied Homogeneous Catalysis with Organometallic Compounds*, Cornils, B. and Herrmann, W. A. (ed.), VCH, New York, **1996**, pp. 1009-1024.
[60] Berrisford, D. J.; Bolm, C.; Sharpless, K. B. *Angew. Chem. Int. Ed.* **1995**, *34*, 1059-1070.
[61] Sharpless, K. B.; Amberg, W.; Bennani, Y. L.; Crispino, G. A.; Hartung, J.; Jeong, K.-S.; Kwong, H.-L.; Morikawa, K.; Wang, Z.-M.; Xu, D.; Zhang, X.-L. *J. Org. Chem.* **1992**, *57*, 2768-2771.
[62] Aldrich catalogue, 2007-2008.
[63] Jonsson, S. Y.; Färnegårdh, K.; Bäckvall, J.-E. *J. Am. Chem. Soc.* **2001**, *123*, 1365-1371.
[64] Döbler, C.; Mehltretter, G. M.; Sundermeier, U.; Beller, M. *J. Am. Chem. Soc.* **2000**, *122*, 10289-10297.
[65] Severeyns, A.; De Vos, D. E.; Jacobs, P. A. *Top. Catal.* **2002**, *19*, 125-131.
[666] van den Berg, T. A. (University of Groningen) **2003**, *personal communication*.
[67] Roelfes, G. *Models for Non-Heme Iron Containing Oxidation Enzymes*, Ph.D. thesis, University of Groningen, The Netherlands, **2000**.
[68] Klopstra, M.; Roelfes, G.; Hage, R.; Kellogg, R. M.; Feringa, B. L. *Eur. J. Inorg. Chem.* **2004**, 846-856.
[69] Kim, C.; Chen, K.; Kim, J.; Que, Jr., L. *J. Am. Chem. Soc.* **1997**, *119*, 5964-5965.
[70] Chen, K.; Que, Jr., L. *J. Am. Chem. Soc.* **2001**, *123*, 6327-6337.
[71] Que, Jr., L. *J. Biol. Inorg. Chem.* **2004**, *9*, 684-690.

[72] Zhang, Y.; Kim. J.; Dong, Y.; Wilkinson, E. C.; Appelman, E. H.; Que, Jr., L. *J. Am. Chem. Soc.* **1997**, *119*, 4197-4205.
[73] Chen, K.; Que, Jr., L. *Angew. Chem. Int. Ed.* **1999**, *38*, 2227-2229.
[74] Bukowski, M. R.; Comba, P.; Lienke, A.; Limberg, C.; Lopez de Laorden, C.; Mas-Ballesté, R.; Merz, M.; Que, Jr., L. *Angew. Chem. Int. Ed.* **2006**, *45*, 3446-3449.
[75] Oldenburg, P. D.; Ke, C.-Y.; Tipton, A. A.; Shteinman, A. A.; Que, Jr., L. *Angew. Chem. Int. Ed.* **2006**, *45*, 7975-7978.
[76] Chen, K.; Costas, M.; Que, Jr., L. *J. Chem. Soc., Dalton Trans.* **2002**, 672-679.
[77] Chen, K.; Costas, M.; Kim, J.; Tipton, A. K.; Que, Jr., L. *J. Am. Chem. Soc.* **2002**, *124*, 3026-3035.
[78] Oldenburg, P. D.; Shteinman, A. A.; Que, Jr., L. *J. Am. Chem. Soc.* **2005**, *127*, 15672-15673.
[79] Mairata i Payeras, M.; Ho, R. Y. N.; Fujita, M.; Que, Jr., L. *Chem. Eur. J.* **2004**, *10*, 4944-4953.
[80] Fujita, M.; Costas, M.; Que, Jr., L. *J. Am. Chem. Soc.* **2003**, *125*, 9912-9913.
[81] Costas, M.; Que, Jr., L. *Angew. Chem. Int. Ed.* **2002**, *41*, 2179-2181.
[82] Mas-Ballesté, R.; Costas, M.; van den Berg, T. A.; Que, Jr., L. *Chem. Eur. J.* **2006**, *12*, 7489-7500.
[83] Quinonero, D.; Morokuma, K.; Musaev, D. G.; Mas-Ballesté, R.; Que, Jr., L. *J. Am. Chem. Soc.* **2005**, *127*, 6548-6549.
[84] Bassan, A.; Blomberg, M. R. A.; Siegbahn, P. E. M.; Que, Jr., L. *Angew. Chem. Int. Ed.* **2005**, *44*, 2939-2941.
[85] Oldenburg, P. D.; Que, Jr., L. *Catal. Today* **2006**, *117*, 15-21.
[86] White, M. C.; Doyle, A. G.; Jacobsen, E. N. *J. Am. Chem. Soc.* **2001**, *123*, 7194-7195.
[87] Ryu, J. Y.; Kim, J.; Costas, M.; Chen, K.; Nam, W.; Que, Jr., L. *Chem. Commun.* **2002**, 1288-1289.
[88] Dubois, G.; Murphy, A.; Stack, T. D. P. *Org. Lett.* **2003**, *5*, 2469-2472.
[89] Fujita, M.; Que, Jr., L. *Adv. Synth. Catal.* **2004**, *346*, 190-194.
[90] Taktak, S.; Flook, M.; Foxman, B. M.; Que, Jr., L.; Rybak-Akimova, E. V. *Chem. Commun.* **2005**, 5301-5303.
[91] Costas, M.; Tipton, A. K.; Chen, K.; Jo, D.-H.; Que, Jr., L. *J. Am. Chem. Soc.* **2001**, *123*, 6722-6723.

Chapter 2
Dinuclear manganese systems - from catalases to oxidation catalysis

Dinuclear manganese based enzymes engage in processes as diverse as α-amino acid hydrolysis and hydrogen peroxide disproportionation. Despite the mechanistic diversity displayed by this class of enzymes, a common feature is the presence of carboxylato residues, which serve to bridge the manganese centres and of hemi-labile oxo-, hydroxo- and aqua- bridges, which show considerable redox state dependence on their lability. The role of carboxylato bridged dinuclear manganese complexes in the disproportionation of hydrogen peroxide is reviewed both in enzymatic and biomimetic systems. The lability of the carboxylato bridge and bridging oxo, hydroxo and aqua ligands during the catalase cycle is discussed in relation to the redox cycle, which the dinuclear manganese center undergoes. The relationship between catalase activity and catalytic oxidation is discussed briefly with regard to understanding the nature of catalytically active species present during the oxidations discussed in this thesis.

Part of this chapter has been published:
J. W. de Boer, W. R. Browne, B. L. Feringa and R. Hage *C. R. Chimie* **2007**, *10*, 341-354.

By virtue of its non-singlet spin state, oxygen, in the form of $^3O_2$, is kinetically inert despite being an energetically very potent oxidant. Its oxidizing power is realized through the formation of 'active oxygen' species, *i.e.* singlet oxygen ($^1O_2$) and its reduced equivalents, the superoxide radical anion ($O_2^{\bullet-}$), hydrogen peroxide (H_2O_2) and hydroxyl radical ($^{\bullet}OH$). Handling active oxygen is a major challenge both *in vivo*[1] and in oxidation catalysis, a challenge which makes it frequently necessary to employ catalytic mediators to control the expression of their oxidizing power.

In vivo, the ability to deal with all forms of active oxygen is central to cellular protection. Any imbalance in the decomposition of active oxygen species leads to oxidative cellular stress and, ultimately, loss of cellular viability. The mechanisms by which nature diffuses active oxygen safely involves the disproportionation of the active species to the inert oxygen species $^3O_2$ and H_2O, through a range of superoxide dismutases and hydrogen peroxide catalase enzymes or through reduction to H_2O with ascorbate or glutathione.[2] Several of these catalase enzymes utilize dinuclear manganese active sites to effect these reactions, a key feature of which is the presence of carboxylato groups, which form bridges between the manganese centers.[3,4] Furthermore, manganese plays a key role in several other important biological processes and other manganese containing enzymes include: the oxygen evolving complex of photosystem II (PS II),[5,6] manganese superoxide dismutase[3,7] and arginase.[8] In this chapter, the nature and role of carboxylato bridging ligands in several of these enzymes, including dinuclear manganese based catalases[9,10] and arginases, and in structural and functional mimics will be explored. The role of carboxylato bridging ligands both in maintaining the dinuclear nature and in controlling the redox and hence ligand exchange chemistry of the complexes and enzyme active sites is discussed. The systems will be compared to related dinuclear manganese complexes employed in the catalytic oxidation of organic substrates, with regard to mechanistic aspects of the catalysis.

2.1 Dinuclear manganese catalase enzymes

Although the majority of known catalase enzymes are iron-heme based enzymes, several organisms ustilise dinuclear manganese-containing enzymes to disproportionate hydrogen peroxide.[9,10] Two crystal structures at atomic resolution have been obtained for enzymes isolated from *Thermus thermophilus*[11,12] and *Lactobacillus plantarum*, respectively.[13] The enzymes originating from both species consist of six identical subunits, each containing a manganese dimer in the active site. In *T. thermophilus*[12] two conformations (form I and II) of the enzyme can be distinguished. The manganese ions are bridged by a μ-carboxylato ligand (Glu70) and μ-oxygen bridges (either aqua, hydroxo or oxo ligands). The Mn ions are each coordinated to one His and one Glu residue. For Mn(2) the Glu is bound via one oxygen, resulting in penta-coordination, while Mn(1) is coordinated to a (labile) terminal molecule of water also, rendering the Mn ion hexa-coordinate. The crystal structure for the dinuclear manganese catalase enzyme from *L. plantarum*[13] reveals a similar first coordination sphere (Figure 2.1). The manganese ions are bridged by a μ-carboxylato from Glu66 and contain two more oxygen bridges, most probably one μ-oxo and one μ-hydroxo (in the resting, Mn^{III}_2, state). Furthermore, one of the Mn ions is bound to one His181 and a chelating Glu148 carboxylato, while the second Mn ion is bound to one His69 and a

monodentate Glu35 carboxylato, with the sixth coordination site again being occupied by a (labile) water molecule.

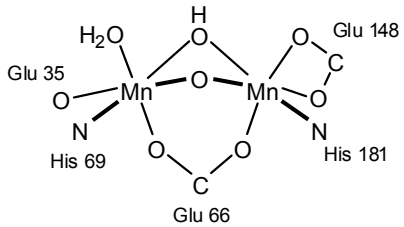

Figure 2.1 The active site of *L. plantarum* catalase.[13]

Four oxidation states are accessible in the dinuclear manganese catalase enzymes (Mn^{II}_2, $Mn^{II}Mn^{III}$, Mn^{III}_2 and $Mn^{III}Mn^{IV}$).[14,15] The majority of the as-isolated enzyme was in the Mn^{III}_2 state, although residual Mn^{II}_2 species and the inactive superoxidized $Mn^{III}Mn^{IV}$ state (*vide infra*) were present also.[16,17]

The activity of these enzymes is dependent on both the pH[10,18] and the oxidation state of the dinuclear manganese centre. During the catalytic decomposition of H_2O_2 the enzyme cycles between the Mn^{III}_2 and Mn^{II}_2 states[14,15] and shows similar activity when starting either in the Mn^{II}_2 and Mn^{III}_2 redox states.[15,20] Treatment with NH_2OH,[16,19,70] which serves as either a one or two electron reductant, depending on local pH,[14] in the presence of H_2O_2 leads to complete conversion of the enzyme to the inactive $Mn^{III}Mn^{IV}$ state (via $Mn^{II}Mn^{III}$). In contrast, reduction with NH_2OH in the absence of H_2O_2 of either the Mn^{III}_2 enzyme or the inactive $Mn^{III}Mn^{IV}$ superoxidized form yields the Mn^{II}_2 state, with full restoration of activity.[16] The interconversion between the different redox states is summarized in Figure 2.2.

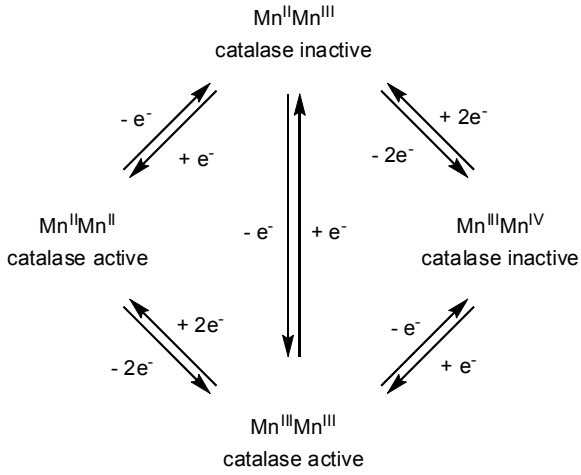

Figure 2.2 Interconversion between the different redox states of the manganese catalase enzymes. H_2O_2 acts as both a two electron oxidant and reductant, whereas NH_2OH acts, predominantly, as a one electron reductant.[16,70]

When the enzyme is in the Mn^{II}_2 state it can be inhibited by the (reversible) binding of several anions (*e.g.* Cl^-, F^-, HPO_4^-)[11,20] and consequently, when H_2O_2 decomposition is performed in the presence of either Cl^- or F^- the enzyme is trapped in the Mn^{II}_2 state.[15] Inhibition by chlorido has been confirmed by X-ray crystallography to be due to replacement of a bridging μ-oxygen ligand by a bridging μ-Cl^- ligand.[11,12] In contrast, azide binds to the terminal position of Mn(1) (in the Mn^{III}_2 state, Figure 2.1) by displacing the terminal labile water molecule from the native enzyme in a mode, which is, possibly, similar to the (initial) binding of H_2O_2.[13]

As mentioned above, the active site of manganese catalase enzymes contains three distinct solvent molecules. From X-ray crystallographic analysis (on the native Mn^{III}_2 enzyme), two solvent molecules bridge between the two Mn centers, while the third water molecule occupies a terminal position on one of the Mn ions. The lability of both the terminal water and the oxygen bridges (either being μ-aqua, μ-hydroxo or μ-oxo) is central to catalytic activity as exemplified by both Cl^- and N_3^- inhibition (*vide supra*). This lability is dependent on the oxidation state of the manganese centers, the Mn-Mn separation and protonation state of the oxygen bridges.[10,13,21] For the Mn^{III}_2 state it has been proposed that the solvent bridges are μ-hydroxo (*trans*-His) and μ-oxo (*trans*-Glu), while for the Mn^{II}_2 state the solvent bridges are believed both to be singly protonated, i.e. both are μ-hydroxo.[12,13] The protonation of the μ–oxo bridges increases their lability and may play a role in governing the differences in the interaction of H_2O_2 with the Mn^{II}_2 and Mn^{III}_2 state.[13,14] Based upon magnetization studies (on the catalase enzyme isolated from *T. thermophilus*) two different pH-dependent bridging modes {(Mn^{III}_2(μO)(OH_2)(OH) (open) and Mn^{III}_2(μ-O)$_2$ (closed)} for the Mn^{III}_2 state have been proposed (Figure 2.3).[22]

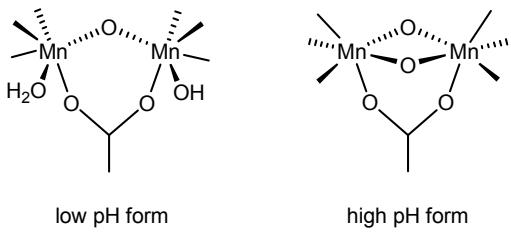

Figure 2.3 Proposed pH-dependent equilibrium between open and closed Mn^{III}_2 catalase enzyme active site.[22]

During catalytic turnover the dinuclear manganese catalase enzymes cycle between Mn^{III}_2 and Mn^{II}_2 and one molecule of H_2O_2 is oxidized to O_2, while another molecule is reduced to H_2O (Figure 2.4).[10,11,14] For the oxidative and reductive half-reactions several different coordination modes for H_2O_2 have been proposed. During the oxidative half-reaction H_2O_2 replaces the terminal H_2O ligand on one of the Mn centers in the Mn^{III}_2 complex, and protonates the μ-oxo bridge.[i] Subsequent reduction of the Mn dimer results in the formation

[i] Before the crystal structures of the (native, Cl^- and N_3^-) inhibited enzymes were known, a similar catalytic mechanism was proposed, however here initial μ-oxygen bridge opening is required to gain a labile water ligand, *e.g.* ref. [9].

and release of O_2. The second equivalent of H_2O_2 binds to the Mn^{II}_2 as a bridging $\mu_{1,1}$-hydroperoxo (either associatively via initial terminal coordination weakening the bridging water, or dissociatively via initial loss of labile H_2O). The $\mu_{1,1}$-bridging mode polarizes the O-O bond and may even be polarized further by *gem*-protonation of hydrogen peroxide, thus facilitating heterolytic O-O bond cleavage, closing the catalytic cycle by reoxidation to Mn^{III}_2 with loss of water.

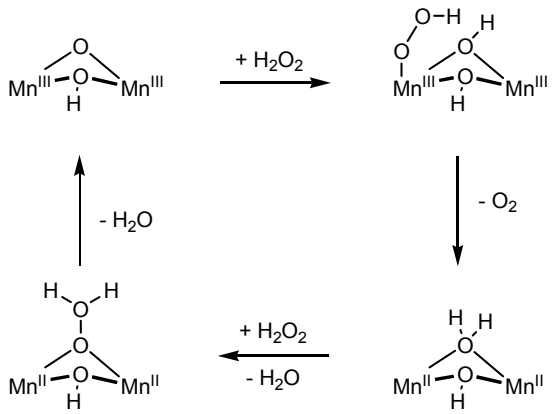

Figure 2.4 Catalytic cycle for a dinuclear manganese catalase enzyme showing two different coordination modes for H_2O_2 during the oxidative and reductive steps.[14]

It is worth noting that, in addition to the manganese catalase enzymes, several other manganese containing enzymes have been tested for catalase activity and, although their biological role is different from that of catalases, they are nevertheless active.[26] An example is arginase, whose physiological role is to cleave L-arginine to L-ornithine hydrolytically and thus plays an important role in mammalian nitrogen metabolism.[3,23] The active site consists of a Mn^{II}_2 dimer (which does not undergo redox change during the hydrolytic catalysis), bridged by two aspartates and one μ-H_2O (Figure 2.5). It has been proposed recently that upon binding of arginine to one of the Mn centers, the μ-H_2O bridge is opened. Deprotonation of the H_2O ligand provides a nucleophilic hydroxide, which then attacks the substrate.[24]

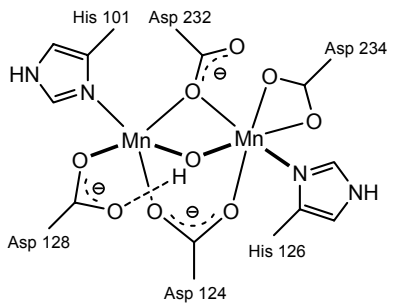

Figure 2.5 Active site of arginase enzyme containing a Mn^{II}_2 dimer.[25,26]

The catalase activity (k_{cat}/K_M) of arginase is five orders of magnitude lower than the catalase enzymes, however its ability to exhibit catalase activity demonstrates the importance of the dinuclear manganese core.[26] The reason for the lower catalase activity of arginase may be due either to the lack of a suitable proton donor/acceptor near the active site (e.g. Lys162 in TTC), which facilitates proton-transfer or the difference in the third bridging ligand (for arginase a $\mu_{1,1}$-carboxylato bridge and for manganese catalases a μ-oxo bridge) in stabilizing the Mn^{II}_2 redox state or both.

Overall it is apparent that the dinuclear μ-carboxylato bridge structural motif is key to the activity of these enzymes in addition to the availability of labile coordination site(s). Importantly, the catalytic activity of these enzymes does not involve loss or partial dissociation of the carboxylato bridge, although in other dinuclear manganese or iron enzymes a carboxylato shift has been found to play an important role in enzyme function (*e.g.* MMO).[27,28]

2.2 Structural, functional and spectroscopic models for catalase enzymes

Modeling the active site of dinuclear manganese catalase enzymes both in terms of structure and function has, over the last two decades, focused on the use of multidentate ligand systems, most notably in the systems described by the groups of Dismukes,[29,30] Wieghardt,[31,32] Pecoraro,[33] Sakiyama[34,35,36,37] and others.[38] In the present chapter the focus will be on functional and structural models for the catalase enzymes,[ii] which present similar dinuclear carboxylato bridged cores.[39] The majority of systems reported are based on a relatively few, albeit structurally diverse, set of non-bridging ligands, in particular phenols,[34,37,40] polypyridyl ligands,[41,42,43] tris(pyrazoyl)-borates[44] and tris(imidazoyl)-phosphines.[45] Overall, four remarkable aspects regarding the diversity in the ligand systems employed in modelling catalase enzymes are i) that structurally very similar complexes can exhibit remarkably different behaviour with respect to both catalase activity and oxidation catalysis, ii) that the lability of ligands, in particular water, is central to activity and decreases with increasing oxidation state of the manganese ions, iii) that whereas in enzymatic systems the carboxylato bridging ligand is generally accepted to be stable and oxo, hydroxo and aqua ligands to be labile with respect to dissociation during catalysis, in biomimetic studies (*vide infra*) the reverse is frequently perceived to be the case and iv) while μ-oxygen bridges generally facilitate communication between two Mn centres, carboxylato bridges both increase the Mn-Mn separation and shield the Mn centres electronically, thus promoting two electron processes instead of two subsequent one electron processes to occur[iii] (*e.g.* Mn^{II}_2/Mn^{III}_2 instead of $Mn^{II}_2/Mn^{II}Mn^{III}/Mn^{III}_2$).

[ii] The phenol based systems of Sakiyama *et al.*, despite containing carboxylato bridges, will not be discussed in detail since their catalase activity is proposed to go via a Mn^{III}_2/Mn^{IV}_2 cycle and thus do not resemble the enzymes (see ref. [34], [35], [36] and [37]).

[iii] The latter is important, at least for the natural enzyme, since formation of the $Mn^{II}Mn^{III}$ state in the presence of H_2O_2 eventually yields the kinetically inert superoxidized $Mn^{III}Mn^{IV}$. In other words, suppression of the formation of the mixed valent $Mn^{II}Mn^{III}$ state is essential for proper functioning of the enzymes. Hence, in addition to acting as a bridging ligand, the carboxylato bridge seems to play a key-role in the enzyme by inhibiting one electron processes and ensuring two electron processes taking place under physiological conditions (see for example ref. [9]).

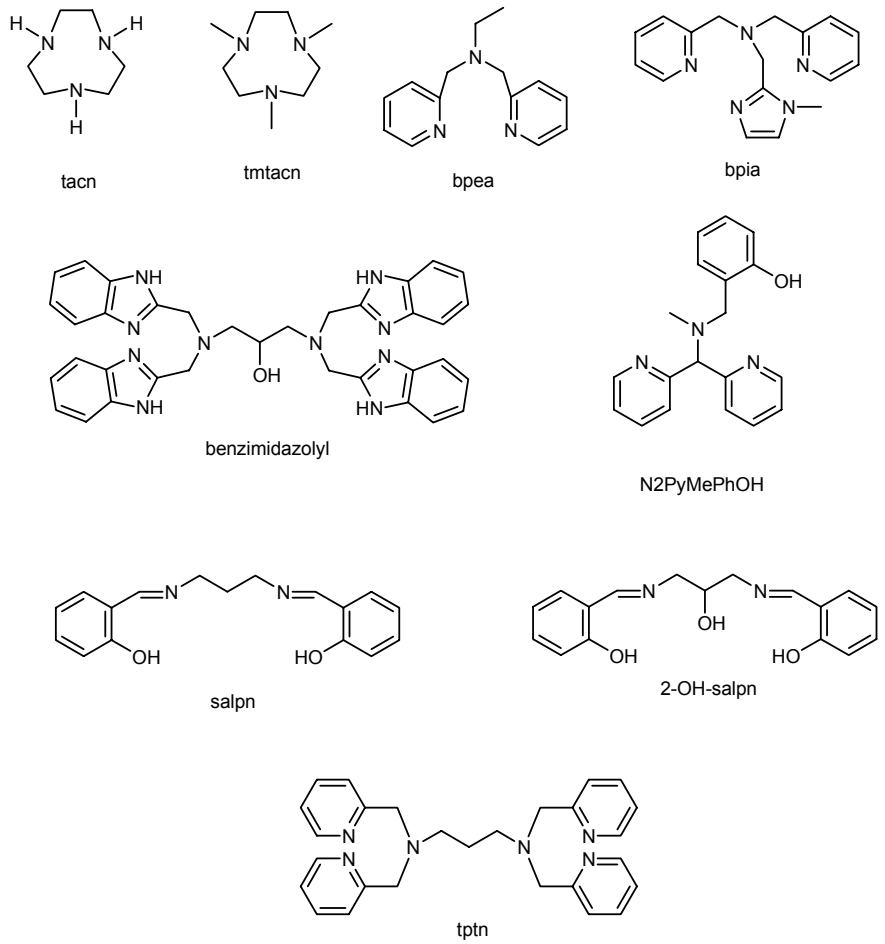

Figure 2.6 Ligands discussed in the text.

2.2.1 TACN based structural models

A structurally and electronically diverse series of mono-, di-, tri- and tetranuclear manganese complexes can be obtained with both the tacn (1,4,7-triazacyclononane) and tmtacn (*N*,*N*',*N*''-trimethyl-1,4,7-triazacyclononane) family of ligands (Figure 2.6).[46,47,48,49,50,51,52] For the dinuclear complexes a series of redox states (Mn^{II}_2 to Mn^{IV}_2) are accessible containing μ-carboxylato bridges and/or μ-oxygen bridges. The solid state (*i.e.* X-ray crystallography) and solution chemistry of these different dinuclear manganese (carboxylato) complexes have been examined in detail and demonstrate the propensity for dinuclear manganese systems to undergo rearrangement of their bridging ligands in response to changes in redox state.[53,54,55,56,57,58] Indeed, the lower oxidation states of the complexes described favour carboxylato and hydroxo bridging ligands whereas the higher oxidation states favour μ-oxo bridging ligands.

bis-Carboxylato $[Mn^{III}_2(\mu\text{-}O)(\mu\text{-}CH_3CO_2)_2L_2]^{2+}$ complexes (with L = tacn or tmtacn) exhibit dynamic solution chemistry.[31] For example, $[Mn^{III}_2(\mu\text{-}O)(\mu\text{-}CH_3CO_2)_2(tmtacn)_2]^{2+}$ can convert between the $Mn^{IV}_2/Mn^{III}Mn^{IV}/Mn^{III}_2/Mn^{II}Mn^{III}$ redox couples in (anhydrous) acetonitrile, retaining the mono-μ-oxo/di-μ-carboxylato core. The same holds for $[Mn^{II}_2(\mu\text{-}OH)(\mu\text{-}CH_3CO_2)_2(tmtacn)_2]^{+}$, which can be oxidized by two separate, reversible, one electron processes: $Mn^{III}_2/Mn^{II}Mn^{III}/Mn^{II}_2$. On the other hand, in aqueous solutions disproportionation reactions can occur resulting in the formation of, for example, $[Mn^{IV}_4(\mu\text{-}O)_6(tacn)_4]^{4+}$ and $[Mn^{IV}_2(\mu\text{-}O)_3(tmtacn)_2]^{2+}$.[46,31]

The latter complex $[Mn^{IV}_2(\mu\text{-}O)_3(tmtacn)_2]^{2+}$, although kinetically stable towards ligand exchange, can undergo electrochemically induced ligand exchange reactions of the μ-oxo bridges in carboxylato containing buffer systems, forming carboxylato bridged $[Mn^{III}_2(O)(\mu\text{-}RCO_2)_2(tmtacn)_2]$ complexes.[59] Mixing equimolar amounts of $[Mn^{III}_2(\mu\text{-}O)(\mu\text{-}CH_3CO_2)_2(tmtacn)_2]^{2+}$ and $[Mn^{III}_2(\mu\text{-}O)(\mu\text{-}CH_3CO_2)_2(tacn)_2]^{2+}$ results in slow formation of mixed ligand species $[Mn^{III}_2(\mu\text{-}O)(\mu\text{-}CH_3CO_2)_2(tmtacn)(tacn)]^{2+}$ [60] as shown by ^{1}H-NMR spectroscopy.[61] The lability of both the μ-oxo and μ-acetato bridges is demonstrated further by the formation of mononuclear complexes of the type $[Mn^{III}(X)_3(tmtacn)]$ (X = N_3^-, Cl^- or NCS^-) when $[Mn^{III}_2(\mu\text{-}O)(CH_3CO_2)(tmtacn)_2]^{2+}$ is reacted with the corresponding anion in ethanol.[31,62]

$[Mn^{III}_2(\mu\text{-}O)(\mu\text{-}CH_3CO_2)_2(tacn)_2]^{2+}$, under aerobic conditions in acidified aqueous media, forms the mixed valent $[Mn^{III,IV}_2(\mu\text{-}O)_2(\mu\text{-}CH_3CO_2)(tacn)_2]^{2+}$ complex (in which one of the acetates is replaced by μ-oxo bridge). By contrast $[Mn^{III}_2(\mu\text{-}O)(\mu\text{-}CH_3CO_2)_2(tmtacn)_2]^{2+}$ retains both acetato bridges to form $[Mn^{III,IV}_2(\mu\text{-}O)(\mu\text{-}CH_3CO_2)_2(tmtacn)_2]^{3+}$ in (anaerobic) acidic aqueous solution.[31,63] Subsequent replacement of the μ-acetato in $[Mn^{III,IV}_2(\mu\text{-}O)_2(\mu\text{-}CH_3CO_2)(tacn)_2]^{2+}$ by either two chlorido or fluorido ligands yields $[Mn^{IV}_2(\mu\text{-}O)_2(tacn)_2(X)_2]^{2+}$ (X=F^-, Cl^-) with a terminal bound halide anion on each Mn-centre upon (aerobic) reaction in water with either $NaBF_4$ or conc. HCl, respectively.[63]

Suprisingly, despite their structural diversity, the catalase activity of this family of complexes has received relatively little attention, in part due to its remarkable catalytic activity with respect to oxidation of organic compounds with H_2O_2 (*vide infra*). Indeed, considerable effort has been expended on suppressing catalase activity.[64] Nevertheless a Mn-tmtacn dinuclear complex has been reported, the first to contain a μ-peroxo bridge. The complex $[Mn^{IV}_2(O)_2(\mu\text{-}O_2)(tmtacn)_2]$ releases O_2 at room temperature, yielding, initially, a Mn^{III}_2 complex which undergoes rapid disproportionation to the Mn^{II} and Mn^{IV}_2 state.[65] The observation of this bridging mode is of particular relevance to the oxidation of H_2O_2 during catalase activity.

Mixed ligand complexes based upon Mn-tmtacn were also prepared: both $[(tmtacn)Mn^{IV}(\mu\text{-}O)_2(\mu\text{-}CH_3CO_2)Mn^{III}(CH_3CO_2)_2]$ and $[(tmtacn)Mn^{IV}(\mu\text{-}O)_2(\mu\text{-}CH_3CO_2)Mn^{III}(bipy)(MeOH)]^{2+}$.[32] Both complexes showed catalase activity in aqueous acetate buffer and the activity was approximately five orders of magnitude lower than the natural enzymes.

2.2.2 Bpea-based catalase mimics

As for the tacn and tmtacn family of ligands, the bpea (*N*,*N*'-bis(2-pyridylmethyl)-ethylamine, Figure 2.6) ligand allows for the preparation of a diverse range of dinuclear manganese complexes in several oxidation states and bridging modes, including $Mn^{II}_2(\mu\text{-}$

$CH_3CO_2)_3$, $Mn^{III}_2(\mu\text{-}O)(\mu\text{-}CH_3CO_2)_2$, $Mn^{III,IV}_2(\mu\text{-}O)_2(\mu\text{-}CH_3CO_2)$ and $Mn^{IV}_2(\mu\text{-}O)_2(\mu\text{-}CH_3CO_2)$ cores which show electrochemically induced inter-conversion.[66] As for the catalase enzymes, the catalytic cycle for the catalase activity exhibited by these types of complexes is proposed to involve a Mn^{II}_2/Mn^{III}_2 couple as depicted in Figure 2.7, with 'opening' of the μ-oxo bridge of the Mn^{III}_2 complex being central to allow for ligand exchange with H_2O_2. For $[(bpea)_2Mn^{II}_2(\mu\text{-}CH_3CO_2)_3]^+$ catalase activity was found to decrease with increasing acetato concentration (the measured O_2 evolution rate decreases from 1.8 to 0.9 to 0.5 ml/min in the presence of 0, 1 and 5 equiv. of NaOAc with respect to the complex, respectively), attributed to the stabilization of the tris-acetato bridged complex in which the labile sites are 'blocked' to H_2O_2 coordination. However, it should be noted also that the addition of acetato leads to a change in pH, which favours the formation of the μ-oxo bridged Mn^{III}_2 complex, and thereby may prevent ligand exchange with H_2O_2.

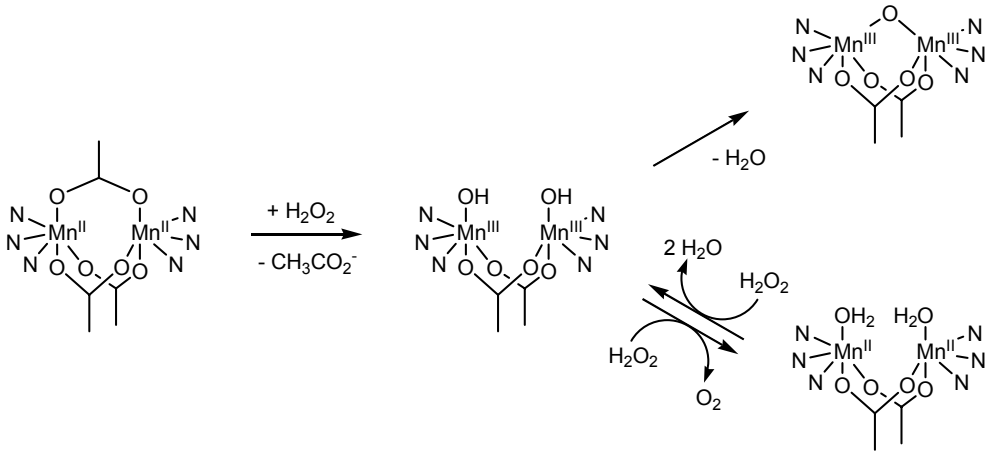

Figure 2.7 Catalase activity by $[(bpea)_2Mn^{II}_2(CH_3CO_2)_3]^{2+}$.[66]

2.2.3 Bpia-based catalase mimics

A series of (mono- and dinuclear) manganese complexes based on the ligand bpia (bis(picolyl)(*N*-methylimidazol-2-yl)amine, Figure 2.6) with various oxidation states and bridging modes have been reported by Krebs and Pecoraro,[67] e.g. $[Mn^{II}_2(\mu\text{-}CH_3CO_2)_2(bpia)_2]^{2+}$, $[Mn^{III}_2(\mu\text{-}O)(\mu\text{-}CH_3CO_2)(bpia)_2]^{3+}$, $[Mn^{III,IV}_2(\mu\text{-}O)_2(bpia)_2]^{3+}$ and $[Mn^{III}_2(\mu\text{-}O)(bpia)(Cl)_2]^{2+}$. Although H_2O_2 is an efficient reductant of the chlorido complex, containing a single μ-oxo bridge and a terminal chlorido on each Mn-centre, it is incapable of reoxidising the reduced complex, and hence this complex does not exhibit catalase activity. By contrast, $[Mn^{II}_2(\mu\text{-}CH_3CO_2)_2(bpia)_2]^{2+}$ is an efficient manganese catalase model with a k_{cat}/K_M of only 2-3 orders of magnitude lower than that of the manganese catalase enzymes. Similarly, $[Mn^{III}_2(\mu\text{-}O)(\mu\text{-}CH_3CO_2)(bpia)_2]^{3+}$ showed catalase activity and was converted to the $[Mn^{III,IV}_2(\mu\text{-}O)_2(bpia)_2]^{3+}$ complex in the presence of H_2O_2.[iv]

[iv] Although $[Mn^{III,IV}_2(\mu\text{-}O)_2(bpia)_2]$ is a structural model for the inactive $Mn^{III,IV}_2$ state of the catalase enzyme, it does show catalase activity.

2.2.4 Benzimidazolyl-based catalase mimics

In a series of reports, Dismukes and coworkers described the redox chemistry and catalase activity of a series of binuclear manganese complexes based on chelating heptadentate, benzimidazolyl-based ligand (L) (*N*,*N*',*N*'',*N*'''-tetrakis(2-methylenebenzimidazolyl)-1,3-diaminopropan-2-ol, Figure 2.6).[68] The complexes isolated initially were $[Mn^{II}_2(L)(\mu\text{-}Cl)(Cl)_2]$ and $[Mn^{II}_2(L)(\mu\text{-}OH)(Br)_2]$, containing a μ-chlorido and a μ-hydroxo bridge, respectively, in addition to a μ-alkoxy bridge from the ligand. The complexes were isolated in the Mn^{II}_2 oxidation state, however during H_2O_2 decomposition (typically up to 200 t.o.n.) the predominant oxidation state was found to be $Mn^{III}_2(\mu\text{-}O)$, determined by UV-Vis and IR spectroscopy, suggesting that a Mn^{II}_2/Mn^{III}_2 cycle was in operation, *i.e.* similar to that observed for the manganese catalase enzymes.

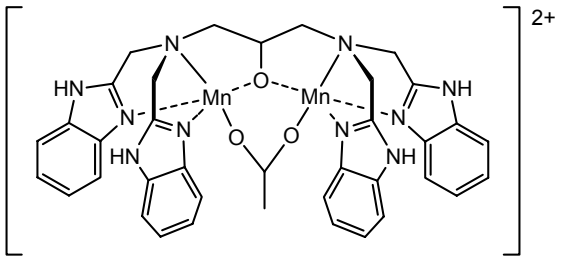

Figure 2.8 $[Mn^{II}_2(CH_3CO_2)(L)]^{2+}$ complex as functional model for catalase.[69]

Three separate redox processes were observed for $[Mn^{II}_2(L)(\mu\text{-}OH)(Br)_2]$ complex (*i.e.* $Mn^{II}_2/Mn^{II}Mn^{III}/Mn^{III}_2/Mn^{III}Mn^{IV}$), while for the μ–Cl bridged complex a one electron, followed by a two electron oxidation was observed ($Mn^{II}_2/Mn^{II}Mn^{III}/Mn^{III}Mn^{IV}$).[68] However, upon replacement of the halide by an acetato ligand, *i.e.* $[Mn^{II}_2(L)(\mu\text{-}CH_3CO_2)]^{2+}$ (Figure 2.8), the first oxidation becomes a two electron process followed by an one electron oxidation, *i.e.* Mn^{II}_2/Mn^{III}_2 and $Mn^{III}_2/Mn^{III}Mn^{IV}$.[69] The effect of the acetato bridge in this class of complexes is intriguing. While for both the related μ-Cl and the μ-OH complexes a $Mn^{II}_2/Mn^{II}Mn^{III}$ couple is observed (*vide supra*; $E_{1/2}$=0.49 and 0.54V vs. SCE, respectively), the μ-acetato complex shows a two electron Mn^{II}_2/Mn^{III}_2 process at 0.81 V.[69,70] Thus introduction of a μ-acetato bridge induces a two electron process in place of two sequential one electron processes, thus circumventing the mixed-valent $Mn^{II}Mn^{III}$ state. The behavior of the $[Mn^{II}_2(L)(\mu\text{-}CH_3CO_2)]$ complex with water, hydroxide and oxygen (in acetone) was studied by several techniques (electrochemistry, ^1H NMR, ESR, FT-IR spectroscopy and MS spectrometry).[2] The penta-coordinate dinuclear manganese complex $[Mn^{II}_2(L)(\mu\text{-}CH_3CO_2)]$ shows a two electron Mn^{II}_2/Mn^{III}_2 process (in acetone), while addition of one equivalent of hydroxide changes this to two single electron processes ($Mn^{II}_2/Mn^{II}Mn^{III}/Mn^{III}_2$), attributed to formation of hexa-coordinate $[Mn^{II}_2(L)(\mu\text{-}CH_3CO_2)(\mu\text{-}OH)]^+$. Addition of another equivalent of hydroxide is proposed to yield $[Mn^{II}_2(L)(\mu\text{-}CH_3CO_2)(OH)_2]$ with two terminal hydroxides, leading to the (re)appearance of a two electron processes ($Mn^{II}_2/Mn^{III}_2/Mn^{IV}_2$). Overall, the redox behavior suggests that the acetato remains bound as a bridging ligand and the changes (from $2e^-$ to $1e^-$ processes, and

vice versa) can be rationalized by the differing coordination modes of the oxygen ligands (*i.e.* hydroxide), with μ-O/μ-OH, μ-Cl and μ-Br ligands facilitating electronic communication between the manganese centers. By contrast the acetato bridges serve to reduce electronic communication and allow for two electron redox processes to take place.

From UV-Vis and EPR spectroscopy and kinetic studies the catalase activity of the acetato bridged complex was determined to involve a Mn^{II}_2/Mn^{III}_2 cycle.[29] Two notable observations with respect to water and acetato content of the reaction mixture were made: *i.e.* the use of up to 2 v/v% of water (in MeOH) resulted in a decrease in the lag-time observed normally, while above 2 v/v% water,[v] a lower catalase rate was observed. Addition of (tetra-*N*-ethylammonium) acetato resulted in a decrease in the rate of H_2O_2 decomposition (4-fold reduction in rate for 20 equiv. of acetato). These results were initially interpreted as shown in the following mechanistic scheme (Figure 2.9).[29] Acetato inhibition was thought to arise from coordination of a second μ-acetato bridge to the five-coordinate manganese centres (not shown), while replacement of the single μ-acetato bridge by two terminally bound water molecules was proposed to be responsible for the lag-time observed (while at higher water concentration binding of water competes with peroxide). Alternatively, the binding mode of the acetato might simply change from bridging to terminal monodentate.

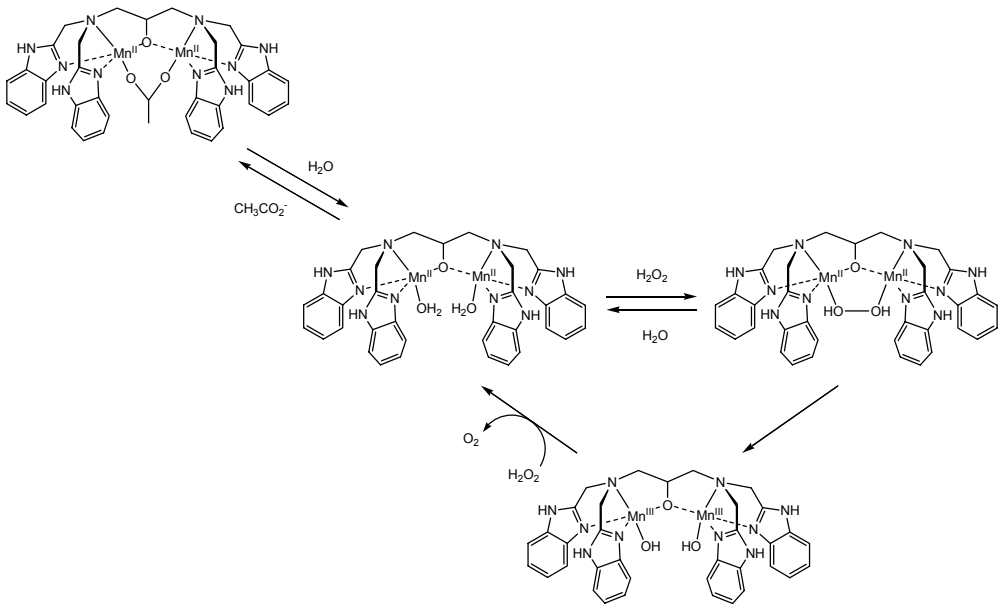

Figure 2.9 Proposed mechanistic scheme.[29]

[v] However, in the presence of 5 equiv. of hydroxide, an *increase* of the rate was observed with increasing water content of the reaction, see ref. [30].

The kinetics of the catalytic decomposition of H_2O_2 by $[Mn^{II}_2(L)(\mu\text{-}CH_3CO_2)]^{2+}$ in MeOH and MeOH/H_2O (98:2 and 11:89) was studied by monitoring the rate of O_2-evolution in a more recent study. The species present during and after catalysis were characterized by UV-Vis and ^{1}H NMR spectroscopy and structural assignments made, primarily by comparison with species assigned in earlier studies.[30] $[Mn^{II}_2(L)(\mu\text{-}CH_3CO_2)]^{2+}$ is an efficient catalase mimic, reaching >2000 t.o.n. with no detectable catalyst decomposition. As for the related catalase enzyme, H_2O_2 disproportionation proceeds via a Mn^{II}_2/Mn^{III}_2 cycle (Figure 2.10). The lag-phase normally observed for this reaction was shown to either decrease upon pre-equilibration with water (*vide supra*) or was completely eliminated upon pretreatment with one equivalent of hydroxide (and the steady state rate of H_2O_2 decomposition increases linearly with up to 5 equiv. of hydroxide). Addition of one equivalent of hydroxide converts $[Mn^{II}_2(L)(\mu\text{-}CH_3CO_2)]^{2+}$ to $[Mn^{II}_2(L)(\mu\text{-}CH_3CO_2)(\mu\text{-}OH)]^{+}$ (based upon electrochemistry). While the effect of water was rationalized by the formation of equal amounts of the (active) $[Mn^{II}_2(L)(\mu\text{-}CH_3CO_2)(\mu\text{-}OH)]^{+}$ species (via deprotonation of $[Mn^{II}_2(L)(\mu\text{-}CH_3CO_2)(\mu\text{-}H_2O)]^{2+}$ formed initially) and (inactive) protonated complex $[Mn^{II}_2(LH)(\mu\text{-}CH_3CO_2)(\mu\text{-}H_2O)]^{3+}$ (observed by ESR as an uncoupled Mn^{II}_2 species). The catalase rate shows saturation kinetics at high H_2O_2 concentrations, indicating peroxide/catalyst complex formation.

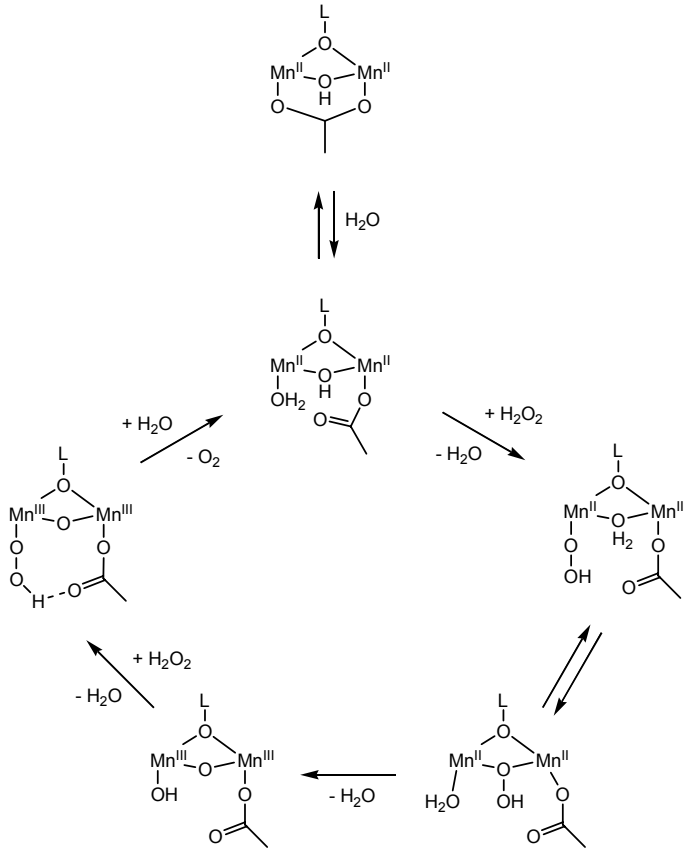

Figure 2.10 Proposed catalytic cycle for catalase activity of $[Mn^{II}_2(L)(\mu\text{-}CH_3CO_2)]^{2+}$.[30]

Two species appeared to be important precursors (*i.e.* $[Mn^{II}_2(L)(\mu\text{-}CH_3CO_2)(\mu\text{-}OH)]^+$ and $[Mn^{III}_2(L)(\mu\text{-}CH_3CO_2)(\mu\text{-}OH)]^{3+}$) to the catalytically active species.[2,30] The reactivity of $[Mn^{II}_2(L)(\mu\text{-}CH_3CO_2)(\mu\text{-}OH)]^+$ is increased by either addition of hydroxide or water (the non-coordinating base 2,6-di-*tert*-butylpyridine has no effect) and upon reaction with H_2O_2 $[Mn^{III}_2(L)(\mu\text{-}CH_3CO_2)(\mu\text{-}OH)]^{3+}$ undergoes a change to a species proposed to be $[Mn^{III}_2(L)(CH_3CO_2)(OH)(\mu\text{-}O)]^+$, in which the acetato bridge has changed its coordination mode to a terminal position. During catalytic turnover, $[Mn^{II}_2(L)(\mu\text{-}CH_3CO_2)(\mu\text{-}OH)]^+$ is proposed to be in equilibrium with 'open' species $[Mn^{II}_2(L)(\mu\text{-}OH)(CH_3CO_2)(H_2O)]^+$ in which the acetato has shifted to a terminal position. The terminal water undergoes ligand exhange with H_2O_2 and the terminal peroxo ligand subsequently exchanges with the μ-OH to form a μ,η_2-peroxo bridge. In the next step the O-O bond of the peroxide is cleaved and the complex undergoes a two electron oxidation to $[Mn^{III}_2(L)(CH_3CO_2)(OH)(\mu\text{-}O)]^+$. Binding of a second H_2O_2 yields a terminally bound peroxide and subsequently O_2 is released together with reduction of the complex to reform $[Mn^{II}_2(L)(\mu\text{-}OH)(CH_3CO_2)(H_2O)]^+$ and closing the catalytic cycle.

2.2.5 SALPN-based catalase mimics

Carboxylato shifts, although implicit in the conclusions of Dismukes and coworkers, are not suspected to play a significant role in effecting H_2O_2 disproportionation in the catalase enzymes themselves. Indeed in the SALPN (1,3-bis(salicylideneamino)propane, Figure 2.6) based series of catalase mimics, carboxylato bridging ligands are not present, yet they have shown catalase type activity also. The dinuclear manganese complexes based on SALPN ligands operate as binuclear catalysts through a Mn^{II}_2/Mn^{III}_2 redox cycle, reminiscent of the redox cycle of the catalase enzymes.[71,72,73,74] The SALPN ligands react with manganese(III) acetate to form a large variety of complexes depending upon reaction conditions, including mono- and dinuclear complexes and polymeric chains.[75,76] Reaction of these 'Mn^{III}(SALPN)' complexes with H_2O_2 yields dinuclear[vi] $[Mn^{IV}_2(SALPN)(\mu\text{-}O)_2]$ complexes.[77]

Modification of the SALPN ligand by incorporation of an alcohol functional group into the propane bridge, *i.e.* 2-OH-SALPN (1,3-bis(salicylideneamino)-2-propanol, Figure 2.6), allows for similar dinuclear complexes to be obtained. Dinuclear $[Mn^{III}_2(2\text{-OHsalpn})_2]$ acts as an efficient functional model for manganese catalase enzymes and the corresponding $Na_2[Mn^{II}_2(2\text{-OH-SALPN})_2]$.2MeOH has been prepared under anaerobic conditions also.[78] The catalytic cycle for H_2O_2 decomposition is proposed to involve a Mn^{II}_2/Mn^{III}_2 cycle and, as for the manganese catalase enzymes, the combination of H_2NOH and H_2O_2 results in the formation of a catalytically inactive $Mn^{III}Mn^{IV}$ dimer. Reactivity can be restored by reaction with H_2NOH in the absence of H_2O_2.

[vi] While a mixture of $[Mn^{IV}_2(SALPN)_2(\mu\text{-}O)_2]$ and $[Mn^{IV}_2(3,5\text{-}Cl_2\text{-SALPN})_2(\mu\text{-}O)_2]$ does not give rise to the formation of mixed ligands, however, when a mixture of both catalysts is used to decompose H_2O_2, the mixed ligand species $[Mn^{IV}_2(SALPN)(3,5\text{-}Cl_2\text{-SALPN})(\mu\text{-}O)_2]$ is formed. This, together with the observation that only $^{18}O_2$ is formed for the decomposition of $H_2{}^{18}O_2$ using $[Mn^{IV}_2(SALPN)_2(\mu\text{-}^{16}O)_2]$, indicates that the μ-oxo bridges are quite labile and monomers might be involved in the catalytic cycle (proposed to be via a Mn^{IV}_2/Mn^{III}_2 cycle). See: Larson, E. J.; Pecoraro, V. L. *J. Am. Chem. Soc.* **1991**, *113*, 7809-7810.

Kinetic studies on a series of $[Mn^{II}_2(2\text{-OH-X-SALPN})_2]^{2-}$ (X = 5-OCH_3, H, 5-Cl, 3,5-diCl, or 5-NO_2) complexes with electron donating and electron withdrawing substituents showed that these systems are effective functional mimics of dinuclear manganese catalase enzymes.[33,79] The 2-OH-SALPN based dinuclear manganese complexes are bridged by two alkoxides and each of the manganese dimers is further coordinated to two oxygen and two nitrogen atoms from the 2-OH-SALPN ligands. As with catalase, the catalytic cycle involves the Mn^{II}_2/Mn^{III}_2 couple. An inactive $Mn^{III}Mn^{IV}$ is formed when oxygen is present at high concentration during H_2O_2 decomposition, however reactivity can be restored upon reaction with H_2NOH. The catalyst can undergo at least 5000 t.o.n.'s. Upon binding of H_2O_2 to $[Mn^{III}_2(2\text{-OH-(X)-SALPN})_2]$, one of the alkoxido bridges changes its coordination mode from bridging to monodentate (alkoxido shift), thus facilitating terminal coordination of the peroxide to the other Mn-ion (Figure 2.11). Subsequent reduction of the manganese dimer and release of O_2 is the rate limiting step. A second H_2O_2 molecule oxidizes the Mn^{II}_2 to Mn^{III}_2, closing the proposed catalytic cycle.

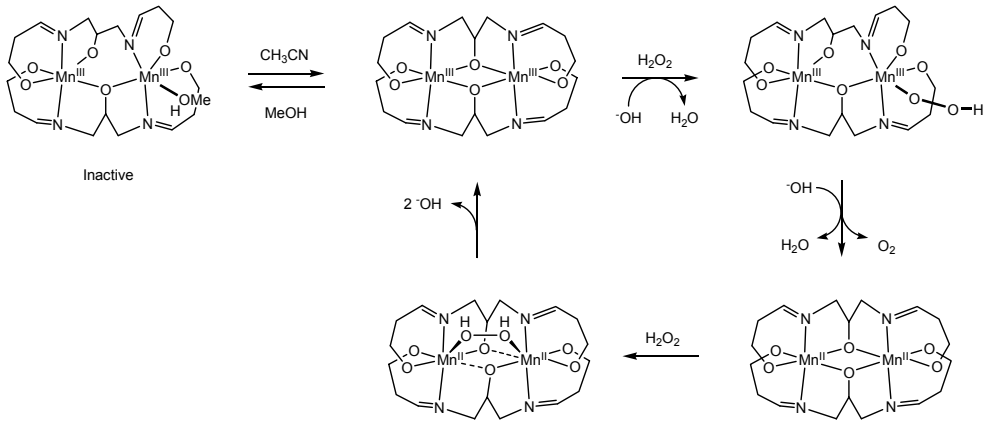

Figure 2.11 Proposed catalytic cycle for H_2O_2 decomposition by Mn-salpn.[33]

2.3 From catalase to oxidation catalysis - dinuclear carboxylato-bridged manganese catalysts

Whereas during catalase activity the dinuclear manganese complexes act as both an alternating $2e^-$ reductant and oxidant of H_2O_2 (Figure 2.12a), for these manganese complexes to act as oxidation catalysts it is required that the oxidised state of the catalyst oxidizes the organic substrate instead of oxidizing H_2O_2 (Figure 2.12b). Indeed carboxylato-bridged dinuclear complexes based on a range of multidentate pyridyl, phenolate and amine based ligands, most notably those based on tmtacn,[80,81,82,83,84,85,86,87,88,89,90] and tptn (*N*,*N*',*N*'',*N*'''-tetrakis(2-pyridylmethyl)-1,3-propanediamine, Figure 2.6),[91,92,93,94] have proven to be effective oxidation catalysts over the last several decades.[95,96,97,98,99,100]

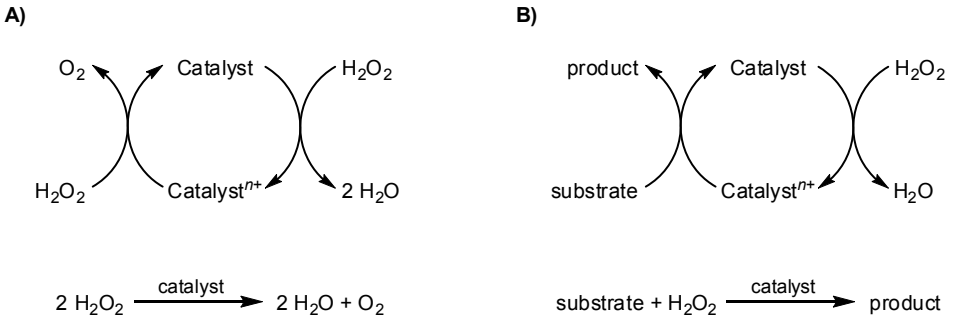

Figure 2.12 H_2O_2 activation: a) catalase activity and b) oxidation catalysis.

2.3.1 Complexes based on Mn-N2PyMePhOH

This change in reactivity frequently involves only minor changes to the coordination environment of the dinuclear manganese core, exemplified in two different dinuclear complexes based on the same pyridyl/phenolate ligand (Figure 2.13).[101,102] Both complexes share similar coordination chemistry with a N2PyMePhOH ligand (2-{[[di(2-pyridyl)methyl](methyl)amino]methyl}phenol, Figure 2.6) coordinating to each manganese centre and a bridging carboxylato ligand. However, if the phenolate ligands act as μ-O bridges between the manganese centres then the complex shows strong catalase activity whereas if the phenolates coordinate to only one of the metal centres and the manganese centres are bridged by a μ-hydroxy bridge then no catalase activity is observed, but instead the complex engages in the catalytic oxidation of organic substrates. For both the role of the carboxylato as a stable bridging ligand rather than a hemi-labile ligand has been demonstrated.[102]

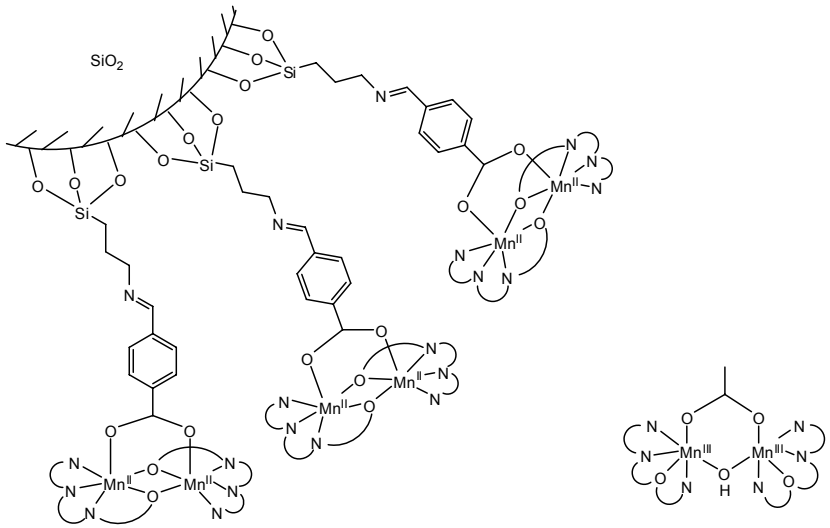

Figure 2.13 Surface bound catalase active Mn-dimers (left) and dinuclear $[Mn^{III}_2(\mu\text{-OH})(N2PyMePhO)_2]^{2+}$ active in epoxidation of styrene (right).[101,102]

2.3.2 Complexes based on Mn-tptn and related ligands

Dinuclear carboxylato-bridged complexes based on the ligands tpen and tptn[103,104] have been shown to be active oxidation catalysts for epoxidation of alkenes,[93] sulfoxidation[91] of thioethers and oxidation of alcohols[92] using H_2O_2 as oxidant (Figure 2.14).[105] High turnover numbers have been obtained for several substrates, however, the mechanism by which these catalysts operate remains elusive.

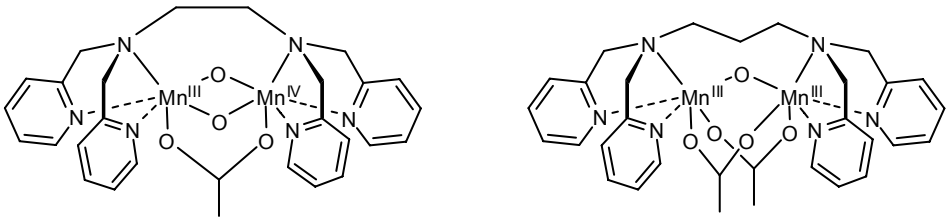

$[Mn^{III,IV}_2(O)_2(CH_3CO_2)(tpen)]^{2+}$ $[Mn^{III}_2(O)(CH_3CO_2)_2(tptn)]^{2+}$

Figure 2.14 Mn-tpen and Mn-tptn.

2.3.3 Complexes based on Mn-tmtacn

Complexes based on Mn-tmtacn have been studied extensively as oxidation catalysts for bleaching of laundry and for oxidative transformation of a wide range of organic substrates: epoxidation, *cis*-dihydroxylation, sulfoxidation, C-H activation and alcohol oxidation,[95,96,97,98] although a detailed understanding of the mechanism(s) by which these Mn-tmtacn catalysts operate is not available. The important role of μ-carboxylato bridges in dinuclear Mn-tmtacn catalysts will be discussed in more detail in the following chapters.

2.4 Conclusions

Perhaps the most sweeping conclusion that may be drawn from the many examples of carboxylato-bridged dinuclear manganese complexes that have been described to date is that the perception of the carboxylato bridging ligand simply as a labile/hemilabile ligand, which can be conveniently displaced by hydrogen peroxide during both catalase activity and oxidation catalysis, is perhaps unwise. Indeed studies of enzymatic active sites provide strong support for the counterview that bridging carboxylato ligands serve to stabilize the dinuclear complexes during catalysis. In contrast to enzymatic and biomimetic catalase systems, the role of carboxylates in oxidation catalysis is at best unclear and in particular the nature of the active states in many manganese carboxylato based catalytic systems has proven somewhat elusive, in part, due to the reluctance to recognize the close relationship between catalase activity and hydrogen peroxide activation. It is apparent then that in order to understand the catalytic activity of manganese carboxylato oxidation systems, the role of the carboxylato as a non-labile bridging unit both in the resting and active states should be considered in addition to the more commonly postulated mononuclear high valent manganese-oxo species.

2.5 References

[1] Lane, N. *Oxygen, the Molecule that Made the World*, Oxford University Press, Oxford, **2002**.
[2] Boelrijk, A. E. M.; Khangulov, S. V.; Dismukes, G. C. *Inorg. Chem.* **2000**, *39*, 3009-3019.
[3] Christianson, D. W. *Prog. Biophys. Molec. Biol.* **1997**, *67*, 217-252.
[4] Wieghardt, K. *Angew. Chem. Int. Ed. Engl.* **1989**, *28*, 1153-1172.
[5] Rüttinger, W.; Dismukes, G. C. *Chem. Rev.* **1997**, *97*, 1-24.
[6] Sivaraja, M.; Philo, J. S.; Lary, J.; Dismukes, G. C. *J. Am. Chem. Soc.* **1989**, *111*, 3221-3225.
[7] Landis, G. N.; Tower, J. *Mech. Ageing Dev.* **2005**, *126*, 365-379.
[8] Wu, G.; Morris, S. M.; *Biochem. J.* **1998**, *336*, 1-17.
[9] Dismukes, G. C. *Chem. Rev.* **1996**, *96*, 2909-2926.
[10] Wu, A. J.; Penner-Hahn, J. E.; Pecoraro, V. L. *Chem. Rev.* **2004**, *104*, 903-938.
[11] Barynin, V. V.; Hempstead, P. D.; Vagin, A. A.; Antonyuk, S. V.; Melik-Adamyan, W. R.; Lamzin, V. S.; Harrison, P. M.; Artymiak, P. J. *J. Inorg. Biochem.* **1997**, *67*, 196.
[12] Antonyuk, S. V.; Melik-Adamyan, V.R.; Popov, A.N.; Lamzin, V. S.; Hempstead, P. D.; Harrison, P. M.; Artymyuk, P. J.; Barynin, V. V. *Crystallography Reports* **2000**, *45*, 111-122.
[13] Barynin, V. V.; Whittaker, M. M.; Antonyuk, S. V.; Lamzin, V. S.; Harrison, P. M.; Artymiuk, P. J.; Whittaker, J. W. *Structure* **2001**, *9*, 725-738.
[14] Whittaker, M.M.; Barynin, V. V.; Antnyuk, S. V.; Whittaker, J. W. *Biochemistry* **1999**, *38*, 9126-9136.
[15] Waldo, G. S.; Penner-Hahn, J. E. *Biochemistry* **1995**, *34*, 1507-1512.
[16] Waldo, G. S.; Fronko, R. M.; Penner-Hahn, J. E. *Biochemistry* **1991**, *30*, 10486-10490.
[17] Zheng, M.; Khangulov, S. V.; Dismukes, G. C.; Barynin, V. V. *Inorg. Chem.* **1994**, *33*, 382-387.
[18] Khangulov, S. V.; Goldfeld, M. G.; Gerasimenko, V. V.; Andreeva, N. E.; Barynin, V. V.; Grebenko, A. I. *J. Inorg. Biochem.* **1990**, *40*, 279-292.
[19] Khangulov, S.V.; Voyevodskaya, N. V.; Varynin, V. V.; Grebenko, A. I.; Melik-Adamyan, V. R. *Biophysics* **1987**, *32*, 1044-1051.
[20] Khangulov, S. V.; Barynin, V. V.; Antonyuk-Barynina, S. V. *Biochim. Biophys. Acta* **1990**, *1020*, 25-33.
[21] Penner-Hahn, J. E. in: *Encyclopedia of Inorganic Chemistry*, King, R. B. (ed.),Volume 4, John-Wiley & Sons, New York, **1994**, 2111-2118.
[22] Michaud-Soret, I.; Jacquamet, L.; Debaecker-Petit, N.; Le Pape, L.; Barynin, V. V.; Latour, J.-M. *Inorg. Chem.* **1998**, *37*, 3874-3876.
[23] Christianson, D. W. *Acc. Chem. Res.* **2005**, *38*, 191-201.
[24] Khangulov, S. V.; Sossong, Jr., T. M.; Ash, D. E.; Dismukes, G. C. *Biochemistry* **1998**, *37*, 8539-8550.
[25] Kanyo, Z. F.; Scolnick, L. R.; Ash, D. E.; Christianson, D. W. *Nature*, **1996**, *383*, 554-557.
[26] Sossong, Jr., T. M.; Khangulov, S. V.; Cavalli, R. C.; Robert Soprano, D.; Dismukes, G. C.; Ash, D. E. *J. Biol. Inorg. Chem.* **1997**, *2*, 433-443.
[27] Rardin, R. L.; Tolman, W. B.; Lippard, S. J. *New. J. Chem.* **1991**, *15*, 417-430.
[28] Merkx, M.; Kopp, D. A.; Sazinsky, M. H.; Blazyk, J. L.; Müller, J.; Lippard, S. J. *Angew. Chem. Int. Ed.* **2001**, *40*, 2782-2807.
[29] Pessiki, P. J.; Dismukes, G. C. *J. Am. Chem. Soc.* **1994**, *116*, 898-903.
[30] Boelrijk, A. E. M.; Dismukes, G. C. *Inorg.* Chem. **2000**, *39*, 3020-3028.
[31] Wieghardt, K.; Bossek, U.; Nuber, B.; Weiss, J.; Bonvoison, J.; Corbella, M.; Vitols, S. E. ; Girerd, J. J. *J. Am. Chem. Soc.* **1988**, *110*, 7398-7411.

[32] Bossek, U.; Saher, M.; Weyhermüller, T.; Wieghardt, K. *J. Chem. Soc., Chem. Commun.* **1992**, 1780-1782.
[33] Gelasco, A.; Bensiek, S.; Pecoraro, V. L. *Inorg.* Chem. **1998**, *37*, 3301-3309.
[34] Sakiyama, H.; Ōkawa, H.; Isobe, R. *J. Chem. Soc.,* Chem. *Commun.* **1993**, 882-884.
[35] Sakiyama, H.; Ōkawa, H.; Suzuki, M.. *J. Chem. Soc., Chem. Commun.* **1993**, 3823-3825.
[36] Yamami, M.; Tanaka, M.; Sakiyama, H.; Koga, T.; Kobayashi, K.; Miyasaka, H.; Ohba, M.; Ōkawa, H. *J. Chem. Soc.,* Dalton *Trans.* **1997**, 4595-4601.
[37] Higuchi, C.; Sakiyama, H.; Ōkawa, H.; Fenton, D. E. *J. Chem. Soc., Dalton Trans.* **1995**, 4015-4020.
[38] Godbole, M. D.; Kloskowski, M.; Hage, R.; Rompel, A.; Mills, A. M.; Spek, A. L.; Bouwman, E. *Eur. J. Inorg. Chem.* **2005**, 305-313.
[39] Khangulov, S. V.; Pessiki, P. J.; Barynin, V. V.; Ash, D. E.; Dismukes, G. C. *Biochemistry* **1995**, *34*, 2015-2025.
[40] Dubois, L.; Caspar, R.; Jacquamet, L.; Petit, P.-E.; Charlot, M.-F.; Baffert, C.; Collomb, M.-N.; Deronzier, A.; Latour, J.-M. *Inorg. Chem.* **2003**, *42*, 4817-4827.
[41] Vincent, J. B.; Tsai, H.-L.; Blackman, A. G.; Wang, S.; Boyd, P. D. W.; Folting, K.; Huffman, J. C.; Lobkovsky, E. B.; Hendrickson, D. N.; Christou, G. *J. Am. Chem. Soc.* **1993**, *115*, 12353-12361.
[42] Fernández, G.; Corbella, M.; Alfonso, M.; Stoeckli-Evans, H.; Castro, I. *Inorg. Chem.* **2004**, *43*, 6684-6698.
[43] Albela, B.; Corbella, M.; Ribas, J. *Polyhedron* **1996**, *15*¸ 91-96.
[44] Sheats, J. E.; Czernuszewicz, R. S.; Dismukes, G. C.; Rheingold, A. L.; Petrouleas, V.; Stubbe, J.; Armstrong, W. H.; Beer, R. H.; Lippard, S. J. *J. Am. Chem. Soc.* **1987**, *109*¸1435-1444.
[45] Wu, F.-J.; Kurtz, Jr. D. M.; Hagen, K. S.; Nyman, P. D.; Debrunner, P. G.; Vankai, V. A. *Inorg. Chem.* **1990**, *29*, 5174-5183.
[46] Wieghardt, K.; Bossek, U.; Gebert, W. *Angew. Chem.* **1983**, *95*, 320-321.
[47] Wieghardt, K.; Bossek, U.; Nuber, B.; Weiss, J.; Gehring, S.; Haase, W. *J. Chem. Soc., Chem. Commun.* **1988**, 1145-1146.
[48] Niemann, A.; Bossek, U.; Haselhorst, G.; Wieghardt, K.; Nuber, B. *Inorg. Chem.* **1996**, *35*, 906-915.
[49] Duboc-Toia, C.; Hummel, H.; Bill, E.; Barra, A.-L.; Chouteau, G.; Wieghardt, K. *Angew. Chem. Int. Ed.* **2000**, *39*, 2888-2890.
[50] Penkert, F. N.; Weyhermüller, T.; Bill, E.; Hildebrandt, P.; Lecomte, S.; Wieghardt, K. *J. Am. Chem. Soc.* **2000**, *122*, 9663-9673.
[51] Pavlishchuk, V.; Birkelbach, F.; Weyhermüller, T.; Wieghardt, K.; Chaudhuri, P. *Inorg. Chem.* **2002**, *41*, 4405-4416.
[52] Birkelbach, F.; Flörke, U.; Haupt, H.-J.; Butzlaff, C.; Trautwein, A. X.; Wieghardt, K.; Chaudhuri, P. *Inorg. Chem.* **1998**, *37*, 2000-2008.
[53] Wieghardt, K.; Bossek, U.; Ventur, D.; Weiss, J. *J. Chem.* Soc*., Chem. Commun.* **1985**, 347-349.
[54] Wieghardt, K.; Bossek, U.; Bonvoisin, J.; Beauvillain, P.; Girerd, J.-J.; Nuber, B.; Weiss, J.; Heinze, J. *Angew. Chem.* **1986**, *98*, 1026-1027.
[55] Niemann, A.; Bossek, U.; Wieghardt, K.; Butzlaff, C.; Trautwein, A. X.; Nuber, B. *Angew. Chem. Int. Ed. Engl.* **1992**, *31*, 311-313.
[56] Darovsky, A.; Kezerashvili, V.; Coppens, P.; Weyhermüller, T.; Hummel, H.; Wieghardt, K. *Inorg. Chem.* **1996**, *35*, 6916-6917.
[57] Zweygart, W.; Bittl, R.; Wieghardt, K.; Lubitz, W. *Chem. Phys. Lett.* **1996**, *261*, 272-276.
[58] Schäfer, K.-O.; Bittl, R.; Zweygart, W.; Lendzian, F.; Haselhorst, G.; Weyhermüller, T.; Wieghardt, K.; Lubitz, W. *J. Am. Chem. Soc.* **1998**, *120*, 13104-13120.

[59] Hage, R.; Krijnen, B.; Warnaar, J. B.; Hartl, F.; Stufkens, D. J.; Snoeck, T. L. *Inorg. Chem.* **1995** *34*, 4973-4978.
[60] Hotzelmann, R.; Wieghardt, K.; Flörke, U.; Haupt, H.-J.; Weatherburn, D. C.; Bonvoisin, J.; Blondin, G.; Girerd, J.-J. *J. Am.* Chem. *Soc.* **1992**, *114*, 1681-1696.
[61] Hage, R.; Gunnewegh, E. A.; Niël, J.; Tjan, F. S. B.; Weyhermüller, T.; Wieghardt, K. *Inorg. Chim. Acta* **1998**, *268*, 43-48.
[62] Wieghardt, K.; Bossek, U.; Nuber, B.; Weiss, J. *Inorg. Chim. Acta* **1987**, *126*, 39-43.
[63] Wieghardt, K.; Bossek, U.; Zsolnai, L.; Huttner, G.; Blondin, G.; Girerd, J.-J.; Babonneau, F. *J. Chem. Soc., Chem. Commun.* **1987**, 651-653.
[64] See for example ref. [85] and [86].
[65] Bossek, U.; Weyhermüller, T.; Wieghardt, K.; Nuber, B.; Weiss, J. *J. Am. Chem. Soc.* **1990**, *112*, 6387-6388.
[66] Romero, I.; Dubois, L.; Collomb, M.-N.; Deronzier, A.; Latour, J.-M.; Pécaut, J. *Inorg. Chem.* **2002**, *41*, 1795-1806.
[67] Triller, M. U.; Hsieh, W.-Y.; Pecoraro, V. L.; Rompel, A.; Krebs, B. *Inorg, Chem.* **2002**, *41*, 5544-5554.
[68] Mathur, P.; Crowder, M.; Dismukes, G. C. *J. Am. Chem. Soc.* **1987**, *109*, 5227-5233.
[69] Pessiki, P. J.; Khangulov, S. V.; Ho, D. M.; Dismukes, G. C. *J. Am. Chem. Soc.* **1994**, *116*, 891-897.
[70] Shank, M.; Barynin, V.; Dismukes, G. C. *Biochemistry* **1994**, *33*, 15433-15436.
[71] Larson, E.; Soo Lah, M.; Li, X.; Bonadies, J. A.; Pecoraro, V. L. *Inorg. Chem.* **1992**, *31*, 373-378.
[72] Kessissoglou, D. P.; Kirk, M. L.; Soo Lah, M.; Li, X.; Raptopoulou, C.; Hatfield, W. E.; Pecoraro, V. L. *Inorg. Chem.* **1992**, *31*, 5424-5432.
[73] Baldwin, M. J.; Stemmler, T. L.; Riggs-Gelasco, P. J.; Kirk, M.L.; Penner-Hahn, J. E.; Pecoraro, V. L. *J. Am. Chem. Soc.* **1994**, *116*, 11349-11356.
[74] Caudle, M. T.; Riggs-Gelasco, P.; Gelasco, A. K.; Penner-Hahn, J. E.; Pecoraro, V. L. *Inorg. Chem.* **1996**, *35*, 3577-3584.
[75] Bonadies, J. A.; Kirk, M. L.; Soo Lah, M.; Kessissoglou, D. P.; Hatfield, W. E.; Pecoraro, V. L. *Inorg. Chem.* **1989**, *28*, 2037-2044.
[76] Bonadies, J. A.; Maroney, M. J.; Pecoraro, V. L. Inorg. *Chem.* **1989**, *28*, 2044-2051.
[77] Larson, E. J.; Pecoraro, V. L. *J. Am. Chem. Soc.* **1991**, *113*, 3810-3818.
[78] Gelasco, A.; Pecoraro, V. L. *J. Am. Chem. Soc.* **1993**, *115*, 7928-7929.
[79] Gelasco, A.; Kirk, M. L.; Kampf, J. W.; Pecoraro, V. L. *Inorg. Chem.* **1997**, *36*, 1829-1837.
[80] de Boer, J. W.; Brinksma, J.; Browne, W. R.; Meetsma, A.; Alsters, P. L.; Hage, R.; Feringa, B. L. *J. Am. Chem. Soc.* **2005**, *127*, 7990-7991.
[81] Brinksma, J.; Schmieder, L.; van Vliet, G.; Boaron, R.; Hage, R.; De Vos, D. E.; Alsters, P. L.; Feringa, B.. L. *Teterahedron Lett.***2002**, *43*, 2619-2622.
[82] Zondervan, C.; Hage, R.; Feringa, B. L. *Chem. Commun.* **1997**, 419-420.
[83] Quee-Smith, V. C.; DelPizzo, L.; Jureller, S. H.; Kerschner, J. L.; Hage, R. *Inorg. Chem.* **1996**, *35*, 6461-6465.
[84] Lindsay Smith, J. R.; Gilbert, B.C.; Mairata i Payeras, A.; Murray, J.; Lowdon, T.R.; Oakes, J.; Pons i Prats, R.; Walton, P. H. *J. Mol. Catal. A: Chem.* **2006**, *251*, 114-122 and references cited herein.
[85] Berkessel, A.; Sklorz, C. A. *Tetrahedron Lett.* **1999**, 40, 7965-7968.
[86] De Vos, D.E.; Sels, B. F.; Reynaers, M.; Subba Rao, Y. V.; Jacobs, P. A. *Tetrahedron Lett.* **1998**, *39*, 3221-3224.
[87] De Vos, D. E.; De Wildeman, S.; Sels, B. F.; Grobet, P. J.; Jacobs, P. A. *Angew. Chem. Int. Ed.* **1999**, *38*, 980-983.

[88] Vincent, J.-M.; Raboin, A.; Yachandra, V. K.; Fish, R. H. *Angew. Chem. Int. Ed.* **1997**, *36*¸2346-2349.
[89] Woitiski, C. B.; Kozlov, Y. N.; Mandelli, D.; Nizova, G. V.; Schuchardt, U.; Shul'pin, G. B. *J. Mol. Catal. A: Chem.* **2004**, *222*¸103-119 and references cited herein.
[90] Barker, J. E.; Ren, T. *Tetrahedron Lett.* **2004**, *45*, 4681-4683.
[91] Brinksma, J.; La Crois, R.; Feringa, B. L.; Donnoli, M. I.; Rosini, C. *Tetrahedron Lett.* **2001**, *42*, 4049-4052.
[92] Brinksma, J.; Rispens, M. T.; Hage, R.; Feringa, B. L. *Inorg. Chim. Acta* **2002**, *337*¸ 75-82.
[93] Brinksma, J.; Hage, R.; Kerschner, J.; Feringa, B. L. *Chem. Commun.* **2000**, 537-538.
[94] Brinksma, J.; Zondervan, C.; Hage, R.; Feringa, B. L. *J. Inorg. Biochem.* **1999**, *74*, 82.
[95] Hage, R. *Recl. Trav. Chim. Pays-Bas* **1996**, 115, 385-395.
[96] Hage, R.; Lienke, A. *Angew. Chem. Int. Ed.* **2006**, *45*¸ 206-222.
[97] Hage, R.; Lienke, A. *J. Mol. Catal. A.: Chem.* **2006**, *251*, 150-158.
[98] Sibbons, K. F.; Shastri, K.; Watkinson, M. *Dalton Trans.* **2006**, 645-661.
[99] Lindsay Smith, J.R.; Gilbert, B. C.; Mairata i Payeras, A.; Murray, J.; Lowdon, T. R.; Oakes, J.; Pons i Prats, R.; Walton, P. H. *J. Mol. Catal. A.: Chem.* **2006**, *251*, 114-122.
[100] Hage, R.; Iburg, J.E. Kerschner, J.; Koek, J.H.; Lempers E.L.M.; Martens R.J.; Racherla, U.S.; Russell S.W.; Swarthoff, T.; van Vliet M.R.P.; Warnaar, J.B.; van der Wolf, L.; Krijnen, B. *Nature* **1994**, *369*, 637-639.
[101] La Crois, R. M. *Manganese Complexes as Catalysts in Epoxidation Reactions: a Ligand Approach*, Ph.D. thesis, University of Groningen, The Netherlands, **2000**.
[102] Vicario, J.; Eelkema, R.; Browne, W. R.; Meetsma, A.; La Crois, R. M.; Feringa, B. L. *Chem. Commun.* **2005**, 3936-3938.
[103] Toftlund, H.; Yde-Andersen, S. *Acta Chem. Scand. A* **1981**, *35*, 575-585.
[104] Toftlund, H.; Markiewicz, A.; Murray, K. S. *Acta Chem. Scand.* **1990**, *44*, 443-446.
[105] Brinksma, J. *Manganese Catalysts in Homogeneous Oxidation Reactions*, Ph.D. thesis, University of Groningen, The Netherlands, **2002**.

Chapter 3
Tuning the selectivity of Mn-tmtacn by the use of carboxylic acid additives

The combination of $[Mn^{IV}_2O_3(tmtacn)_2]^{2+}$ and carboxylic acids results in an effective system for the catalytic cis-dihydroxylation and epoxidation of alkenes using H_2O_2 as terminal oxidant. Screening of a series of alkanoic and benzoic acids identified three most effective carboxylic acids. Trichloroacetic acid yields the most active system, while the selectivity of the reaction can be tuned towards either cis-dihydroxylation or epoxidation when 2,6-dichlorobenzoic or salicylic acid are employed, respectively. The combination of $[Mn^{IV}_2O_3(tmtacn)_2]^{2+}$/2,6-dichlorobenzoic acid is the most active Os-free cis-dihydroxylation catalyst reported to date.

Part of this chapter has been published:
J. W. de Boer, J. Brinksma, W. R. Browne, A. Meetsma, P. L. Alsters, R. Hage and B. L. Feringa *J. Am. Chem. Soc.*, **2005**, *127*, 7990-7991.

The Mn-tmtacn family of complexes were developed by Wieghardt and coworkers as model systems for the water splitting component of photosystem II (PS II, a Mn_4 cluster) and dinuclear manganese-based catalase enzymes in the late 1980's (see Chapter 2, section 2.2.1). In 1994, Unilever scientists reported $[Mn^{IV}_2O_3(tmtacn)_2]^{2+}$ (**1**) (Figure 3.1) as an excellent catalyst for clean and efficient low-temperature bleaching as well as its potential use as an epoxidation catalyst.[1] Since then, the Mn-tmtacn family of complexes have been studied extensively as oxidation catalysts[2] for both bleaching of laundry and for the oxidative transformations of a wide range of organic substrates: epoxidation, *cis*-dihydroxylation, sulfoxidation, C-H bond activation and benzyl alcohol oxidation (Figure 3.2).[3,4,5]

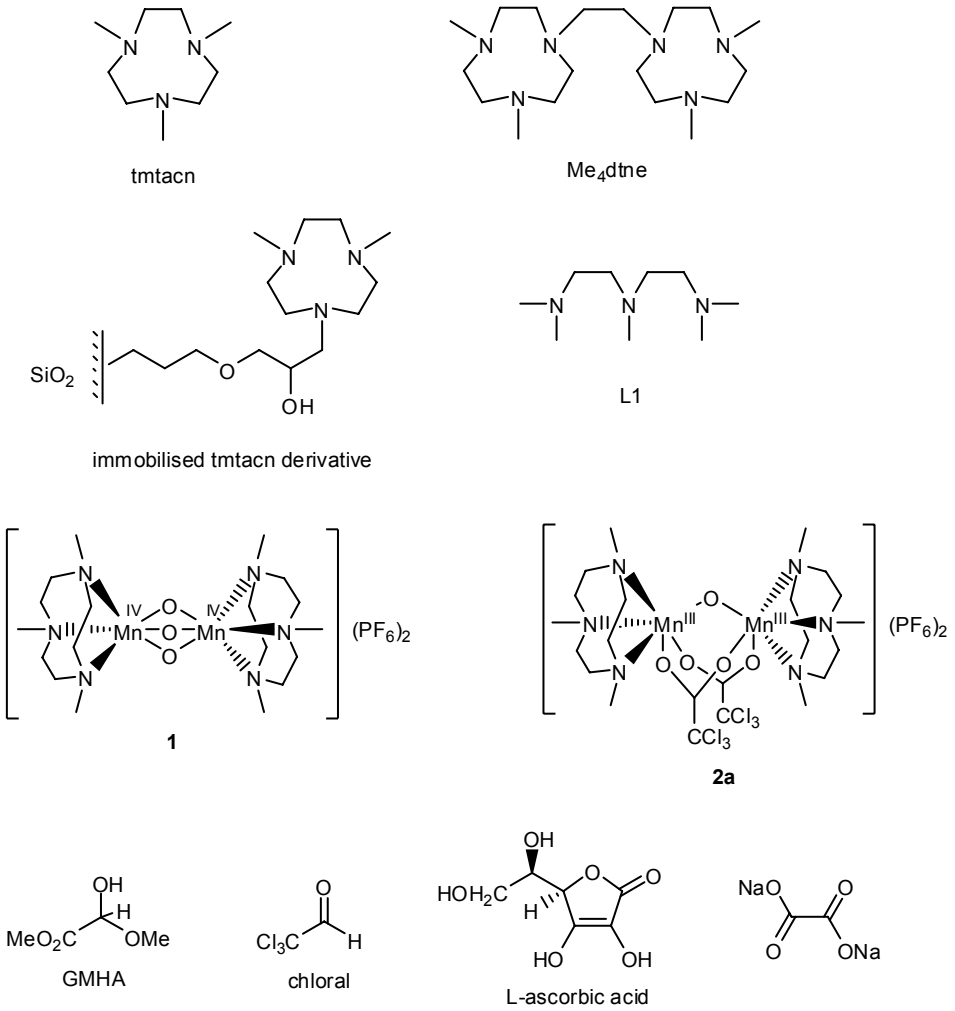

Figure 3.1 Ligands tmtacn, Me_4dtne, **L1** and SiO_2 immobilised tmtacn derivative, complex **1** and **2a** and additives GMHA, chloral, L-ascorbic acid and oxalate.

Whilst complex **1** can be employed as a catalyst, this complex exhibits catalase-type activity. This wasteful disproportionation of H_2O_2 is suppressed either by maintaining a low concentration of H_2O_2 during the reaction (either by slow addition of H_2O_2 or by working in acetone,[i] utilising the formation of the corresponding perhydrate[6,7]) or by the use of additives.[5]

3.1 Suppressing catalase-type activity with additives

As early as 1994, Hage and coworkers reported that complex **1** and related complexes were effective in the epoxidation of styrene and 4-vinylbenzoic acid in an aqueous carbonate buffer at pH 8-9 with a large excess of H_2O_2 (100 equiv. with respect to substrate) as oxidant (Table 3.1, entry 1).[1] Shortly after this, a seminal publication by De Vos *et al.* showed that with acetone as solvent and an excess of H_2O_2 (2 equiv. w.r.t. substrate) added slowly to a mixture of tmtacn and a manganese salt, the epoxidation of a series of alkene substrates could be achieved (entry 2).[8] In a subsequent report oxalate-buffered aqueous CH_3CN enabled efficient epoxidation of a range of alkenes (entry 3).[11] Similarly, Berkessel and coworkers reported the use of a mixture of ascorbic acid and sodium ascorbate in combination with tmtacn and Mn^{2+} in a catalytic system capable of both epoxidation of alkenes and the oxidation of alcohols using excess H_2O_2 (entry 4).[9] In a series of papers Shul'pin and coworkers reported the use of a large excess of acid additives such as acetic acid (*e.g.* 5000 equiv. w.r.t. **1**) to enhance the catalytic activity of the Mn-tmtacn system in CH_3CN using excess of H_2O_2 (2-3 equiv. w.r.t. substrate) giving either C-H bond activation of alkanes[13] or epoxidation of alkenes[10] (entry 5).

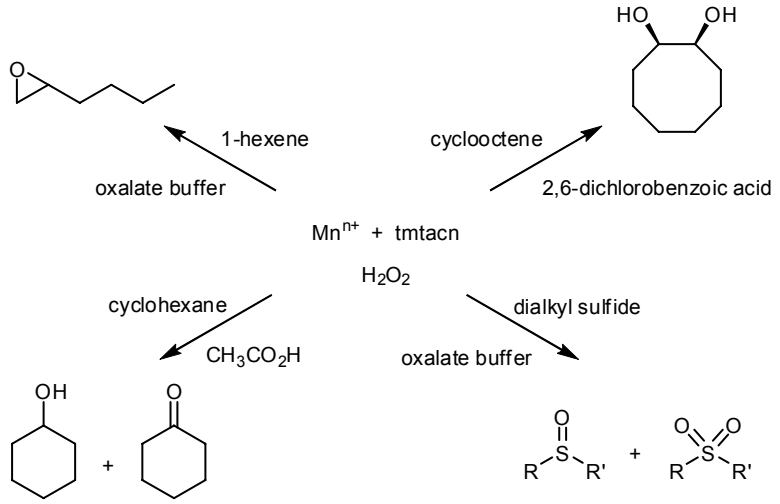

Figure 3.2 Examples of catalytic oxidation reactions using Mn-tmtacn catalyst.[11,12,13,14,15]

[i] Mixtures of H_2O_2 and acetone are potentially explosive, see also ref. [7].

Several other groups have also used additives in an attempt to improve the catalytic activity of Mn-tmtacn. Examples include the use of carboxylate buffers in combination with Mn-tmtacn for C-H bond activation, both at benzylic[16] and at non-activated positions,[17] and the use of biphenols[18] and Rose Bengal[19] for the epoxidation of alkenes. Despite the recognition that additives are capable of enhancing the catalytic activity of Mn-tmtacn, their role was, at best, poorly understood.[ii]

When De Vos *et al.* attached a tacn derivative to a solid support to obtain a heterogeneous version of the Mn-tmtacn catalyst, surprisingly, *cis*-dihydroxylation of alkenes was observed in addition to epoxidation.[20] Although the *cis*-diol/epoxide ratio was low (<0.64 for *cis*-2-hexene), this was the first report on manganese-catalysed *cis*-dihydroxylation.

Table 3.1 Representative examples of Mn-tmtacn catalyzed epoxidations of alkenes employing H_2O_2 as oxidant.

Entry	Product	Catalyst / additive	Solvent	equiv. H_2O_2[a]	Yield	Ref.
1	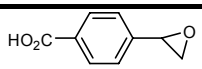	**1** / carbonate buffer[b]	H_2O	100	98%	[1]
2		tmtacn + Mn^{2+} / -	acetone	2	89%	[8]
3	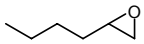	tmtacn + $MnSO_4$ / oxalate buffer	CH_3CN	1.5	>99%	[11]
4	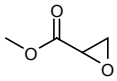	tmtacn + $Mn(OAc)_2$/ sodium ascorbate	CH_3CN	2	97%	[9]
5	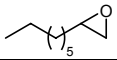	**1** / CH_3CO_2H	CH_3CN	2.6	80%[c]	[10]

[a] With respect to (w.r.t.) substrate. [b] pH 8. [c] Calculated from the reported turnover number (t.o.n.) (see ref. 10).

3.2 Aldehydes and carboxylic acids as additives

3.2.1 *Cis*-dihydroxylation

Previously, aldehydes were found to be effective in the suppression of the catalase type activity of **1** and allowed for good conversion of alkene substrates.[21,22] Moreover, *cis*-dihydroxylation was observed in addition to epoxidation (Scheme 3.1). Both GMHA and chloral hydrate (Figure 3.1 and Table 3.2, entries 1 and 2) provided the *cis*-diol as the major product with cyclooctene as substrate, albeit with a low *cis*-diol/epoxide ratio (1.2). Suppression of catalase-type activity was thought to be due to an equilibrium between the aldehyde and the corresponding perhydrate, thus maintaining a low effective H_2O_2 concentration in solution.[iii]

[ii] The few mechanistic proposals given in literature will be discussed in Chapter 5.

[iii] As will be shown in section 3.2.2, subsequent studies have indicated that this supposed perhydrate formation is likely to be incorrect. An alternative explanation for the role of the aldehyde additive was proposed to be coordination of the hydrate to a mononuclear manganese complex, however, evidence for the latter was inconclusive.

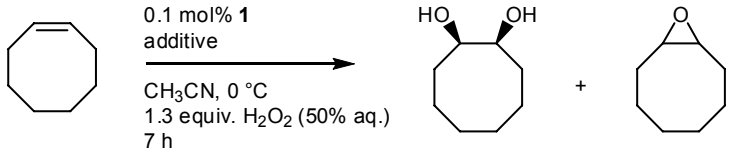

Scheme 3.1 Catalytic oxidation of cyclooctene, employing **1** and an additive.

In this chapter a study of the major aspects of the catalytic oxidation of alkenes by **1** in the presence of additives, specifically carboxylic acids, will be described. In particular the role of additive concentration, possible involvement of peracids, solvents, competitive oxidation processes, catalyst selectivity and substrate scope will be explored.

3.2.2 Results

At the beginning of the research described in this thesis, the results obtained earlier with chloral hydrate were problematic with respect to reproducibility both in terms of activity and selectivity (Table 3.2, entries 1 and 2). The conversion obtained was lower (70%) than described previously (96%); however, the *cis*-diol/epoxide ratio increased from 1.2 to 2.4.[iv] This inconsistency in the outcome of the chloral-promoted reaction was puzzling. When the level of chloral hydrate was reduced from 25 to 1 mol% (entries 3 and 4), low conversion was observed. These results prompted an investigation into the role of the aldehyde additives played in the catalysis.

Although the relatively large amount of aldehyde needed could suggest the involvement of perhydrates, it opened the possibility that a contaminant in the aldehyde might be responsible for the observed activity instead of the aldehyde itself, as was inferred previously.[21,22] Aldehydes are known to react, albeit slowly, during storage over prolonged periods and can contain (trace amounts of) the corresponding alcohol and carboxylic acid.[23] While the use of trichloroethanol as additive did not result in alkene conversion, trichloroacetic acid was found to be active in combination with **1** (Table 3.2, entry 5). Importantly, the amount of CCl_3CO_2H could be reduced from 25 mol% to 1 mol% (w.r.t. substrate, *i.e.* 10 equiv. w.r.t. catalyst) with only a small decrease in reactivity (entries 5 and 6). When using 0.4 and 0.2 mol% of CCl_3CO_2H good conversion was obtained, although the use of 0.1 mol% CCl_3CO_2H resulted in a sharp drop in reactivity (entries 10 and 11).[v]

[iv] The (apparent) higher *cis*-diol/epoxide can be explained by the lower reactivity of the catalytic system in the second case (entry 3) compared to the one reported previously (entry 2, ref. [21] and [22]). The lower reactivity is evident from both the lower conversion and the higher mass-balance, suggesting less overoxidation of the *cis*-diol and thus a higher *cis*-diol/epoxide ratio (see also section 3.5).

[v] As will be discussed in Chapter 5, two carboxylate ligands are needed per manganese dimer to obtain the catalytically active species.

Table 3.2 Catalytic epoxidation and *cis*-dihydroxylation of cyclooctene.[a]

Entry	Co-catalyst (mol%)	conv. (%)[b]	mass bal.[c]	t.o.n.[d]	
				cis-diol	epoxide
1	GMHA (25)[e]	90	88	420	360
2	Chloral hydrate (25)[e]	88	80	370	310
3	Chloral hydrate (25)	70	92	440	185
4	Chloral hydrate (1.0)	3	104	20	15
5	CCl_3CO_2H (25)	96	77	325	405
6	CCl_3CO_2H (1.0)	91	78	440	245
7	HPF_6 (1.0)	3	100	10	20
8	$(Et)_4N.OAc$ (1.0)	0	108	0	6
9	-	3	99	10	5
10	CCl_3CO_2H (0.2)	59	90	340	145
11	CCl_3CO_2H (0.1)	9	100	65	25

a) Reaction conditions: **1**/cyclooctene/H_2O_2 1/1000/1300, H_2O_2 added over 6 h, reported data after 7 h, general procedure A (see Appendix C). All values within +/- 10%. b) Based on substrate consumed. c) Mass balance [%] = unreacted alkene [%] + (*cis*-diol and epoxide products [%]). Deviation from 100% indicates loss through further oxidation of the *cis*-diol to the α-hydroxyketone, see also ref. [21]. d) Turnover number. e) From ref. [21].

Having established that carboxylic acids, present in the aldehydes employed previously, are the active additive of the catalytic system, it was deemed important to examine which other components are essential to obtain an active catalytic system. When **1** alone is used, conversion was not observed (Table 3.3, entry 1). Similarly, activity is not observed when either the ligand tmtacn and manganese(III) acetate are mixed *in situ* (Table 3.3, entry 2), the combination of **1** and tetraethylammonium acetate[vi] (Table 3.2, entry 8) or the combination of **1** and a simple proton source such as HPF_6 (Table 3.2, entry 7) is used. When the tmtacn ligand was mixed *in situ* with either manganese(II) perchlorate or manganese(III) acetate and the reaction was performed in the presence of CCl_3CO_2H, activity was observed (Table 3.3, entries 7 and 8). Ligand **L1** (a linear variant of tmtacn) together with a Mn^{II} or Mn^{III} salt and CCl_3CO_2H gave no activity (Table 3.3, entries 9 and 10). From these results it is clear that the tmtacn ligand, Mn^{II}- or Mn^{III}-ions and a carboxylic acid are required to obtain a catalytically active system.

[vi] The combination of **1**/CH_3CO_2H is catalytically active, see Table 3.6, entry 1.

Table 3.3 Product distribution following oxidation of cyclooctene catalyzed by **1**, Mn^{II} and Mn^{III} salts in CH_3CN, in the absence and presence of tmtacn.[a]

Entry	Catalyst (mol%)	CCl_3CO_2H (mol%)	Conv. (%)	T.O.N. *cis*-diol	T.O.N. epoxide	Mass. bal.(%)
1	**1** (0.1)	-	3	10	5	99
2	tmtacn (0.11)+$Mn(OAc)_3.2H_2O$ (0.1)	-	1	0	26	101
3	$Mn(OAc)_3.2H_2O$ (0.1)	1	0	0	0	109
4	$MnSO_4$ (0.1)	1	0	0	0	101
5	$MnSO_4$ (0.2)	25	0	0	0	102
6	$Mn(ClO_4)_2.6H_2O$ (0.2)	25	3	0	0	97
7	tmtacn (0.11)+$Mn(ClO_4)_2.6H_2O$ (0.1)	1	52	293	141	91
8	tmtacn (0.11)+$Mn(OAc)_3.2H_2O$ (0.1)	1	71	402	204	90
9	**L1**[b] (0.22) +$Mn(ClO_4)_2.6H_2O$ (0.2)	1	0	0	0	100
10	**L1**[b] (0.22) +$Mn(OAc)_3.2H_2O$ (0.2)	1	0	0	0	100

a) See general procedure A (see Appendix C). b) **L1** = *N,N,N',N'',N''*-pentamethyldiethylenetriamine (see Figure 3.1).

3.3 Peracids

Burgess,[24] Stack,[25] Que,[26] and co-workers have demonstrated the use of Mn- and Fe-complexes in combination with peracids (either preformed or prepared *in situ* from the corresponding acid and H_2O_2) in the epoxidation of alkenes. The combination of H_2O_2 and carboxylic acids in the present system, raises the possibility of the involvement of *in situ* formation of peracids.[vii]

Table 3.4 Oxidation of cyclooctene.[a]

Entry	Catalyst	Additive (mol%)	Conv. (%)	t.o.n. *cis*-diol	t.o.n. epoxide	Mass. bal. (%)	Oxidant
1	**1**	CH_3CO_2H (1)	14	78	36	98	H_2O_2
2	**1**[c]	-	97	26	919	97	PAA[b]
3	**3a**	-	70	0	668	97	PAA[b]
4	-[d]	-	85	0	838	99	PAA[b]
5	**1**	3-chlorobenzoic (1)	38	253	113	98	H_2O_2
6	**1**	3-chlorobenzoic (1)	74	6	715	98	*m*CPBA[e]
7	**11**	3-chlorobenzoic (1)	81	8	740	94	*m*CPBA[e]
8	-	-	91	0	899	99	*m*CPBA[e]
9	**2a**	CCl_3CO_2H (1)	10	0	21	92	^{t}BuOOH[f]

a) Employing 0.1 mol% of catalyst (see general procedure A, Appendix C). b) Added by syringe pump over 6 h. c) See also ref. [25c]. d) No lag-period observed. e) Added as a 1.3 M solution in CH_3CN. f) 1 equiv. of ^{t}BuOOH (70 w/w% in H_2O) added over 5 h, reported data after 7 h.

[vii] Stack and coworkers have also used a combination of tmtacn and a Mn^{II}-salt to oxidise 1-octene employing peracetic acid (PAA) (91% yield of the epoxide, see ref. [25c]).

The oxidation of cyclooctene was performed with both peracetic acid (PAA) and *m*-chloroperbenzoic acid (*m*CPBA) as oxidant in place of H_2O_2, to examine whether peracids are involved in the current system (Table 3.4). Whereas **1** and either acetic acid or 3-chlorobenzoic acid afforded a *cis*-diol/epoxide ratio of ~2:1 (*vide infra*, Table 3.6, entry 1 and 8), with peracetic acid (39% in CH_3CO_2H) or *m*CPBA, almost quantitative epoxidation is observed with formation of only minor amounts of *cis*-diol (~3%, Table 3.4, entry 1).[viii] It should be noted that in the absence of Mn-tmtacn both PAA and *m*CPBA give epoxidation of cyclooctene (84 and 90% yield, respectively, Table 3.4, entries 4 and 8), with slightly higher yields than in the presence of Mn-tmtacn (entries 3 and 7). Furthermore, with the alkyl peroxide *tert*-butylperoxide as oxidant, no significant conversion of cyclooctene was observed (entry 9).[ix]

3.4 Reactivity dependence on solvent

Several solvents other than CH_3CN were examined for the oxidation of cyclooctene catalysed by **1**/CCl_3CO_2H. In ^{t}BuOH/H_2O, THF and acetone conversion of cyclooctene was lower than that observed with CH_3CN (Figure 3.3 and Table 3.5). In both DMF and CH_2Cl_2 very low conversion was observed. The activity observed in several, quite different solvents (CH_3CN, acetone, ^{t}BuOH/H_2O and THF) indicates that coordination of organic solvents to the manganese complex is not critical to catalytic activity.[x]

[viii] Commercially available PAA (Fluka) used consists of 39% peracetic acid in acetic acid (45%) and contains up to 6% of H_2O_2. The formation of *cis*-diol can be attributed to the presence of H_2O_2 in commercially available PAA and, hence, allows for the formation of **3** (see also Chapter 4).

[ix] Complex **2a** (see Chapter 4) was employed in this reaction as ^{t}BuOOH is not effective in reducing **1** under catalytic conditions.

[x] Overall the solvent dependence of the reactivity of **1**/CCl_3CO_2H correlates well with the stability of complex $[Mn^{III}_2(\mu\text{-}O)(\mu\text{-}CCl_3CO_2)_2(tmtacn)_2]^{2+}$ (**2a**) (Figure 3.3) under catalytic conditions (see Chapter 5 for details). That is, catalysis takes place only where **2a** can be formed from **1** and is stable. In acetone, for example, the formation of **2a** is very slow (by UV-Vis spectroscopy) and the resulting long lag-period is mainly responsible for the low conversion. In DMF, complex **2a** is not stable and decomposes quickly (as determined by UV-Vis spectroscopy). It should be noted that the absence of activity or reduced activity observed in different solvents can, potentially, be due to competitive solvent oxidation which leads to a reduced efficiency in terms of cyclooctene conversion. However, catalytic activity towards alkene oxidation was observed only when **2a** was present in solution.

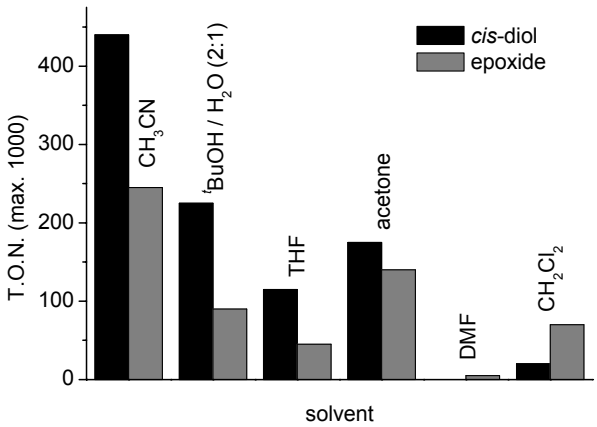

Figure 3.3 Solvent dependence of the oxidation of cyclooctene after 7 h by **1** (0.1 mol%) with CCl_3CO_2H (1 mol%) (see also Table 3.5).

Table 3.5 Product distribution dependence on solvent for the oxidation of cyclooctene catalyzed by **1** or $MnSO_4$ with CCl_3CO_2H (1 mol%).[a]

Entry	Catalyst (mol%)	Solvent	Conv. (%)	t.o.n. *cis*-diol	t.o.n. epoxide	Mass. bal. (%)
1	**1** (0.1)	CH_3CN	91	440	245	78
2	**1** (0.1)	$^tBuOH/H_2O$(2:1 v/v)	39	225	90	93
3	**1** (0.1)	THF	21	115	45	95
4	**1** (0.1)	Acetone	53	175	140	78
5	**1** (0.1)	DMF	20	0	5	80
6	$MnSO_4$ (1)[b]	DMF	3	0	5	98
7	**1** (0.1)	CH_2Cl_2	15	20	70	94

a) See general procedure A (Appendix C). b) 10 mol% CCl_3CO_2H.

3.5 Time course of the reaction

In the optimised reaction conditions for the catalytic oxidation of cyclooctene (100 mol%) a combination of **1** (0.1 mol%) and CCl_3CO_2H (1 mol%) is employed in CH_3CN at 0 °C. H_2O_2 (50% aq.) is added slowly by syringe pump addition over 6 h. When both substrate conversion and product formation are followed in time a significant lag-period is observed (phase I, Figure 3.4), after which *cis*-dihydroxylation and epoxidation begin simultaneously with both processes showing similar time dependence up to 4 h (phase II). Finally, towards the end of the reaction (phase III), the *cis*-diol concentration begins to level off and ultimately decreases. During the lag-period, *i.e.* phase I, the catalytically active species is formed as will be discussed in detail in Chapter 5.

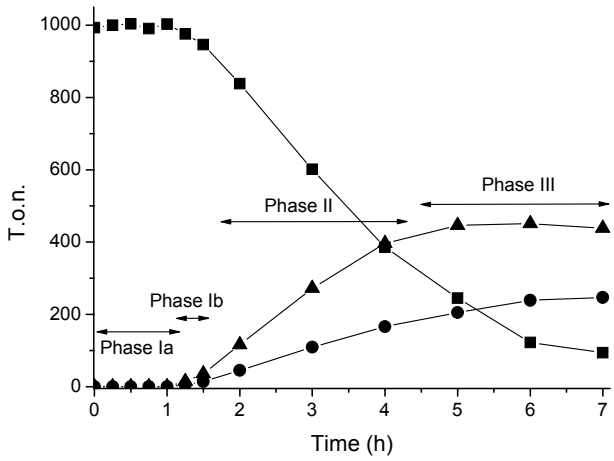

Figure 3.4 Typical time course for product formation (*cis*-diol: triangles and epoxide: circles) and substrate consumption (cyclooctene: squares) under 'standard' conditions (see text for details) in the catalyzed oxidation of cyclooctene with H_2O_2 by **1**/CCl_3CO_2H. Phase I - lag-period, Phase II - normal reactivity observed, Phase III - subsequent oxidation of *cis*-diol product is observed.

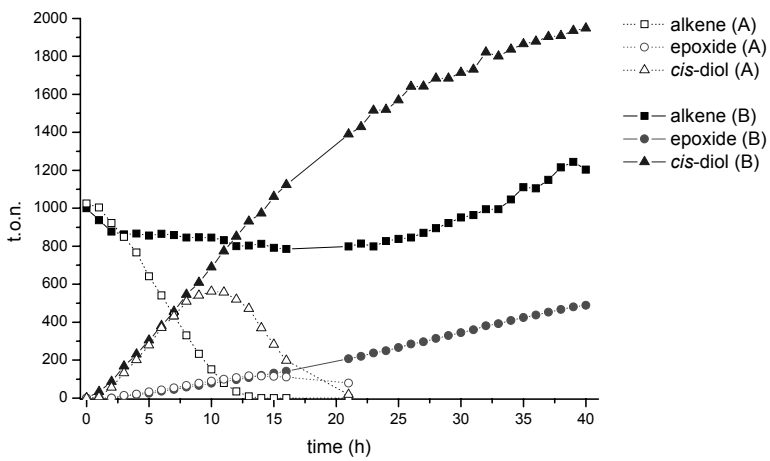

Figure 3.5 Catalytic oxidation of cyclooctene by a combination of **1** (0.1 mol%) and 2,6-dichlorobenzoic acid (3 mol%): a) extended addition of H_2O_2 (dotted lines) and b) maintaining *pseudo*-steady state levels of cyclooctene (solid lines).

Phase III of the reaction is intriguing as it appears that the *cis*-diol/epoxide selectivity of the catalyst decreases in time. This is not the case, however, and the apparent loss of the activity of the catalyst towards *cis*-diol formation is in fact due to further oxidation of the *cis*-diol product to the corresponding α-hydroxyketone.[21] This is best exemplified in the

case where a combination of **1** and 2,6-dichlorobenzoic acid (30 equiv. w.r.t. **1**) is used (Figure 3.5, dotted lines). When the addition of oxidant (H_2O_2) is continued over a longer period,[xi] three observations can be made. First, the cyclooctene substrate is converted completely (after ca. 12 h). Secondly, the formation of the epoxide product is constant in time (after the initial lag-period) and its formation ceases when all cyclooctene has been consumed. Thirdly, the amount of *cis*-diol increases steadily during phase II. However, when most of the alkene substrate has been consumed the amount of *cis*-diol levels off and ultimately all *cis*-diol is oxidised. In an additional experiment the concentration of the cyclooctene substrate is held at a pseudo-steady state level (by addition of cyclooctene at approximately the same rate as it was consumed, Figure 3.5, solid lines). It is apparent that the epoxidation is unaffected and the epoxide is formed at a constant rate throughout the reaction. The formation of the *cis*-diol behaves initially in an identical manner as before. However, the amount of *cis*-diol increases throughout the reaction and after 40 h 2000 t.o.n.'s for *cis*-dihydroxylation are obtained. From these two experiments it can be concluded that the intrinsic (*cis*-diol/epoxide) selectivity of the catalyst is not altered over the 40 h of the reaction. In fact, the catalyst is very active and although it exhibits a preference for the oxidation of the alkene over the *cis*-diol, at low alkene concentration the *cis*-diol competes effectively with the alkene to be oxidised by the catalyst.[xii] Similar suppression of overoxidation is observed when 1-octene is used as substrate (Figure 3.6).

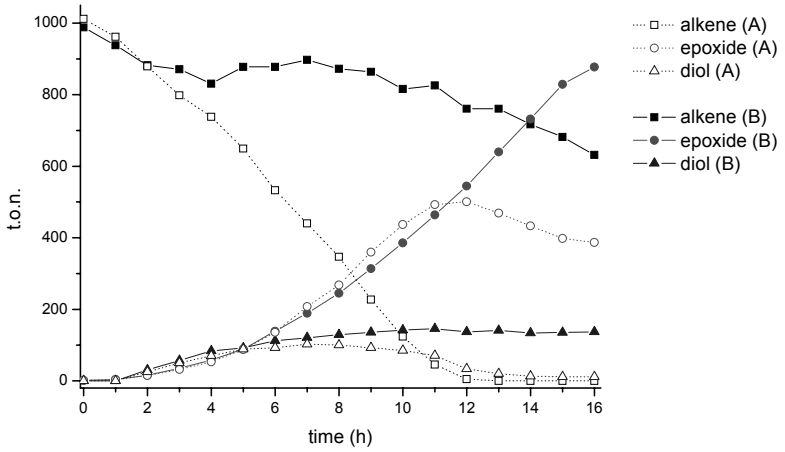

Figure 3.6 Catalytic oxidation of 1-octene by a combination of **1** (0.1 mol%) and 2,6-dichlorobenzoic acid (3 mol%): extended addition of H_2O_2 (dotted lines) and maintaining *pseudo*-steady state levels of 1-octene (solid lines).

[xi] H_2O_2 is being added at the same rate as under 'standard' conditions. As a consequence of the longer addition time, more oxidant than needed for single oxidation of the alkene substrate is being added, *i.e.* 5.2 equiv. of H_2O_2 w.r.t. substrate was added over a period of 21 h.

[xii] Furthermore, the α-hydroxyketone formed is subject to further oxidation, ultimately giving suberic acid (see Appendix C).

3.6 Dependence of activity and selectivity on the carboxylic acid

Since CCl_3CO_2H was identified as an effective additive to i) suppress the catalase activity of **1** and ii) to enable **1** to act as both a *cis*-dihydroxylation and epoxidation catalyst, a series of alkanoic and benzoic acids were tested in combination with **1**, to identify more selective carboxylic acids, both for selective formation of *cis*-diol and selective formation of epoxide products. When comparing the activity and selectivity of different additives, it is, however, important to note the different phases during the reaction (Figure 3.4). Although all carboxylic acids examined promote oxidation of cyclooctene by **1** to both *cis*-diol and epoxide, the duration of the lag-period, the *cis*-diol/epoxide ratio and the conversion are dependent on the specific carboxylic acid employed. In order to compare the intrinsic activity and *cis*-diol/epoxide selectivity of the different additives it is important to take into account both the duration of the lag-period as well as the level of overoxidation. For example, for hexafluoroglutaric acid a lag-period of only 30 min is observed at 0 °C, while for CCl_3CO_2H the lag-period is 60-90 min and for 2,4,6-trichlorobenzoic acid a lag-period of almost 2 h was observed (Figure 3.7 and Table 3.6). Hence, the lag-period should be taken into account: *i.e.* low conversion after 7 h does not necessarily correspond to a low intrinsic activity. Furthermore, a very active system might appear non-selective towards *cis*-dihydroxylation, since due to the high activity substantial overoxidation occurs, resulting in a reduction of the amount of *cis*-diol observed after 7 h.

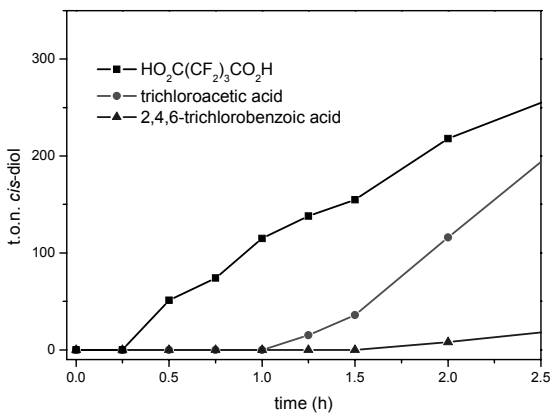

Figure 3.7 Effect of different carboxylic acids on the lag-period for the *cis*-dihydroxylation of cyclooctene by **1**/H_2O_2.

Acetic acid, trichloroacetic acid, trifluoroacetic acid, glutaric acid and hexafluoroglutaric acid (Table 3.6, entries 1-5) all show a *cis*-diol/epoxide ratio of approximately 2, however, with CCl_3CO_2H and CF_3CO_2H higher conversion is observed than with CH_3CO_2H. The ditopic carboxylic acids examined (*i.e.* glutaric and hexafluoroglutaric acid) show similar selectivity with their mono-carboxylic acid counterparts (acetic and trifluoroacetic acid, respectively). For hexafluoroglutaric acid a shorter lag-period is observed compared with

trifluoroacetic acid. For glutaric acid, however, the increased activity observed compared to acetic acid is surprising, when it is considered that glutaric acid exhibits a much longer lag-period (a rational for the latter observations is provided in Chapter 5).

For benzoic acid and its F-, Cl-, HO-, MeO- and Me- substituted analogs, activity towards both *cis*-dihydroxylation and epoxidation is observed. Indeed several inferences regarding the relative importance of steric and electronic effects towards reactivity and selectivity can be drawn from Figure 3.8 (see also Table 3.6). With the exception of 2,4,6-trimethyl- and 4-chlorobenzoic acid, for all substituted benzoic acids examined, an increase in reactivity compared with benzoic acid is observed. Comparison of *ortho*-, *meta*- and *para*-mono-substituted benzoic acids show only minor differences in selectivity, however, overall *para*-substitution results in a significant decrease in activity. A clear correlation between electronic parameters and either reactivity or selectivity is not observed for the benzoic acids. It should be noted, however, that the activity observed is affected significantly by the duration of the lag-period.

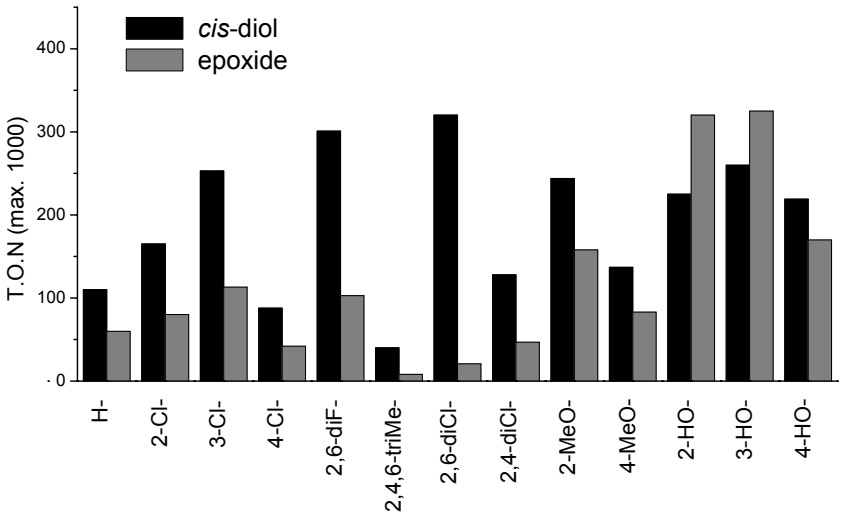

Figure 3.8 *Cis*-dihydroxylation and epoxidation of cyclooctene by **1** (0.1 mol%) in the presence of (selected) chloro-, fluoro-, methyl-, methoxy-, and hydroxy-substituted benzoic acids (1 mol%). See also Table 3.6.

The selectivity of the reaction shows only moderate sensitivity to the position of the hydroxy group in the hydroxybenzoic acid series (*i.e. meta*-OH ~ *ortho*-OH, entries 22 and 21, Table 3.6). By contrast, steric demands at the 2- *and* 6-positions appear to be more important with regard to selectivity, with (bulky) 2,6-disubstituted benzoic acids providing consistently higher *cis*-diol/epoxide ratios without loss in activity, compared with their *ortho*-mono substituted analogs: both 2-chlorobenzoic acid and 2,4-dichlorobenzoic acid exhibit only a moderate *cis*-diol/epoxide ratio (entries 7 and 11), while 2,6-dichlorobenzoic acid is much more selective towards *cis*-dihydroxylation (entry 10). Furthermore, for the 2,6-difluorobenzoic acid promoted system (entry 15), the activity is comparable to the

2,6-dichlorobenzoic acid promoted system, however, the selectivity observed was comparable to that with benzoic acid (entry 6). In the case of the 2,4,6-trimethylbenzoic acid (entry 14) promoted reaction the *cis*-diol/epoxide ratio is high also (~5), although in this case very low reactivity is observed. This suggests that while the activity is driven by both electronic and steric effects, the selectivity is dominated by steric factors with bulky substituents at both the 2- and 6-position favoring *cis*-dihydroxylation over epoxidation.[xiii]

Table 3.6 *Cis*-dihydroxylation and epoxidation of cyclooctene - influence of carboxylic acids.[a]

Entry	Carboxylic acid (mol%)	Conv. (%)	t.o.n.[b] *cis*-diol	t.o.n.[b] epoxide	Mass bal. (%)	Lag-period
1	acetic acid (1.0)	14	78	36	98	>1.5 h
2	glutaric acid (0.5)	38	237	104	96	2-3 h
3	CCl_3CO_2H (1.0)	91	440	245	78	60-90 min
4	trifluoroacetic acid (1.0)	90	296	251	65	30-45 min
5	hexafluoroglutaric acid (0.5)	92	315	256	65	15-30 min
6	benzoic acid (1.0)	21	110	60	96	>2h
7	2-chlorobenzoic acid (1.0)	29	165	80	96	>2h
8	3-chlorobenzoic acid (1.0)	38	253	113	98	N/A
9	4-chlorobenzoic acid (1.0)	16	88	42	97	>2h
10	2,6-dichlorobenzoic acid (1.0)	36	320	21	98	1.5 h
11	2,4-dichlorobenzoic acid (1.0)	21	128	47	97	>2h
12	2,3,6-trichlorobenzoic acid (1.0)	42	362	30	97	1.25 h
13	2,4,6-trichlorobenzoic acid (1.0)	24	197	16	97	2-3 h
14	2,4,6-trimethylbenzoic acid (1.0)	7	40	8	98	>2h
15	2,6-difluorobenzoic acid (1.0)[c]	47	301	103	93	1.5 h
16	2,4-difluorobenzoic acid (1.0)[c]	43	268	106	95	2 h
17	3,4-difluorobenzoic acid (1.0)[c]	34	206	82	95	2 h
18	3,5-difluorobenzoic acid (1.0)[c]	33	194	82	95	1.25 h
19	2-methoxybenzoic acid (1.0)	47	244	158	93	2 h
20	4-methoxybenzoic acid (1.0)	26	137	83	96	>2h
21	2-hydroxybenzoic acid (1.0)	64	225	320	90	1.25 h
22	3-hydroxybenzoic acid (1.0)	69	260	325	89	1.5 h
23	4-hydroxybenzoic acid (1.0)	46	219	170	93	> 2 h
24	5-bromosalicylic acid (1.0)	62	252	296	92	N/A

a) Employing **1** (0.1 mol%), see also general procedure A (Appendix C). b) Turnover number. c) Mn^{III}_2 bis(carboxylato) complexes **17-20** used instead of **1** (see Figure 4.2, Chapter 4).

3.7 Me_4dtne

In order to get an indication of the relative importance of the dinuclear structure of **1**, a related manganese-dimer was tested for catalytic activity as well. The complex $[Mn^{III,IV}_2(\mu\text{-}O)_2(\mu\text{-}CH_3CO_2)(Me_4dtne)]^{2+}$ is based on the ethylene-bridged tmtacn type

[xiii] The electron withdrawing/donating nature of the various acids is inferred from the redox potentials of the bis(carboxylate) complexes, see Chapter 4, Table 4.1.

ligand, Me_4dtne.[1] Its reactivity was tested on cyclooctene using selected carboxylic acids (Table 3.7). As with the combination **1**/CH_3CO_2H low activity is observed with $[Mn^{III,IV}_2(\mu\text{-}O)_2(\mu\text{-}CH_3CO_2)(Me_4dtne)]^{2+}$ in combination with CH_3CO_2H (entry 1). However, when CH_3CO_2H is replaced by CCl_3CO_2H, the conversion increases to 31% and a *cis*-diol/epoxide ratio of 1:1 is obtained (entry 2). The use of both 2,6-dichlorobenzoic acid and salicylic acid results in low conversion (7 and 8%, respectively) and both acids give a *cis*-diol/epoxide ratio of 0.7 (entries 3 and 4).[xiv]

Table 3.7 Catalytic oxidation of cyclooctene by $[Mn^{III,IV}_2(\mu\text{-}O)_2(\mu\text{-}CH_3CO_2)(Me_4dtne)]^{2+}$ (0.1 mol%) at 0 °C.[a]

Entry	acid (mol%)	Conv. (%)	t.o.n.		mass.
			cis-diol	epoxide	bal. (%)
1	acetic acid (1)	3	0	6	98
2	trichloroacetic (1)	31	154	150	100
3	2,6-dichlorobenzoic (3)	7	37	50	101
4	salicylic acid (1)[b]	8	38	58	102

a) See general procedure A (Appendix C). b) Single run.

3.8 Substrate scope

3.8.1 Alkenes

From the screening of a range of carboxylic acids, three carboxylic acids stand out. CCl_3CO_2H is one of the most active additives, while overoxidation of the *cis*-diol is limited. 2,6-Dichlorobenzoic acid exhibits the highest selectivity for *cis*-dihydroxylation and salicylic acid gives the epoxide as the main product. These three acids were employed in the oxidation of a series of alkenes representing key structural classes (Table 3.8).

As for cyclooctene, for *cis*-2-heptene either the *cis*-diol is obtained as the major product when using 2,6-dichlorobenzoic acid or the *cis*-epoxide when salicylic acid is used (Table 3.8). Furthermore, retention of configuration (RC)[27] for both the *cis*-diol (RC >96%) and epoxide (RC >95%) is observed, indicating that the reaction between the alkene and the activated catalyst proceeds via a concerted pathway. *Trans*-heptene on the other hand gives lower conversion and the very poor mass-balance indicates that competing processes are taking place. For the terminal alkenes styrene and 1-octene epoxidation is observed to be the major process even with CCl_3CO_2H or 2,6-dichlorobenzoic acid. The same holds for cyclopentene and cyclohexene where the epoxide is observed as the major product. The general trend that 2,6-dichlorobenzoic acid favors *cis*-dihydroxylation and salicylic acid

[xiv] A possible explanation for the similar selectivity observed for the reaction promoted by 2,6-dichlorobenzoic and salicylic acid, respectively, is that the corresponding carboxylates are too sterically demanding to replace the μ-acetate ligand in $[Mn^{III,IV}_2(\mu\text{-}O)_2(\mu\text{-}CH_3CO_2)(Me_4dtne)]^{2+}$. While in the case of **1** (containing two tmtacn ligands) replacement of two μ-oxo bridges by two (sterically demanding) carboxylates can be facilitated by increasing the Mn-Mn separation, this would not be possible in the complex with the ethylene-bridged ligand Me_4dtne.

favors epoxidation holds for these substrates. It should be noted that both for cyclopentene and cyclohexene only minor amounts of allylic oxidation products were observed. While high conversion is achieved with electron-rich alkenes, electron-deficient alkenes (*i.e.*, dimethyl-maleate and -fumarate) show low conversion, indicating that the catalyst is electrophilic in character.

Table 3.8 *Cis*-dihydroxylation and epoxidation of various alkenes.[a]

	2,6-dichlorobenzoic acid (3 mol%)		**CCl_3CO_2H (1 mol%)**		**salicylic acid (1 mol%)**	
Substrate Product(s)	**(*conv.*)[b] t.o.n.[c]**	**Mass bal.**	**(*conv.*)[b] t.o.n.[c]**	**Mass bal.**	**(*conv.*)[a] t.o.n.[c]**	**Mass bal.**
cyclooctene	(*67%*)[d]	93%	(*82%*)	85%[f]	(*64%*)	90%
cis-diol	525		445		225	
epoxide	75		225		320	
***cis*-2-heptene**	(*86%*)	72%[g]	(*94%*)	70%[g]	(*82%*)	82%[g]
erythro-/*threo*-diol	440 / 10		295 / 5		145 / 5	
cis-/*trans*-epoxide	125 / 5		330 / 10		485 / 15	
***trans*-2-heptene**	(*64%*)	54%[g]	(*79%*)	55%[g]	(*72%*)	67%[g]
erythro-/ *threo*-diol	0 / 85		0 / 240		0 / 90	
cis-/*trans*-epoxide	10 / 90		25 / 85		15 / 285	
cyclohexene	(*92%*)	75%	(*94%*)	76%	(*100%*)	80%
cis-diol	110		70		0	
epoxide	400		570		735	
2-cyclohexen-1-ol	25		30		0	
2-cyclohexen-1-one	135		35		60	
cyclopentene	(*n.d.*)	(*n.d.*)	(*n.d.*)	(*n.d.*)	(*n.d.*)	(*n.d.*)
cis-diol	305		190		120	
epoxide	360		460		505	
2-cyclopenten-1-one	85		35		60	
1-octene	(*71%*)	71%[g]	(*66%*)	65%[g]	(*75%*)	87%[g]
diol	125		115		30	
epoxide	295		200		590	
styrene	(*97%*)	80%	(*74%*)	91%	(*100%*)	81%
diol	0		35		0	
epoxide	770		615		815	
dimethylmaleate[e]	(*< 1%*)	98%	(*< 1%*)	101%	(*6%*)	102%
meso- / *D,L*-diol	0 / 0		0 / 0		0 / 0	
cis-/*trans*-epoxide	0 / 0		0 / 0		0 / 20	
dimethylfumarate[e]	(*5%*)	97%	(*21%*)	99%	(*32%*)	96%
meso- / *D,L*-diol	0 / 15		0 / 105		0 / 105	
cis-/*trans*-epoxide	0 / 0		0 / 0		0 / 40	

a) See general procedure B and C in Appendix C. All values +/- 10%. b) Based on substrate consumed. c) Turnover number. d) Isolated yield *cis*-cyclooctane diol: 46%. e) Reaction conditions: **1**/alkene/H_2O_2 1/500/650, see also general procedure D in Appendix C. Under these conditions, using CCl_3CO_2H as additive, cyclooctene gives: 79% conversion, 122 t.o.n. epoxide, 166 t.o.n. *cis*-diol (mass-balance: 78%). f) The discrepancy in the mass balance is due to further oxidation of the *cis*-diol to the α-hydroxyketone, see also ref. [21]. g) Multiple (minor) oxidation side products observed by GC. [h] Benzaldehyde is the major oxidation side product.

3.8.2 Benzyl alcohol oxidation and C-H bond activation

Previously, Mn-tmtacn based catalysts were found to be active in the oxidation of benzylalcohols to their corresponding aldehydes in acetone (and to the carboxylic acids when excess H_2O_2 was used).[12] Furthermore, overoxidation of the *cis*-cyclooctanediol to the corresponding α-hydroxyketone (at high conversion of cyclooctene, Figure 3.5) and the formation of a number of (unidentified) by-products in trace amounts in the catalytic oxidation of *trans*-heptene (Table 3.8) were observed. Therefore, the current system was tested for activity for both alcohol oxidation and C-H bond activation.

The combination of **1** and either 2,6-dichlorobenzoic acid, CCl_3CO_2H or salicylic acid resulted in good conversion of benzyl alcohol (69-100%) with benzoic acid being the major product (Table 3.9). Catalytic oxidation of cyclooctane using **1**/CCl_3CO_2H provided 52% conversion of the substrate and cyclooctanone was found as the major product. Using the same system, *n*-octane was partly oxidized to a complex mixture of various alcohols and ketones.

Table 3.9 Catalytic oxidation of benzylalcohol, cyclooctane and *n*-octane.

	2,6-dichlorobenzoic acid[a]		**CCl_3CO_2H**[b]		**salicylic acid**[b]	
Substrate Products	**(*conv.*)**[c] **t.o.n.**[d]	**Mass Bal.**[e]	**(*conv.*)**[c] **t.o.n.**[d]	**Mass bal.**[e]	**(*conv.*)**[c] **t.o.n.**[d]	**Mass Bal.**[e]
benzylalcohol	(*100%*)	79%	(*69%*)	102%	(*83%*)	99%
benzaldehyde	0		305		275	
benzoic acid	785		410		545	
cyclooctane			(*52%*)	82%		
cyclooctanol			30			
cyclooctanone			310			
***n*-octane**			(*21%*)	(n.d.)		
alcohol / ketone			(n.d.)			

a) Reaction conditions: **1**/substrate/H_2O_2 1/1000/1800, H_2O_2 added over 7 h, reported data after 8 h, see general procedure C in Appendix C. All values +/- 10%. b) Reaction conditions: **1**/substrate/H_2O_2 1/1000/1300, H_2O_2 added over 6 h, reported data after 7 h, see general procedure B in Appendix C. c) Based on substrate consumed. d) Turnover number.

3.9 Summary

The complex $[Mn_2O_3(tmtacn)_2]^{2+}$ (**1**) itself does not show catalytic activity in the oxidation of organic substrates with H_2O_2 as oxidant;[xv] in fact it catalyses the decomposition of H_2O_2 (catalase type activity). However, carboxylic acid additives such as CCl_3CO_2H suppress catalase-type activity. Examination of a range of carboxylic acids confirmed that both the

[xv] In their paper, Hage *et al.*[1] did not describe the use of additives. However, **1** was used as epoxidation catalyst under basic aqueous conditions using a *carboxylate* buffer.

activity and the selectivity of the catalyst can be tuned by the use of the appropiate carboxylic acid. CCl_3CO_2H was identified as providing the most active system. The most selective additive for *cis*-dihydroxylation is 2,6-dichlorobenzoic acid, while the use of salicylic acid results in the highest preference for epoxidation.

Based on the results of the reactions performed with peracids (PAA and *m*CPBA) and the lack of activity of Mn^{II} and Mn^{III} salts with trichloroacetic acid and H_2O_2, it can be excluded that *cis*-dihydroxylation arises from the *in situ* formation of peracids. For epoxidation, involvement of peracids formed *in situ* cannot be excluded completely. However, it is unlikely since i) the combination of Mn-salts and acids do not result in epoxidation and ii) in the absence of CCl_3CO_2H the complex **2a** gives the same *cis*-diol/epoxide ratio as in the presence of CCl_3CO_2H (see Chapter 5, Figure 5.5 and Table 5.1).

The catalytic oxidation of a series of alkenes representing key structural classes revealed that reaction between the active catalyst and the alkene substrate occurs via a concerted pathway (section 3.8.1). Comparison between electron-rich and electron-poor substrates showed that the catalyst is electrophilic in nature with the highest selectivities for *cis*-dihydroxylation observed for electron-rich *cis*-alkenes.

The system **1**/2,6-dichlorobenzoic acid (>2000 t.o.n. for *cis*-1,2-cyclooctanediol) is the most active Os-free *cis*-dihydroxylation catalyst reported to date. However, this very high activity of the present system was found to be its Achilles' heel as exemplified by the oxidation of several of the substrates. Besides *cis*-dihydroxylation and epoxidation, the catalytic system is also capable of alcohol oxidation and C-H bond activation. In general, the activated catalyst prefers to oxidise (electron-rich) alkenes. However, when the alkene concentration becomes low (*e.g.* at high conversion of cyclooctene, Figure 3.5) or is not accessible (*e.g. trans*-2-heptene, Table 3.8), the catalyst will oxidise alcohols or C-H bonds, respectively. Overoxidation can be circumvented by maintaining pseudo-steady state concentrations of substrate.

Thus, the use of carboxylic acids suppresses the catalase activity of **1** and instead a very active and selective oxidation catalyst is obtained, of which the selectivity can be tuned towards either *cis*-dihydroxylation or epoxidation by the use of the appropriate carboxylic acid additive. Furthermore, the combination **1**/carboxylic acid results in a very H_2O_2 efficient catalyst and nearly all H_2O_2 is used in oxidation events (see also Chapter 5, Figure 5.9).

These results are promising, but raise several questions. First of all, the considerable lag-period, during which catalytic activity is not observed, is not understood. Moreover, the observations described in this chapter do not explain the role of the carboxylic acids in controlling activity and selectivity. Neither has the catalytically active species been identified. These issues will be addressed in Chapter 5, however, to understand the present catalytic system it is essential to understand first the complexes involved. In the next chapter the ligand exchange and redox chemistry of several Mn-tmtacn complexes relevant to catalysis will be explored.

3.10 References

[1] Hage, R.; Iburg, J. E.; Kerschner, J.; Koek, J. H.; Lempers E. L. M.; Martens R. J.; Racherla, U. S.; Russell S. W.; Swarthoff, T.; van Vliet M. R. P.; Warnaar, J. B.; van der Wolf, L.; Krijnen, B. *Nature* **1994**, *369*, 637-639.
[2] Hage, R. *Recl. Trav. Chim. Pays-Bas* **1996**, *115*, 385-395
[3] Hage, R.; Lienke, A. *Angew. Chem. Int. Ed.* **2006**, *45*¸ 206-222.
[4] Hage, R.; Lienke, A. *J. Mol. Catal. A.: Chem.* **2006**, *251*, 150-158.
[5] Sibbons, K. F.; Shastri, K.; Watkinson, M. *Dalton Trans.* **2006**, 645-661.
[6] Sauer, M. C. V.; Edwards, J. O. *J. Phys. Chem.* **1971**, *75*, 3004-3011.
[7] a) Brewer, A. D. *Chem. Brit.* **1975**, *11*, 335. b) Bodner, G. M. *J. Chem. Educ.* **1985**, *62*¸ 1105-1107.
[8] De Vos, D. E.; Bein, T. *Chem. Commun.***1996**, 917-918.
[9] Berkessel, A.; Sklorz, C. A. *Tetrahedron Lett.* **1999**, *40*, 7965-7968.
[10] See for example: Woitiski, C. B.; Kozlov, Y. N.; Mandelli, D.; Nizova, G. V.; Schuchardt, U.; Shul'pin, G. B. *J. Mol. Catal. A: Chem.* **2004**, *222*¸103-119 and references cited herein.
[11] De Vos, D.E.; Sels, B. F.; Reynaers, M.; Subba Rao, Y. V.; Jacobs, P. A. *Tetrahedron Lett.* **1998**, *39*, 3221-3224.
[12] Zondervan, C.; Hage, R.; Feringa, B.L. *Chem. Commun.* **1997**, 419-420.
[13] See for example: a) Lindsay Smith, J. R.; Shul'pin, G. B. *Tetrahedron Lett.* **1998**, *39*, 4909-4912, b) Shul'pin, G. B. *J. Mol. Catal. A: Chem.* **2002**, *189*, 39-66, and references cited herein.
[14] Lindsay Smith, J. R.; Gilbert, B. C.; Mairata i Payeras, A.; Murray, J.; Lowdon, T. R.; Oakes, J.; Pons i Prats, R.; Walton, P. H. *J. Mol. Catal. A: Chem.* **2006**, *251*, 114-122.
[15] Barker, J. E.; Ren, T. *Tetrahedron Lett.* **2004**, *45*, 4681-4683.
[16] Bennur, T. H.; Sabne, S.; Deshpande, S. S.; Srinivas, D.; Sivasanker, S. *J. Mol. Catal. A: Chem.* **2002**, *185*, 71-80.
[17] Ryu, J. Y.; Kim, S. O.; Nam, W.; Heo, S.; Kim, J. *Bull. Korean Chem. Soc.* **2003**, *24*, 1835-1837.
[18] Gilbert, B. C.; Lindsay Smith, J. R.; Mairata i Payeras, A.; Oakes, J.; Pons i Prats, R. *J. Mol. Catal. A: Chem.* **2004**, *219*, 265-272.
[19] Liu, B.; Chen, Y.; Yu, C.-Z.; Shen, Z.-W. *Chin. J. Chem.* **2003**, *21*, 833-838.
[20] De Vos, D. E.; de Wildeman, S.; Sels, B. F.; Grobet, P. J.; Jacobs, P. A. *Angew. Chem. Int. Ed.* **1999**, *38*, 980-983.
[21] Brinksma, J.; Schmieder, L.; Van Vliet, G.; Boaron, R.; Hage, R.; De Vos, D. E.; Alsters, P. L.; Feringa, B. L. *Tetrahedron Lett*. **2002**, *43*, 2619-2622.
[22] Brinksma, J. *Manganese catalysts in homogeneous oxidation reactions*, Ph.D. Thesis, University of Groningen, **2002**.
[23] March, J. *Advanced Organic Chemistry, Reactions, Mechanism and Structure*, fourth edition, Wiley, New York, **1992**, pp.1233-1235.
[24] a) Lane, B. S.; Burgess, K. *J. Am. Chem. Soc.* **2001**, *123*, 2933-2934. b) Lane, B. S.; Vogt, M.; DeRose, V. J.; Burgess, K. *J. Am. Chem. Soc.* **2002**, *124*, 11946-11954.
[25] a) Murphy, A.; Dubois, G.; Stack, T. D. P. *J. Am. Chem. Soc.* **2003**, *125*, 5250-5251. b) Dubois, G.; Murphy, A.; Stack, T. D. P. *Org. Lett.*, **2003**, *5*, 2469-2472. c) Murphy, A.; Pace, A.; Stack, T. D. P. *Org. Lett.* **2004**, *6*, 3119-3122.
[26] Fujitta, M.; Que, Jr., L. *Adv. Synth. Catal.* **2004**, *346*, 190-194.
[27] RC (retention of configuration) = 100% × (A – B)/(A + B) where A = yield of product with retention of configuration and B = yield of epimer: Fujita, M.; Costas, M.; Que, Jr., L. *J. Am. Chem. Soc.* **2003**, *125*, 9912-9913.

Chapter 4
Redox-state dependent coordination chemistry of the Mn-tmtacn family of complexes

The solution chemistry of Mn-tmtacn complexes in CH_3CN is explored, with focus on the various μ-oxo and/or μ-carboxylato bridged manganese dimers and their interconversion. The nature of the non-carboxylato bridging ligands of the manganese dimers is determined by both the redox state of the manganese centres and presence or absence of carboxylic acids and/or water in the reaction medium.

Part of this chapter has been published:
J. W. de Boer, W. R. Browne, J. Brinksma, P. L. Alsters, R. Hage and B. L. Feringa
Inorg. Chem. **2007**, *46*, 6353-6372.

The study of the coordination chemistry of Mn-tmtacn was initiated and developed by Wieghardt and coworkers in the late 1980's because of the relevance of these complexes as model compounds for biologically important manganese-containing enzymes such as manganese catalases and photosystem II (PS II).[1,2] A series of dinuclear Mn-tmtacn complexes containing oxo and/or acetato bridging ligands, such as $[Mn^{III}_2(\mu\text{-}O)(\mu\text{-}CH_3CO_2)_2(tmtacn)_2]^{2+}$ **3a**, $[Mn^{II}_2(\mu\text{-}OH)(\mu\text{-}CH_3CO_2)_2(tmtacn)_2]^{+}$ **3b**, $[Mn^{II}_2(\mu\text{-}CH_3CO_2)_3(tmtacn)_2]^{+}$, $[Mn^{III,IV}_2(\mu\text{-}O)(\mu\text{-}CH_3CO_2)_2(tmtacn)_2]^{3+}$ **4** and $[Mn^{IV}_2(\mu\text{-}O)_3(tmtacn)_2]^{2+}$ **1** were described.[1,2] In their work, Wieghardt and coworkers focused on the synthesis of the Mn-tmtacn family of complexes and on the characterisation of their physical properties, with emphasis on single crystal X-ray structure analysis and magnetic properties (*e.g.* ESR and magnetic susceptibility).[3,4,5]

For these dinuclear complexes, containing μ-acetato and/or μ-oxo bridges, a series of redox states (Mn^{II}_2 to Mn^{IV}_2) are accessible. The solid state structure (*i.e.* X-ray crystallography) and the study of the solution chemistry of the dinuclear manganese (μ-acetato) complexes demonstrates the propensity for dinuclear manganese systems to undergo rearrangement of their bridging ligands in response to changes in redox state.[6,7,8,9] Indeed, in lower oxidation states the complexes favour acetato and hydroxo bridging ligands whereas in higher oxidation states μ-oxo bridging ligands are favoured.

For the complex $[Mn^{III}_2(\mu\text{-}O)(\mu\text{-}CH_3CO_2)_2(tmtacn)_2]^{2+}$ **3a** the $Mn^{IV}_2/Mn^{III}Mn^{IV}/Mn^{III}_2/Mn^{II}Mn^{III}$ redox couples are fully reversible in (anhydrous) CH_3CN.[2,6,7] Also the complex $[Mn^{II}_2(\mu\text{-}OH)(\mu\text{-}CH_3CO_2)_2(tmtacn)_2]^{+}$ **3b** exhibits two separate, reversible one-electron oxidation steps ($Mn^{III}_2/Mn^{II,III}_2/Mn^{II}_2$).[2]

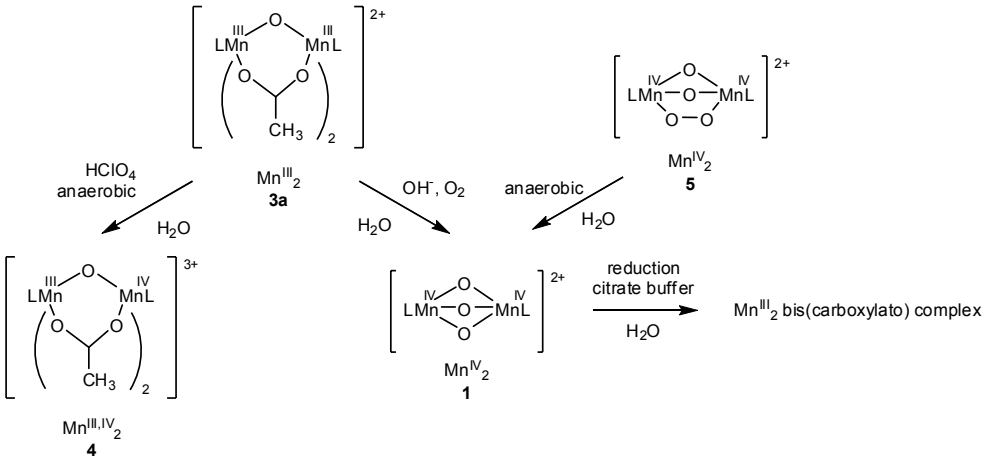

Figure 4.1 Summary of aqueous solution chemistry of Mn-tmtacn complexes, reported by Wieghardt *et al.*[2,10] and Hage *et al.*[11]

While in anaerobic acidic aqueous solution complex **3a** disproportionates to yield $[Mn^{III,IV}_2(\mu\text{-}O)(\mu\text{-}CH_3CO_2)_2(tmtacn)_2]^{3+}$ **4** as the only isolable complex,[1a,2] in alkaline aqueous solution and in the presence of oxygen, complex **3a** is oxidized to form **1** (and trace amounts of MnO_2) (Figure 4.1).[2] Another interesting complex isolated by Wieghardt

and coworkers is the $\mu_{1,2}$-peroxo bridged complex $[Mn^{IV}_2(\mu\text{-}O)_2(\mu\text{-}O_2)(tmtacn)_2]^{2+}$ **5** that releases O_2 in anaerobic aqueous solution upon formation of a Mn^{III}_2 intermediate which in turn forms **1** after a series of disproportionation reactions.[10] Investigation of the complex electrochemical properties of **1** by Hage and coworkers showed by UV-Vis spectroscopy that the *in situ* formation of dinuclear Mn^{III}_2 bis(μ-carboxylato) species upon bulk reduction of **1** in citrate buffer occurred, however, this complex was not isolated.[11]

Mixing equimolar amounts of $[Mn^{III}_2(\mu\text{-}O)(\mu\text{-}CH_3CO_2)_2(tmtacn)_2]^{2+}$ and $[Mn^{III}_2(\mu\text{-}O)(\mu\text{-}CH_3CO_2)_2(tacn)_2]^{2+}$ results in slow formation of the mixed ligand species $[Mn^{III}_2(\mu\text{-}O)(\mu\text{-}CH_3CO_2)_2(tmtacn)(tacn)]^{2+}$ [12] as shown by ^{1}H NMR spectroscopy.[13] The lability of both the μ-oxo and μ-acetato bridges is demonstrated further by the formation of mononuclear complexes of the type $[Mn^{III}(X)_3(tmtacn)]$ (X = N_3^-, Cl^- or NCS^-) when $[Mn^{III}_2(\mu\text{-}O)(CH_3CO_2)(tmtacn)_2]^{2+}$ is in the presence of the corresponding anion in ethanol.[2,14]

In this chapter the preparation and physical properties of bis(trichloroacetato) complexes **2a**-**2d** (Figure 4.2) will be discussed first. Furthermore, the rich solution chemistry of these complexes in CH_3CN will be explored, building upon the work of Wieghardt and coworkers. Finally, the conversion of tris(μ-oxo) complex **1** into bis(carboxylato) complexes such as **2a** will be described.

4.1 Synthesis and characterisation of Mn^{III}_2 bis(μ-carboxylato) complexes

The synthesis of the dinuclear Mn^{III}_2 bis(μ-carboxylato) complexes (**2a**, **3a** and **6**-**27**) was carried out via a net two-electron reduction of **1** (Scheme 4.1). Upon addition of 1.1 equivalents of *L*-ascorbic acid to an aqueous solution of **1** in the presence of two equivalents of the carboxylic acid of interest, the clear red solution darkened immediately and a purple/brown precipitate formed within 30-60 sec due to exchange of two of the bridging μ-oxo ligands by two bridging carboxylato groups. The stability of the Mn^{III}_2 bis(carboxylato) complexes in aqueous solution is dependent on the nature of the acid employed and it is thus important to remove the precipitated complex quickly from the aqueous environment by filtration. Furthermore, for several of the less polar carboxylic acids, the use of a minimal amount of methanol or acetone as co-solvent was required to assure the dissolution of the carboxylic acid prior to addition of *L*-ascorbic acid.

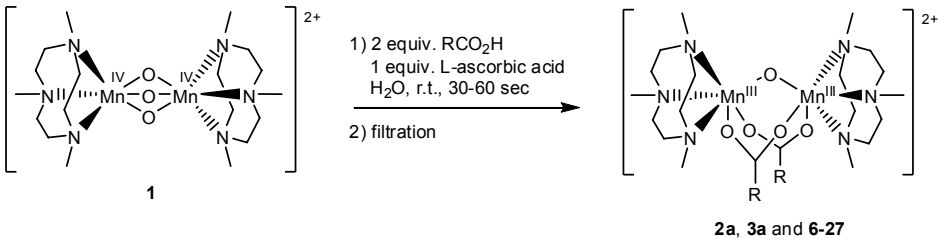

Scheme 4.1 Synthesis of **2a**, **3a** and **6**-**27** from **1** (9-88 % yield).

Crystals suitable for structure determination by single crystal X-ray diffraction of complexes **2a**, **6**, **7** and **8** were grown by slow infusion of ethyl acetate or diethyl ether into

a solution of the respective complexes in CH_3CN (see Figure 4.3 for ORTEP drawings and Appendix B for more details). All four dinuclear complexes show the facial coordination of one tmtacn ligand to each manganese(III) cation. The two manganese centres are bridged by one μ-oxo and two μ-carboxylato ligands.

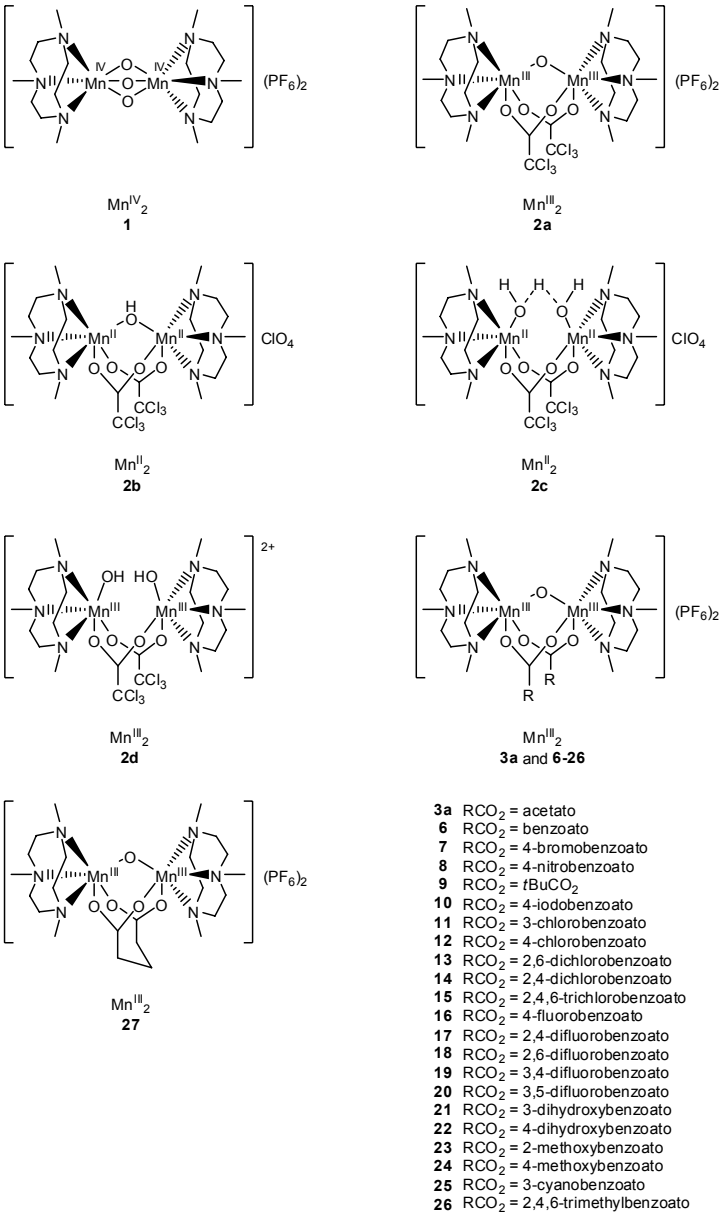

3a RCO_2 = acetato
6 RCO_2 = benzoato
7 RCO_2 = 4-bromobenzoato
8 RCO_2 = 4-nitrobenzoato
9 RCO_2 = *t*$BuCO_2$
10 RCO_2 = 4-iodobenzoato
11 RCO_2 = 3-chlorobenzoato
12 RCO_2 = 4-chlorobenzoato
13 RCO_2 = 2,6-dichlorobenzoato
14 RCO_2 = 2,4-dichlorobenzoato
15 RCO_2 = 2,4,6-trichlorobenzoato
16 RCO_2 = 4-fluorobenzoato
17 RCO_2 = 2,4-difluorobenzoato
18 RCO_2 = 2,6-difluorobenzoato
19 RCO_2 = 3,4-difluorobenzoato
20 RCO_2 = 3,5-difluorobenzoato
21 RCO_2 = 3-dihydroxybenzoato
22 RCO_2 = 4-dihydroxybenzoato
23 RCO_2 = 2-methoxybenzoato
24 RCO_2 = 4-methoxybenzoato
25 RCO_2 = 3-cyanobenzoato
26 RCO_2 = 2,4,6-trimethylbenzoato

Figure 4.2 Complexes **1**-**27**.

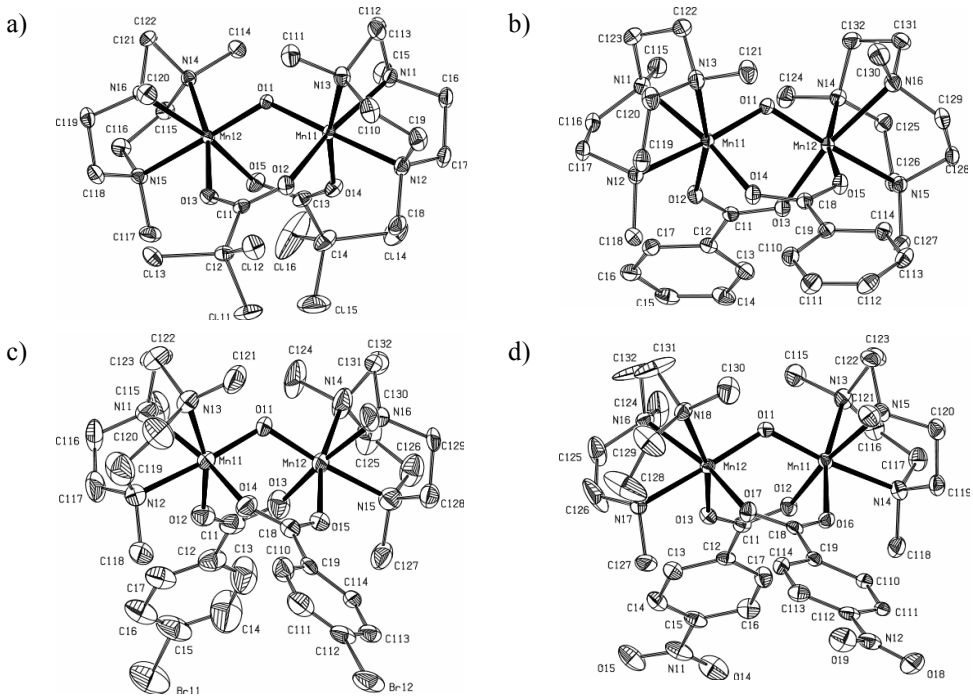

Figure 4.3 ORTEP drawing of a) **2a** (trichloroacetato), b) **6** (benzoato), c) **7** (4-bromobenzoato) and d) **8** (4-nitrobenzoato) complexes (PF_6^- anions omitted for clarity). For details, see Appendix B.

The dinuclear nature of the Mn^{III}_2 bis(μ-carboxylato) complexes is retained in (acetonitrile) solution as shown by ^{1}H NMR, UV-Vis and FT-IR spectroscopy, mass spectrometry and electrochemistry (*vide infra*). ^{1}H NMR spectra of complexes **2a**, **3a** (Figure 4.4b) and **6**-**27** exhibit very large chemical shifts and broad signals similar to those of $[Mn^{III}_2(O)(CH_3CO_2)_2(tmtacn)_2]^{2+}$ **3a**, reported by Hage *et al.*[13] (Figure 4.4a). Electrospray ionisation mass spectrometry (ESI-MS) of the Mn^{III}_2 complexes **2a** and **6**-**27** show both the dication $[Mn^{III}_2(O)(RCO_2)_2(tmtacn)_2]^{2+}$ and the ion pair $[\{Mn^{III}_2(O)(RCO_2)_2(tmtacn)_2\}(PF_6)]^+$ (see Figure 4.5a for the spectrum of **2a**).

It is worth noting, especially in light of the use of mass spectrometry as a mechanistic probe (see Chapter 5), that the magnitude of the voltages applied can have a dramatic effect on the number and type of the species observed.[i] While at low voltages the dinuclear species $[Mn^{III}_2(\mu\text{-}O)(\mu\text{-}CH_3CO_2)_2(tmtacn)_2]^{2+}$ (*m/z* 293.2) and $[\{Mn^{III}_2(\mu\text{-}O)(\mu\text{-}CH_3CO_2)_2$

[i] A second word of caution holds for the presence of additives such as formic or acetic acid. While typically these acids are used to allow for the observation of (the protonated forms of) organic analytes by ESI-MS, in the present case their presence is detrimental to the spectra obtained, since ligand exchange of the carboxylato bridges with formato and/or acetato ligands occurs, resulting in the disappearance of the signal of the bis(μ-carboxylato) complexes under examination.

$(tmtacn)_2\}(PF_6)]^+$ (*m/z* 731.2) are observed, at higher voltages the replacement of these signals by signals of mononuclear species such as $[Mn^{II}(CH_3CO_2)(tmtacn)]^+$ (*m/z* 285.3) is observed (see Figure 4.5b for details).

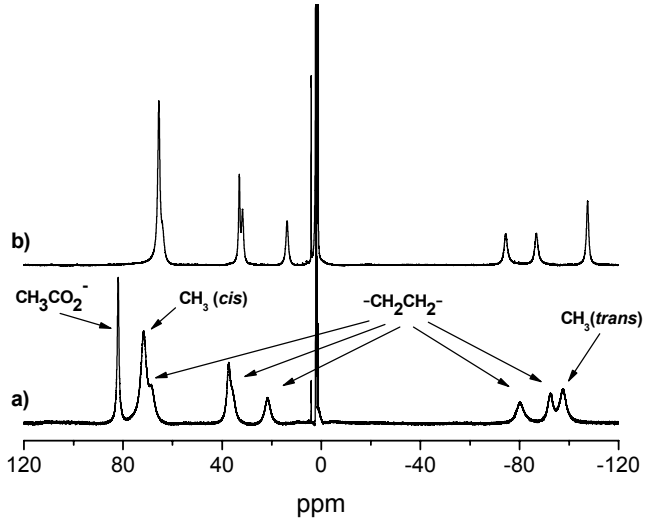

Figure 4.4 ^1H NMR spectra in CD_3CN of a) **3a** (20 mM) and b) **2a** (20 mM). Assignments for **3a** as reported by Hage *et al.*[13]

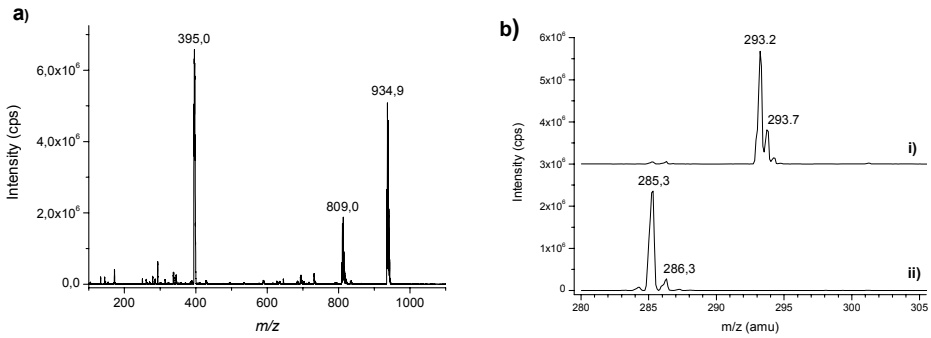

Figure 4.5 a) ESI-MS of **2a** in CH_3CN showing *m/z* 395.0 $[Mn^{III}_2(\mu\text{-}O)(\mu\text{-}CCl_3CO_2)_2(tmtacn)_2]^{2+}$ and 934.9 $[\{Mn^{III}_2(\mu\text{-}O)(\mu\text{-}CCl_3CO_2)_2(tmtacn)_2\}(PF_6)]^+$. The signal at *m/z* 809.0 $[Mn^{II}_2(\mu\text{-}O_2H_3)(\mu\text{-}CCl_3CO_2)_2(tmtacn)_2]^+$ is generated inside the mass spectrometer. b) ESI-MS of **3a** in CH_3CN at i) low voltages (ionspray voltage 5200V, OR +10V, ring +50V, Q0 -3V) showing only the dimer *m/z* 293.2 $[Mn^{III}_2(\mu\text{-}O)(\mu\text{-}CH_3CO_2)_2(tmtacn)_2]^{2+}$ and ii) high voltages (ionspray voltage 5200V, OR +15V, ring +150V, Q0 -5V) showing only monomer *m/z* 285.3 $[Mn^{II}(CH_3CO_2)(tmtacn)]^+$.

The Mn^{III}_2 bis(μ-carboxylato) complexes **2a**, **3a** and **6-27** are ESR silent at 77 K in CH_3CN. UV-Vis spectroscopy shows absorption bands at 485, 530, 725 and 1000 nm for **2a** (Figure 4.6). These bands are typical for the absorption spectrum of $\{Mn^{III}_2(O)(RCO_2)_2\}$ complexes such as **3a**.[6,7,11] The complexes **2a**, **3a** and **6-27** show similar UV-Vis spectra (Figure 4.6). The solid state FT-IR spectrum of **2a** (in KBr) shows a μ-carboxylato bridge absorption at 1659 cm^{-1}, an absorption which is retained upon dissolution in CH_3CN (Figure 4.12 and 4.13, *vide infra*).

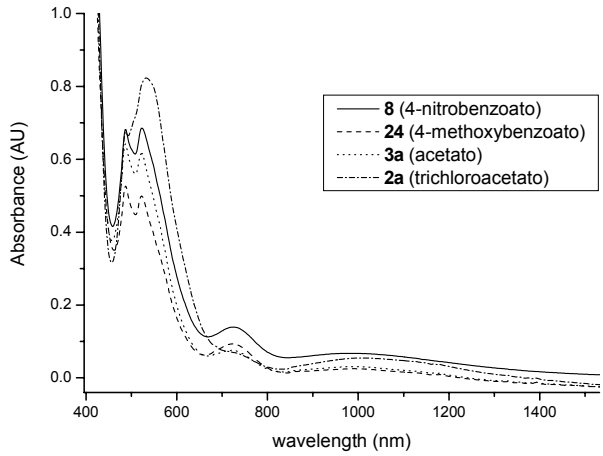

Figure 4.6 UV-Vis spectra of complexes **2a**, **3a**, **8** and **24** (1 mM in CH_3CN).

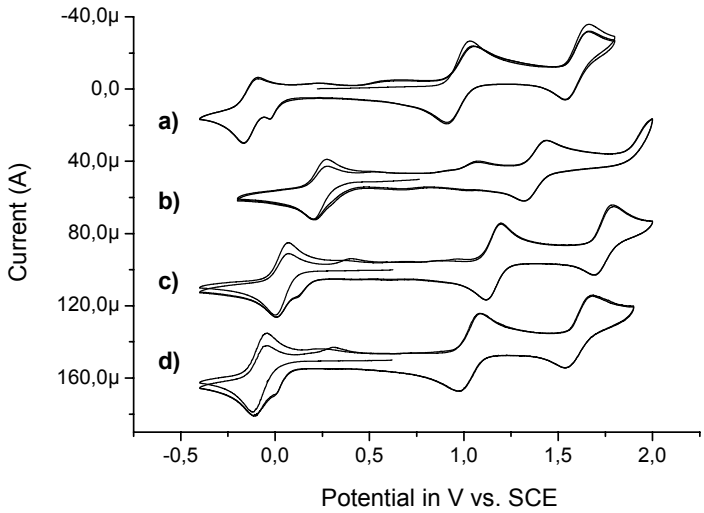

Figure 4.7 Cyclic voltammetry in CH_3CN (0.1 M $TBAPF_6$), scan rate 100 mVs^{-1}, of a) **3a**, b) **2a**, c) 4-nitrobenzoato complex **8** and d) 4-methoxybenzoato complex **24**.

The cyclic voltammetry of **3a** in CH_3CN (Figure 4.7a) is in agreement[ii] with that reported earlier by Wieghardt and coworkers.[2,7] Reversible one-electron reduction of **3a**$\{Mn^{III}_2\}$ to $\{Mn^{II,III}_2\}$ is observed at $E_{½}$ -0.14 V and two separate one-electron oxidations to form the corresponding $\{Mn^{III,IV}_2\}$ and $\{Mn^{IV}_2\}$ species are observed at $E_{½}$ 0.98 and 1.60 V, respectively. Similar processes are observed for **2a** (Figure 4.7b). The anodic shift of both the reduction and oxidation potentials of **2a** compared to **3a** is in accordance with the more electron-withdrawing nature of the μ-trichloroacetato bridges compared with the μ-acetato bridges. Redox data for other $[Mn^{III}_2(O)(RCO_2)_2(tmtacn)_2]^{2+}$ complexes (**6-27**) in CH_3CN (0.1 M $TBAPF_6$) are reported in Table 4.1.

Table 4.1 Redox data for $[Mn_2(\mu\text{-}O)(\mu\text{-}RCO_2)_2(tmtacn)_2]^{n+}$ complexes.[a]

Complex	RCO_2^-	$E_{½}^{II,III-III,III}$	$E_{½}^{III,III-III,IV}$	$E_{½}^{III,IV-IV,IV}$
2a	$CCl_3CO_2^-$	0.26 (70)	1.40 (120)	2.06 ($E_{p,a}$)
3a	$CH_3CO_2^-$	-0.14 (80)	0.98 (120)	1.60 (120)
27	$^-O_2C(CH_2)_3CO_2^-$	-0.25 ($E_{p,c}$)	1.05 (155)	1.73 (230)
9	^{t}Bu-CO_2^-	-0.11 (60)	1.07 (110)	1.74 (120)
6	benzoato	-0.06 (60)	1.06 (90)	1.65 (115)
10	4-iodobenzoato	-0.03 (70)	1.08 (95)	1.67 (130)
7	4-bromobenzoato	-0.03 (70)	1.09 (100)	1.68 (125)
11	3-chlorobenzoato	0.02 (70)	1.15 (110)	1.70 (150)
12	4-chlorobenzoato	-0.07(80)	1.10 (95)	1.69 (125)
13	2,6-dichlorobenzoato	0.08 (70)	1.24 (100)	1.85 (130)
14	2,4-dichlorobenzoato	0.01 (76)	1.16 (100)	1.78 (130)
15	2,4,6-trichlorobenzoato	0.08 (110)	1.25 (170)	1.86 (120)
16	4-fluorobenzoato	-0.04(70)	1.08 (105)	1.67 (140)
17	2,4-difluorobenzoato	-0.02 (75)	1.11 (90)	1.68 (120)
18	2,6-difluorobenzoato	0.01 (90)	1.16 (130)	1.72 (100)
19	3,4-difluorobenzoato	0.00 (60)	1.11 (80)	1.69 (120)
20	3,5-difluorobenzoato	0.01 (75)	1.15 (120)	1.71 (110)
21	3-hydroxybenzoato	-0.07 ($E_{p,c}$)	1.07 (95)	-
22	4-hydroxybenzoato	-0.08 ($E_{p,c}$)	1.01 (130)	-
23	2-methoxybenzoato	-0.12 (70)	1.00 (95)	1.58 (135)
24	4-methoxybenzoato	-0.09 (75)	1.03 (110)	1.61 (135)
8	4-nitrobenzoato	0.03 (65)	1.15 (80)	1.74 (100)
25	3-cyanobenzoato	0.04 (80)	1.17 (99)	1.76 (130)
26	2,4,6-trimethylbenzoato	-0.04 ($E_{p,c}$)	1.19 (173)	-

a) All complexes are 1 mM in CH_3CN (0.1 M $TBAPF_6$), scan rate 100 mVs^{-1}. $E_{½}$ in V vs. SCE ($|E_{p,a}-E_{p,c}|$ in mV). For irreversible processes only $E_{p,c}$ or $E_{p,a}$ is given. All values +/- 10 mV.

[ii] That is, the potentials and assignments of the redox processes of **3a** in CH_3CN are in agreement with those reported by Wieghardt and coworkers (ref. [2] and [6]). However, while Wieghardt *et al.* reported that two-electron reduction of **3a** in CH_3CN in the presence of H_2O resulted in dissociation into two Mn^{II} monomers, it will be shown in sections 4.3 and 4.4 that the $\{Mn^{III}_2(\mu\text{-}O)(RCO_2)_2\}$ complexes retain their dinuclear structure upon reduction in the presence of carboxylic acid and/or water. The irreversibility of the two-electron reduction wave is due to protonation and opening of the μ-oxo bridge, yielding $\{Mn^{III}_2(\mu\text{-}O_2H_3)(RCO_2)_2\}$ species.

4.2 Synthesis and characterisation of Mn^{II}_2 bis(μ-carboxylato) complexes

Complex **2b** was prepared from $Mn(ClO_4)_2.6H_2O$, tmtacn and CCl_3CO_2Na in MeOH under N_2 by the same procedure as reported by Wieghardt *et al.* for the corresponding acetate complex.[2] Crystals suitable for single crystal X-ray diffraction were obtained upon storing the reaction mixture at 6 °C (Figure 4.8). Both manganese(II) centres are each coordinated to a tmtacn ligand. Two μ-trichloroacetato ligands and one μ-hydroxo ligand bridge the dinuclear structure. ESI-MS shows the $[Mn^{II}_2(\mu\text{-}OH)(CCl_3CO_2)_2(tmtacn)_2]^+$ (*m/z* 791.0) cation, thus showing that this structure is retained in CH_3CN solution. The complex does not absorb in the near UV or visible region (Figure 4.9).

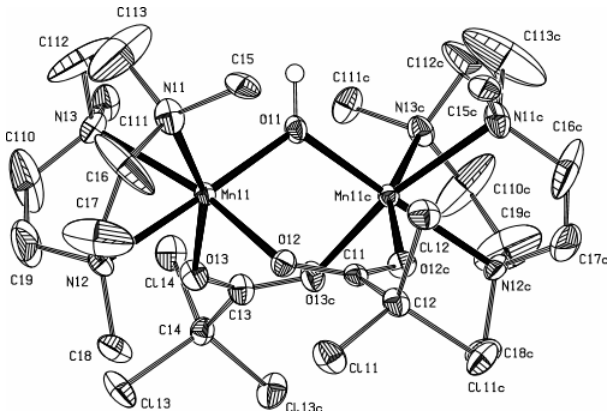

Figure 4.8 ORTEP drawing of **2b**, see Appendix B for selected bond angles etc. (ClO_4^- anion is omitted for clarity).

Complex **2c** was prepared by reduction of **1** with two equivalents of H_2NNH_2 in CH_3CN in the presence of two equivalents of CCl_3CO_2H and was isolated as a white powder. Unfortunately crystals suitable for single crystal X-ray diffraction were not obtained, due to the instability of **2c** in solution. The observation of the $[Mn^{II}_2(\mu\text{-}O_2H_3)(\mu\text{-}CCl_3CO_2)_2(tmtacn)_2]^+$ cation by ESI-MS at *m/z* 808.9 is in agreement with the structure depicted in Figure 4.2 containing a $\mu\text{-}O_2H_3$ bridge.[15] However, it should be noted that ESI-MS on itself is not sufficient proof for this assignment of the $\mu\text{-}O_2H_3$ bridge. The alternative assignment of this signal as a simple H_2O adduct of **2b**, *i.e.* $[\mathbf{2b}.H_2O]^+$, is also conceivable since solvent adducts of (cationic) complexes can be observed readily by ESI-MS. In the following sections, further evidence will be provided that the Mn^{II}_2 complexes **2b** and **2c** contain different non-carboxylato bridges, *i.e.* μ-OH and $\mu\text{-}O_2H_3$ respectively. Magnetic susceptibility measurements indicate that the bridging ligands in **2b** and **2c** are different and both ESR and FT-IR spectroscopy give strong indications for the $\mu\text{-}O_2H_3$ bridging motif upon comparison with similar $\{Zn^{II}_2(\mu\text{-}O_2H_3)\}$ complexes.[18]

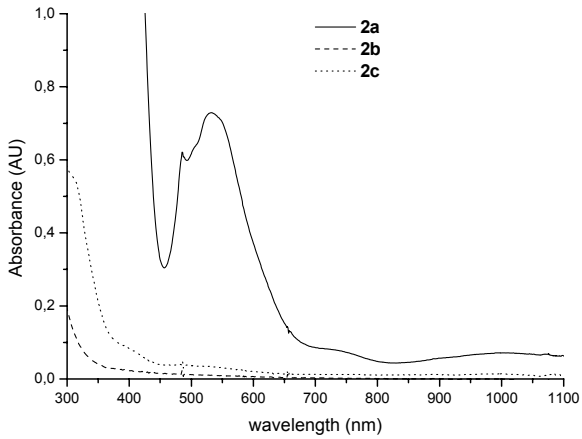

Figure 4.9 UV-Vis spectra of **2a** (solid line), **2b** (dashed line) and **2c** (dotted line)[iii] (1 mM in CH_3CN).

4.2.1 Magnetic susceptibility

At 300 K, the complex **2b** exhibits a $\chi_M T$ value of 6.54 cm^3 K mol^{-1} which is lower than the theoretical value of 8.754 cm^3 K mol^{-1} expected for two high-spin non-interacting manganese(II) ions (S=5/2) (Figure 4.10). The $\chi_M T$ value decreases monotonically with decreasing temperature, behavior which indicates that the two manganese(II) ions experience antiferromagnetic interactions ($J = -16.8$ cm^{-1}, g = 2, R = 3×10^{-5}). These results are very similar to those observed for $[Mn^{II}_2(\mu\text{-}OH)(\mu\text{-}CH_3CO_2)_2(tmtacn)_2]^+$ as reported by Wieghardt and coworkers (J = -18 cm^{-1}, g = 2.00).[2]

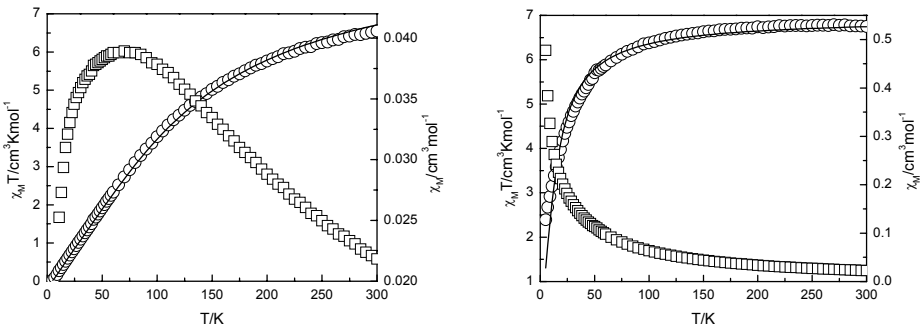

Figure 4.10 Temperature dependence of $\chi_M T$ (circles) and χ_M (squares) for: **2b** (left), J = -16.8 cm^{-1}, g = 2, R = 3×10^{-5} and **2c** (right), J = -2.1 cm^{-1}, g = 2, R = 3×10^{-3}. The solid line in all graphs represents the best fit.

[iii] The absorption seen for **2c** around 530 nm is due to a minor amount of Mn^{III}_2 dimer.

For **2c** at 300 K, the complex exhibits a $\chi_M T$ value of 6.74 cm^3 K mol^{-1}, which is lower than the theoretical value of 8.754 cm^3 K mol^{-1} expected for two S=5/2 non-interacting manganese(II) ions (albeit slightly higher when compared with **2b**) (Figure 4.10). Again, the $\chi_M T$ value decreases monotonically with decreasing temperature, indicating the presence of antiferromagnetic interactions ($J = -2.1$ cm^{-1}, g = 2, R = 3×10^{-3}). For **2c**, the antiferromagnetic exchange coupling between the two manganese(II) ions is considerably smaller than the antiferromagnetic exchange coupling observed for the complex **2b**, thus suggesting that the μ-hydroxo bridge is primarily responsible for the magnetic interaction, rather than the μ-carboxylato bridges.

4.2.2 ESR

The ESR spectra of both **2b** and **2c** in CH_3CN (at 77 K, Figure 4.11) are characterized by broad features at g ~ 2, which do not show discernible hyperfine splitting. The spectrum of **2c** itself in CH_3CN is unaffected by addition of CCl_3CO_2H (Figure 4.11b i and iii). While broad signals are observed for **2c** in CH_3CN, the appearance of a distinct hyperfine-coupling pattern (a = 45 G) is observed upon addition of cyclooctene in the presence of CCl_3CO_2H (Figure 4.11b iv), although the overall shape and intensity of the spectrum is not affected.
Addition of 10 equiv. of CCl_3CO_2H (10 mM) to **2b** (1 mM, Figure 4.11a i and iii) results in the appearance of a spectrum identical to that of **2c**[iv] and subsequent addition of cyclooctene (1 M) results in the appearance of a distinct[16] hyperfine splitting (a = 45 G). The observation of a solvent polarity dependence on the resolution of the hyperfine structure for **2c** is in agreement with the assignment of a μ-O_2H_3 bridging unit being present.

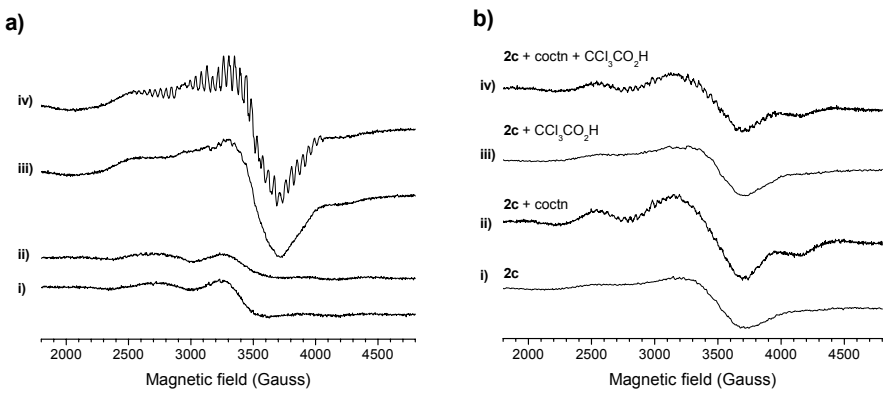

Figure 4.11 X-band ESR spectra at 77 K in CH_3CN. a) complex **2b** (1 mM) in the presence of 1,2-dichlorobenzene (0.5 M) i) with and ii) without cyclooctene (1 M). iii) **2b** and CCl_3CO_2H (10 mM) and iv) **2b** in the presence of cyclooctene (1 M) and CCl_3CO_2H (10 mM). b) **2c** (1 mM) i) with and ii) without cyclooctene (1 M). iii) **2c** with CCl_3CO_2H (10 mM), iv) **2c** with CCl_3CO_2H (10 mM) and cyclooctene (1 M).

[iv] The quantitative conversion of **2b** to **2c** upon addition of CCl_3CO_2H was observed by cyclic voltammetry as well, see section 4.3.1.

4.2.3 FT-IR spectroscopy

In the solid state a sharp absorption at 3620 cm^{-1}, assigned to the μ-OH bridge, is observed in the spectrum of **2b** (Figure 4.12). The μ-OH absorption band corresponds to that of the related $[Mn^{II}_2(\mu\text{-}OH)(\mu\text{-}CH_3CO_2)_2(tmtacn)_2]^+$ complex (3520 cm^{-1})[2] and, for example, dinuclear $Zn^{II}_2(\mu\text{-}OH)$ complexes (3618 cm^{-1}).[17] Complex **2c** on the other hand, exhibits a set of three broad absorption bands at 3593, 3433 and 3251 cm^{-1} assigned to a $\mu\text{-}O_2H_3$ bridge, based upon comparison with dinuclear $\{Zn^{II}_2(\mu\text{-}O_2H_3)\}$ complexes.[18]

The μ-carboxylato absorptions (Figure 4.12) of **2b** and **2c** (1692 and 1695 cm^{-1}, respectively) are similar to that of **2a** (1659 cm^{-1}). The absorptions assigned to the $CCl_3CO_2^-$ moieties of **2a** and **2b** are blue shifted significantly (80-90 cm^{-1}) from the corresponding $CH_3CO_2^-$ bridged complexes (1570 and 1615 cm^{-1}, respectively).[2,19] Both **2b** (1 mM, Figure 4.13) and **2c** (data not shown) show a strong absorption at 1695 cm^{-1} in CH_3CN solution, identical to that observed in their solid state spectra. Similarly, for **2a** the absorption at 1659 cm^{-1} is retained in CH_3CN solution (Figure 4.13).

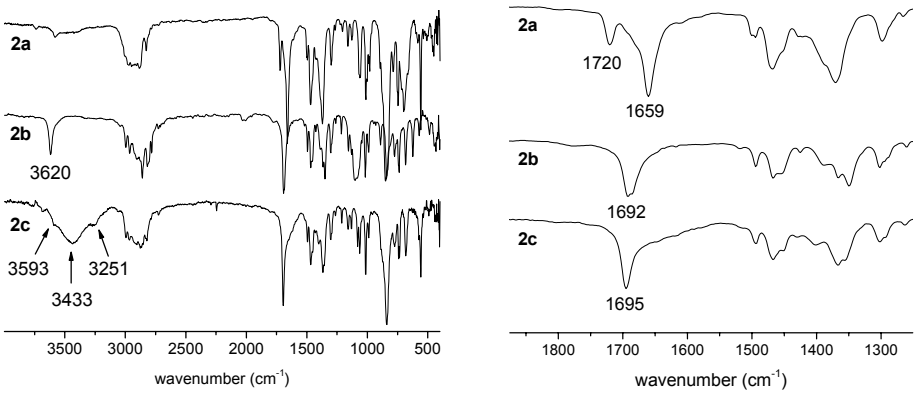

Figure 4.12 Solid state FT-IR spectra (in KBr powder) of **2a**, **2b** and **2c**.

Addition of CCl_3CO_2H (10 equiv.) to a solution of **2b** in CH_3CN results in the disappearance of the absorption band at 1695 cm^{-1} and the appearance of a strong absorption band at 1720 cm^{-1} (Figure 4.13 i and ii). Addition of D_2O results in the partial recovery of the absorption band at 1695 cm^{-1} (Figure 4.13 v). The carboxylato vibrations of the tris(carboxylato) bridged complex $[Mn^{II}_2(\mu\text{-}CH_3CO_2)_3(tmtacn)_2]^+$, reported by Wieghardt *et al.* at 1636 cm^{-1}, are at higher energy than for the corresponding bis(carboxylato) complex $[Mn^{II}_2(\mu\text{-}OH)(\mu\text{-}CH_3CO_2)_2(tmtacn)_2]^+$ (1615 cm^{-1}).[2] This supports the assignment of the absorption at 1720 cm^{-1} as being due to the tris(carboxylato) complex $[Mn^{II}_2(\mu\text{-}CCl_3CO_2)_3(tmtacn)_2]^+$, formation of which is suppressed by addition of water. Thus, bis(carboxylato) complex **2c** is in equilibrium with the tris(carboxylato) complex

$[Mn^{II}_2(\mu\text{-}CCl_3CO_2)_3(tmtacn)_2]^+$ in the presence of excess CCl_3CO_2H;[v] however, the presence of water favours the formation of the corresponding bis(carboxylato) complex, *i.e.* **2c**.

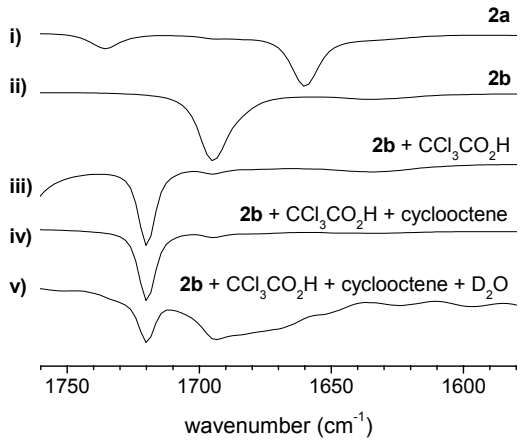

Figure 4.13 FT-IR spectra (solvent substracted) in CH_3CN of i) **2a** (1 mM), ii) **2b** (1 mM), iii) **2b** (1 mM) with CCl_3CO_2H (10 mM), iv) **2b** (1 mM) with CCl_3CO_2H (10 mM) and cyclooctene (1 M) and v) as for iv) except with 5% D_2O.

4.3 Electrochemical properties of 2a-d

4.3.1 Cyclic voltammetry of 2a

The cyclic voltammetry of **2a** in CH_3CN shows three redox waves. Scanning cathodically from the open circuit potential (OCP) reveals a reversible one-electron reduction of **2a** $\{Mn^{III}_2(\mu\text{-}O)\}$ to form the corresponding $\{Mn^{II,III}_2(\mu\text{-}O)\}$ complex at $E_{½}$ 0.26 V (Figure 4.14). Anodically two redox processes are observed. The reversible one-electron oxidation at $E_{½}$ 1.40 V forms $Mn^{III,IV}_2$ and at higher potential an irreversible one-electron oxidation to Mn^{IV}_2 is observed at $E_{p,a}$ 2.06 V. The effect of addition of 10 equiv. of CCl_3CO_2H on the anodic process of **2a** is minimal (Figure 4.14); however, the reversible one-electron reduction ($Mn^{III}_2/Mn^{II,III}_2$) changes to an irreversible two-electron reduction ($E_{p,c}$ 0.29 V). The return wave of this latter process occurs at $E_{p,a}$ 1.10 V, and this process in turn has a return wave at $E_{p,c}$ 0.74 V (see Figure 4.14 for scans over a narrower potential window). Both the irreversibility of the reduction at $E_{p,c}$ 0.29 V and the occurrence of the new redox waves at $E_{p,a}$ 1.10 V and $E_{p,c}$ 0.74 V indicates that the complex undergoes a

[v] For example, the corresponding complex $[Mn^{II}_2(\mu\text{-2,6-dichlorobenzoato})_3(tmtacn)_2]^+$ (*m/z* 1019) has been observed by ESI-MS in the presence of 10 equiv. of 2,6-dichlorobenzoic acid and cyclooctene (data not shown).

structural change upon change of the oxidation state of the manganese centres. Assignment of these redox-driven structural changes is aided considerably by examination of the electrochemical properties of both **2b** and **2c**.

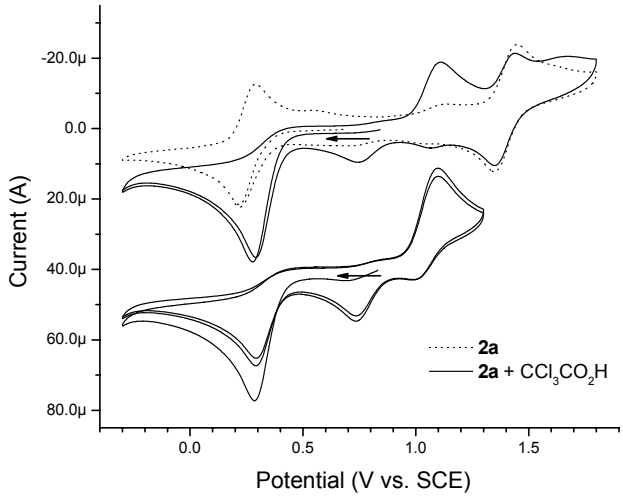

Figure 4.14 Cyclic voltammetry (100 mV s^{-1}) of **2a** (1 mM) in CH_3CN (0.1 M $TBAPF_6$), in the absence (dotted lines) and presence (solid lines) of CCl_3CO_2H (10 mM) and (below) over a narrower potential window (offset for clarity).

Table 4.2 Redox data for **2a-c** (1 mM) in CH_3CN (0.1 M $TBAPF_6$).[a]

Starting complex	$E_{p,c}^{II,II-III,III}$	$E_{p,a}^{II,II-III,III}$	$E_{½}^{II,II-II,III}$	$E_{½}^{II,III-III,III}$	$E_{½}^{III,III-III,IV}$
without CCl_3CO_2H					
2a				0.26 (70)	1.40 (100)
2b			0.53 (100)		
2c	0.30, 0.54, 0.76	1.11			
with CCl_3CO_2H[b]					
2a	0.29 and 0.74[c]	1.10			1.40 (90)
2b	0.17 and 0.72[c]	1.08			
2c	0.75	1.09			1.63 ($E_{p,a}$)

a) All values +/- 10 mV. $E_{½}$, $E_{p,c}$ and $E_{p,a}$ in V vs. SCE, $|E_{p,a}-E_{p,c}|$ between parentheses (in mV). b) 10 mM c) Assigned to **2d**.

4.3.2 Cyclic voltammetry of 2c

For **2c** $\{Mn^{II}_2(\mu\text{-}O_2H_3)\}$ oxidation is observed at $E_{p,a}$ 1.11 V in the absence of CCl_3CO_2H (Figure 4.15). The three return waves observed correspond to further chemical reaction of the $\{Mn^{III}_2(\mu\text{-}O_2H_3)\}$ complex formed upon oxidation, including formation of **2a** ($E_{p,c}$ 0.30 V). In the presence of 10 equiv. of CCl_3CO_2H, the $\{Mn^{II}_2(\mu\text{-}O_2H_3)\}$ to

$\{Mn^{III}_2(\mu\text{-}O_2H_3)\}$ two-electron oxidation remains unchanged; however, only a single return wave is observed: a two-electron reduction of Mn^{III}_2 to Mn^{II}_2 at $E_{p,c}$ 0.75 V. This wave is assigned to the deprotonated form of the complex, *i.e.* **2d** $\{Mn^{III}_2(\mu\text{-}OH)_2\}$, since the cathodic shift of over 300 mV implies that the species responsible for the return at $E_{p,c}$ 0.75 V is not $\{Mn^{III}_2(\mu\text{-}O_2H_3)\}$ itself,[20] but its deprotonated form since it occurs at a more negative potential.

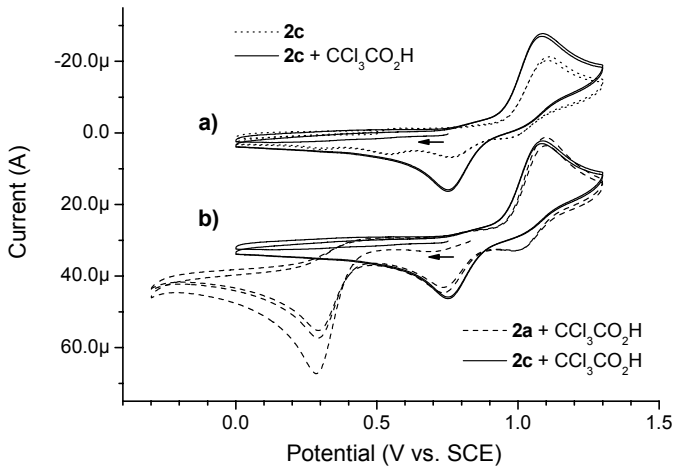

Figure 4.15 Cyclic voltammetry (100 mV s^{-1}) in CH_3CN (0.1 M $TBAPF_6$). a) **2c** (1 mM) in the absence (dotted lines) and presence (solid lines) of CCl_3CO_2H (10 mM). b) **2c** (solid lines) and **2a** (dashed lines) with CCl_3CO_2H (10 mM) (offset for clarity).

4.3.3 Cyclic voltammetry of 2b

For **2b** $\{Mn^{II}_2(\mu\text{-}OH)\}$ in the absence of CCl_3CO_2H, a reversible one-electron oxidation to $\{Mn^{II,III}_2(OH)\}$ is observed at $E_{½}$ 0.53 V. Addition of 10 equiv. of CCl_3CO_2H results in a dramatic change to the cyclic voltammetry of **2b** (Figure 4.16) with behavior identical to that observed for **2c** $\{Mn^{II}_2(\mu\text{-}O_2H_3)\}$ in the presence of CCl_3CO_2H (Figure 4.15). In the presence of 10 equiv. of CCl_3CO_2H the one-electron oxidation at $E_{½}$ 0.53 V from **2b** is replaced by an irreversible two-electron oxidation at $E_{p,a}$ 1.08 V (assigned to **2c**). Thus, in the presence of CCl_3CO_2H, **2b** $\{Mn^{II}_2(\mu\text{-}OH)\}$ is converted quantitatively to **2c** $\{Mn^{II}_2(\mu\text{-}O_2H_3)\}$.

Comparison of the cyclic voltammetry of **2a**, **2b**, and **2c** in the presence of 10 equiv. of CCl_3CO_2H reveals remarkable similarities (Figures 4.14, 4.16 and 4.15, respectively) and allows for assignment of the structural changes that **2a** undergoes in the presence of CCl_3CO_2H (Figure 4.14). However, the relative number of electrons involved in the different processes, which follow the two-electron reduction of **2a** in the presence of 10 equiv. of CCl_3CO_2H (Mn^{III}_2 to Mn^{II}_2) is unclear when examined by diffusion controlled cyclic voltammetry as displayed in Figure 4.14. Therefore, cyclic voltammetry of **2a** in the presence of CCl_3CO_2H was applied under thin layer conditions, in order to 'trap' the

electrochemically generated species close to the working electrode (Figure 4.17). From the peak current of the return wave ($E_{p,a}$ 1.17 V) observed after reduction ($E_{p,c}$ 0.26 V) of **2a** {Mn^{III}_2(μ-O)}, it is clear that the return process is a two-electron process (Mn^{II}_2 to Mn^{III}_2) also. The species generated by this oxidation (**2d**) is itself reduced again at $E_{p,c}$ 0.73 V (Mn^{III}_2 to Mn^{II}_2) yielding a series of three EC processes.

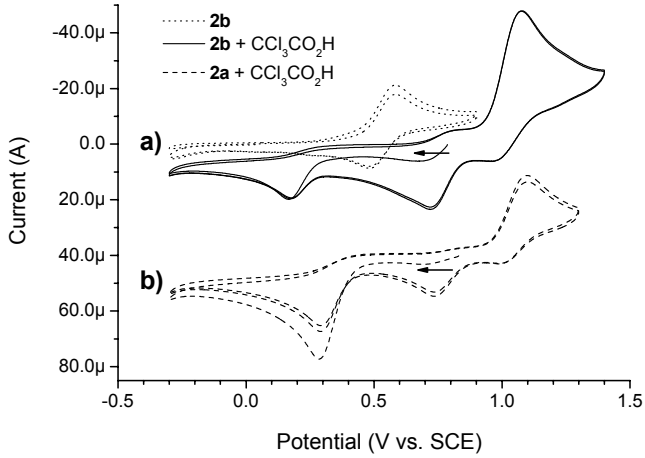

Figure 4.16 Cyclic voltammetry (100 mV s^{-1}) in CH_3CN (0.1 M $TBAPF_6$). a) **2b** (1 mM) in the absence (dotted line) and presence (solid line) of CCl_3CO_2H (10 mM). b) **2a** (dashed line) with CCl_3CO_2H (10 mM).

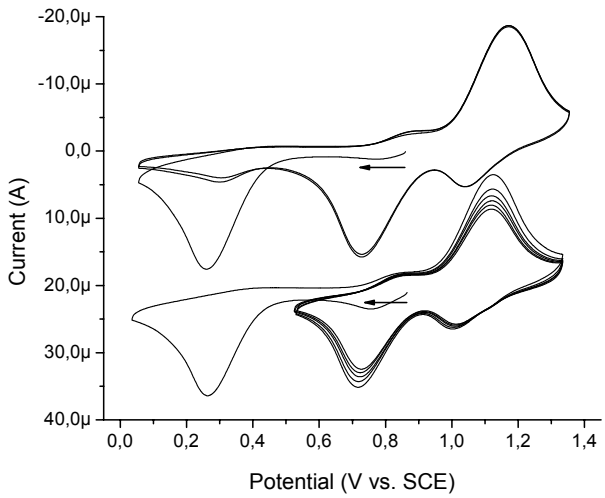

Figure 4.17 Cyclic voltammetry (100 mV s^{-1}) of **2a** (1 mM) in CH_3CN (0.1 M $TBAPF_6$), in presence of CCl_3CO_2H (10 mM) under thin layer conditions (lower graph offset for clarity).

Addition of one equivalent of CCl_3CO_2H to **2a** was found to be sufficient to render the reduction of **2a** $\{Mn^{III}_2(O)\}$ irreversible, indicating that the process is a $2e^-/1H^+$ coupled process. The bielectronic nature of the reduction wave, apparent from its intensity relative to the $Mn^{III}_2/Mn^{III,IV}_2$ oxidation waves, may be misleading in that the initial reduction is H^+/e^- coupled followed by a structural change and a subsequent one-electron reduction. It should be noted that for **2b** the $Mn^{II,III}_2$ reduction is 240 mV more anodic than for **2a** (in the presence of CCl_3CO_2H). Hence, the (overall) two-electron reduction of **2a** under acidic conditions may be described more accurately by an ECE mechanism, *i.e.* one-electron reduction of **2a** is coupled with protonation of the μ-oxo bridge which is followed by a second one-electron reduction.

4.3.4 Influence of [CCl_3CO_2H] and [H_2O] on the non-carboxylato bridging ligand

Overall the electrochemistry of **2a** in the presence of 10 equiv. of CCl_3CO_2H is not affected by a further increase in CCl_3CO_2H concentration (up to 250 equiv.); however, several minor changes are observed (Figure 4.18). Whereas in the absence of CCl_3CO_2H acid for **2a** redox processes are not observed between 0.4 and 1.2 V, in the presence of increasing amounts of CCl_3CO_2H acid, the concentration of **2d** increases ($E_{p,c}$ 0.7 V). Concomitantly, the intensity of the reduction wave of **2a** at $E_{p,c}$ 0.29 V decreases. This indicates that at higher acid concentrations, an equilibrium between **2a** and **2d** changes in favor of the latter. Likewise, the effect of H_2O addition was investigated. For **2a**, in the presence of 10 equiv. of CCl_3CO_2H, an increase of the concentration of H_2O has a similar effect as an increase of the concentration of CCl_3CO_2H (Figure 4.18), confirming that the equilibrium is not dominated by $[H^+]$ but rather by the presence of water required to effect opening of the μ-oxo bridge of **2a** to form **2d**.

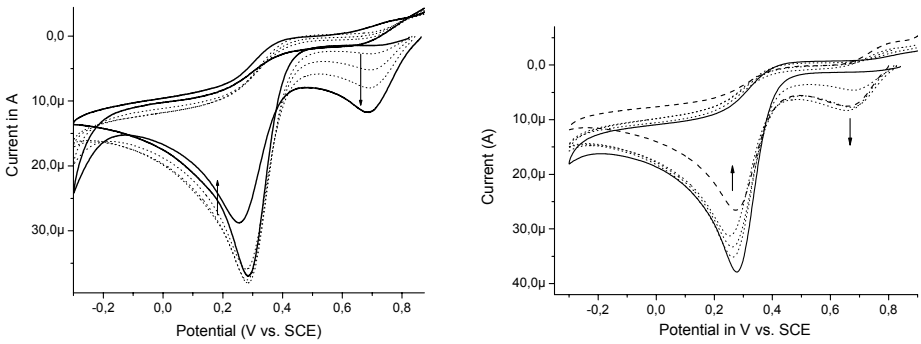

Figure 4.18 Cyclic voltammetry (100 mV s^{-1}) of **2a** (1 mM) in CH_3CN (0.1 M $TBAPF_6$). a) presence of 1 mM (thick line), 5, 10, 50 mM (dotted lines) and 250 mM (thin line) CCl_3CO_2H. and b) in the presence of 0 mM (thick line), 5, 10, 50 mM (dotted lines) and 500 mM (dashed line) H_2O. Initial scan direction is cathodic beginning at OCP.

4.3.5 Interaction of 2a-d with H_2O_2.

The cyclic voltammetry of **2a** in the presence of H_2O_2 is depicted in Figure 4.19. Upon addition of H_2O_2, the irreversible two-electron reduction of **2a** is unaffected ($E_{p,c}$ 0.29 V). However, addition of H_2O_2 renders the oxidation of **2c** ($E_{p,a}$ 1.10 V) completely irreversible, *i.e.* the return reduction steps are no longer observed at $E_{p,c}$ 0.99 and 0.71 V. In addition a new irreversible oxidation wave at $E_{p,a}$ 1.00 V is observed, which remains until all H_2O_2 has been consumed. It is reasonable to conclude that this new redox wave is due to ligand exchange of H_2O with H_2O_2 for complex **2c** (an equilibrium, which would benefit from the increased ligand lability[21] expected for a Mn^{II}_2 complex compared with Mn^{III}_2). However, the new oxidation wave is not electrocatalytic in nature, *i.e.* its intensity is not influenced significantly by the presence of excess of H_2O_2 (50 equiv.). The irreversible oxidation of this new species to a Mn^{III}_2 state results in formation of **2a** rather than **2d**. Indeed it is apparent that complex **2d** reacts with H_2O_2 very rapidly, in stark contrast to **2a**, which is largely unaffected by even a 50 fold excess of H_2O_2. The stability of **2a** in the presence of H_2O_2 indicates that the interaction of **2a** with H_2O_2 is a kinetically slow process.

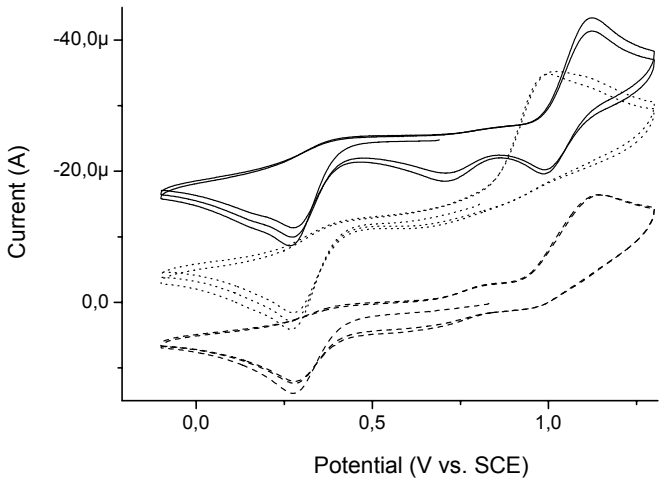

Figure 4.19 Cyclic voltammetry (100 mV s^{-1}) in CH_3CN (0.1 M $TBAPF_6$). Complex **2a** (1 mM) with CCl_3CO_2H (10 mM) prior to (upper/solid line), after (ca. 30 s, middle/dotted line) addition of H_2O_2 (50 equiv. w.r.t. **2a**), and 20 min after (lower/dashed line).

4.4 Formation of $[Mn^{III}_2(O)(RCO_2)_2(tmtacn)_2]^{2+}$ complexes from $[Mn^{IV}_2(O)_3(tmtacn)_2]^{2+}$

4.4.1 Electrochemical reduction in the presence of trichloroacetic acid

As reported previously by Hage *et al.*,[11] in CH_3CN complex **1** exhibits a chemically irreversible reduction at $E_{p,c}$ -0.61 V (vs. SCE, Figure 4.20). However, in the presence of acid (either inorganic acids such as sulphuric acid[11] or HPF_6 or carboxylic acids such as CCl_3CO_2H) one of the μ-oxo bridges of **1** is protonated.[11] This protonation results in an anodic shift of 600 mV (Figure 4.20). In the presence of a carboxylic acid, the new return waves indicate that the chemical changes in complex **1** result in the formation of bis(μ-carboxylato) species (*e.g.* the processes at $E_{p,a}$ 1.10 and $E_{p,c}$ 0.74 V, Figure 4.20, solid line). Bulk reduction of **1** in the presence of 10 equiv. CCl_3CO_2H or CH_3CO_2H was followed by both cyclic voltammetry, UV-Vis and ESR spectroscopy.

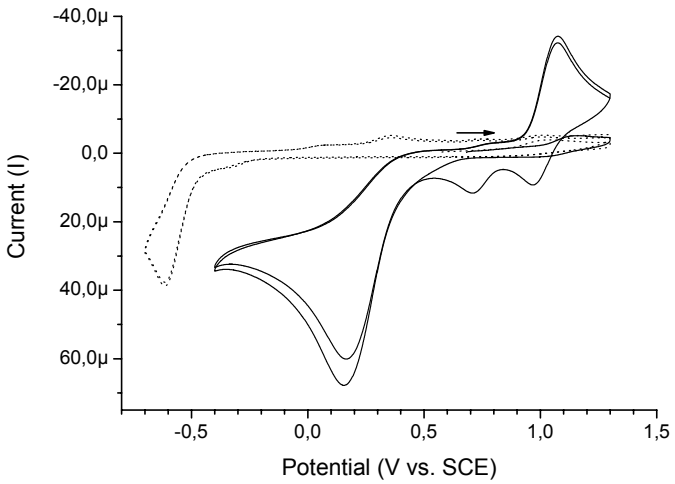

Figure 4.20 Cyclic voltammetry in CH_3CN (0.1 M $TBAPF_6$), scan rate 100 mVs^{-1}. **1** (mM) in the absence (dotted line) and presence of CCl_3CO_2H (10 mM) (solid line).

Comparision between the cyclic voltammetry before and after addition of CCl_3CO_2H indicates that the initial reduction of $H\mathbf{1}^+$ becomes a four electron process[vi] (Figure 4.20). Bulk electrochemical reduction of **1** in the presence of 10 equiv. of CCl_3CO_2H at -0.2 V

[vi] As estimated from the area of the cathodic wave in the presence of CCl_3CO_2H ($E_{p,c}$ 0.15 V), relative to the area of the cathodic wave in the absence of CCl_3CO_2H ($E_{p,c}$ -0.61 V) (Figure 4.20) and assumes no change in diffusion coefficients. Coulometry was not practical due to H_2 evolution at the counter electrode which in turn affects the pH of the solution.

results in the formation of **2c**. This assignment is based upon UV-Vis spectroscopy (Figure 4.21a) and cyclic voltammetry (Figure 4.21b) by comparison with a sample synthesised independently (Figure 4.14-4.16). Subsequent bulk oxidation at 1.10 V results in the formation **2d** (Figure 4.21).

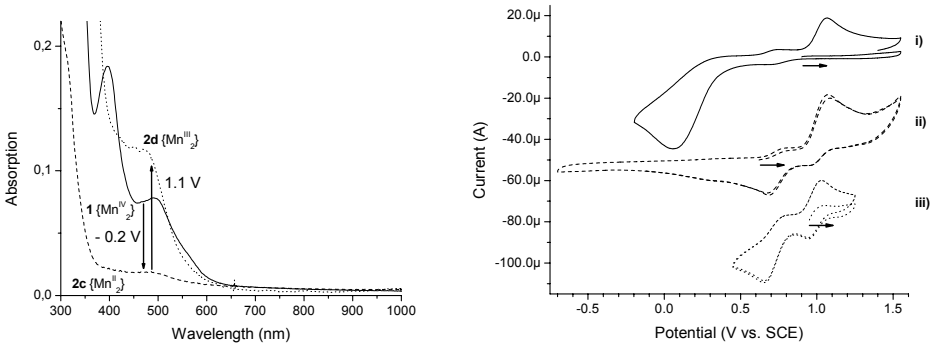

Figure 4.21 a) UV.Vis spectroscopy of **1** (1 mM) in the presence of CCl_3CO_2H (10 mM) in CH_3CN (0.1 M KPF_6) before (solid line), after bulk reduction at -0.2 V (dashed line) and after bulk reoxidation at 1.10 V (dotted line). b) Cyclic voltammetry (0.1 V s^{-1}) of **1** (1 mM) in the presence of CCl_3CO_2H (10 mM) in CH_3CN (0.1 M KPF_6) i) before and ii) after bulk reduction at -0.2 V and iii) after reoxidation at 1.10 V, initial scan direction anodic starting from OCP as indicated by the arrows.

4.4.2 Electrochemical reduction in the presence of acetic acid

When the bulk electrolysis of **1** is performed in the presence of 10 equiv. of CH_3CO_2H, in place of CCl_3CO_2H, similar changes are observed. However, upon bulk oxidation (at 0.76 V) of the Mn^{II}_2 complex formed initially (*i.e.* the μ-acetato equivalent of **2c**) the μ-oxo bridged dinuclear complex **3a** $\{Mn^{III}_2(\mu\text{-}O)\}$ is obtained and not the μ-acetato analogue of **2d** $\{Mn^{III}_2(OH)_2\}$ apparent from the reduction at $E_{p,c}$ -0.17 V (Figure 4.22).

Bulk reduction at -0.3 V of **3a** (1 mM) in CH_3CN (in the presence of CH_3CO_2H, 10 mM) resulted in the formation of the corresponding $\{Mn^{II}_2(\mu\text{-}O_2H_3)(\mu\text{-}CH_3CO_2)_2\}$ species, analoguous to **2c** (Figure 4.23 i). Wieghardt *et al.*[2,6] have reported the irreversibility of the two-electron reduction of **3a**, which was observed in the presence of H_2O and this irreversibility was thought to be due to dissociation of the resulting Mn^{II}_2 dimer into two Mn^{II} monomers. However, the ESR spectrum after bulk reduction of **3a** shows that the dinuclear structure of the Mn^{II}_2 complex remains essentially intact. Instead, the reduction is accompanied with protonation and subsequent opening of the μ-oxo bridge by water, resulting in the formation of the corresponding $\{Mn^{II}_2(\mu\text{-}O_2H_3)(CH_3CO_2)_2\}$ complex, *i.e.* the bis(acetato) variant of **2c**.

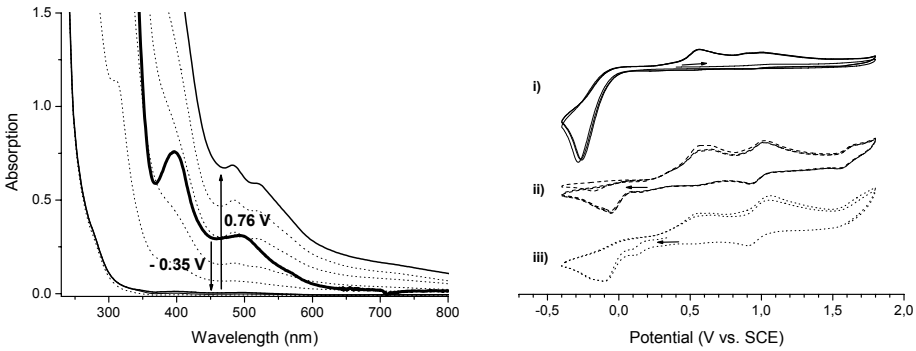

Figure 4.22 a) UV.Vis spectra of 1 (1 mM) with CH_3CO_2H (10 mM) in CH_3CN (0.1 M KPF_6) before (thick solid line) and after (lower solid line) bulk reduction at -0.35 V, and after bulk reoxidation at 0.76 V (upper solid line). b) Cyclic voltammetry (0.1 Vs^{-1}) of 1 (1 mM) with CH_3CO_2H (10 mM), i) before (black line) and ii) after bulk reduction at -0.35 V (blue line) and iii) after reoxidation at 0.76 V (red line) initial scan direction cathodic from OCP.

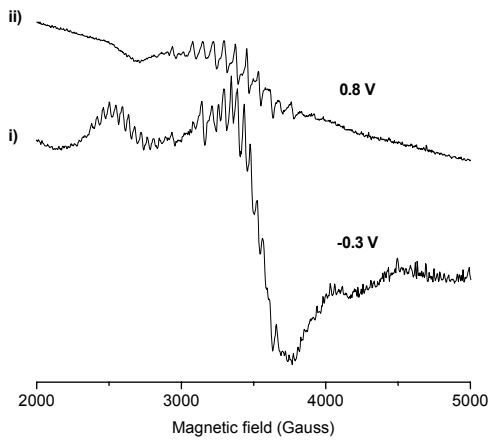

Figure 4.23 X-band ESR spectra of **3a** (1 mM) in CH_3CN (0.1 M $TBAPF_6$) i) after bulk reduction at -0.3 V and ii) followed by reoxidation at 0.8 V.

4.4.3 Chemical reduction

In addition to electrochemical reduction, chemical reduction of **1** in the presence of carboxylic acids can be achieved with various reductants as well, for example by H_2O_2, H_2NNH_2 or, as was already mentioned during the description of the synthesis of complexes **2a** and **6-27** (section 4.1), by L-ascorbic acid.

Strong acids such as $HClO_4$ or H_2SO_4 are known to protonate complex **1** in CH_3CN solution, as can be observed by UV-Vis spectroscopy.[8,11] Similarly, addition of 10 equiv. of HPF_6 or CCl_3CO_2H to **1** in CH_3CN results in (partial) protonation.

When H_2O_2 is added to a solution of **1** in CH_3CN, catalase activity is observed. However, in the presence of acid, this catalase activity is suppressed. Moreover, when H_2O_2 is added to a solution of **1** in the presence of 10 equiv. of CCl_3CO_2H, complete conversion of **1** is observed together with the formation of **2a** (Figure 4.24a). A lag period is found for this conversion to **2a**, together with a sigmoidal shape in the kinetics of the conversion (Figure 4.24b). The kinetics of the formation of **2a** from **1** suggest an autocatalytic process.[vii] When the corresponding sodium salt (*i.e.* CCl_3CO_2Na) was employed instead of CCl_3CO_2H, catalase activity was noticeable and the formation of **2a** was not observed.

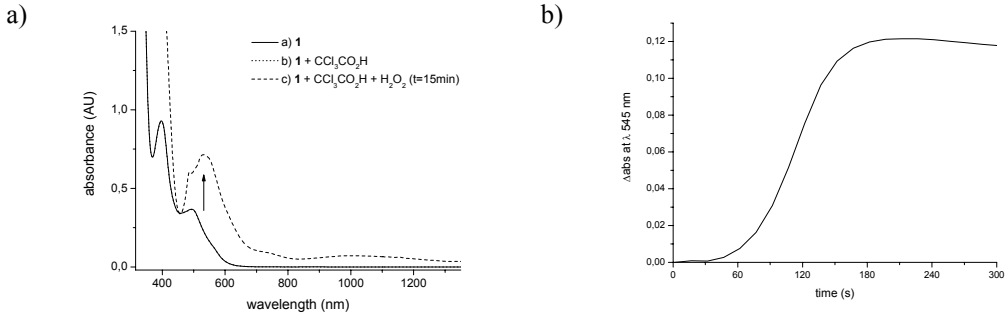

Figure 4.24 a) UV-Vis of i) **1** (1 mM), ii) **1** (1 mM) and CCl_3CO_2H (10 mM) and iii) same as (ii) after 15 min of adding H_2O_2 (53 equiv.). b) formation of **2a** from **1** followed at 545 nm.

Although both **1**[22] and **2a** are ESR silent, the reduction of **1** to **2a** by H_2O_2 was followed by ESR spectroscopy over a series of concentrations of CCl_3CO_2H (Figure 4.25a). In the absence of CCl_3CO_2H no signals were observed. However, in the presence of 1 equivalent of CCl_3CO_2H, a weak 16-line signal (A = 76 G) is observed, which is attributed to the presence of the mixed valent complex $[Mn^{III,IV}_2(\mu\text{-}O)_2(\mu\text{-}CCl_3CO_2)(tmtacn)_2]^{2+}$ based upon comparison with the complex $[Mn^{III,IV}_2(\mu\text{-}O)_2(\mu\text{-}CH_3CO_2)(TMEM\text{-}2)]^{2+}$. At higher concentrations of CCl_3CO_2H (2-250 equiv.), a weak 6-line signal (A = 100 G) was observed, with its intensity increasing with increasing concentration of CCl_3CO_2H. This signal is assigned to a minor amount[viii] of mononuclear $[Mn^{II}(CCl_3CO_2)_3]^-$, which is formed

[vii] The conversion of **1** into **2a** proceeds via a complex set of (ligand exchange and redox) reactions which is not understood fully and most likely involves a number of (carboxylato bridged) intermediates. It is apparent that one of these intermediates is capable of reducing H**1**$^+$, resulting in the (auto)catalytic chemistry involved.

[viii] It should be noted that the amount of free Mn^{II} formed is minor as judged by comparison with $Mn^{II}(ClO_4)_2/CCl_3CO_2H$ (Figure 4.25b). Moreover, following the formation of **2a** from **1** in the presence of 10 equiv. of CCl_3CO_2H by UV-Vis spectroscopy has revealed that at least 90% of the manganese can be accounted for in the form of the dinuclear complex **2a** (Figure 5.1).

as a result of dissociation of the tmtacn ligand. This assignment was confirmed by comparison with the signal of a mixture of $Mn^{II}(ClO_4)_2.6H_2O$ and 250 equiv. CCl_3CO_2H in CH_3CN (Figure 4.25b) and by the observation of the anion by negative mode ESI-MS (*m/z* 538 $[Mn^{II}(CCl_3CO_2)_3]^-$, data not shown).

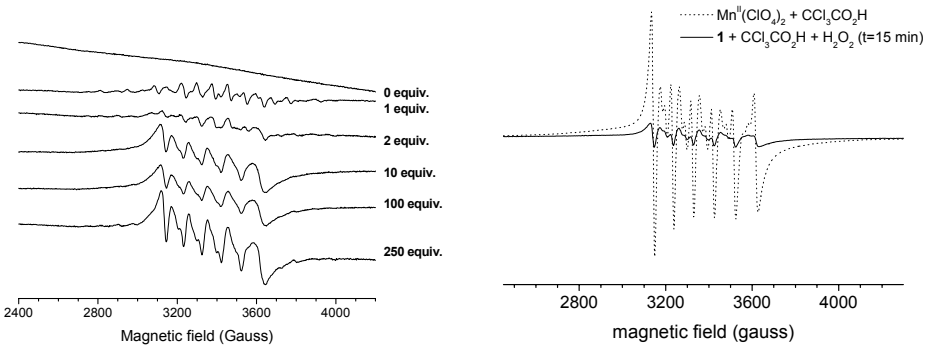

Figure 4.25 X-band ESR spectra at 77 K in CH_3CN. a) **1** (1 mM) with CCl_3CO_2H (0-250 mM) 15 min after addition of H_2O_2 (53 equiv.). b) **1** (1 mM) with CCl_3CO_2H (250 mM) 15 min after addition of H_2O_2 (53 equiv.) (solid line) and $Mn^{II}(ClO_4)_2.6H_2O$ (2 mM) in the presence of CCl_3CO_2H (250 mM) (dotted line).

The quantitative conversion of **1** in the presence of CCl_3CO_2H and H_2O_2 was confirmed by ESI-MS and ^1H NMR spectroscopy (Figure 4.26). However, due to the paramagnetic nature of the Mn^{III}_2 bis(μ-carboxylato) complexes, non-standard catalytic concentrations (*i.e.* [**1**] = 20 mM, and $[CCl_3CO_2H]$ 200 mM) are required to observe ^1H NMR spectra of the complexes.[ix] Addition of excess of H_2O_2 (53 equiv.) to a mixture of **1** and 10 equiv. of CCl_3CO_2H in CH_3CN resulted in a series of new signals assigned to **2a** (Figure 4.26c), in addition to weaker ^1H NMR signals assigned to **2d** $[Mn_2^{III}(OH)_2]^{2+}$.[x]

[ix] Changing to higher concentration is not without consequences. Although most measurements described in this chapter, unless indicated otherwise, were performed at the same concentrations as employed in the catalytic studies reported in Chapter 3 and 5, *i.e.* 1 mM manganese dimer and 10 mM carboxylic acid, increasing the concentration of carboxylic acid results in the formation of a species not normally encountered under catalytic conditions. Mononuclear $[Mn^{II}(CCl_3CO_2)_3]^-$ was observed by both ESR (6-line, A = 100 G) and ESI-MS (*m/z* 538) upon *in situ* formation of **2a** from **1** with H_2O_2 using higher CCl_3CO_2H concentrations.

[x] The assignment of this new species as **2a** was based on comparison with the ^1H NMR spectrum of the related bis(μ-acetato) complex **3a**, published by Hage *et al.* (ref. [13]) Addition of 10 equiv. of CCl_3CO_2H to a solution of **3a** results in the appearance of a similar spectrum, due to ligand exhange of the two μ-acetato ligands with two trichloroacetato bridges (Figure 4.26c and 4.26d).

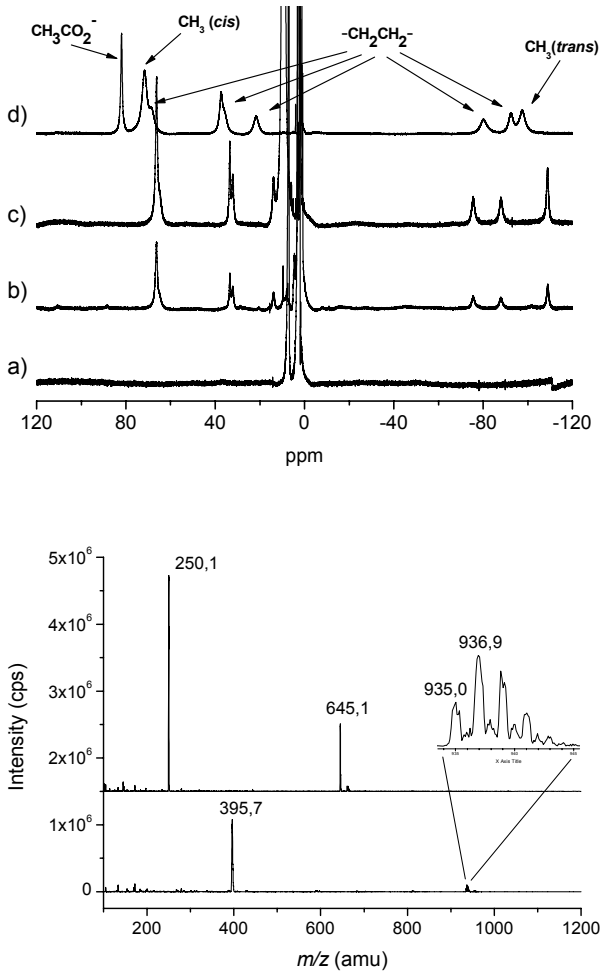

Figure 4.26 (top) ^{1}H NMR (400 MHz, CD_3CN) spectra of a) **1** (20 mM) with CCl_3CO_2H (200 mM). b) as for (a) except 1 h after addition of H_2O_2 (53 equiv.) in two portions. c) **3a** (20 mM) with CCl_3CO_2H (200 mM) after 24 h. d) **3a** (20 mM). (bottom) ESI-MS of **1** (1 mM) in CH_3CN in the presence of 10 equiv. CCl_3CO_2H (10 mM) i) before and ii) 15 minutes after addition of 53 equiv. of H_2O_2, showing conversion of **1** and formation of **2a**.

4.5 Ligand exchange in Mn^{III}_2 complexes

The dynamic solution chemistry of the dinuclear Mn^{III}_2 bis(μ-carboxylato) complexes was explored further through the ligand exchange of the μ-oxo, μ-carboxylato and tmtacn

ligands in **2a** and **3a**. As was observed by ^{1}H NMR spectroscopy, the μ-acetato ligands of **3a** are replaced slowly by μ-trichloroacetato ligands in the presence of CCl_3CO_2H in CD_3CN (Figure 4.26).

The exchange of the μ-oxo bridge in **2a** with the oxygen of (solvent) water was monitored by using ESI-MS employing ^{18}O-labelled water (data not shown). The exchange of the μ-oxo bridge in **2a** (1 mM) in the presence of CCl_3CO_2H (10 mM) in $CH_3CN/H_2{}^{18}O$ (9:1) with solvent water is complete within 1 min (*i.e.* within the time resolution of the experiment). Ligand exchange of the μ-oxo bridge of **3a** is slower than for **2a** (*vide infra*).[xi]

The availibility of deuterated acetic acid and complex **3a**-d_{18} with partly deuterated tmtacn ligands (*i.e.* $(CD_3)_3$-tacn) allows for comparison of the ligand exchange rates of the μ-oxo, μ-acetato and tmtacn ligands of **3a** (Figure 4.27). For $[Mn^{III}{}_2(\mu\text{-}^{16}O)(\mu\text{-}CH_3CO_2)_2(tmtacn)_2]^{2+}$ (**3a**) (*m/z* 293.4) relatively slow exchange of the μ-oxo ligand with ^{18}O from water was observed and the exchange was complete within 8 min (Figure 4.27 a and b) in $CH_3CN/H_2{}^{18}O$ (9:1) in the presence of 10 equiv. CH_3CO_2H. This rate is comparable to that reported recently by Brudvig and coworkers for related dinuclear complexes.[23] The exchange of the μ-acetato ligands with CD_3CO_2H occurs on a comparable time scale, with no further change in the relative ratios of the $\{Mn^{III}{}_2(\mu\text{-}CH_3CO_2)_2\}$ (*m/z* 293.4), $\{Mn^{III}{}_2(\mu\text{-}CH_3CO_2)(\mu\text{-}CD_3CO_2)\}$ (*m/z* 294.9) and $\{Mn^{III}{}_2(\mu\text{-}CD_3CO_2)_2\}$ (*m/z* 296.4) signals after circa 8 min (Figure 4.27 c and d). The incomplete formation of $\{Mn^{III}{}_2(\mu\text{-}CD_3CO_2)_2\}$ is expected statistically, since the addition of 10 equiv. of CD_3CO_2H to **3a** results in a final ratio of non-deuterated and deuterated acetate of 1:5.[xii]

Mixing equimolar amounts of **3a** $\{Mn^{III}{}_2(tmtacn)_2\}$ and **3a**-d_{18} $\{Mn^{III}{}_2(tmtacn\text{-}d_9)_2\}$ in CH_3CN/H_2O (9:1) in the presence of 10 equiv. of CH_3CO_2H results in slow formation of the mixed ligand species **3a**-d_9 $\{Mn^{III}{}_2(tmtacn)(tmtacn\text{-}d_9)\}$.[xiii] Even after 60 min only a small amount of the mixed ligand species is formed, far from equilibration to the statistically expected ratio of 25:50:25 (for **3a** : **3a**-d_9 : **3a**-d_{18}) (Figure 4.27). The slow formation of the mixed ligand species **3a**-d_9 compared with the μ-oxo and μ-acetato exchange means that during the ligand exhange of both the μ-oxo ligand and the μ-carboxylato ligands in **3a** the dinuclear structure of the complex remains intact.

[xi] As shown by electrochemistry (sections 4.4.1 and 4.4.2), complex **3a** $\{Mn^{III}{}_2(\mu\text{-}O)\}$ is less prone to form the corresponding $\{Mn^{III}{}_2(\mu\text{-}OH)_2\}$ complex (similar to **2d**) then complex **2a**. Since a smaller (equilibrium) concentration of the 'open' complex is present in case of **3a**, slower ^{18}O exchange with solvent water is expected (and is observed).

[xii] When a larger excess of CD_3CO_2D was used (50 mM, 50 equiv. w.r.t. to **3**) almost complete conversion was observed.

[xiii] Similarly, mixing **3** and $[Mn^{III}{}_2(\mu\text{-}O)(\mu\text{-}CH_3CO_2)_2(tacn)_2]^{2+}$ in CD_3CN resulted in (partial) formation of mixed ligand species $[Mn^{III}{}_2(\mu\text{-}O)(\mu\text{-}CH_3CO_2)_2(tmtacn)(tacn)]^{2+}$ after 4 d at r.t. as reported by Hage *et al.* (ref. [13]).

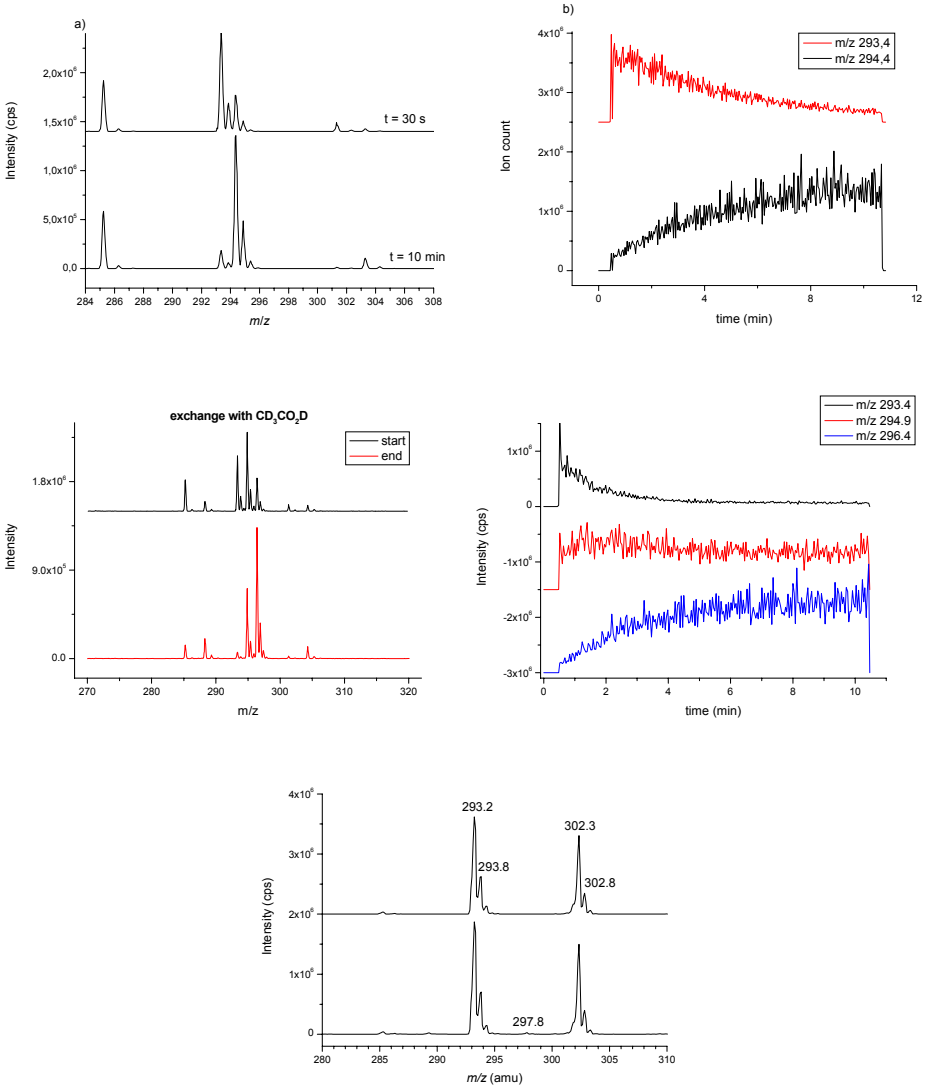

Figure 4.27 a) ESI-MS spectrum of **3a** (1 mM) in CH_3CO_2H (10 mM) with $H_2{}^{18}O/CH_3CN$ 1:9 v/v, at t= 30 s and t = 10 min. b) Time dependence of intensity at 293.4 and 294.4 m/z (traces offset for clarity). c) CD_3CO_2-exchange performed in CH_3CN/H_2O-16 (9:1). t = 0 is time of addition of 10 equiv. of CD_3CO_2D. d) Time dependence of intensity at 293.4, 294.9 and 296.4 m/z (traces offset for clarity). e) mixture of **3a** (0.5 mM) and **3a**-d_{18} (0.5 mM) in CH_3CN/H_2O (9:1) containing CH_3CO_2H (10 mM) at t = 30 sec (upper) and after 60 min (lower).

4.6 Summary

4.6.1 Dinuclear Mn_2 bis(carboxylato) complexes

All data are consistent with the structures for **2a-d** shown in Figure 4.2 and Scheme 4.2 and, moreover, these structures are retained in CH_3CN solution. These complexes are manganese dimers, where each Mn-cation is coordinated to a 'capping' tmtacn ligand. The differences between the complexes are in the oxidation state of the Mn-centres and in the bridging ligands. Complex **2a** is a Mn^{III}_2 dimer with one μ-oxo bridge and two μ-trichloroacetate bridges. **2b** is similar to **2a**; however, it is a Mn^{II}_2 dimer and the μ-oxo bridge is protonated giving a μ-hydroxo bridge. Complex **2c** is a Mn^{II}_2 dimer also, containing two μ-trichloroacetato bridges. However, the μ-hydroxy bridge is 'opened' by H_2O and thus **2c** contains a μ-O_2H_3 bridge. Finally, complex **2d** is a Mn^{III}_2 dimer containing two μ-trichloroacetato bridges and both Mn-centres are each coordinated to a hydroxo group.

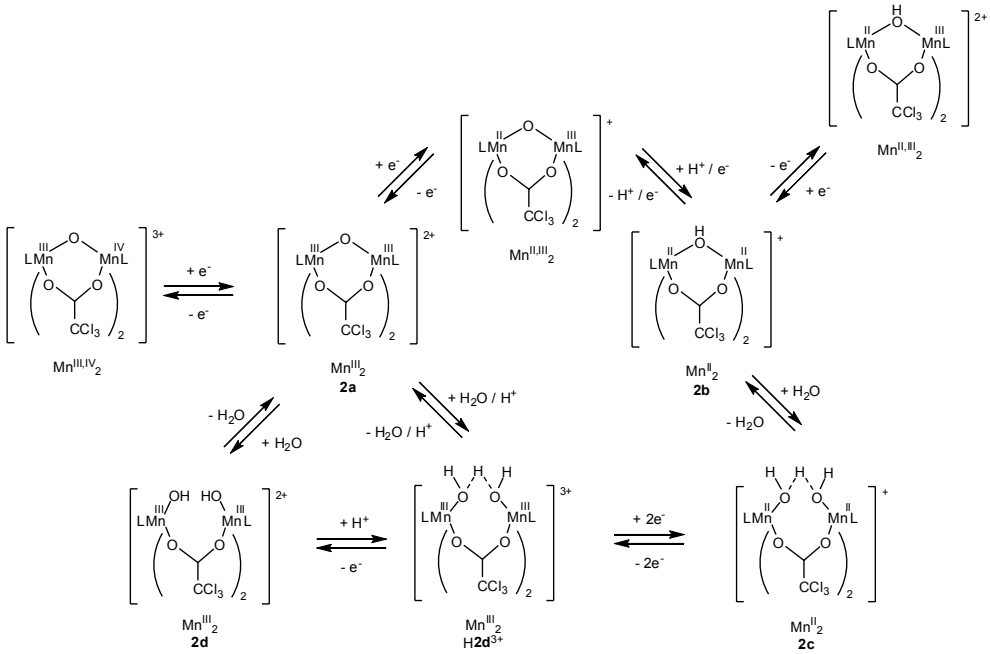

Scheme 4.2 Summary of redox chemistry of **2a-d** in 0.1 M $TBAPF_6/CH_3CN$ in the absence and in the presence of CCl_3CO_2H (middle and lower).

The dinuclear manganese bis(μ-trichloroacetato) complexes **2a-d** show rich electrochemistry, both in the absence and, especially, in the presence of CCl_3CO_2H (Scheme 4.2). In the absence of CCl_3CO_2H both **2a** and **2b** undergo reversible one-electron reduction and oxidation, respectively. Complex **2c** undergoes chemically irreversible two-electron oxidation to form H**2d**$^{3+}$ $\{Mn^{III}_2(\mu\text{-}O_2H_3)\}$, which, depending upon the conditions

employed either shows i) a (quasi)reversible two-electron reduction (to form **2c**), ii) undergoes deprotonation to form **2d** $\{Mn^{III}_2(OH)_2\}$ or iii) undergoes a further chemical change: elimination of H_2O to reform **2a**.

In the presence of CCl_3CO_2H the interchange between the various species is more complex and a series of chemically irreversible redox processes is observed. Although significant structural changes accompany some of the redox processes, overall 'decomposition' of **2a** does not occur, *i.e.* the dinuclear bis(carboxylato) structure remains intact. The proton-coupled two-electron reduction of **2a** to form **2b** is followed, in the presence of CCl_3CO_2H, by opening of the μ-OH bridge to form the corresponding μ-O_2H_3 bridged complex, **2c**. This species undergoes a (chemically) irreversible two-electron oxidation to form H**2d**$^{3+}$ $\{Mn^{III}_2(\mu\text{-}O_2H_3)\}$, which undergoes deprotonation to form **2d**. Thus, although the dinuclear structure of the manganese bis(μ-carboxylato) complexes is not affected upon change of the redox state of the manganese centres, the nature of the bridging, non-carboxylato ligand does change upon interaction with excess of CCl_3CO_2H and/or water and μ-O, μ-OH, μ-O_2H_3 and μ-O_2H_2 bridges are observed for **2a**, **2b**, **2c** and **2d**, respectively.

Complexes **2a** and **2d** are in equilibrium with each other, as is inferred from the exchange of the μ-oxo bridge of **2a** with solvent water. This equilibrium is affected both by the acid and H_2O content of the CH_3CN solvent. High acid and/or high H_2O concentration favours the formation of **2d** at the expense of **2a**. During the μ-oxo and μ-carboxylato exchange the dinuclear structure of the Mn^{III}_2 bis(μ-carboxylato) complexes is retained.

4.6.2 Redox driven ligand exchange of 1

Partial protonation of one of the μ-oxo bridges of **1** occurs in the presence of acids such as CCl_3CO_2H. Reduction is then followed by ligand exchange of two μ-oxo bridges by two μ-carboxylato ligands to form **2c** (Scheme 4.3). Subsequent oxidation and loss of H_2O results in the formation of **2a**. In addition to electrochemical reduction, the initial reduction can be achieved using chemical reductants also, as for example, with *L*-ascorbic acid, which is used during the synthesis of the dinuclear Mn^{III}_2 bis(μ-carboxylato) complexes from **1** (Scheme 4.1 and Appendix B) or with H_2O_2 to prepare **2a** in CH_3CN *in situ* (Figure 4.24 and 4.26).

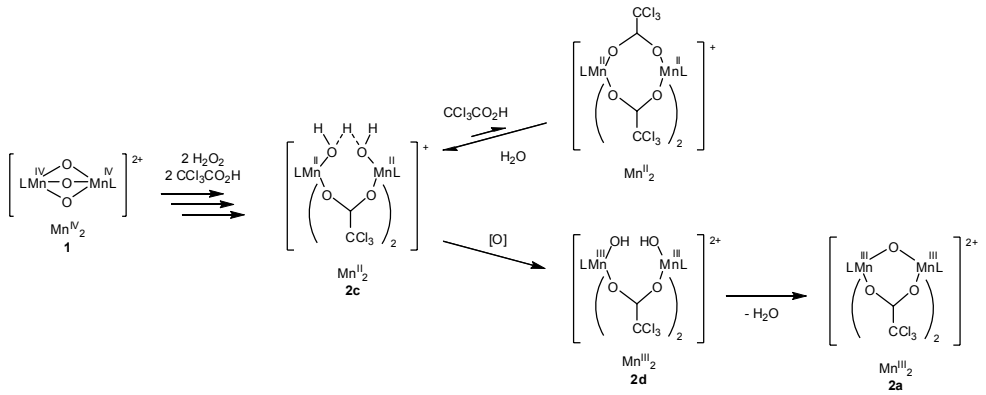

Scheme 4.3 Formation of **2a** from **1**.

4.7 Conclusions

Upon either electrochemical or chemical reduction in the presence of carboxylic acids complex **1** is converted to the corresponding Mn^{III}_2 bis(μ-carboxylato) complexes such as **2a**. It is important to note that these Mn^{III}_2 bis(μ-carboxylato) complexes retain their dinuclear structure upon two-electron reduction, as opposed to the dissociation into two Mn^{II} monomers as proposed earlier by Wieghardt and coworkers.[2,19] The nature of the non-carboxylato bridging ligand in **2a-d** (*i.e.* μ-O, μ-OH, μ-O_2H_3 and μ-O_2H_2, respectively) is both dependent on the oxidation state of the Mn-centres and on the presence of carboxylic acids or water in the CH_3CN solution.

The dynamic solution chemistry of these manganese dimers holds not only relevance to manganese-containing enzymes. The understanding of this dynamic solution chemistry is key to understanding the oxidation catalysis exhibited by Mn-tmtacn, certainly in light of the poor understanding of the mode of action of Mn-tmtacn catalysts. Many of the effects and processes described here will therefore be related to the catalytic activity of Mn-tmtacn in the following chapters.

4.8 References

[1] See for example: a) Wieghardt, K.; Bossek, U.; Zsolnai, L.; Huttner, G.; Blondin, G.; Girerd, J.-J.; Babonneau, F. *J. Chem. Soc., Chem. Commun.* **1987**, 651-653. b) Bossek, U.; Weyhermüller, T.; Wieghardt, K.; Nuber, B.; Weiss, J. *J. Am. Chem. Soc.* **1990**, *112*, 6387-6388. See Chapter 2 for a more extensive list of references.
[2] Wieghardt, K.; Bossek, U.; Nuber, B.; Weiss, J.; Bonvoisin J.; Corbella, M.; Vitols, S.E.; Girerd, J.J. *J. Am. Chem. Soc.* **1988**, *110*, 7398-7411
[3] Wieghardt, K.; Bossek, U.; Nuber, B.; Weiss, J.; Gehring, S.; Haase, W. *J. Chem. Soc., Chem. Commun.* **1988**, 1145-1146.
[4] Birkelbach, F.; Flörke, U.; Haupt, H.-J.; Butzlaff, C.; Trautwein, A. X.; Wieghardt, K.; Chaudhuri, P. *Inorg. Chem.* **1998**, *37*, 2000-2008.
[5] Marlin, D. S.; Bill, E.; Weyermüller, T.; Bothe, E.; Wieghardt, K. *J. Am. Chem. Soc.* **2005**, *127*, 6095-6108.
[6] Wieghardt, K.; Bossek, U.; Ventur, D.; Weiss, J. *J. Chem. Soc., Chem. Commun.* **1985**, 347-349.
[7] Wieghardt, K.; Bossek, U.; Bonvoisin, J.; Beauvillain, P.; Girerd, J.-J.; Nuber, B.; Weiss, J.; Heinze, J. *Angew. Chem.* **1986**, *98*, 1026-1027.
[8] Niemann, A.; Bossek, U.; Wieghardt, K.; Butzlaff, C.; Trautwein, A. X.; Nuber, B. *Angew. Chem. Int. Ed. Engl.* **1992**, *31*, 311-313.
[9] Darovsky, A.; Kezerashvili, V.; Coppens, P.; Weyhermüller, T.; Hummel, H.; Wieghardt, K. *Inorg. Chem.* **1996**, *35*, 6916-6917.
[10] Bossek, U.; Weyhermüller, T.; Wieghardt, K.; Nuber, B.; Weiss, J. *J. Am. Chem. Soc.* **1990**, *112*, 6387-6388.
[11] Hage, R.; Krijnen, B.; Warnaar, J. B.; Hartl, F.; Stufkens, D. J.; Snoeck, T. L. *Inorg. Chem.* **1995**, *34*, 4973-4978.

[12] Hotzelmann, R.; Wieghardt, K.; Flörke, U.; Haupt, H.-J.; Weatherburn, D. C.; Bonvoisin, J.; Blondin, G.; Girerd, J.-J. *J. Am. Chem. Soc.* **1992**, *114*, 1681-1696.
[13] Hage, R.; Gunnewegh, E. A.; Niël, J.; Tjan, F. S. B.; Weyhermüller, T.; Wieghardt, K. *Inorg. Chim. Acta* **1998**, *268*, 43-48.
[14] Wieghardt, K.; Bossek, U.; Nuber, B.; Weiss, J. *Inorg.* Chim. *Acta* **1987**, *126*, 39-43.
[15] For examples of the bridging μ-O_2H_3 structural motif see: a) Stibrany, R.T.; Gorun, S. M. *Angew. Chem. Int. Ed. Engl.* **1990**, *29*, 1156-1158. b) Jaime, E.; Weston, J. *Eur. J. Inorg. Chem.* **2006**, 793-801. c) Bauer-Siebenlist, B.; Meyer, F.; Farkas, E.; Vidovic, D.; Dechert, S. *Chem. Eur. J.* **2005**, 4349-4360. d) De Munno, G.; Viterbo, D.; Caneschi, A.; Lloret, F.; Julve, M. *Inorg. Chem.* **1994**, 33, 1585-1586. e) Dong, Y.; Fujii, H.; Hendrich, M. P.; Leising, R. A.; Pan, G.; Randall, C. R.; Wilkinson, E. C.; Zang, Y.; Que, Jr., L.; Fox. B. G.; Kauffmann, K.; Münck, E. *J. Am. Chem. Soc.*, **1995**, *117*, 2778-2792. f) Ardon, M.; Bino, A.; Michelsen, K.; Pedersen, E.; Thompson, R. C. *Inorg. Chem.*, **1997**, *36*, 4147-4150.
[16] Pessiki, P. J.; Khangulov, S. V.; Ho, D. M.; Dismukes, G. C. *J. Am. Chem. Soc.* **1994**, *116*, 891-897.
[17] Meyer, F.; Rutsch, P. *Chem. Commun*. **1998**, 1037-1038.
[18] Ruf, M.; Weis, K.; Vahrenkamp, H. *J. Am. Chem. Soc.* **1996**, *118*, 9288-9294.
[19] Wieghardt, K.; Bossek, U.; Ventur, D.; Weiss, J. *J. Chem. Soc., Chem. Commun.* **1985**, 347-349.
[20] Sawyer, D. T.; Sobkowiak, A.; Roberts, Jr., J. L. *Electrochemistry for Chemists* (second edition), Wiley, New York, **1995**.
[21] McAuliffe, C. A.; Godfrey, S. M.; Watkinson, M. *Manganese: Inorganic & Coordination Chemistry*, in: Encyclopedia of Inorganic Chemistry, volume 4, King, B. R. (ed.), Wiley, New York, **1994**, 2075-2118.
[22] Hage, R.; Iburg, J. E.; Kerschner, J.; Koek, J. H.; Lempers E. L. M.; Martens R. J.; Racherla, U. S.; Russell S. W.; Swarthoff, T.; van Vliet M. R. P.; Warnaar, J. B.; van der Wolf, L.; Krijnen, B. *Nature* **1994**, *369*, 637-639.
[23] Tagore, R.; Chen, H.; Crabtree, R. H.; Brudvig, G. W. *J. Am.Chem.Soc.* **2006**, *128*, 9457-9465.

Chapter 5
Cis-dihydroxylation and epoxidation of cyclooctene by Mn-tmtacn/CCl_3CO_2H - speciation analysis

*A range of spectroscopic techniques was employed to determine both the factors responsible for the lag period and the species present in solution during the catalytic cis-dihydroxylation and epoxidation of alkenes by the system **1**/CCl_3CO_2H described in Chapter 3. Analysis of the effects of variation in reaction parameters on both the behaviour and stability of Mn-tmtacn complexes and on the catalytic performance, together with isotopic labeling studies, led to insight into the mode of action of this powerful catalyst. A Mn^{III}_2-η^1-peroxo species, rather than the involvement of a high-valent Mn-oxo species, is proposed to be the active species that engages in oxidation of the alkene substrates.*

Part of this chapter has been published:
J. W. de Boer, W. R. Browne, J. Brinksma, P. L. Alsters, R. Hage and B. L. Feringa
Inorg. Chem. **2007**, *46*, 6353-6372.

As discussed in Chapter 3, the key factor for effective *cis*-dihydroxylation and/or epoxidation of alkenes by $[Mn^{IV}_2(\mu\text{-}O)_3(tmtacn)_2]^{2+}$ (**1**) employing H_2O_2 is the presence of a carboxylic acid. While the nature of the carboxylic acid affects both the selectivity and activity of the catalytic system and the duration of the lag-time, its mode of action is not understood. To gain better insight into the mechanism(s) by which the current catalytic system operates, it is first important to explore which species are present in solution during the different stages of the reaction. Furthermore, since dramatic changes are observed on the (redox) properties of Mn-tmtacn complexes (Chapter 4), the effects of the carboxylic acid and water concentration on both the activity and selectivity of the catalytic system need to be explored.

The 'standard' reaction that will be discussed in this chapter is the catalytic oxidation of cyclooctene by **1** (0.1 mol%, 1 mM) in the presence of CCl_3CO_2H (1 mol %, 10 mM) at 0 °C in CH_3CN with H_2O_2 (50 w/w % aq., 1.3 equiv. w.r.t. substrate) added continuously over 6 h, followed by 1 h without addition of H_2O_2 (Scheme 5.1).[i] These 'standard' conditions are advantageous as they allow for the maintenance of a low concentration of H_2O_2 and thus allow for suppression of both oxidant and catalyst decomposition. In addition, the concentration of **1** employed facilitates direct spectroscopic study of the reaction mixture. As discussed in Chapter 3, a significant lag period is observed under these 'standard' conditions (phase I, Figure 3.4), after which *cis*-dihydroxylation and epoxidation begin simultaneously and both processes show similar time dependence up to 4 h (phase II).[ii] Finally, towards the end of the reaction (phase III), the *cis*-diol concentration begins to decrease due to oxidation to the corresponding α-hydroxyketone,[1] while the epoxide concentration continues to increase steadily.

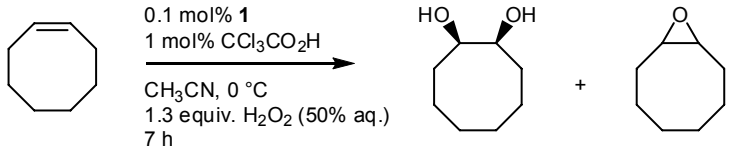

Scheme 5.1. Catalytic *cis*-dihydroxylation and epoxidation of alkenes by **1**/CCl_3CO_2H.

---

[i] The system described in this chapter involving **1**/CCl_3CO_2H has been chosen as representative for the study of alkene oxidation for several reasons; its high activity, product distribution (which allows for facile quantification of the effect of changes on selectivity), moderately short lag-period and the utility of $^{35/37}Cl$ isotope patterns for mass spectral analysis. Similarly, cyclooctene is chosen as the model substrate primarily due to the excellent conversions achievable, even with less active **1**/carboxylic acids combinations, and the absence of significant and potentially interfering side reactions, such as allylic oxidation.

[ii] At higher temperatures (*i.e.* 20 °C) a decreased lag period is observed (30-45 min), however, overall conversion and turnover numbers are not affected significantly, although the amount of *cis*-diol is reduced somewhat due to increased overoxidation (Table 5.1, entries 1 and 2). As for the results obtained at 0 °C, the lag-period for both initiation of the reaction and formation of **2a** coincide.

5.1 Macroscopic parameters affecting the catalytic performance

5.1.1 CCl_3CO_2H as bridging ligand

During the lag-period of the reaction (30-45 min at 20 °C and 60-90 min at 0 °C), no change in either the UV-Vis or ESI-MS[iii] spectra occurs, and only weak ESR signals are observed (see section 5.2). At the end of the lag-period, *i.e.* the time at which conversion of cyclooctene begins, UV-Vis and ^{1}H NMR spectroscopy and ESI-MS[2] show quantitative conversion of **1** (predominantly to **2a**, Figure 5.1). It is also apparent from the intensity of the UV-Vis spectrum that the major species (> 95 %, by comparison with an authentic sample of **2a**) present after the lag-period is **2a**. The remainder (< 5 %), however, is certainly not **1**, as after the lag period **1** is not detectable by ESI-MS.

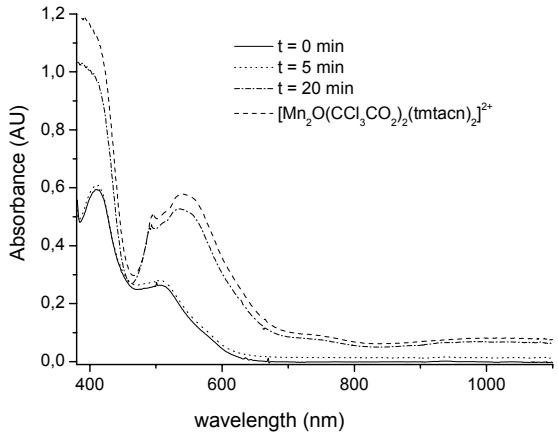

Figure 5.1 UV-Vis spectrum of a mixture of **1** (1 mM)/CCl_3CO_2H (10 mM)/cyclooctene (1 M) after 0 (solid line), 5 (dotted line) and 20 min (dash-dot-dash line) at 20 °C in CH_3CN and of **2a** (1 mM, dashed line).

Although the pKa of **1** is -2,[3] in CH_3CN containing CCl_3CO_2H (10 mM), a significant amount of the complex is present in the protonated form. The reduction of H**1**$^+$ is, primarily, responsible for the lag-period observed prior to the onset of catalytic activity.

[iii] Mass spectrometry has proven to be a powerful tool in the identification of species present in solution, see for example ref. [2]. However, caution should be exercised in its use as a mechanistic probe due to the potential of observation of experimental artifacts. For example, the presence of minor impurities in commercial grade chemicals such as cyclooctene highlights this point. One source of cyclooctene contained such a component, which provided signals in the ESI-MS experiments assignable to possible catalytic intermediates. The use of cyclooctene from a second source or triple distillation of the cyclooctene to remove this component, while having no effect on other spectroscopic properties or catalysis, did result in the elimination of these spurious signals.

However, as H_2O_2 is incapable of reducing **1** at an appreciable rate even in the presence of a proton source such as HPF_6, it is clear that the formation of the Mn^{II}_2 and Mn^{III}_2 bis(carboxylato) bridged systems, *e.g.* **2a-d**, results from an autocatalytic reduction of H**1**$^+$ (see also section 4.4.3, Chapter 4). Notably the onset and rate of the autocatalytic conversion of H**1**$^+$ is delayed by the presence of cyclooctene (Figure 5.2).

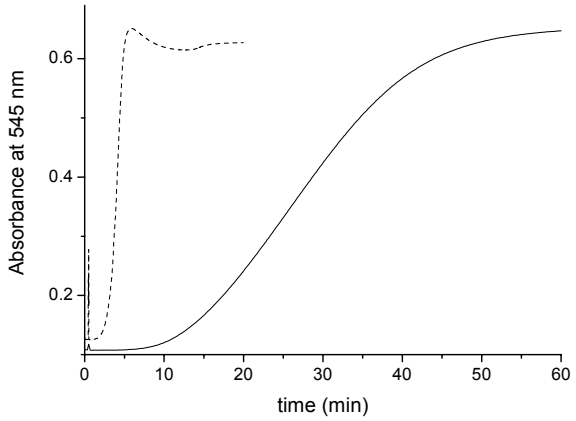

Figure 5.2 Conversion of **1** (1 mM) to **2a** in CH_3CN in the presence of CCl_3CO_2H (10 mM) after addition of H_2O_2 (50 mM) at t = 0 min, in the absence (dashed line) and presence (solid line) of cyclooctene (1 M).

The formation of Mn^{III}_2 bis(μ-carboxylato) complexes, such as **2a**, coincides with the onset of catalytic activity of **1**/CCl_3CO_2H. Since the presence of cyclooctene slows down the formation of **2a** from **1**, it was anticipated that the lag-period could be circumvented either by converting **1** to **2a** *in situ* prior to addition of cyclooctene or by using **2a** prepared independently (in place of **1**). Indeed the formation of the complex *in situ* by addition of excess H_2O_2 (53 equiv) to **1** (1 mM) and CCl_3CO_2H (10 mM) at 20 ^oC 20 min prior to addition of cyclooctene and cooling to 0 ^oC, results in a significant reduction in the length of the lag period (Figure 5.3).[iv] Similarly, when complex **2a** (prepared independently) is used as catalyst (1 mM) a reduced lag-period is observed also (data not shown). This underlines that the formation of **2a** is a prerequisite for catalytic activity. It should be noted that both conversion and *cis*-diol/epoxide ratio after 7 h are similar (Table 5.1, entries 1, 3 and 4), regardless of which complex was used at the start of the reaction (*i.e.*, **1**/CCl_3CO_2H, preparing **2a** *in situ* before the start of the reaction or using an independently prepared sample of **2a**). However, the incomplete reduction of the lag-period, in terms of activity, and the synchronization of the reaction with the standard reaction after 1.5 h, indicate that the formation of **2a** is not the sole factor responsible for the lag period.

[iv] H_2O_2 can reduce H**1**$^+$ in the presence of CCl_3CO_2H, ultimately leading to the formation of **2a**, as discussed in Chapter 4 (section 4.4.3).

Table 5.1 Product distribution following catalytic oxidation of cyclooctene with **1, 2a, 2b** and **2c** (0.1 mol%) at 0 °C.

Entry	Catalyst	CCl_3CO_2H	H_2O[a]	conv. (%)	t.o.n. *cis*-diol	t.o.n. epoxide	mass. bal. (%)[f]
1	**1**	1 mol%	-	91	438	247	78
2	**1**[b]	1 mol%	-	91	380	280	75
3	**1**[c]	1 mol%	-	82	445	227	85
4	**2a**	1 mol%	-	93	380	259	71
5	**2a**	-	-	44	269	112	94
6	**2b**	1 mol%		90	378	280	76
7	**2b**[c]	1 mol%	-	76	403	217	86
8	**2c**	1 mol%	-	91	372	252	71
9	**2a**	1 mol%	110 µL	96	357	250	65
10	**2b**	1 mol%	110 µL	93	390	251	71
11	**2a**	1 mol%	-[d]	29	151	102	96
12	**2a**	1 mol%	-[e]	38	245	104	96

a) Added prior to addition of cyclooctene and H_2O_2. b) Reaction performed at room temperature (lag period: 30-45 min). c) 30 µl of H_2O_2 added at 20 °C prior to addition of cyclooctene. d) A dried solution of H_2O_2/CH_3CN was used (0.46 equiv. H_2O_2). e) As for d) except a normal amount of water was added (see Figure 5.8 for details also). f) Deviation from 100% is due to further oxidation of the *cis*-diol to the α-hydroxyketone, as discussed in more detail in section 3.5 (Chapter 3).

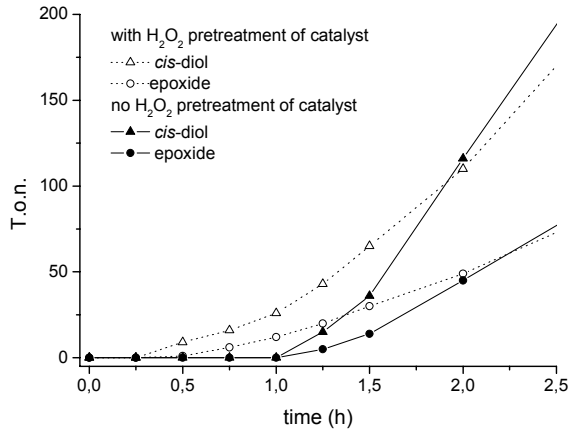

Figure 5.3 Catalytic oxidation of cyclooctene (1 M) in CH_3CN by **1** (1 mM) and CCl_3CO_2H (10 mM) (solid lines). Effect of pre-treatment of the catalyst with H_2O_2 prior to addition of substrate on lag period (dotted lines).

5.1.2 [CCl_3CO_2H] dependence on activity and selectivity

The dependence of the activity and selectivity of **1** on the relative concentration of CCl_3CO_2H is shown in Figure 5.4. With less then 2 equiv. of CCl_3CO_2H (w.r.t. complex **1**), low activity is observed, in agreement with the necessity for two carboxylato ligands to form **2a** from **1**. With 2 equiv. of CCl_3CO_2H present, a large increase in activity is observed, however, a further increase in acid concentration affects the reaction less, with only a modest increase in activity and increased further oxidation of the *cis*-diol product. Notably, increasing the concentration of acid to 25 mol % results in enhanced selectivity for epoxidation over *cis*-dihydroxylation.

The change in selectivity observed with changes in CCl_3CO_2H concentration is due to changes in the water content rather than other effects such as peracid formation (see also Chapter 3, Table 3.4). When CH_3CN/H_2O (9:1 v/v) is used in place of CH_3CN as solvent for the reaction catalyzed by **1** (0.1 mol%) with 25 mol% CCl_3CO_2H, the *cis*-diol/epoxide selectivity increases from 0.79 to 1.5 (Figure 5.4, and entries 7 and 8 in Table 5.2) with a negligible change in overall cyclooctene conversion. The ratio 1.5 is comparable to the ratio 1.8 observed using 1 mol% CCl_3CO_2H (Table 5.1, entry 1). Hence, the difference in selectivity with increasing acid concentration can be attributed to reduction of the effective water content of the reaction mixture.

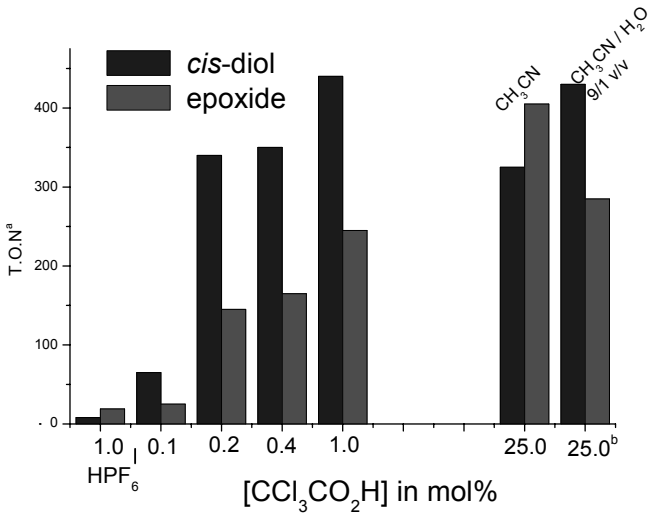

Figure 5.4 Effect of relative acid concentration on the catalytic oxidation of cyclooctene by **1** (0.1 mol%) at 0 °C. a) Maximum total t.o.n. = 1000. b) Reaction performed in CH_3CN/H_2O (9:1 v/v). See also Table 5.2. Note that although simple proton sources, *e.g.* HPF_6, together with **1**, are inactive towards cyclooctene oxidation, they are effective in suppressing catalase activity.

Table 5.2 Effect of [CCl_3CO_2H] on activity and selectivity.[a]

Entry	additive (mol%)	conv. (%)	t.o.n. cis-diol	t.o.n. epoxide	mass. bal. (%)
1	HPF_6 (1)	3	10	20	100
2	trichloroacetic (0.1)	9	65	25	100
3	trichloroacetic (0.2)	59	340	145	90
4	trichloroacetic (0.4)	65	350	165	86
5	trichloroacetic (1)	91	440	245	78
6	trichloroacetic (1)[b]	91	380	280	75
7	trichloroacetic (25)	96	325	405	77
8	trichloroacetic (25)[c]	94	430	285	77

a) Catalyst **1** (0.1 mol%) in CH_3CN at 0 ^oC (general procedure A, Appendix C). b) At 20 ^oC c) In CH_3CN/H_2O 9:1.

5.1.3 Dependence of activity and selectivity on [2a]

When the amount of catalyst **2a** is varied between 0.375 and 0.0075 mol% under otherwise identical conditions (*i.e.* 1 mol% of CCl_3CO_2H and 1.3 equiv. of H_2O_2 w.r.t. cyclooctene) the intrinsic selectivity of the catalyst remains unaltered (Table 5.3, entries 1-4). Although at higher catalyst concentration the *cis*-diol/epoxide ratio is lowered, this can be attributed to increased overoxidation of the *cis*-diol (analogous to the process described in more detail in section 3.5, Chapter 3). At low catalyst concentration, *i.e.* 0.0075 mol%, the conversion decreases, however, 5500 turnovers were achieved.

Table 5.3 Concentration dependence of [**2a**] on the catalytic oxidation of cyclooctene in the presence of CCl_3CO_2H (1 mol%).

Entry	2a (mol%)	Conv. (%)	t.o.n.[a] (% yield[b]) *cis*-diol	epoxide	Mass bal. (%)
1	0.375	98	80 (30)	70 (25)	57
2	0.1	93	380 (38)	260 (26)	71
3	0.0375	94	925 (35)	660 (25)	65
4	0.0075	63	3350 (25)	2120 (16)	78

a) Turnover number w.r.t. Mn-dimer. b) Yield based on alkene substrate.

5.1.4 Excess of CCl_3CO_2H

That the carboxylic acid acts as a ligand in the manganese dimer is apparent from structural data and the reduction of the lag period when **2a** is used in place of **1**. However, the carboxylic acid has another role to play also. Figure 5.5 shows the time course for the oxidation of cyclooctene catalysed by **2a** (0.1 mol%) in the presence and in the absence of CCl_3CO_2H (1 mol%). During the initial stage, the two reactions behave similarly. However, without additional CCl_3CO_2H, the catalyst becomes less active towards the end of the reaction and at ca. 5 h becomes inactive.

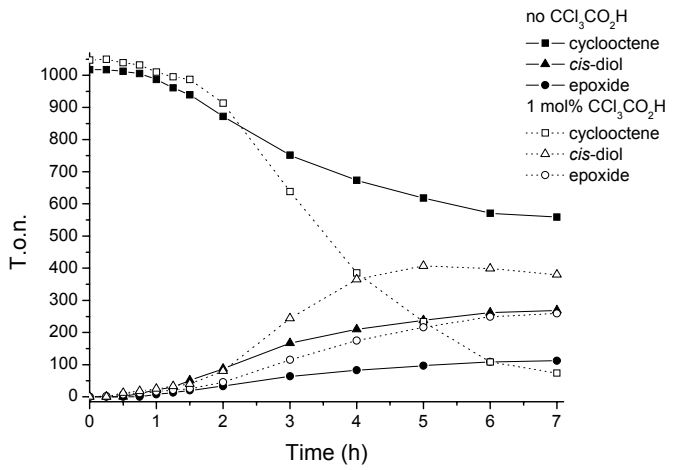

Figure 5.5 Catalytic oxidation of cyclooctene (squares) by **2a** (1 mM) with CCl_3CO_2H (10 mM) (dotted lines) and without CCl_3CO_2H present (solid lines) yielding *cis*-diol (triangles) and epoxide (circles).

The loss in activity is related to the dissociation of the carboxylato ligands from the complex. This is best exemplified in a similar catalytic experiment employing 3,5-difluorobenzoato as bridging ligand, *i.e.* by using $[Mn^{III}_2(O)(3,5\text{-difluorobenzoato})_2(tmtacn)_2]^{2+}$ **20** instead of **2a** (Table 5.4). The fluoro substituents in the carboxylic acid allow for monitoring the carboxylato ligands by ^{19}F NMR spectroscopy at standard catalytic concentrations (Figure 5.6). During the initial stages of the reaction (where normal reactivity is observed), the two 3,5-difluorobenzoato bridges are ligands in the Mn^{III}_2 complex (-99 ppm). However, as the reaction progresses, the intensity of the signal of the 3,5-difluorobenzoato bridges of the Mn^{III}_2 complex decreases and free 3,5-difluorobenzoic acid is observed (-112 ppm). Upon complete dissociation of the carboxylato ligands catalytic activity ceases. Thus, although excess carboxylic acid is not essential for catalytic activity, its presence stabilizes the bis(μ-carboxylato) complexes involved.

Table 5.4 Catalytic oxidation of cyclooctene.[a]

Entry	Cat./carboxylic acid (mol%)	conv. (%)[b]	t.o.n.[c] *cis*-diol	t.o.n.[c] epoxide	mass bal.	lag period
1	**1** / 3,5-difluorobenzoic acid (1.0)	20	101	51	95	60-90 min
2	**20** / 3,5-difluorobenzoic acid (1.0)	33	194	82	95	75-90 min
3	**20** / -	10	50	23	97	2-3 h

a) Conditions: see general procedure A in Appendix C. b) Based on substrate consumed. c) Turnover number (t.o.n.).

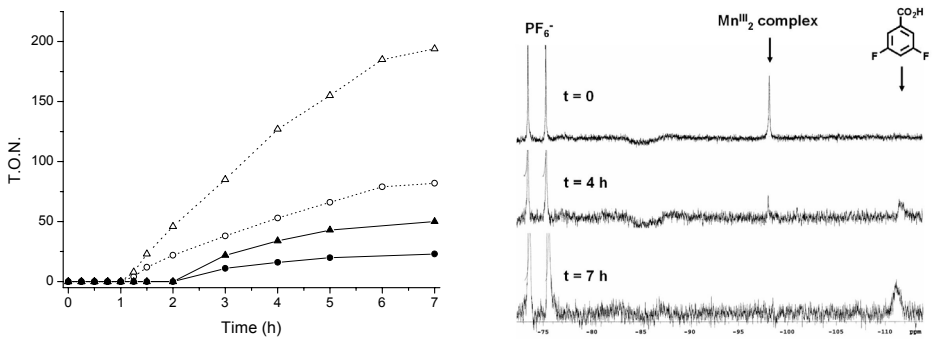

Figure 5.6 a) *Cis*-dihydroxylation (triangles) and epoxidation (circles) of cyclooctene by $[Mn^{III}_2(\mu\text{-}O)(\mu\text{-}3,5\text{-difluorobenzoato})_2(tmtacn)_2]^{2+}$ **20** (1 mM) with 3,5-difluorobenzoic acid (10 mM) (dotted lines) and without 3,5-difluorobenzoic acid present (solid lines). b) ^{19}F NMR spectra during the oxidation of cyclooctene at t = 0, 4 h and 7 h (top to bottom) with **20** (1 mM) in the absence of 3,5-difluorobenzoic acid. PF_6^- anion is used as internal reference (-75 ppm).

5.1.5 Initial oxidation state

The use of the Mn^{III}_2 complex **2a** in place of **1**, allows for the near complete elimination of the lag-period (Figure 5.7a). For both **2b** and **2c** a negligible lag period is observed also (Figure 5.7b, Table 5.1). The identical behavior of **2b** and **2c** is, however, not surprising, considering that under reaction conditions (*i.e.* in the presence of CCl_3CO_2H), **2b** undergoes quantitative conversion to **2c** (see Chapter 4, section 4.6.1). The activity over the first hour with respect to formation of the epoxide product is similar to that observed after 1.5 h. However, with either **2b** or **2c**, the *cis*-diol/epoxide ratio is lower over the first 1.5 h of the reaction than observed at later stages of the reaction. The difference in selectivity and the increased reactivity observed for **2c** (and **2b**) compared with **2a** in the early stages (phase I) of the reaction, is remarkable considering that within 15 min of the start of the reaction complex **2a** is the predominant species present in solution (80-90% by UV-Vis and ESR spectroscopy, see section 5.2). After ca. ~90 min the selectivity of the reaction with **2b** or **2c** is almost identical to that with **1** and **2a**. Furthermore, whether the catalytic oxidation of cyclooctene is performed starting with complex **1, 2a** $\{Mn^{III}_2(\mu\text{-}O)\}$, **2b** $\{Mn^{II}_2(\mu\text{-}OH)\}$ or **2c** $\{Mn^{II}_2(\mu\text{-}O_2H_3)\}$, the turnover numbers with respect to both *cis*-diol, epoxide and the conversion of cyclooctene are very similar after 7 h (Table 5.1, entries 1, 4, 6 and 8, respectively).

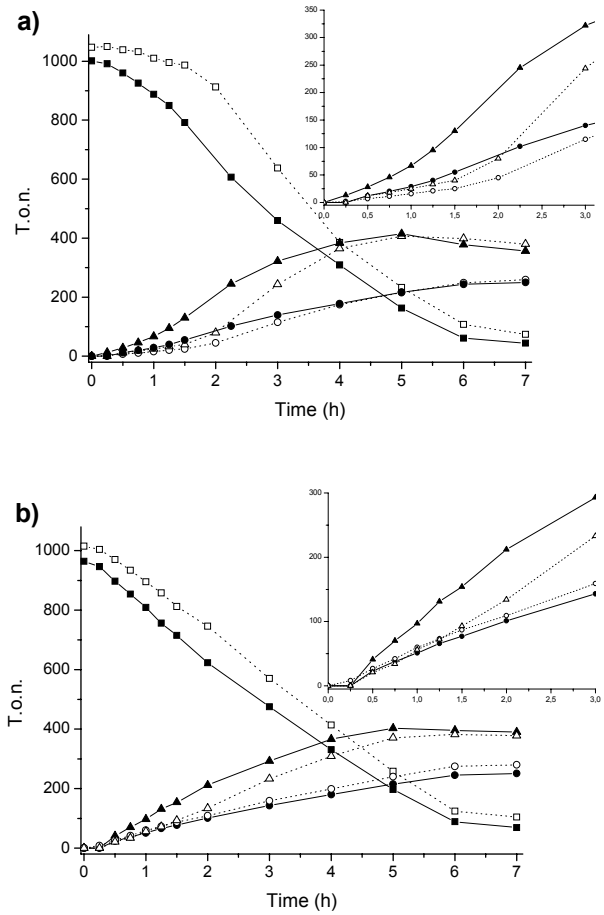

Figure 5.7 Effect of oxidation state and addition of H_2O prior to start of catalysis on the product distribution in the oxidation of cyclooctene catalyzed by a) **2a** and b) **2b.** With no H_2O added (dotted lines/open symbols) and with added H_2O (solid lines/filled symbols). Insets: expansion of 1st 3 h period (0.1 mol% of catalyst, 1 mol% of CCl_3CO_2H) (cyclooctene/squares, epoxide/circles, *cis*-diol/triangles). See Table 5.1 for further details.

5.1.6 Effect of water

The difference in both reactivity and selectivity of the different complexes during phase I of the reaction (Figures 5.5 and 5.7) is intriguing and could indicate the presence of a second catalytically active species or catalytic pathway during the early period of the reaction; however, solvent effects should be considered also. During the catalysis, H_2O_2 (50 % aqueous solution) is added continuously and, hence, the water content of the reaction

mixture increases as the reaction progresses. Indeed, addition of H_2O prior to the start of the reaction[v] catalyzed by either **2a** or **2b**, results in a significant difference in the time-dependence of product formation observed (Figure 5.7). Importantly, the *cis*-diol/epoxide ratio for both the **2a** and **2b** catalyzed reactions becomes identical to that observed later in the reaction. Furthermore the reactivity of **2a** is increased to match that observed after 1.5 h.

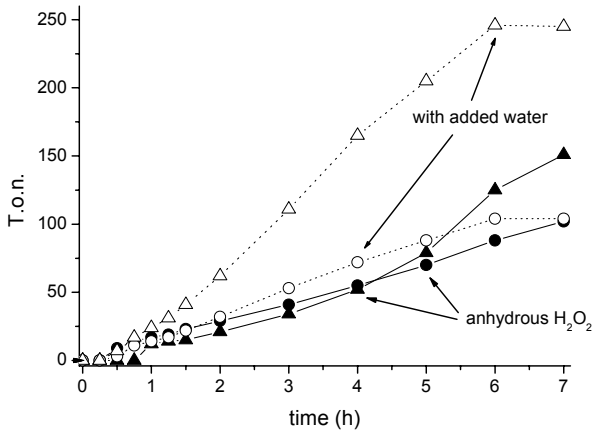

Figure 5.8 Time course for the formation of *cis*-diol (triangles) and epoxide (circles) from cyclooctene with anhydrous H_2O_2 (solid lines) and with additional water added with time (dotted lines). H_2O_2 is added at one third of the normal amount and rate of addition (see also Table 5.1, entries 11 and 12).

The influence of the water content of the reaction mixture was explored further using H_2O_2/CH_3CN, from which water has been removed[4] (Figure 5.8).[vi] From the time profile of the reaction it is apparent that addition of anhydrous H_2O_2/CH_3CN solution to the reaction mixture with **2a** results in a 1:1 *cis*-diol/epoxide ratio.[vii] A control reaction with anhydrous H_2O_2/CH_3CN to which H_2O was added continuously to achieve the same water content as used normally, showed a typical *cis*-diol/epoxide ratio of ca. 2.3. This high *cis*-diol/epoxide

---

[v] Pretreatment with H_2O: the amount of H_2O added is equal to the amount of H_2O which is added over 105 min during continuous addition of H_2O_2 (50 w/w%) (see also procedure A in Appendix C).

[vi] H_2O_2 (50% w/w in H_2O) was diluted in CH_3CN and dried over $MgSO_4$ (caution). The use of dry H_2O_2 sources such as urea hydrogen peroxide (UHP, $CO(NH_2)_2.H_2O_2$) was considered however, practical difficulties, most notably the insolubility of the reagents in CH_3CN render this approach ineffective in assessing the role of H_2O content. It should be noted that during the time course of the reaction some H_2O is formed due to epoxide formation (since only one of the oxygens of H_2O_2 is incorporated in the epoxide product).

[vii] The increase in *cis*-diol/epoxide ratio observed towards the end of the reaction (ca. 5-7 h) is due to the release of water from H_2O_2 during epoxidation. A reduced rate of H_2O_2 addition (1/3rd normal) was employed to minimize this effect.

ratio of 2.3 compared to 1.8 under normal conditions is due to the low level of overoxidation of the *cis*-diol at low substrate conversion. Under normal conditions a *cis*-diol/epoxide ratio of 2.5 is observed for the same (40%) conversion.

The difference in the *cis*-diol/epoxide ratio's observed during the initial phase of the reaction when using **2a**, **2b** or **2c** can thus be attributed to the low water content of the reaction mixture during this earlier period, rather than to a difference in oxidation state (Mn^{II}_2 vs. Mn^{III}_2). Importantly, the level of activity towards epoxidation is affected much less by the addition of H_2O and the increase in the overall activity is due to increased *cis*-diol formation. This latter observation may be related to the ligation strength of *cis*-diols compared to epoxides, and hence the need to displace *cis*-diol once formed from the catalyst by H_2O (see also section 5.4.2.2).

5.1.7 H_2O_2 efficiency

A key feature of the present system is the efficiency with respect to the terminal oxidant (H_2O_2). The efficiency of the reaction, *i.e.* conversion of substrate and further oxidation of the *cis*-diol, with respect to H_2O_2 added, is demonstrated in Figure 5.9. For the catalytic system **1**/CCl_3CO_2H, the H_2O_2 added during the lag period is consumed only partly after the lag period, however, once catalysis commences the efficiency in terms of oxidant consumption is close to 100%. For **2a**/CCl_3CO_2H, almost all of the oxidant added is used in oxidation of the substrate, albeit with a small amount of H_2O_2 used in the further oxidation of the *cis*-diol, in the final stages of the reaction. The efficiency confirms that a near complete suppression of catalase type activity occurs. It is important to note that the rate of H_2O_2 addition is matched by the consumption of H_2O_2 by the catalyst. This indicates that overall the rate of oxidation is limited by the addition of oxidant and not the intrinsic activity of the catalyst.

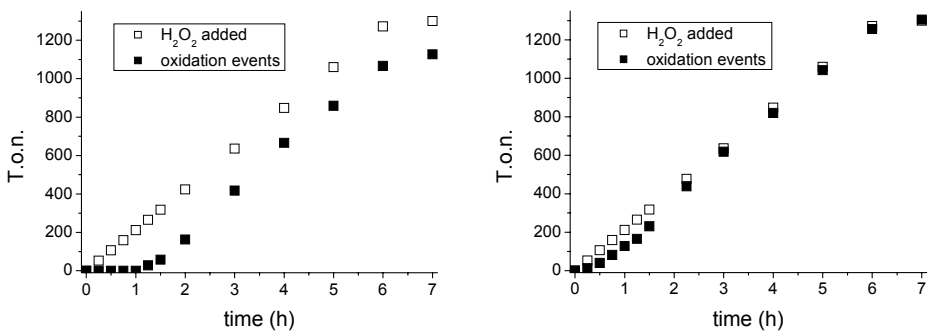

Figure 5.9 Total number of oxidation events (this is the total t.o.n. for oxidation of cyclooctene + oxidation of the *cis*-diol formed) compared with number of equivalents of H_2O_2 added. Left: **1** (0.1 mol%) /CCl_3CO_2H (1 mol%); Right: **2a** (0.1 mol%) /CCl_3CO_2H (1 mol%) with H_2O (110 µl) added at t = 0 (see text for details).

5.2 Speciation analysis

Regardless of whether **1**, **2a**, **2b** or **2c** is employed as catalyst, the major species in solution during the period when catalysis occurs is **2a**, which accounts for 80-90% of all manganese present in the reaction mixture (Figure 5.10). As was noted in section 5.1.1, during the lag-time **1** is converted to **2a** (Figure 5.10a). Complete conversion of **1** during the lag period was confirmed by ESI-MS (loss of the signals at *m/z* 250.1 $[Mn^{IV}_2(O)_3(tmtacn)_2]^{2+}$ and 645.1 $[\{Mn^{IV}_2(O)_3(tmtacn)_2\}(PF_6)]^+$) and formation of **2a** was observed (*m/z* 395.7 $[Mn^{III}_2(O)(CCl_3CO_2)_2(tmtacn)_2]^{2+}$ and 935.0 $[\{Mn^{III}_2(O)(CCl_3CO_2)_2(tmtacn)_2\}(PF_6)]^+$). When the starting complex is **2a**, this complex remains the main species in solution, although a small part of **2a** is 'lost' (Figure 5.10b). When the reaction is started with **2c** (or **2b**), within 5 min complex **2a** is the predominant species present in solution (Figure 5.10c).

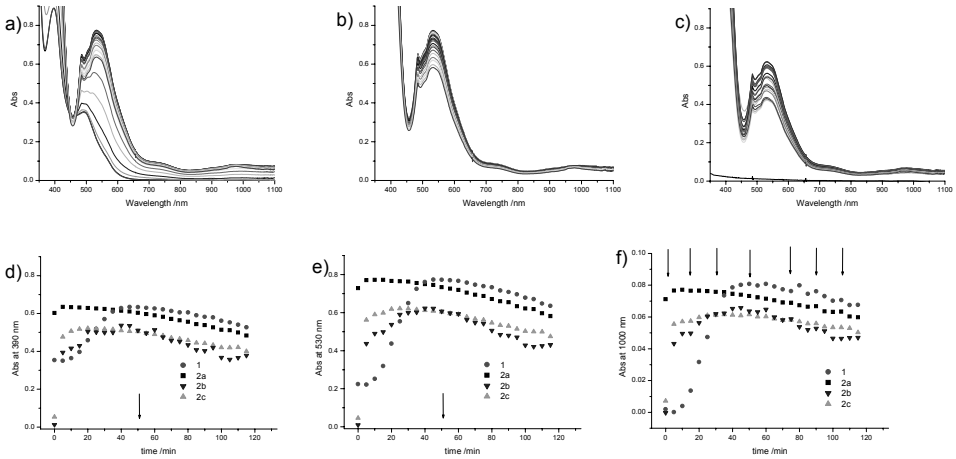

Figure 5.10 Changes observed in the UV-Vis spectrum of the reaction mixture during the oxidation of cyclooctene (1 M) by H_2O_2 (added batch-wise at a rate of 55 equiv w.r.t catalyst every 15 min) catalyzed by a) **1** (1.26 mM), b) **2a** (1.25 mM) and c) **2b** (1.32 mM) at 20 ^oC with CCl_3CO_2H (10 mM). Changes in absorption observed during catalysis with **1**, **2a**, **2b**, and **2c** (1.25 mM) with CCl_3CO_2H (10 mM) at d) 390, e) 530 and f) 1000 nm. The points of H_2O_2 batch addition are indicated by black arrows in graph f.

ESR spectroscopy presents a powerful tool in the study of manganese-based catalytic systems. Although it is clear from UV-Vis spectroscopy and mass spectrometry that the major species present in solution are ESR silent Mn^{III}_2 dinuclear complexes, such as **2a**, the availability of ESR active (Mn^{II}_2) complexes such as **2b** and **2c** allows for assessment of their involvement during catalysis. The same holds for any other ESR active species (*e.g.* mononuclear Mn^{II} or Mn^{IV} species) that might be present (at low concentrations) in addition to **2a**.

The oxidation of cyclooctene by H_2O_2 catalyzed by **1** (1 mM) in the presence of CCl_3CO_2H (10 mM) at 20 ^oC was followed by ESR spectroscopy under standard catalytic concentrations. After 15 min, a multiline signal is observed (attributed to **2c**, *cf.* Figure 4.11, Chapter 4), present at low concentrations (Figure 5.11), based on intensity compared with **2c** (1 mM) under identical conditions. This weak signal decreases in intensity over the first hour of the reaction with the appearance of a weak 6 line signal (a = 100 G). Interestingly a weak signal, assigned to **2c**, is observed in the ESR spectrum of **2a** (1 mM), in the presence of cyclooctene and CCl_3CO_2H (10 mM), prior to addition of H_2O_2. Addition of H_2O_2 results in the disappearance of this signal. After 45 min the appearance of a weak 6 line signal is observed (a = 100 G). This 6 line species is assigned as $[Mn^{II}(CCl_3CO_2)_3]^-$ on the basis of comparison with $Mn^{II}(ClO_4)_2/CCl_3CO_2H$ 1:10 in CH_3CN (see also Chapter 4, Figure 4.25).

Thus, ESR spectroscopy confirms the conversion of **2b** and **2c** in the presence of CCl_3CO_2H to an ESR silent complex (*i.e.* **2a**) upon addition of H_2O_2 (Figure 5.12), in agreement with UV-Vis spectroscopy (Figure 5.10c). Overall, although several species are observed by ESR spectroscopy, namely **2c** and free mononuclear Mn^{II}-tris(carboxylato) complexes, the ESR signal is remarkably weak during catalysis, in agreement with electrochemical, ESI-MS and UV-Vis spectroscopic studies in which the major species observed is the ESR silent Mn^{III}_2 complex **2a.**

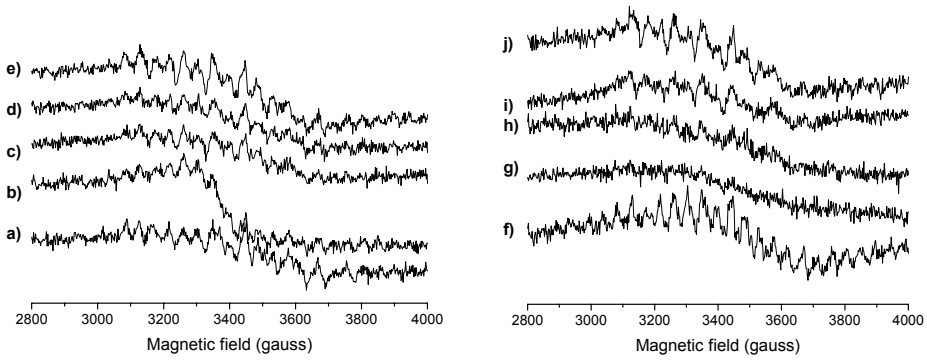

Figure 5.11 X-Band ESR spectra at 77 K in CH_3CN in the presence of CCl_3CO_2H (10 mM), cyclooctene (1 M) and 1,2-dichlorobenzene (0.5 M). Left: **1** (1 mM), from bottom to top, a) t = 15, b) 30, c) 45, d) 46 (immediately after H_2O_2 addition) and e) 60 min. Right: **2a (**1 mM) at f) t = 0, g) 15, h) 30, i) 45 and j) 60 min.

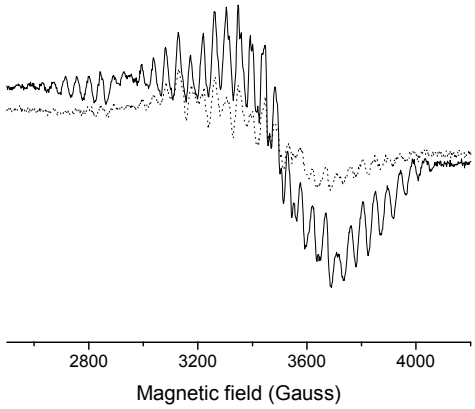

Figure 5.12 X-band ESR spectra of **2b** 1 mM in CH_3CN with 10 equiv. of CCl_3CO_2H acid during the oxidation of cyclooctene with H_2O_2: t = 0 (solid line) and 60 min (dotted line).

5.2.1 Electrochemistry under catalytic conditions

Cyclic voltammetry under catalytic conditions, in the presence of both cyclooctene and H_2O_2, is depicted in Figure 5.13 for both complexes **2a** and **2c** (formed *in situ* from **2b** in the presence of CCl_3CO_2H).

When H_2O_2 (50 equiv. w.r.t. manganese dimer) is added (compare Figure 5.13a.ii and 5.13b.ii with 5.13a.i and 5.13b.i, respectively) there are three important aspects of note. First of all, the redox wave at $E_{p,a}$ 0.25 V (*i.e.* two-electron reduction of **2a**) is unaffected by the presence of (excess) H_2O_2. This shows that there is no significant interaction between **2a** and H_2O_2. Secondly, a new irreversible oxidation wave at $E_{p,a}$ 1.00 V is observed (Figure 5.13a.ii and 5.13b.ii), which persists until all H_2O_2 has been consumed (Figure 5.13a.iii and 5.13b.iii), as observed in the absence of cyclooctene (see Chapter 4, section 4.3.5 and Figure 4.19). This new cathodic wave is tentatively assigned to a Mn^{II}_2-peroxo species, derived from **2c** where one of the water ligands has been replaced by hydrogen peroxide. This Mn^{II}_2-peroxo species is stable in the presence of a large excess of cyclooctene substrate (1000 equiv. w.r.t. the manganese dimer), excluding this species as active species in the oxidation of alkenes. Thirdly, the oxidation of both the Mn^{II}_2-peroxo species and of species **2c** ($E_{p,a}$ 1.00 and 1.10 V, respectively) is completely irreversible in the presence of H_2O_2, *i.e.* the return reduction steps are no longer observed at $E_{p,c}$ 0.99 and 0.71 V (Figure 5.13a.ii and 5.13b.ii). When all H_2O_2 is consumed (Figure 5.13a.iii and 5.13b.iii), these cathodic waves due to H**2d**$^+$ and **2d** (at $E_{p,c}$ 0.99 and 0.71 V, respectively) are observed again. It is apparent that H_2O_2 reacts with **2d** quickly and the resulting Mn^{III}_2-peroxo species (species A in Scheme 5.3) in turn reacts quickly with the alkene substrate.

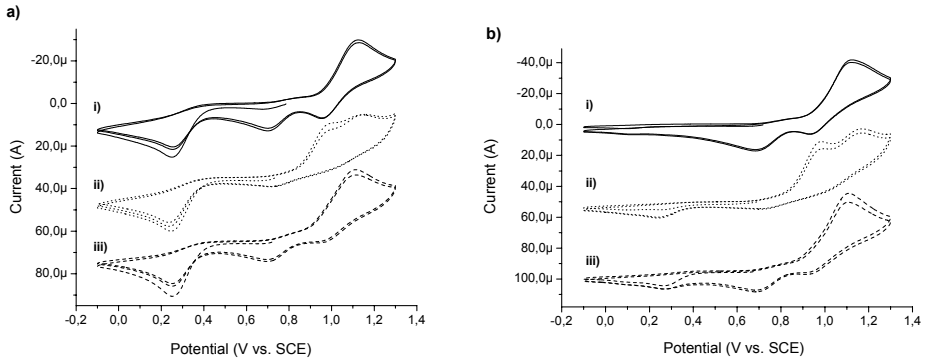

Figure 5.13 a) Complex **2a** (1 mM) and b) **2b** (1 mM) in CH_3CN (0.1 M $TBAPF_6$) in the presence of CCl_3CO_2H (10 mM), cyclooctene (1000 mM) and 1,2-dichlorobenzene (500 mM) before (solid lines) and just after (t ~ 30 sec) addition of H_2O_2 (50 equiv. w.r.t Mn-dimer) (dotted lines) and ~15 min after (dashed lines).

5.3 ^{18}O labeling and ^{2}D isotope effects

A key probe in 'tracking' oxygen atoms in oxidation catalysis is through $^{16}O/^{18}O$ isotope labeling. Both labelled hydrogen peroxide ($H_2{}^{18}O_2$) and/or labeled water ($H_2{}^{18}O$) were employed to identify the origin of the oxygen atoms incorporated into both *cis*-diol and epoxide products. To circumvent the lag-period observed with **1**/CCl_3CO_2H, **2a** (1 mM) was used as the catalyst source.[viii]

With the combination of **2a**/CCl_3CO_2H (1 mM/10 mM) and employing 2% v/v $H_2{}^{18}O_2/H_2{}^{16}O$, single ^{18}O incorporation in the *cis*-diol product is observed, while ^{18}O incorporation into the epoxide product is 71% (Table 5.5, entry 1). For the complementary experiment with 2% v/v $H_2{}^{16}O_2/H_2{}^{18}O$, again single ^{18}O incorporation in the *cis*-diol product and 38% ^{18}O incorporation in the epoxide product is found (entry 2). Similar results were obtained in the *cis*-dihydroxylation/epoxidation of *cis*-2-heptene (entry 5). Interestingly, when using 25 mol% CCl_3CO_2H, no significant difference in ^{18}O incorporation in either the *cis*-diol or epoxide product is observed compared with the reaction with 1 mol% of CCl_3CO_2H (entry 4). In the absence of CCl_3CO_2H (using **2a** as catalyst), reduced ^{18}O incorporation from $H_2{}^{18}O$ into the *cis*-diol (single incorporation, 80%) and the epoxide (21%) is observed, as well as greatly reduced conversion (entry 3).

[viii] $H_2{}^{18}O_2$ is only available as a 2% v/v solution in $H_2{}^{16}O$ while 50 % w/w H_2O_2 solution is employed in typical catalysis experiments. However, the presence of water in the reaction medium allows for 'normal' catalysis to take place, *i.e.* no lag-period is observed. The *cis*-diol/epoxide ratio obtained at several H_2O_2/H_2O ratios (50, 30, 20 and 2% H_2O_2 in H_2O) indicates that no significant difference in the chemistry observed under labelling conditions compared with standard reaction conditions.

Table 5.5 Catalytic oxidation of cyclooctene by **2a** (0.1 mol%) at 0 °C in the presence of trichloroacetic with $H_2{}^{18}O_2/H_2{}^{16}O$ and $H_2{}^{16}O_2/H_2{}^{18}O$ (corrected for H_2O_2/H_2O isotopic composition).[a,b]

Entry	H_2O	H_2O_2	Acid (mol%)	*cis*-diol %$^{16}O^{18}O$	epoxide %^{18}O	t.o.n. *cis*-diol	t.o.n. epoxide
1	^{16}O	^{18}O	CCl_3CO_2H (1)	104	71	120	55
2	^{18}O	^{16}O	CCl_3CO_2H (1)	93	38	105	50
3	^{18}O	^{16}O	-	80	21	12	18
4	^{18}O	^{16}O	CCl_3CO_2H (25)	93	34	95	50
5[c]	^{18}O	^{16}O	CCl_3CO_2H (1)	95	38	67	58
6[d]	^{18}O	^{16}O	CCl_3CO_2H (1)	95	32	425	235

a) ^{18}O-labeling studies were performed on cyclooctene on 1/20th scale of the standard conditions, with the adjustment that a 2% H_2O_2 (aq.) solution was used and the peroxide was added batchwise in four portions every 15 min (*i.e.* at the same rate and amount of H_2O_2 addition under typical reaction conditions). See procedure E in Appendix C. ^{18}Oxygen incorporation was determined by GC-MS (CI) after 60 min reaction time. b) Values +/-5%. c) *Cis*-heptene as substrate. d) With 20 % $H_2O_{2(aq)}$ solution.

As with **2a**, for other μ-carboxylato bridged complexes (*i.e.* 2,6-dichlorobenzoato (**13**), 2,4-dichlorobenzoato (**14**) and 4-hydroxybenzoato (**22**)), ^{18}O incorporation from $H_2{}^{18}O$ into the *cis*-diol product is relatively insensitive to the nature of the acid (82-94%, single oxygen incorporation from H_2O, Table 5.6). However, for the epoxide product the extent of ^{18}O incorporation from $H_2{}^{18}O$ ranges from 3-38% depending on the bridging carboxylato ligand.

Table 5.6 $^{16/18}O$ isotopic distribution in the oxidation products of cyclooctene by $[Mn^{III}{}_2(\mu\text{-}O)(\mu\text{-}RCO_2)_2(tmtacn)_2]^{2+}$ complexes (0.1 mol%) at 0 °C in the presence of the corresponding carboxylic acid with $H_2{}^{18}O/H_2{}^{16}O_2$ (corrected for H_2O/H_2O_2 isotopic composition).[a]

Entry	Catalyst[b]/acid (mol%)	*cis*-diol $^{16}O^{18}O$ (%)	epoxide ^{18}O (%)	T.O.N. *cis*-diol	T.O.N. epoxide
1	**13** / 2,6-dichlorobenzoic acid (3)	93	19	115	15
2	**14** / 2,4-dichlorobenzoic acid (1)	90	13	60	25
3	**14** / 2,4-dichlorobenzoic acid (25)	94	11	110	40
4	**22** / 4-hydroxybenzoic acid (1)	86	12	20	35
5	**29** / 2-hydroxybenzoic acid (1)	82	3	25	50

a) ^{18}O-labelling studies where performed on cyclooctene on $^{1}/_{20}{}^{th}$ scale of standard conditions, with the adjustment that a 2% H_2O_2 was added in four portions each every 15 min, reported data after 60 min reaction time. See general procedure E (Appendix C) for full experimental details. b) 0.1 mol% $[Mn^{III}{}_2(\mu\text{-}O)(\mu\text{-}RCO_2)_2(tmtacn)_2]^{2+}$.

The use of D_2O_2/D_2O in place of H_2O_2/H_2O resulted in no significant changes to either the time dependence of product formation or the overall conversion (Table 5.7, entries 1-4), indicating that proton (or hydrogen atom) transfer does not play a role in determining the outcome of the reaction with respect to *cis*-diol/epoxide formation.

Table 5.7 Oxidation of cyclooctene catalyzed by **2a** (0.1 mol%) at 0 °C in the presence of CCl_3CO_2H (1.0 mol%) with H_2O_2 and D_2O_2.

Entry	Oxidant[a]	conv. (%)	t.o.n. *cis*-diol	t.o.n. epoxide	mass. bal. (%)
1	30% H_2O_2 [b]	89	425	240	77
2	30% H_2O_2 (diluted from 50% with H_2O)	92	405	240	73
3	30% H_2O_2 (diluted from 50% with D_2O)	90	415	240	75
4	30% D_2O_2 (in D_2O)[b]	94	395	250	70

a) Reactions were performed in 15 ml instead of 10 mL of CH_3CN to prevent phase separation of the CH_3CN and cyclooctene. b) Used as received (without dilution).

5.4 Mechanistic considerations

5.4.1 Speciation analysis

A summary of the complexes involved during phase I-III of the catalytic *cis*-dihydroxylation and epoxidation of alkenes is provided in Scheme 5.2. In the carboxylic acid promoted catalytic oxidation of alkenes by **1**, the first step is reduction of H**1**$^+$ by H_2O_2, followed by ligand exchange to form **2a**. Hence the use of dinuclear manganese bis(carboxylato) complexes, either prepared or generated *in situ* prior to initiation of catalysis, results in the elimination of the lag period.

Alternatively to using **1**, complex **2b** can be used as catalyst precursor. Under the reaction conditions, prior to addition of H_2O_2, the Mn^{II}_2 complex **2b** is converted immediately and quantitatively to **2c**, and upon addition of H_2O_2 almost complete conversion of **2c** to **2a** is observed within the first 10 min of the reaction. Although Mn^{II}_2 complexes, *i.e.* **2c**, may be present during the lag period, the onset of catalytic activity does not coincide with their formation. Furthermore, the observation that **2c** can interact with H_2O_2 to form a meta-stable complex (as observed by electrochemistry), supports the conclusion that Mn^{II}_2 complexes are not directly involved in the catalytic cycle.

Regardless of the various processes that occur prior to the onset of catalytic activity (depending on the manganese dimer used), it is evident that catalysis is observed only when either **2a** and/or **2d** are present in solution. Cyclic voltammetry in the presence of H_2O_2 shows that **2d** is not observed until all H_2O_2 has been consumed (see Figure 5.13), whereas the amount of **2a** is relatively unaffected by the addition of H_2O_2. Hence, it is reasonable that the species, which interacts with H_2O_2, is the dinuclear Mn^{III}_2 complex, **2d**. The preponderance of **2a** in solution (>85% depending on conditions) compared with **2d** suggests that **2a** is directly involved in the catalytic cycle and that the opening of the μ-oxo

bridge of **2a** is limiting reactivity. That is, **2a** acts as a catalyst resting point, which is in equilibrium with **2d**. Coordination of H_2O_2 to **2d** is followed by reaction of the H_2O_2-activated species with the substrate to reform **2a** (and/or **2d**).

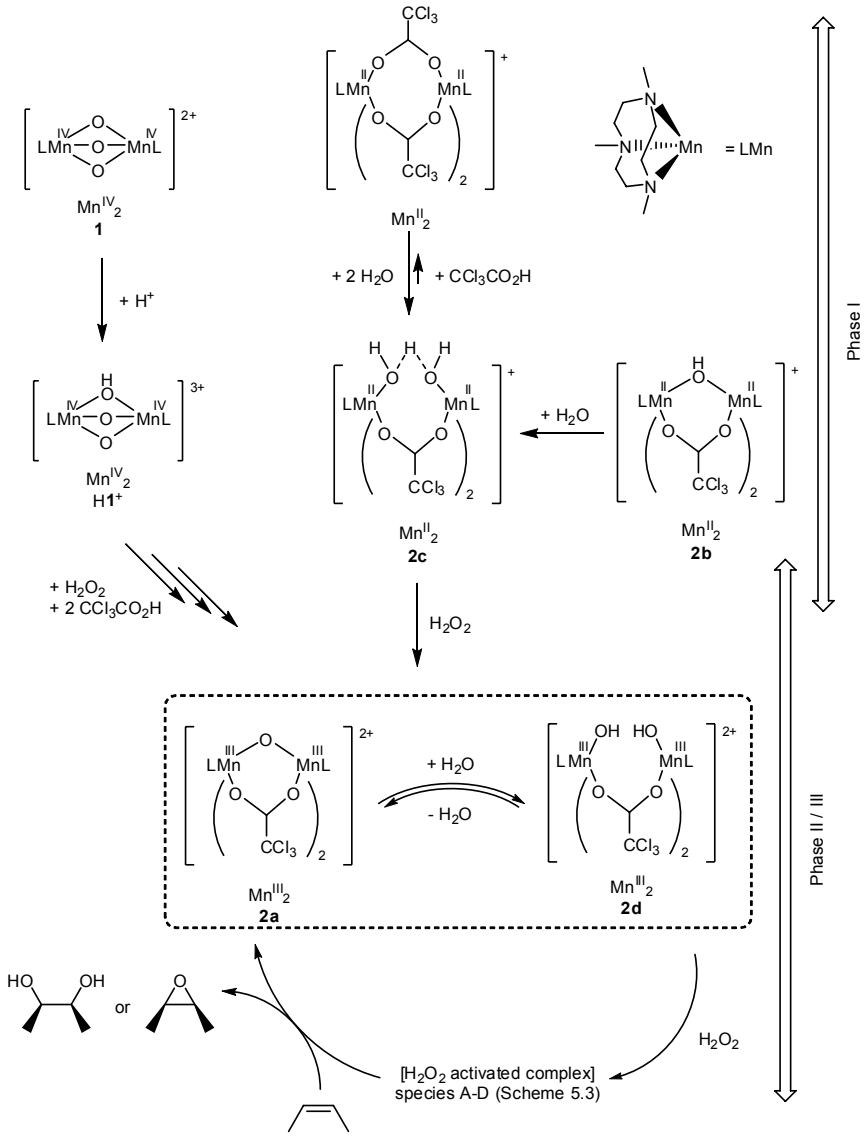

Scheme 5.2 Summary of processes which occur during phases I to III during the catalytic oxidation of alkenes (see Figure 3.4, Chapter 3). Complexes **1**[5] and **2a-c** have been isolated (see Chapter 4). Evidence for the structure of complex **2d** is provided in Chapter 4.

The primary role of H_2O in determining activity appears to be the formation of **2d**. The equilibrium between **2d**, which interacts with H_2O_2, and **2a** is affected strongly by both the amount of H_2O present and the carboxylic acid concentration. That this is the case is supported further by comparison of glutaric and acetic acid promoted reactions. In the case of glutaric acid, formation of the Mn^{III}_2 'open' species (analogous to **2d**) occurs much more readily than for the corresponding acetato complex and the glutarato bridged complexes shows much higher reactivity than the corresponding acetato complexes, despite being 'electronically' equivalent. Furthermore, the rate of exchange of the μ-oxo bridge of the Mn^{III}_2 bis(carboxylato) complexes is dependent on the nature of the carboxylato ligands with the rate increasing with increasing electron withdrawing character of the ligand as was apparent from exchange of the μ-oxo bridge with the oxygen-18 from solvent $H_2{}^{18}O$ (section 4.5, Chapter 4)

Hence, both **2a** and **2d** can be implicated directly in the catalytic cycle and the prerequisite for activity is the formation of **2d** from **2a**. Once formed, **2d** interacts with H_2O_2 followed by oxidation of the substrate by the 'H_2O_2-activated complex' to reform **2a**.

5.4.2 H_2O_2-activated species

Although two complexes in the catalytic cycle, *i.e.* **2a**/**2d**, have been identified experimentally, a key question now arises: are two catalytically active species involved (one for *cis*-dihydroxylation and one for epoxidation) or, if a common H_2O_2-activated intermediate is responsible for both oxidation processes, what is the nuclearity (mono- or dinuclear) and nature of such species (peroxo or high valent Mn-oxo).

Several aspects of the current catalytic system indicate that a common intermediate is involved, or at least that there is a common immediate precursor to the species responsible for *cis*-diol and epoxide formation, respectively. Firstly, the conversion of cyclooctene to *cis*-diol and epoxide products commences simultaneously and the processes, which change the duration of the lag period (*e.g.* catalyst preactivation, initial oxidation state of the catalyst, H_2O content of the reaction mixture, nature of carboxylic acid) all affect the lag period for both *cis*-dihydroxylation and epoxidation in the same manner. Secondly, both *cis*-dihydroxylation and epoxidation show a similar time dependence over the course of the reactions. Significantly lower *cis*-diol/epoxide ratios are observed during the initial stages of the reaction when the well defined complexes **2a**, **2b** or **2c** are used as catalysts or high acid concentrations are employed. However, this decrease is due to the low water content of the reaction mixture during the early stages and the 'dehydrating' effect of high acid concentrations since addition of H_2O restores normal catalytic behavior. Hence, any reaction mechanism should take into consideration a common catalyst being, most probably, responsible for both *cis*-dihydroxylation and epoxidation.

5.4.2.1 Active species proposed in literature

The majority of mechanisms, proposed previously for the tmtacn family of manganese catalysts, have favored the formation of high-valent oxidizing species,[6] with the vast majority being mononuclear species. In the most detailed study available to date, based on ESI-MS, mononuclear high-valent Mn^{IV}=O (**5.1**) and Mn^{V}=O species (**5.2**) were proposed

by Lindsay Smith and co-workers during the oxidation of phenols[7] and the epoxidation of cinnamic acid[8] derivatives by Mn^{II}-tmtacn (in the presence of oxalic acid and other additives) (Figure 5.14).[9,10] De Vos and coworkers have proposed a similar structure as active species to account for the effect of oxalate additive.[11]

From Hammett parameters on a series of substituted cinnamic acid derivatives Lindsay Smith and coworkers concluded that the active species is electrophilic in nature and ^{18}O-labelling studies showed incorporation of oxygen in the epoxide mainly from H_2O_2 (93%) in addition to from H_2O (ca. 10%) using oxalic acid as additive in basic aqueous CH_3CN.[8] ^{18}O-labeling studies on the epoxidation of 4-vinylbenzoic acid in aqueous carbonate buffer (pH 8) by Hage *et al.* had already revealed that oxygen in the epoxide product was exclusively derived from H_2O_2 also, showing that both Mn-oxo or Mn-peroxo intermediates could be involved in catalysis.[12]

Although most studies thus far have favoured the formation of high-valent oxidizing species in the Mn-tmtacn catalyzed oxidations of alkenes, there is relatively scant empirical evidence to support such proposals. The most detailed study uses ESI-MS as a single (spectroscopic) technique to support the proposal.[8] However, to base a (proposed) mechanism on a single technique, in particular mass spectrometry,[ix] is delicate and it is important to ensure that the species observed hold relation to the species present in solution during catalysis and are on the catalytic reaction pathway. Moreover, it was noted in this particular study that the additives leading to the most easily detected Mn^{V}=O species, *i.e.* biphenols, actually resulted in slower rates of epoxidation by Mn-tmtacn than in the absence of these additives[8] (thus suggesting that these detected Mn^{V}=O species are not responsible for the observed epoxidation activity).

Shul'pin and coworkers on the other hand, proposed a high-valent dinuclear $Mn^{IV,V}{}_2$ species (**5.4**) (Figure 5.14) to be responsible for epoxidation based upon limited kinetic data alone.[13] However, no spectrosopic data was provided for this species, nor for any other species they proposed to be involved in the catalytic cycle. These kinetic studies are based on only a limited number of data points (typically 3-6 data points) and the large number of parameters used to fit the data are at best an indication of the number of species involved. Hence the assignment of catalyst structures without the support of spectroscopic evidence should be taken with great care.

Che and coworkers have reported on the stoichimetric reaction between $[(tmtacn)(CF_3CO)Ru^{VI}(O)_2)]^+$ **5.5** (Figure 5.14) and alkenes in $^{t}BuOH/H_2O$ (5:1) to yield the corresponding *cis*-diols via a concerted pathway.[14] Their proposition for [3+2] cycloaddition between the *cis*-dioxoruthenium(VI) complex and alkene was based on isolation of a Ru^{III} cycloadduct. Although this study on the stoichiometric reaction between mononuclear Ru-tmtacn and alkenes might hold relevance to the Mn-tmtacn catalyzed oxidations due to the diagonal relationship between Mn and Ru, data were not provided for the claim of preliminary results on catalytic *cis*-dihydroxylation and epoxidation of cyclooctene using $[(tmtacn)(CF_3CO_2)_2Ru^{III}(OH_2)]^+$ in combination with H_2O_2.[14]

[ix] For example, as was shown in Chapter 4 (Figure 4.5b) either only monomers or only dimers can be observed depending upon minor changes of the voltages of the mass spectrometer.

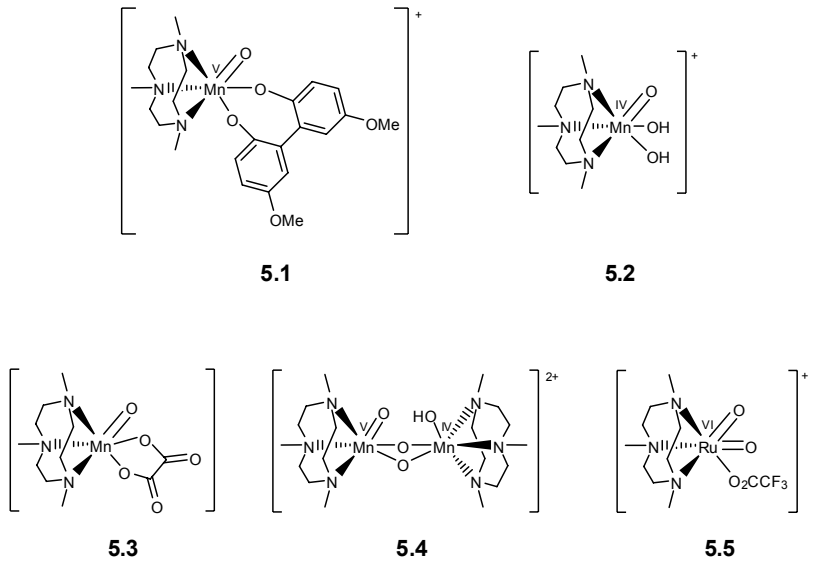

Figure 5.14 Active species proposed by Lindsay Smith[8,9] (**5.1**, **5.2**), De Vos[11] (**5.3**), Shul'pin[13] (**5.4**) and Che[14] (**5.5**).

Recently, in a related 1,4,8,11-tetraazacyclohexadecane-based system, Busch and coworkers[15] have suggested a mononuclear Mn^{IV} peroxy complex $[(Me_2EBC)Mn^{IV}(O)(OOH)]^+$ as being the activated oxidant in the epoxidation of olefins (Figure 5.15), a so-called inorganic peracid,[16,17] based upon the observation of this complex with ESI-MS and a series of ^{18}O labeling experiments.[15] A related η^2-peroxido complex $[Mn^{III}(tmc)(O_2)]^+$ (tmc = 1,4,8,11-tetramethyl-1,4,8,11-tetraazacyclotetradecane) recently isolated by Nam and coworkers, is not capable of oxygenating substrates (*e.g.* cyclooctene) through an electrophilic reaction, however it is capable of deformylating aldehydes via a nucleophilic reaction.[18]

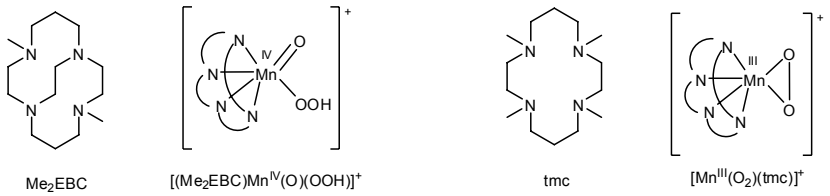

Figure 5.15 Structure of inorganic peracid $[(Me_2EBC)Mn^{IV}(O)(OOH)]^+$ proposed by Busch and coworkers[15] and $[Mn^{III}(tmc)(O_2)]^+$ complex isolated by Nam and coworkers[18].

5.4.2.2 Catalytic oxidations by the system 1/carboxylic acid

Although most mechanisms suggested for the Mn-tmtacn family of catalysts propose the involvement of high-valent manganese-oxo species, no such mononuclear Mn-tmtacn species have been observed in the present catalytic system, despite extensive spectroscopic and electrochemical characterization.[x] While that does not exclude their involvement completely, these observations require that a mechanism, which recognizes that throughout the reaction >95% of the manganese is present in solution as dinuclear Mn^{III}_2 complexes (*e.g.* **2a** and **2d**), is considered also.

The absence of spectroscopic evidence for any H_2O_2-activated complexes during catalysis, indicates that the rate determining step in the catalytic cycle involves formation of **2d** from **2a**. Subsequent coordination of H_2O_2 to **2d** takes place followed by rapid reaction of the H_2O_2-activated complex with the alkene substrate (Scheme 5.2). In addition, the reformation of **2a**, after oxidation of the substrate, is fast and virtually complete.

The inability of H_2O_2 either to reduce or oxidize the Mn^{III}_2 dinuclear complex **2a** and the rapid and irreversible interaction of **2d** with H_2O_2 suggests that the system may bear more similarity with dinuclear carboxylato bridged catalase enzymes and that the formation of high-valent species is at most transient, *i.e.* during the oxygen transfer to the substrate (or hydrogen abstraction in the case of C-H activation). As for dinuclear manganese containing catalase enzymes[19] one role of the carboxylato bridges might be to suppress the occurrence of one-electron processes, thus avoiding radical chemistry.

It is clear that neither **2a**, **2c** nor **2d** can effect direct oxygen transfer as all three complexes are stable in the presence of cyclooctene. However, in the present system it is improbable that the dinuclear complex 'splits' to form two mononuclear complexes prior to interaction with H_2O_2. The stability of the complex throughout the reaction and the deactivation of the catalyst observed upon loss of a carboxylato ligand provides credence to this conclusion (Figure 5.5 and 5.6).

The transient nature of the H_2O_2-activated complex (*i.e.* the formation of **2d** from **2a** is slower than the subsequent reaction of the H_2O_2-activated species with the alkene) and the absence of distinct spectroscopic features requires that indirect methods be employed to gain information as to the species nature. ^{18}O isotopic labeling of both H_2O and H_2O_2, provides a powerful probe. Although it is clear that only one of the oxygen atoms incorporated into the *cis*-diol product originates from H_2O_2 and the other oxygen atom from H_2O, the situation is less clear for the epoxide products, where either H_2O_2 or H_2O provide the oxygen atom. The dependence of ^{18}O incorporation into the epoxide from $H_2{}^{18}O$ on the specific acid employed is as striking as is the relative insensitivity of the 1:1 oxygen incorporation into the *cis*-diol from H_2O and H_2O_2. However, for the epoxide there is a correlation between the *cis*-diol/epoxide selectivity of the catalyst/carboxylic acid system and the incorporation of oxygen into the epoxide from H_2O. The incorporation of oxygen

---

[x] Although $[Mn^{II}(CCl_3CO_2)_3]^-$ has been observed by ESR and ESI-MS (see section 5.2), control experiments have shown that it is not involved in catalysis (see Table 3.3, Chapter 3). Likewise, $[Mn^{III}(tmtacn)(salicylate)]^+$ is very unlikely to be involved in catalysis either, see Chapter 6, section 6.1).

from water into the epoxide product ranges from for 18 % for the 2,6-dichlorobenzoate complex (*cis*-diol/epoxide ratio 7) to 13 % for the 2,4-dichlorobenzoic acid complex (*cis*-diol/epoxide ratio 2.7) to 3 % for salicylic acid (*cis*-diol/epoxide ratio 0.7). Furthermore, for the electron withdrawing acid CCl_3CO_2H, although the selectivity towards *cis*-diol formation is lower than that observed for 2,6-dichlorobenzoic acid, the incorporation of oxygen from water into the epoxide product is much higher (33%). In the absence of added carboxylic acid more oxygen from the H_2O_2 is incorporated into both the *cis*-diol and epoxide products, with a significant amount of *cis*-diol showing both oxygen atoms originating from H_2O_2. This observation can be rationalized by considering that the rate of exchange of Mn-OH with H_2O is slower in the absence of an excess of carboxylic acid.

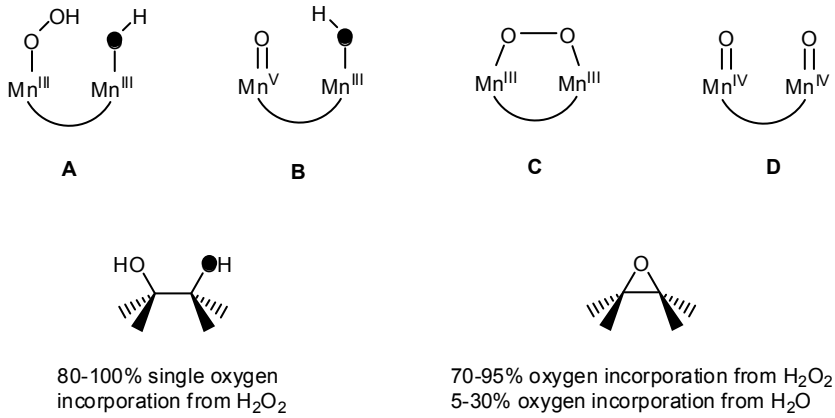

Scheme 5.3 Possible H_2O_2 activated species and observed oxygen incorporation from H_2O_2 and H_2O into *cis*-diol and epoxide products (oxygen originating from H_2O as black circle).

Several dinuclear structures for the 'H_2O_2 activated' complex are proposed in Scheme 5.3. Coordination of H_2O_2 to Mn^{III}_2 dimer **2d** could form either a η^1-O-OH species (A) or $\mu_{1,2}$-peroxo species (C). In the case of species A, homolysis of the O-O bond to form OH· radicals is highly unlikely as the involvement of hydroxyl radicals in the catalytic oxidation has been excluded experimentally (Chapter 3). The ability to engage in oxidation of alkanes and alcohols (Table 3.9, Chapter 3) would suggest that a high-valent (*e.g.* $Mn^V{=}O$)[20] species is involved; however, although heterolysis of the O-O bond in species A would yield a $Mn^{III,V}_2$ species (B), such a species can exist only transiently before intramolecular electron transfer takes place to form a $(Mn^{IV}{=}O)_2$ species (D).

For species C, direct reaction with the substrate is unlikely as this would result in both oxygens of H_2O_2 being incorporated into the *cis*-diol product and 100% incorporation into the epoxide and this is not in agreement with the ^{18}O-labeling studies. Homolysis of the O-O bond, however, would lead to the formation of the Mn^{IV}_2 species D and although exchange of one of the oxygen atoms with water would rationalize the ^{18}O incorporation into the products, a fast exchange of only one of the oxygen atoms with water is required with the remaining oxygen from the hydrogen peroxide being kinetically inert to exchange.

For a symmetric species such as D, such behavior is highly unlikely. The incorporation of oxygen from water into the epoxide would demand that slow exchange takes place as the degree of incorporation is not statistical. Indeed the incorporation of oxygen from water is highly dependent on the nature of the carboxylate employed whilst for the *cis*-diol product the ratio appears to be dependent, albeit only moderately, on the rate of Mn-OH exchange with water.

It is therefore, a reasonable assumption that the reaction of H_2O_2 with **2d** leads, initially, to the formation of a $\{Mn^{III}_2(OOH)(OH)\}$ structure (species A). The Mn^{III} center polarizes the O-O bond to a much greater extent than would be the case in a corresponding Mn^{II}_2 species. Such polarization, and hence reactivity, is facilitated by electron deficient ligands such as $CCl_3CO_2^-$. Hence the catalyst is expected to be electrophilic in nature, as is observed experimentally. The polarization of the O-O bond is reminiscent of the reductive step of the manganese catalase cycle where the O-OH bond is cleaved by transfer of a proton to the terminal oxygen (*i.e.* -O-OH_2).[21] The proton required is available proximally in the present model from the neighboring Mn-OH unit. The more electron withdrawing the carboxylic acid, the greater the acidity of this Mn-OH group will be and hence the more reactive the system.

A mechanism in which a high-valent manganese centre is present as a transient intermediate is proposed in Scheme 5.4.[xi] From the results discussed in Chapter 3 it is clear that the oxygen transfer is a concerted process for both the *cis*-dihydroxylation and epoxidation. Hence the transfer of the oxygen atom(s) to the alkene substrate should occur in a single step. This mechanism proposes that the oxygen atom of the η^1-peroxo bound to the manganese centre, and to a lesser extent the oxygen atom on the adjacent manganese site, engage in an electrophilic interaction with the substrate to form the transition state.[xii] It is at this point that the differentiation in mechanisms between *cis*-dihydroxylation and epoxidation would be expected to take place. Loss of H_2O, coupled with formation of a Mn-O-Mn bond will result in reformation of (*e.g.*) **2a** together with formation of the epoxide product. This step favors the transfer of the oxygen atom of the Mn-O-O-H unit to the alkene but with more electron withdrawing carboxylate ligands, the Mn-O-H oxygen can compete with this process. Such a mechanism is in full agreement with ^{18}O labeling studies for the epoxide product.

For the *cis*-diol product, the loss of H_2O from the transition state is not coupled to formation of a Mn-O-Mn bridge. Instead the diol remains bound via both oxygens and must be displaced subsequently by H_2O before re-entering the catalytic cycle either as (*e.g.*) **2a** or **2d**. Hence it would be expected that carboxylato ligands which inhibit formation of complexes such as **2a** in favor of **2d** should also inhibit the formation of epoxide in favor of *cis*-diol. As was discussed in Chapter 3, steric hinderance is the most important factor in

---

[xi] It should be noted that the active species and mechanism, proposed in Scheme 5.4, are the most likely and most consistent with the experimental data available. However, alternatives should be considered in future investigations, *e.g.* by theoretical calculations.

[xii] This mechanism is similar to one proposed by Busch and coworkers (see Figure 5.15). However, there the *non-coordinated* oxygen atom of the inorganic peracid species $[(Me_2EBC)Mn^{IV}(O)(OOH)]^+$ is proposed to be activated for oxygen transfer.

determining selectivity with more sterically hindered systems favoring *cis*-dihydroxylation. Such a mechanism requires the incorporation of one oxygen atom from H_2O_2 and one from H_2O into the *cis*-diol product, which is indeed the case.

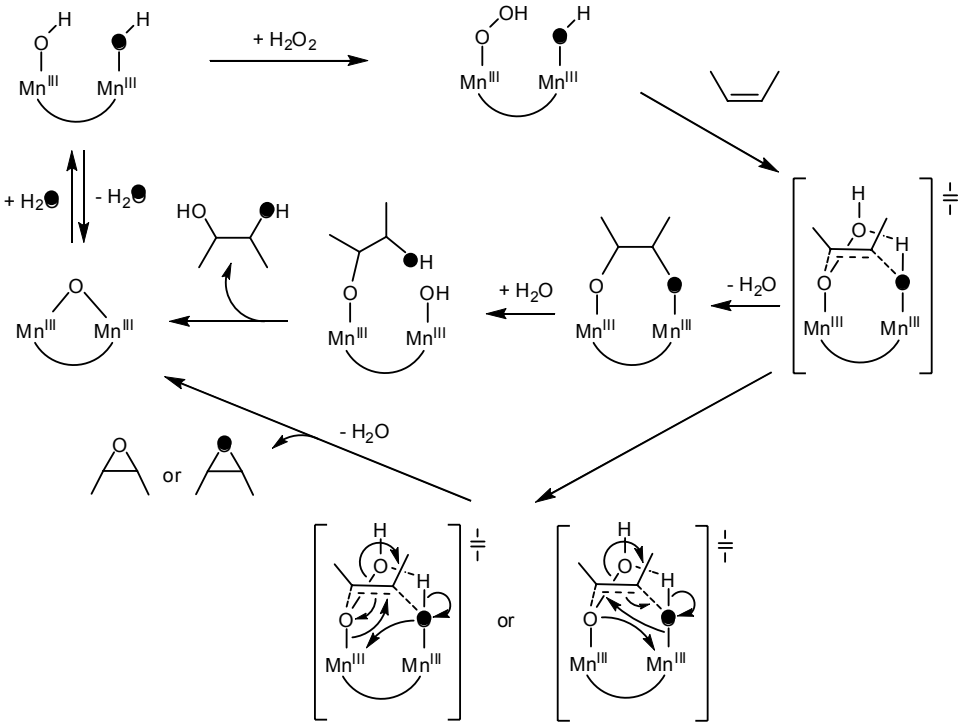

Scheme 5.4 Rationalization of H_2O_2 activation by dinuclear Mn^{III}_2 bis(carboxylato) bridged complexes.

5.5 Summary and conclusions

Over the past decade considerable successes in enhancing the activity of **1** towards catalytic oxidative transformations were achieved most notably through the use of additives (see also section 3.1, Chapter 3). Among the various approaches taken, the use of carboxylic acids has proven to be the most effective in both suppression of the wasteful disproportionation of H_2O_2 and in controlling the activity and selectivity of the catalytic system.

The lag period typically observed in the catalytic system **1**/carboxylic acid is due to two factors. First of all, complex **1** has to be converted to Mn^{III}_2 bis(carboxylato) species such as **2a**, however, this is not the sole factor responsible for the lag period. Secondly, complex **2a** is in equilibrium with the corresponding 'opened' complex **2d**. Interaction of H_2O_2 with the latter species is thought to form the H_2O_2 activated species. The equilibrium between species **2a** and **2d** is governed by the amount of H_2O present in the reaction medium, by the carboxylic acid concentration and by the nature of the carboxylato bridges, that is,

carboxylato ligands which promote formation of such 'opened' species show higher activity compared with electronically equivalent carboxylato ligands which favor μ-oxo bridged species.

The role of the carboxylic acid additive is threefold. First of all, (partial) protonation of one of the μ-oxo bridges in **1** by the carboxylic acid enables reduction by H_2O_2 and subsequent ligand exchange, ultimately giving Mn^{III}_2 bis(carboxylato) species such as **2a**. Secondly, it is in acting as a ligand, that the carboxylate can exert control over both the activity and selectivity of the catalyst. Steric factors appear to be dominant with regard to selectivity, with increasing steric hindrance at the 2- and 6-position of the benzoic acid favoring *cis*-dihydroxylation over epoxidation. Thirdly, the presence of excess carboxylic acid in solution helps stabilising the dinuclear Mn^{III}_2 bis(carboxylato) catalyst and thus enhances its catalytic activity.

Speciation analysis has shown that the vast majority of manganese present in solution is present as bis(carboxylato) bridged Mn^{III}_2 dimers, *i.e.* as **2a** and **2d**. The H_2O_2-activated species, once formed, reacts very quickly with the alkene substrate and as a consequence could not be detected spectroscopically. However, ^{18}O-labeling results are consistent with Mn^{III}_2-η^1-peroxo complex **A** being the catalytically active species.

5.6 References

[1] Brinksma, J.; Schmieder, L.; van Vliet, G.; Boaron, R.; Hage, R.; De Vos, D. E.; Alsters, P. L.; Feringa, B. L. *Tetrahedron Lett.* **2002**, *43*, 2619-2622.
[2] Bortolini, O.; Conte, V. *Mass Spectrom. Rev.* **2006**, *25*, 724-740.
[3] Hage, R.; Krijnen, B.; Warnaar, J. B.; Hartl, F.; Stufkens, D.J.; Snoeck, T. L. *Inorg. Chem.* **1995**, *34*, 4973-4978.
[4] Fujitta, M.; Que, Jr., L. *Adv. Synth.* Catal. **2004**, *346*, 190-194.
[5] Wieghardt, K.; Bossek, U.; Nuber, B.; Weiss, J.; Bonvoisin J.; Corbella, M.; Vitols, S.E.; Girerd, J.J. *J. Am. Chem. Soc.* **1988**, *110*, 7398-7411.
[6] For recent reviews see: a) Hage, R.; Lienke, A. *Angew. Chem. Int. Ed.* **2006**, *45*, 202-222. b) Hage, R.; Lienke, A. *J. Mol. Catal. A: Chem.* **2006**, *251*, 150-158. c) Sibbons, K. F.; Shastri, K.; Watkinson, M. *Dalton Trans*. **2006**, 645-661.
[7] Gilbert, B. C.; Kamp, N. W. J.; Lindsay Smith, J. R.; Oakes, J. *J. Chem. Soc., Perkin Trans. 2* **1998**, 1841-1843.
[8] Gilbert, B. C.; Lindsay Smith, J. R.; Mairata i Payeras, A.; Oakes, J.; Pons i Prats, R. *J. Mol. Cat. A: Chem.*, **2004**, *219*, 265-272.
[9] Gilbert, B.C.; Smith, J. R. L.; Mairata i Payeras, A.; Oakes, J. *Org. Biomol. Chem.* **2004**, *2*, 1176-1180.
[10] Lindsay Smith, J. R.; Gilbert, B. C.; Mairata i Payeras, A.; Murray, J.; Lowdon, T. R.; Oakes, J.; Pons i Prats, R.; Walton, P. H. *J. Mol. Catal. A: Chem.* **2006**, *251*¸114-122.
[11] De Vos, D. E.; De Wildeman, S.; Sels, B. F.; Grobet, P. J.; Jacobs, P. A. *Angew. Chem. Int. Ed.* **1999**, *38*, 980-983.
[12] Hage, R.; Iburg, J. E.; Kerschner, J.; Koek, J. H.; Lempers E. L. M.; Martens R. J.; Racherla, U. S.; Russell S. W.; Swarthoff, T.; van Vliet M. R. P.; Warnaar, J. B.; van der Wolf, L.; Krijnen, B. *Nature* **1994**, *369*, 637-639.

[13] Woitiski, C. B.; Kozlov, Y. N.; Mandelli, D.; Nizova, G. V.; Schuchardt, U.; Shul'pin, G. B. *J. Mol. Catal. A: Chem.* **2004**, *222*, 103-119.
[14] Yip, W.-P.; Yu, W.-Y.; Zhu, N.; Che, C.-M. *J. Am.* Chem. *Soc.* **2005**, *127*, 14239-14249.
[15] a) Yin, G.; Buchalova, M.; Danby, A. M.; Perkins, C. M.; Kitko, D.; Carter, J. D.; Scheper, W. M.; Busch, D. H. *J. Am. Chem. Soc.* **2005**, *127*, 17170-17171. b) Yin, G.; Buchalova, M.; Danby, A. M.; Perkins, C. M.; Kitko, D.; Carter, J. D.; Scheper, W. M.; Busch, D. H. *Inorg. Chem.* **2006**, *45*, 3467-3474. c) Yin, G.; McCormick, J. M.; Buchalova, M.; Danby, A. M.; Rodgers, K.; Day, V. W.; Smith, K.; Perkins, C. M.; Kitko, D.; Carter, J. D.; Scheper, W. M.; Busch, D. H. *Inorg. Chem.* **2006**, *45*, 8052-8061.
[16] Deubel, D. V.; Frenking, G.; Gisdakis, P.; Herrmann, W. A.; Rösch, N.; Sundermeyer, J. *Acc. Chem. Res.* **2004**, *37*, 645-652.
[17] Sheldon, R. A.; Kochi, J. K. *Metal-Catalyzed Oxidations of Organic Compounds*, Academic Press, New York, **1981**.
[18] Seo, M. S.; Kim, J. Y.; Annaraj, J.; Kim, Y.; Lee, Y.-M.; Kim, S.-J.; Kim, J.; Nam, W. *Angew. Chem. Int. Ed.* **2007**, *46*, 377-380.
[19] See Chaper 2 and references cited therein.
[20] a) Adam, W.; Roschmann, K. J.; Saha-Möller, C. R.; Seebach, D. *J. Am. Chem. Soc.* **2002**, *124*, 5068-5073. b) Meunier, B.; Guilmet, E.; De Carvalho, M.; Poilblanc, R. *J. Am. Chem. Soc.* **2000**, *122*, 2675. c) Bernadou, J.; Meunier, B. *Chem. Commun.* **1998**, 2167-2173. d) Balahura, R. J.; Sorokin, A.; Bernadou, J.; Meunier, B. *Inorg. Chem.* **1997**, *36*, 3488-3492. e) Nam, W.; Valentine, J. S. *J. Am. Chem. Soc.* **1993**, *115*, 1772-1778.
[21] Whittaker, M. M.; Barynin, V. V.; Antonyuk, S. V.; Whittaker, J. W. *Biochemistry* **1999**, *38*, 9126-9136.

Chapter 6
Salicylic, L-ascorbic and oxalic acid additives

*A comparison is made between the **1**/carboxylic acid promoted oxidation of alkenes and the combination of **1** with salicylic acid, L-ascorbic acid and oxalic acid additives with the aim to establish whether these systems behave, mechanistically, in a similar manner as the system **1**/carboxylic acid discussed in the previous chapters. While the use of salicylic acid results in a similar catalytic system, the systems employing either L-ascorbic or oxalic acid exhibit a more complicated behaviour.*

Emphasis thusfar has rested on the **1**/CCl_3CO_2H promoted catalytic oxidation of alkenes, however, it should be stressed that all (substituted) alkanoic and benzoic acids tested act essentially by the same mode of action (Chapter 3, Table 3.6 and Chapter 5). That is, when the reaction is carried out with the combination **1**/carboxylic acid, a lag period is observed before c*is*-dihydroxylation and epoxidation commence simultaneously and this time corresponds with the formation of Mn^{III}_2 bis(μ-carboxylato) complexes and, as for the combination **1**/CCl_3CO_2H, the formation of Mn^{III}_2 bis(μ-carboxylato) complexes is key to catalytic activity. However, with salicylic acid the reaction exhibited some spectroscopic pecularities, although, as will be shown, it behaves similar to the other carboxylic acids employed.

Furthermore, during the course of these studies, the question arose as to whether the additives used by others, *i.e.* L-ascorbic acid[1] (Berkessel *et al.*) and oxalate buffer[2] (De Vos *et al.*), play a similar role as CCl_3CO_2H. In order to make a realistic comparison between the additives found to be effective for the epoxidation of alkenes by the groups of Berkessel and De Vos, both L-ascorbic acid and oxalic acid where tested under the 'standard' conditions[i] used for the **1**/CCl_3CO_2H promoted reaction as described in this thesis.

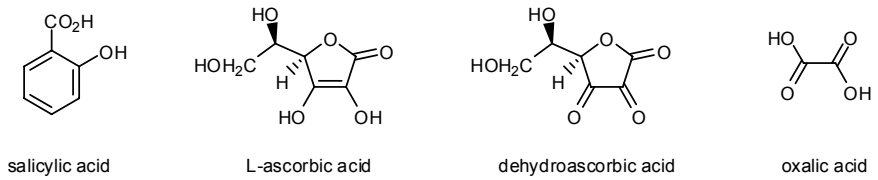

Figure 6.1 Salicylic acid, L-ascorbic acid, dehydroascorbic acid and oxalic acid additives.

6.1 Salicylic acid

6.1.1 Catalytic oxidation of cyclooctene

From the time course of the reaction (1 mol% of salicylic acid) (Figure 6.2 and Table 6.1, entry 1), it is apparent that i) there is an initial lag period and ii) both *cis*-diol and epoxide formation start concurrently, as for all other carboxylic acids examined (see Chapter 3). The lag period is due to the delayed transformation of the $\{Mn^{IV}_2(\mu\text{-}O)_3\}$ bridged complex **1** to a Mn^{III}_2 bis(carboxylato) complexes such as **2a**/**2d** (see Chapter 5).

Upon increasing the concentration of salicylic acid (5 and 10 mol%), it is apparent that epoxidation is favored over *cis*-dihydroxylation (Table 6.1, entries 1-3). A higher preference for epoxidation at increased carboxylic acid concentration was observed for other carboxylic acids such as CCl_3CO_2H also (section 5.1.2, Chapter 5). Similarly, 5-bromosalicylic acid and 3-hydroxybenzoic acid show preferential epoxidation over

[i] See general procedure A in Appendix C. It should be noted that neither Berkessel *et al.* nor De Vos *et al.* have reported on using cyclooctene as substrate.

cis-dihydroxylation (entries 8 and 6). 4-Hydroxybenzoic acid gives a substantially lower *cis*-diol/epoxide ratio (1.3, entry 7, Table 6.1) compared with the other benzoic acids examined (typically 2-3:1, Table 3.6, Chapter 3). The mononuclear $[Mn^{III}(salicylato)(tmtacn)]^+$ complex **29** (1 mol%) (*vide infra*) (in combination with 1 mol% of salicylic acid) gives similar results as when the system **1**/salicylic acid is used as catalyst precursor (entries 5 and 1, respectively), however the lag period is reduced from 2 h to 45 min, and as a consequence the t.o.n.'s obtained are somewhat higher (the *cis*-diol/epoxide ratio is not affected). For the substrate 1-octene the system **1**/salicylic acid gives mainly epoxidation (entry 4). Both oxalic acid and L-ascorbic acid additives give slightly higher conversion then salicylic acid (entry 2 in Table 6.3 and entry 2 in Table 6.4, respectively), however, for all these three additives the epoxide is the main product.

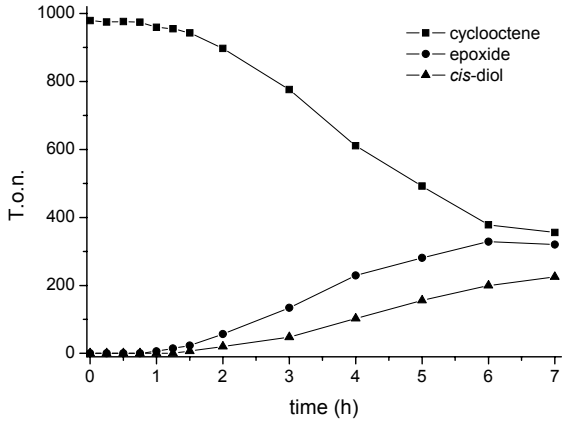

Figure 6.2 Catalytic oxidation of cyclooctene by **1** (1 mM) in the presence of salicylic acid (10 mM, 1 mol%) in CH_3CN employing H_2O_2.

Table 6.1 Catalytic oxidation of cyclooctene employing hydroxy- and methoxy-substituted benzoic acids as additives.[a]

Entry	Catalyst / carboxylic acid (mol%)	conv. (%)	t.o.n. *cis*-diol	t.o.n. epoxide	mass. bal. (%)
1	**1** / salicylic (1)	64	225	320	90
2	**1** / salicylic (5)	74	132	510	90
3	**1** / salicylic (10)	61	102	431	92
4	**1** / salicylic (1)[b]	75	30	590	87
5	**29** / salicylic (1)	75	249	371	87
6	**1** / 3-hydroxybenzoic acid (1)	69	260	325	89
7	**1** / 4-hydroxybenzoic acid (1)	46	219	170	93
8	**1** / 5-bromosalicylic acid (1)	62	252	296	92
9	**1** / 2-methoxybenzoic acid (1)	47	244	158	93
10	**1** / 4-methoxybenzoic acid (1)	26	137	83	96

a) According to general procedure A (Appendix C). b) 1-Octene as substrate.

6.1.2 Salicylic acid complexes

The Mn^{III}_2 bis(carboxylato) complex of salicylic acid (complex **28**) could be generated *in situ* by hydrazine reduction of **1** in CH_3CN in the presence of 2 equiv. of salicylic acid. Although the dinuclear complex $[Mn^{III}_2(\mu\text{-}O)(\mu\text{-}2\text{-hydroxybenzoato})_2(tmtacn)_2]^{2+}$ **28** could be isolated once in very low yield by the general synthesis method employing ascorbic acid as reductant (see Appendix C), even in dry CH_3CN this complex is unstable and converts readily to the more stable green mononuclear complex $[Mn^{III}(salicylato)(tmtacn)]^+$ **29**. The latter mononuclear complex was isolated also (see Appendix B for the synthesis, ^1H NMR, ESI-MS and elemental analysis data). Although this conversion is much faster in water, it also occurs readily in CH_3CN. Both compounds exhibit distinctive UV-Vis spectra (Figure 6.4). ESI-MS of the dinuclear complex **28** in CH_3CN established the presence of the dinuclear complex (*m/z* 371 $[\mathbf{28}]^{2+}$ and 887 $[\mathbf{28}+PF_6]^+$), however, the mononuclear complex $[\mathbf{29}]^+$ (*m/z* 362) was observed as well.

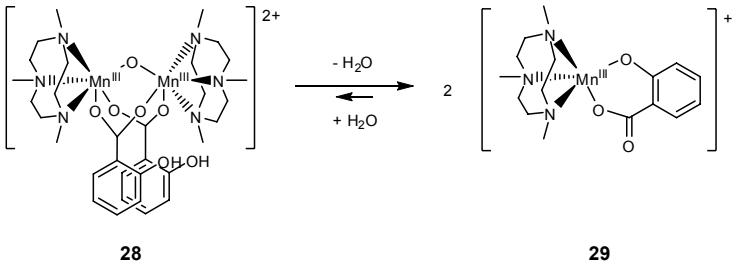

Figure 6.3 Equilibrium between dinuclear $[Mn^{III}_2(\mu\text{-}O)(\mu\text{-}2\text{-hydroxybenzoato})_2(tmtacn)_2]^{2+}$ **28** and mononuclear $[Mn^{III}(salicylato)(tmtacn)]^+$ **29** complexes.

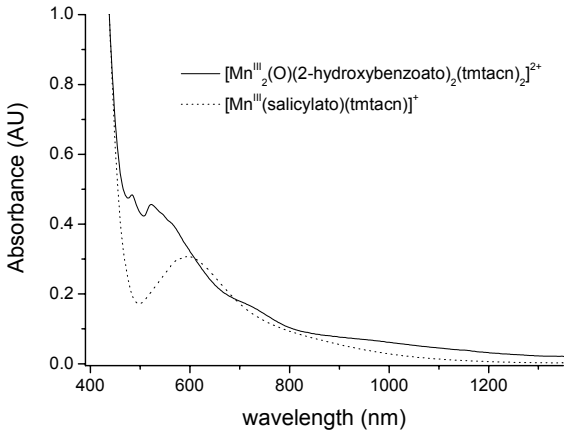

Figure 6.4 UV-Vis spectra in CH_3CN of $[Mn^{III}_2(\mu\text{-}O)(\mu\text{-hydroxybenzoato})_2(tmtacn)_2]^{2+}$ **28** (1 mM) and $[Mn^{III}(salicylato)(tmtacn)]^+$ **29** (2 mM).

6.1.3 Spectroscopic examination

Although, UV-Vis spectroscopy indicated formation of Mn^{III}_2 bis(μ-carboxylato) species from **1** during the lag period for the majority of carboxylic acids studied, for **1**/salicylic acid the increase in absorbance is larger and the spectrum is atypical of Mn^{III}_2 bis(μ-carboxylato) complexes (Figure 6.5). The differences in the absorption spectra of the **1**/salicylic acid catalyzed reaction compared with those of the other carboxylic acids can be assigned, tentatively, being due to a ring-opened dinuclear complex similar to **2d**. When the complex $[Mn^{III}(salicylato)(tmtacn)]^+$ is used as catalyst precursor an identical UV-Vis spectrum is observed as for the reaction with **1**/salicylic acid after the lag period (data not shown). This is in agreement with the observation that the system **1**/salicylic acid and **29**/salicylic acid give essentially the same catalytic reactivity (Table 6.1, entries 1 and 5). The resemblance of both the selectivity and UV-Vis spectra for the system **1**/salicylic acid and **29**/salicylic acid indicates that the same species are present in both cases, most likely a ring-opened dinuclear complex similar to **2d**.

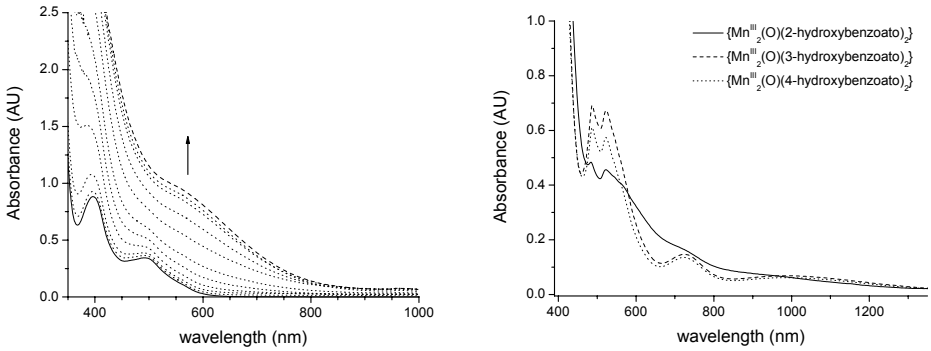

Figure 6.5 a) UV-Vis spectra during the catalytic oxidation of cyclooctene (1 M) in CH_3CN at 0 °C employing **1** (1 mM) and salicylic acid (10 mM) (between 0-2 h). b) UV-Vis spectra in CH_3CN (1 mM) of complexes **29** (2-hydroxybenzoato), **21** (3-hydroxybenzoato) and **22** (4-hydroxybenzoato).

ESI-MS during catalysis does not show formation of a Mn^{III}_2 bis(carboxylato) dimer and instead the mononuclear compound $[Mn^{III}(salicylato)(tmtacn)]^+$ is observed. However, it should be noted that even the Mn^{III}_2 bis(carboxylato) complex of salicylic acid shows this mononuclear species by ESI-MS and that the dinuclear Mn^{III}_2 bis(μ-carboxylato) complex **28** and the mononuclear complex **29** are in equilibrium. During the catalytic oxidation of cyclooctene with the system **1**/salicylic acid, significant ESR signals were not observed at any stage during catalysis, as was the case for **1**/CCl_3CO_2H. This is not surprising considering both the Mn^{III}_2 bis(carboxylato) complexes and the $[Mn^{III}(salicylato)(tmtacn)]^+$ complex are ESR silent (X-band, 77 K).

6.1.4 ^{18}O-labeling

For both salicylic acid and 4-hydroxybenzoic acid oxygen incorporation in the *cis*-diol and epoxide follows the same trend as found for CCl_3CO_2H and a selected set of other carboxylic acids (see also Chapter 5, section 5.3). That is, for the *cis*-diol product one of the oxygen atoms originates from H_2O_2 and the other oxygen originates from H_2O (Table 6.2). For the majority of epoxide product the oxygen incorporated originates from H_2O_2, although part of the product derives its oxygen from H_2O, the ratio depending on the specific carboxylic acid used.

Table 6.2 Catalytic oxidation of cyclooctene by **28** and **29** (0.1 and 0.2 mol%, respectively) at 0 °C in the presence of the corresponding carboxylic acid with $H_2{}^{16}O_2/H_2{}^{18}O$.[a]

Entry	H_2O / H_2O_2	Catalyst	Acid (mol%)	*cis*-diol %$^{16}O^{18}O$	epoxide %^{18}O
1	^{18}O / ^{16}O	**22**	4-hydroxybenzoic acid (1)	86	12
2	^{18}O / ^{16}O	**29**	salicylic acid (1)	82	3

a) ^{18}O-labelling studies were performed on cyclooctene on 1/20 scale of standard conditions, with the adjustment that a 2% H_2O_2 solution was used (see procedure E, Appendix C). Values are corrected for H_2O_2/H_2O isotopic composition. Samples to determine the oxygen incorporation where taken after 60 min and were analysed by GC-MS.

6.1.5 Discussion of the role of salicylic acid

Although it is tempting to consider the involvement of the proximal -OH group of salicylic acid in ligation to the manganese ions, or as proton donor/acceptor group in rationalising preferred epoxidation over *cis*-dihydroxylation for the system **1**/salicylic acid, it should be noted that the selectivity achieved with 3-hydroxybenzoic acid is similar to that of salicylic acid (Table 6.1, entry 1 and 6). Similarly, 4-hydroxybenzoic acid exhibits a *cis*-diol/epoxide ratio of 1.3, which is substantially lower than for all other benzoic acids investigated (typically 2-3:1, Table 3.6, Chapter 3). These observations indicate that the position of the hydroxyl group in salicylic acid is not critical for the low *cis*-diol/epoxide ratio observed and that interactions of this hydroxyl group (*e.g.* via hydrogen bonding) as being the prime factor for this low ratio is unlikely.

For both 3- and 4-hydroxybenzoic acid the synthesis and characterisation of the Mn^{III}_2 bis(carboxylato) complexes was achieved by standard methods (see Appendix B) and the formation of mononuclear complexes was not observed. For salicylic acid the corresponding Mn^{III}_2 bis(carboxylato) complex can be generated in CH_3CN solution from **1**/salicylic acid upon reduction with H_2NNH_2. However, this complex is in equilibrium with the mononuclear complex $[Mn^{III}(salicylato)(tmtacn)]^+$ and only this latter complex could be isolated or observed by ESI-MS during the catalytic oxidation reaction. UV-Vis spectroscopy shows that the mononuclear complex **29** is not present during the catalytic oxidation of cyclooctene by **1**/salicylic acid. Furthermore, ^{18}O-labeling results show similar incorporation of the oxygens in the *cis*-diol and epoxide products for the reaction catalysed

by **1**/salicylic acid as was found for other carboxylic acids (see Chapter 5, section 5.3). Thus, also for the catalytic system **1**/salicylic acid the results are in agreement with a mechanism as that described for **1**/CCl_3CO_2H (Chapter 5, Scheme 5.2 and 5.4).

6.2 L-ascorbic acid

6.2.1 Catalytic oxidation of cyclooctene and 1-octene by 1/L-ascorbic acid

The use of L-ascorbic acid/sodium ascorbate as an effective additive in the catalytic epoxidation of two terminal alkenes (methyl acrylate and 1-octene) and the oxidation of both 2-pentanol (to 2-pentanone) and 1-butanol (to butanoic acid) by Mn(II)/tmtacn has been reported previously by Berkessel and coworkers.[1] The oxidation of 1-octene in the presence of 1 mol% of L-ascorbic acid under our 'standard' conditions resulted in epoxidation with only trace amounts of the *cis*-diol product being formed (Table 6.3, entry 2), in agreement with the results of Berkessel *et al.*[1] (entry 1). In contrast, oxidation of cyclooctene resulted in the formation of substantial amounts of the corresponding *cis*-diol in addition to the epoxide (entry 3).

For L-ascorbic acid, 'normal' reactivity was observed with both *cis*-dihydroxylation and epoxidation occurring concurrently and continuing to do so throughout the reaction (Figure 6.6). However, a lag period was not observed due to immediate reduction of **1** by ascorbic acid. In contrast to L-ascorbic acid, dehydroascorbic acid[ii] exhibited hardly any reactivity, primarily due to its inability to reduce **1** and the absence of a proton source to enable H_2O_2 to engage in reduction of H**1**$^+$ either (see also Chapter 4, section 4.4).

Table 6.3 Catalytic oxidation of 1-octene and cyclooctene by **1** (0.1 mol%) at 0 °C in the presence of L-ascorbic acid (1 mol%).[a]

Entry	Additive (mol%)	Substrate	conv (%)	t.o.n. *cis*-diol	t.o.n. epoxide	Mass. bal. (%)
1	ascorbic acid / Na ascorbate (0.04/0.16)[b]	1-octene	n.d.	0	1110 (max. 1333)	n.d.
2	L-ascorbic (1)[c]	1-octene	89	36	672	82
3	L-ascorbic (1)[c]	cyclooctene	83	275	384	83
4	dehydroascorbic acid (1)[c]	cyclooctene	3	52	76	110

a) Conditions: alkene (1000 mM), 1 (1 mM), L-ascorbic acid (10 mM), 1,2-dichlorobenzene (500 mM) in CH_3CN at 0 °C. H_2O_2 (50 % aq., 1300 mM) was added by syringe pump addition over 6 h, t.o.n. and conversion reported after 7 h (see Appendix C, general procedure A). b) From ref. [1], conditions: 1-octene:H_2O_2:$Mn^{II}(OAc)_2$:tmtacn:L-ascorbic acid:Na ascorbate 1333:3500:1:1.3:0.5:2.1 in CH_3CN/H_2O (6:4). c) No lag period.

[ii] It should be noted that dehydroascorbic acid is only partly soluble at the start of the reaction.

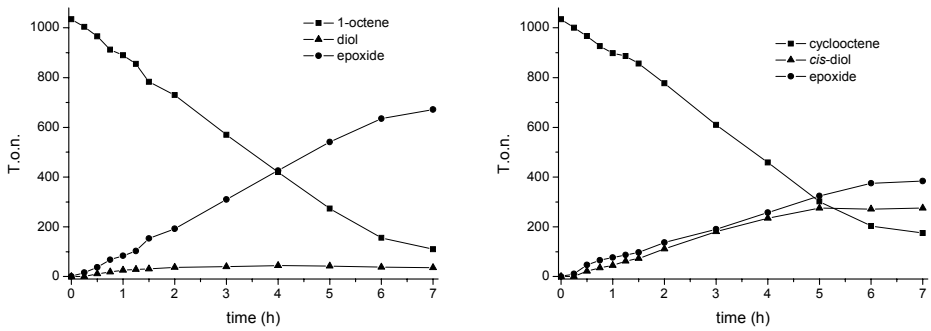

Figure 6.6 Catalytic oxidation of 1-octene (left) and cyclooctene (right) by **1** (1 mM) / L-ascorbic acid (10 mM) in CH_3CN.

6.2.2 Spectroscopic examination

The reaction catalyzed by **1**/ascorbic acid was monitored by UV-Vis spectroscopy. When ascorbic acid (10 mM, 1 mol%) is added to the mixture of **1** (1 mM) and cyclooctene (1 M) in CH_3CN, the absorbance due to **1** (395 and 495 nm) decreases slowly over several min (data not shown). However, once H_2O_2 (50 equiv.) is added an intense, broad spectrum is obtained, which decreases in intensity slowly over time, and eventually, at low concentration of H_2O_2, a spectrum typical for a $\{Mn^{III}_2(\mu\text{-O})(\mu\text{-carboxylato})_2\}$ species is observed (Figure 6.7, dotted line). When more H_2O_2 is added, the same intense featureless spectrum is obtained, which again decreases in intensity slowly in time (Figure 6.7b).

a) b)

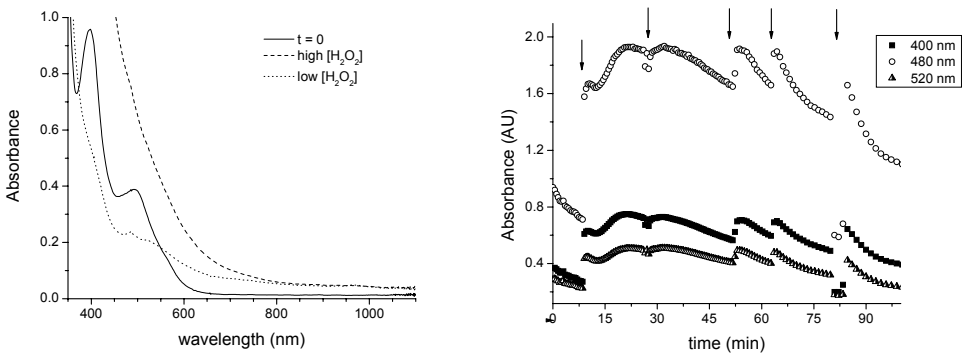

Figure 6.7 UV-Vis spectra obtained during the catalytic oxidation of cyclooctene (1 M) by **1** (1 mM) and L-ascorbic acid (10 mM) in CH_3CN. a) Just after each addition of H_2O_2 (53 mM, every 15 min) an intense featureless spectrum is observed (dashed line), while at low H_2O_2 concentrations (14 min after addition of each batch of H_2O_2) a spectrum typical for a Mn^{III}_2 bis(carboxylato) complex is observed (dotted lines). b) Absorbance in time monitored at 400, 480 and 520 nm (addition of H_2O_2 indicated by arrows).

When followed by EPR spectroscopy, a 16-line spectrum is observed immediately upon addition of ascorbic acid (a = 69 G, Figure 6.8a i). This 16-line species is indicative for a mixed valent $Mn^{III,IV}_2$ species, most likely $\{Mn^{III,IV}_2(\mu\text{-}O)_3\}$, and the unusual small a-value is identical to the value reported by Hage *et* al.[3] for the one-electron reduction of **1** by $Co(Cp)_2$ in CH_3CN. Addition of H_2O_2 (50 equiv.) results in a change in the hyperfine splitting of the 16-line ESR spectrum to 76 G (Figure 6.8a ii-iv).[iii] The intensity of this latter 16-line species decreases slowly over time, but increases in intensity again immediately upon addition of the next batch of H_2O_2 (50 equiv.) (Figure 6.8b). This new 16-line signal is also attributed to a mixed valent $Mn^{III,IV}_2$ species, however, the change in hyperfine coupling constant indicates a change in the nature of the bridging ligand(s).

Attempts to identify this new $Mn^{III,IV}_2$ species (and the Mn^{III}_2 bis(carboxylato) species observed by UV-Vis spectroscopy) by ESI-MS were unsuccessful: *i.e.* **1** was converted completely within 30 min and a series of weak unidentified signals were observed. A possible source of the carboxylato ligands is suberic acid, which can form as an overoxidation product from the *cis*-diol (see Chapter 3, section 3.5). Alternatively, either hydrolysis of the γ-lactone of L-ascorbic acid or dehydroascorbic acid or an oxidation product of either compound (*e.g.*, C-C bond cleavage between the ketone functional groups of dehydroascorbic acid or oxidation of the primary alcohol[iv]) would yield a carboxylic acid.

a) b)

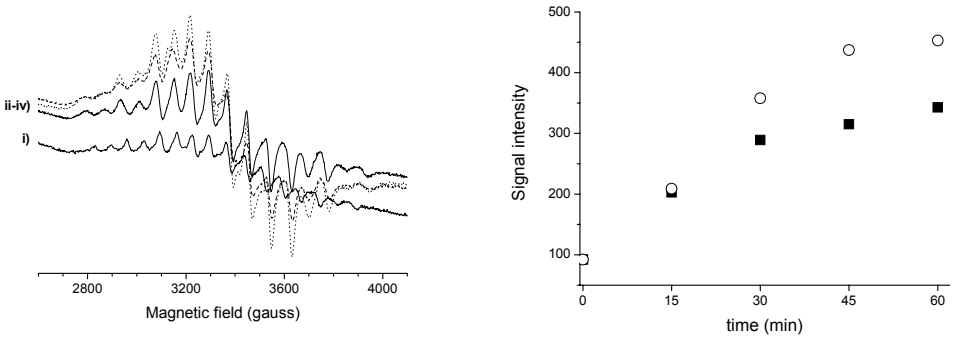

Figure 6.8 ESR spectra during the catalytic oxidation of cyclooctene (1 M) in CH_3CN by **1** (1 mM) and L-ascorbic acid (10 mM): i) after stirring for 15 min without H_2O_2 present (lower solid line, y-axis offset for clarity), ii) 15 mins after 1st addition of H_2O_2 (solid line), iii) 15 min after 2nd addition of H_2O_2 (dashed line); iv) 1 min after 3rd addition of H_2O_2 (dotted) (10 db/20.1 mW) b) Signal intensity just before (solid squares) and just after (open circles) addition of H_2O_2 (50 equiv. w.r.t. Mn_2).

[iii] The interchange between these two $Mn^{III,IV}_2$ species (with a = 69 and 76 G, respectively) is not understood and neither is the relative importance of several other compounds present in solution for this process to occur (*e.g.* H_2O_2, water, L-ascorbic acid, L-dehydroascorbic acid, cyclooctene).

[iv] Note that the combination Mn-tmtacn/L-ascorbic acid is an effective catalytic system for the oxidation of primary alcohols, as reported by Berkessel *et al.*, see ref. [1].

6.2.3 Discussion of the role of L-ascorbic acid

Berkessel and coworkers reported the epoxidation of terminal alkenes by the combination of Mn-tmtacn and L-ascorbic acid.[1] In the present study these results were confirmed; however, especially when cyclooctene is used as substrate with L-ascorbic acid as additive, substantial *cis*-dihydroxylation is observed in addition to epoxidation. That the system **1**/L-ascorbic acid shows higher levels of *cis*-dihydroxylation for cyclooctene than for terminal alkenes is in agreement with the trends observed for the substrate scope of the **1**/carboxylic acid promoted catalytic oxidation of alkenes (Table 3.8, Chapter 3), where the highest levels of *cis*-dihydroxylation were found for internal *cis*-alkenes.

The absence of a lag period for the system **1**/L-ascorbic acid can be attributed to the reducing power of L-ascorbic acid (Scheme 6.1). From UV-Vis spectroscopic data it is clear that a Mn^{III}_2 bis(carboxylato) complex is present at low H_2O_2 concentration. Although a $Mn^{III,IV}_2$ bis(carboxylato) species might be involved as well, as observed by EPR, not all Mn complexes are necessarily in the $Mn^{III,IV}_2$ state at high H_2O_2 concentration.

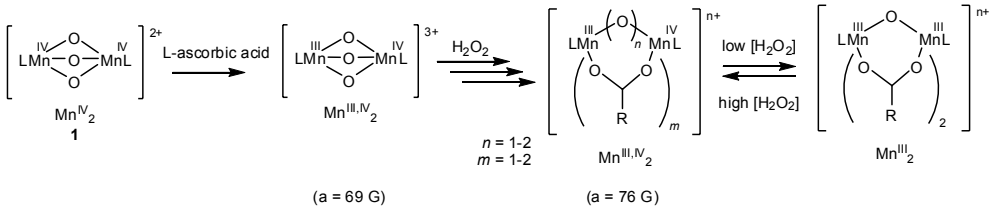

Scheme 6.1 Summary of species present during catalytic oxidation of alkenes by **1**/L-ascorbic acid.

6.3 Oxalic acid

6.3.1 Catalytic oxidation of cyclooctene and 1-octene

The use of oxalate buffer as additive for the catalytic epoxidation of several alkenes by Mn(II)/tmtacn in CH_3CN/H_2O was reported by De Vos and coworkers.[2] Again, in order to make a comparison with the catalytic system **1**/CCl_3CO_2H, reactions were performed under the 'standard' conditions used in this thesis (*i.e.* 0.1 mol% of **1** and 1 mol% of oxalic acid, Table 6.4, entry 2). In accordance with the results obtained by De Vos *et al.* (entry 1), under these 'standard' conditions effective epoxidation of 1-octene was observed. However, when cyclooctene is used as substrate, *cis*-dihydroxylation takes place in addition to epoxidation (entry 3).

The time course of the catalytic oxidation of cyclooctene by **1**/oxalic acid shows two remarkable features compared with all 'normal' carboxylic acids[v] examined. First of all, the

[v] Normally a lag-time is observed and both *cis*-diol and epoxide formation start at the same moment (see Chapter 3).

conversion of the substrate starts directly upon the addition of H_2O_2, *i.e.* no lag period is observed. Secondly, the **1**/oxalic acid system is the only example in which *cis*-dihydroxylation and epoxidation do not start simultaneously: epoxide formation is observed before the commencement of *cis*-diol formation. The time course of the reaction (in terms of substrate consumption and product formation) indicates that there is a distinct change in the nature of the reaction after 3 h (at r.t., 4-5 h at 0 °C), at which point *cis*-dihydroxylation commences and *cis*-diol and epoxide formation occur concurrently (Figure 6.10d).

Table 6.4 Catalytic oxidation of cyclooctene by **1** (0.1 mol%) at 0 °C in the presence of oxalic acid (1 mol%).[a]

Entry	additive (mol%)	substrate	conv. (%)	t.o.n. *cis*-diol	t.o.n. epoxide	mass. bal. (%)
1	oxalic acid / Na oxalate (0.2/0.2)[b]	1-hexene	> 99	0	660	> 98
2	oxalic acid (1)[c]	1-octene	86	0	724	86
3	oxalic acid (1)[d]	cyclooctene	92	169	599	85
4	oxalic acid (1)[c,e]	cyclooctene	97	154	622	81
5	oxalic acid (1)[f]	cyclooctene	99	14	860	89
6	oxalic acid (1)[d,g]	cyclooctene	94	176	564	80
7	oxalic acid (1)[g,h]	cyclooctene	99	15	838	87

a) See general procedure A (Appendix C). b) From ref. [2], conditions: 1-hexene:H_2O_2:oxalate:Mn 666:1000:3:1 in CH_3CN:H_2O (3.5:1). c) No lag period. d) No lag period for epoxidation, lag period for *cis*-dihydroxylation, see also Figure 6.10. e) H_2O_2 and H_2O pretreatment. f) Extra 1 mol% of oxalic acid added at t = 3.5 h, single run. g) Performed at r.t. h) Extra 1 mol% of oxalic acid added at t = 2.5 h.

During the catalytic oxidation of cyclooctene using the **1**/oxalic acid system, two phases can be distinguished: i) up to 3 h (at r.t.[vi]) epoxidation is the main process, while ii) from 3 h onwards both epoxidation and *cis*-dihydroxylation occur at similar rates. This change in product distribution occurs at a time coincident with a pronounced change in the UV-Vis spectrum of the reaction mixture (Figure 6.10 c and d). During the first 3 h of the catalytic oxidation of cyclooctene by **1**/oxalic acid, 7 t.o.n.'s of *cis*-diol and 272 t.o.n.'s of epoxide are obtained, giving a *cis*-diol/epoxide ratio of 0.03. Between 3-5 h[vii], however, 136 t.o.n.'s for the *cis*-diol product and 91 t.o.n.'s of epoxide occur, resulting in a *cis*-diol/epoxide ratio of 1.5 (over this 2 h period). After commencement of substantial *cis*-dihydroxylation, the *cis*-diol/epoxide selectivity in the later stage of the reaction is similar to that found for alkanoic acids (ca. 2-3:1, Table 3.6, Chapter 3) or that reported for **1**/gmha[4] (*cis*-diol/epoxide 1.2). When at 2.5 h another 1 mol% of oxalic acid is added to the reaction mixture, the formation of *cis*-diol (from 3 h onwards) is suppressed in favor of continued epoxide formation (Figure 6.9).

[vi] The same phases and processes are observed at 0 °C, however at slightly longer times. For practical reasons the reaction discussed in this section was performed at r.t.

[vii] Thus during the linear region, before substantial overoxidation occurs.

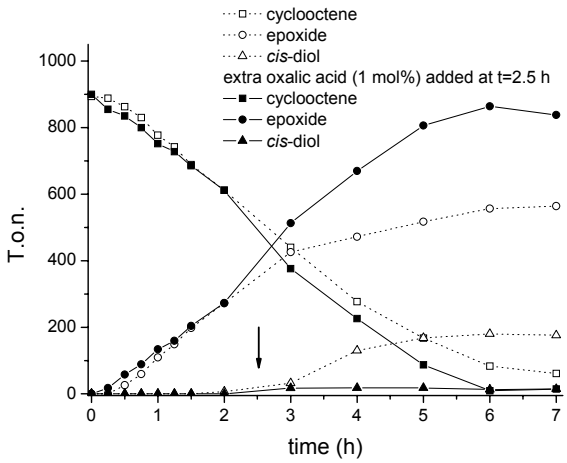

Figure 6.9 Catalytic oxidation of cyclooctene (1 M, squares) in CH_3CN at r.t. employing **1** (1 mM) and oxalic acid (10 mM) yielding both epoxide (circles) and *cis*-diol (triangles) products (dotted lines). When an extra batch of oxalic acid (10 mM) is added at t = 2.5 h (arrow), under otherwise identical conditions, *cis*-dihydroxylation is suppressed and epoxidation remains the predominant process (solid lines).

6.3.2 Spectroscopic examination

Despite the several changes in the UV-Vis spectrum of the manganese catalyst observed during the reaction, EPR active species were not observed. Surprisingly, when the reaction mixture is allowed to stand overnight, the UV-Vis spectrum becomes that typical of a $[Mn^{III}_2(\mu\text{-O})(\mu\text{-carboxylato})_2(tmtacn)_2]^{n+}$ complex (Figure 6.10b). The observation of a UV-Vis spectrum typical for $[Mn^{III}_2(\mu\text{-O})(\mu\text{-carboxylato})_2]^{2+}$ species demonstrates the presence of carboxylic acids capable of acting as bridging ligands. Attempts to identify this/these carboxylato ligand(s) (*e.g.* by ESI-MS, both positive and negative mode) where unsuccessful. Possible candidates for carboxylato ligands on the manganese dimer are oxalic acid or carboxylic acid(s) derived form overoxidation of the *cis*-diol product formed initially. As was shown in section 3.5 (Chapter 3) suberic acid can be formed during the catalytic oxidation of cyclooctene. Since both oxalic acid and suberic acid are diacids, a possible explanation for the absence of clear signal due to a Mn^{III}_2 bis(carboxylato) species with ESI-MS is deprotonation of the non-coordinated carboxylic acid group, resulting in the formation of neutral and thus uncharged species which are not detected by ESI-MS.

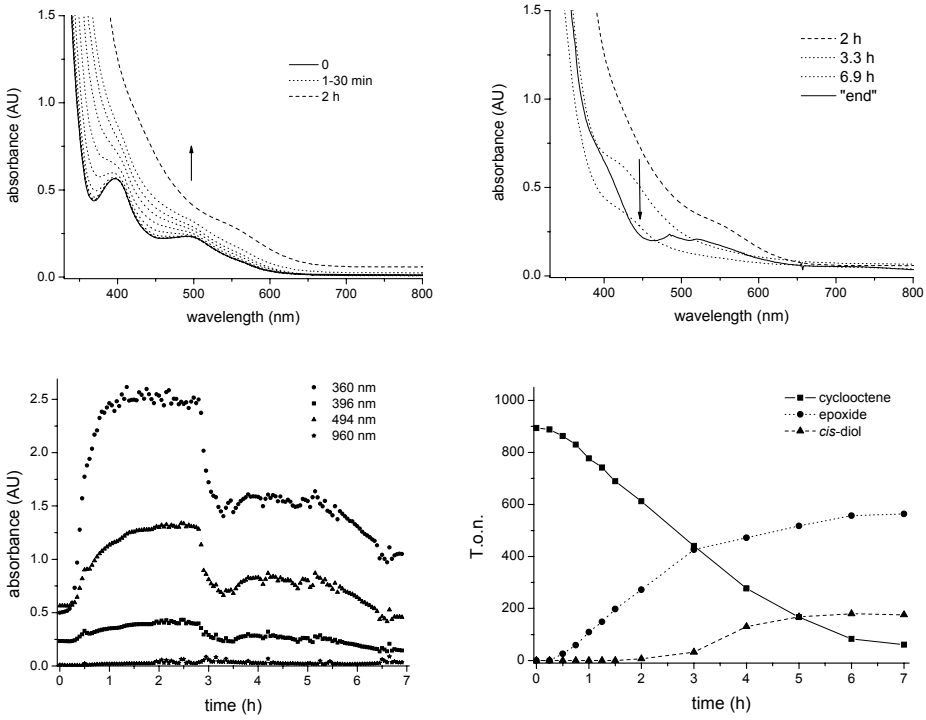

Figure 6.10 Catalytic oxidation of cyclooctene (1 M) in CH_3CN at room temperature employing **1** (1 mM) and oxalic acid (10 mM). a) UV-Vis spectra between 0-2 h. b) UV-Vis absorption as function of time at different times. c) Changes in absorbance in time at 360, 396, 494 and 960 nm. d) Time profile showing cyclooctene (squares, solid line), epoxide (circles, dotted line) and *cis*-diol (triangles, dashed line).

6.3.3 ^{18}O-labeling

Since two phases are observed for the reaction catalysed by **1**/oxalic acid, ^{18}O-labeling studies are complicated. The possibility that two different catalysts operate in these two distinct phases requires examination of these phases separately; otherwise only 'average' results are obtained. While for the first phase the procedure described earlier (Chapter 5, see also Appendix C) can be used, to enable the isotope distribution to be studied during the later stages in the reaction, it is necessary to pretreat the catalyst in such a way that the ^{18}O-percentages are not 'mixed' with products formed during the initial phase of the reaction. This was achieved by first using cycloheptene as substrate and using cyclooctene only during the later stage of the reaction (see Appendix C for details). Whether the differences in ^{18}O-labelling during both phases are significantly different is difficult to address since the actual amount of ^{18}O-labelled water present is difficult to estimate due to the pretreatment procedure with *cis*-2-heptene. However, the results show clearly that oxygen originating from H_2O is incorporated into the *cis*-diol product (Table 6.5), as was

also observed for the combination of **1** and the other carboxylic acids examined (Chapter 5, section 5.3).

Lindsay Smith and coworkers have previously found mainly oxygen incorporation (93 %) from H_2O_2 for the epoxidation of cinnamic acid catalysed by Mn-tmtacn in combination with oxalic acid.[5] However, it should be noted that the substrate they employed (*i.e.* cinnamic acid) contains a free carboxylic acid group, which is possibly involved in the formation of Mn^{III}_2 bis(carboxylato) species considering the results described in Chapter 5.

Table 6.5 Catalytic oxidation of cyclooctene by **1**/oxalic acid at 0 °C with $H_2{}^{16}O_2/H_2{}^{18}O$.

Entry	H_2O	H_2O_2	Catalyst	Acid (mol%)	*cis*-diol $\%^{16}O^{18}O$	epoxide $\%^{18}O$
1	^{18}O	^{16}O	**1**	Oxalic acid (1)	55	2
2	^{18}O	^{16}O	**1**[b]	Oxalic acid (1)	69	9

a) ^{18}O-labelling studies where performed on cyclooctene on 1/20 scale of standard conditions, with the adjustment that a 2% H_2O_2 was used (see procedure E, Appendix C). Values corrected for H_2O_2/H_2O isotopic composition. b) Procedure F (Appendix C). Due to this 'pretreatment' procedure with *cis*-2-heptene only an estimate of the actual ^{18}O labelled water content could be made and thus the numbers are less accurate, although the differences with the previous entry are significant.

6.3.4 Discussion of the role of oxalic acid

The use of the combination of **1**/oxalic acid resulted in the selective epoxidation of a terminal alkene (*i.e.* 1-octene), in agreement with the report of De Vos and coworkers.[2] From the time course of the reaction it is clear that a lag period, which is normally observed for the combination **1**/carboxylic acid, is not present. It is possible that oxalic acid facilitates the reduction[6] of **1** and thus activates the catalyst.[viii]

When cyclooctene was used as substrate, *cis*-dihydroxylation was observed in addition to epoxidation. However, substantial amounts of the *cis*-diol are formed only after 3 h at room temperature (and after ca. 4-5 h at 0 °C), indicating that two distinct catalytically active species are operating. Furthermore, a sudden change in the UV-Vis spectrum of the reaction mixture coincides with the onset of substantial levels of *cis*-dihydroxylation. It should be noted that if a second batch of oxalic acid (1 mol%) is added after 2.5 h, the occurrence of this second phase is suppressed, *i.e.* no *cis*-dihydroxylation is observed during the full time course of the reaction and only selective epoxidation takes place.

While the nature of the catalytically active species during the first 3 h of the reaction remains elusive, during the latter period of the reaction, the oxalic acid system bears close resemblance to that of other 'normal' carboxylic acids. UV-Vis spectroscopy indicates the presence of a dinuclear Mn^{III}_2 bis(carboxylato) complex. However, the nature of this bridging carboxylato ligand(s) is as yet unclear. A possible candidate is suberic acid (formed from cyclooctene by C=C cleavage).

[viii] Oxalic acid → 2 CO_2 + 2 H^+ + 2 e^- (see for example ref. [6]).

6.4 Summary and conclusions

The use of L-ascorbic acid and oxalic acid to suppress the catalase activity of Mn-tmtacn in order to attain effective epoxidation of alkenes was reported by the groups of Berkessel[1] and De Vos[2], respectively. Under the 'standard' conditions (described in this thesis for **1**/carboxylic acid, see also Chapter 3) these additives gave effective epoxidation of (terminal) alkenes. However, when cyclooctene was used as substrate[ix], the combination of **1** and L-ascorbic acid or oxalic acid resulted in a catalytic system capable of *cis*-dihydroxylation in addition to epoxidation, as for the other carboxylic acid additives examined (see Chapters 3 and 5).

It is remarkable that neither the use of L-ascorbic acid as additive nor when using oxalic acid, a lag period is observed prior to commencement of catalysis. This is most likely due to their role in accelerating the reduction of **1**.

Oxalic acid behaves somewhat differently compared to all other carboxylic acids examined. Although **1** undergoes reduction and presumably ligand exchange reactions in the very early stages of the catalysis (observed as a rapid change in the UV-Vis spectrum), epoxidation is observed during the first 3 h of the reaction and only after a sudden change in the UV-Vis spectrum of the reaction mixture substantial amounts of *cis*-diol are being formed besides epoxidation during the second phase of the **1**/oxalic acid promoted reaction. In contrast, for all other carboxylic acids examined *cis*-dihydroxylation and epoxidation commence simultaneously. The sudden change in selectivity of the catalytic system indicates the sudden formation of a different active species.

It is clear that at least the possibility of formation of dinuclear Mn^{III}_2 bis(carboxylato) species either early (L-ascorbic acid) or later in the reaction (oxalic acid) is indicated in the present study. However, when L-ascorbic acid is used as additive a mixed-valent $Mn^{III,IV}_2$ species is observed at high H_2O_2 concentration also. The hyperfine splitting constant indicates that this mixed valent species contains different bridging ligands than present in **1** (which contains three μ-oxo bridges), possibly two carboxylato bridges.

Although a mononuclear complex $[Mn^{III}(salicylato)(tmtacn)]^+$ was isolated, UV-Vis spectroscopy showed that this mononuclear species is not present during the catalytic oxidation reaction by the system **1**/salicylic acid. Instead, just like for all other (substituted) benzoic acids, tentatively, a dinuclear Mn^{III}_2 bis(carboxylato) complex similar to **2d** is present.

As discussed in detail in Chapter 5 (section 5.4.2.1), additives such as oxalic acid have been proposed to induce the formation of mononuclear species[7] responsible for catalytic oxidation of alkenes. However, from the data presented here, it is clear that definitely for salicylic acid and very likely for L-ascorbic acid and oxalic acid (that is, during the second

---

[ix] It should be noted that both Berkessel and co-workers and De Vos and coworkers did not use cyclooctene as substrate. Also, they did not observe *cis*-dihydroxylation activity for the other substrates they examined when using the combination of Mn-tmtacn and L-ascorbic acid or oxalic acid, respectively.

phase of the reaction) dinuclear Mn^{III}_2 bis(carboxylato) complexes are present and are likely to be involved in the catalytic *cis*-dihydroxylation and epoxidation of cyclooctene. Unfortunately, the exact nature of the bridging carboxylato ligands in the case of the L-ascorbic and oxalic acid promoted reactions remains elusive.

6.5 References

[1] Berkessel, A.; Sklorz, C. A. *Tetrahedron Lett.* **1999**, *40*, 7965-7968.
[2] De Vos, D. E.; Sels, B. F.; Reynaers, M.; Subba Rao, Y. V.; Jacobs, P. A. *Tetrahedron Lett.* **1998**, *39*, 3221-3224.
[3] Hage, R.; Krijnen, B.; Warnaar, J. B.; Hartl, F.; Stufkens, D. J.; Snoeck, T. L. *Inorg. Chem.* **1995**, 34, 4973-4978.
[4] Brinksma, J.; Schmieder, L.; Van Vliet, G.; Boaron, R.; Hage, R.; De Vos, D. E.; Alsters, P. L.; Feringa, B. L. *Tetrahedron Lett.* **2002**, *43*, 2619-2622.
[5] Gilbert, B. C.; Lindsay Smith, J. R.; Mairata i Payeras, A.; Oakes, J.; Pons i Prats, R. *J. Mol. Catal. A: Chem.* **2004**, *219*, 265-272.
[6] Yamazaki, S.; Yamada, Y.; Fujiwara, N.; Ioroi, T.; Siroma, Z.; Senoh, H.; Yasuda, K. *J. Electroanal. Chem.* **2007**, *602*, 96-102.
[7] De Vos, D. E.; de Wildeman, S.; Sels, B. F.; Grobet, P. J.; Jacobs, P. A. *Angew. Chem. Int. Ed.* **1999**, *38*, 980-983.

Chapter 7
Enantioselective *cis*-dihydroxylation

The first enantioselective cis-dihydroxylation catalyst based on manganese is reported. The catalyst uses H_2O_2 as oxidant and enantioselectivities up to 47% were obtained with complexes of the type $[Mn^{III}_2(\mu\text{-}O)(\mu\text{-}RCO_2)_2(tmtacn)_2]^{2+}$, which contain two chiral carboxylato bridging ligands.

As discussed in Chapter 1, two important challenges in oxidation chemistry are the development of a robust epoxidation catalyst, which employs either O_2 or H_2O_2 as terminal (stoichimetric) oxidant and the development of an Os-free asymmetric *cis*-dihydroxylation catalyst,[i] which preferably employs O_2 or H_2O_2 also.[1,2] The Os-free catalyst for the enantioselective *cis*-dihydroxylation of alkenes reported by Que and coworkers,[3] which is based on Fe, shows that *cis*-dihydroxylation can be achieved in an enantioselective way in Os-free systems, albeit with low t.o.n.'s (up to 17), limiting the synthetic utility of this system so far (see also section 1.2.2, Chapter 1). As discussed in Chapters 3 and 5, the system **1**/carboxylic acid is an active catalytic system and both the selectivity and activity can be tuned by varying the carboxylic acid employed. The next challenge is thus to develop an enantioselective version of this Mn-tmtacn catalyst.

The presence of two different ligands in the catalysts such as $[Mn^{III}_2(\mu\text{-}O)(\mu\text{-}CCl_3CO_2)_2(tmtacn)_2]^{2+}$ **2a**, *i.e.* the 'capping' tmtacn ligand on each Mn-centre and the bridging carboxylato ligands, offers two approaches for the introduction of stereochemical elements such as a stereogenic centre in the complex, and thus rendering it a chiral catalyst. First of all, the use of a chiral carboxylic acid is synthetically the most straightforward option, since many chiral carboxylic acids are either commercially available or are relatively easy to prepare.[4] Secondly, the introduction of one or more stereogenic centres in the tmtacn ligand would produce a chiral catalyst also.[ii] Although synthetically more challenging, conceptually this would result in a catalyst from which the enantioselectivity can be tuned by one ligand (*i.e.* the modified tacn), while changing the carboxylato bridging ligand allows for obtaining either a *cis*-dihydroxylation or an epoxidation catalyst. Finally, the use of both a chiral carboxylic acid and a chiral tacn derivative might result in improved enantioselectivities compared to the use of only one chiral ligand type. The first approach will be explored in the present chapter.

7.1 Epoxidation catalysts based on chiral tacn derivatives

Several groups have prepared chiral derivatives of the tmtacn ligand and tested these ligands for the enantioselective epoxidation of vinylarenes, usually styrene.[5] In 1997, Bolm and coworkers reported the first enantioselective epoxidation employing chiral Mn-tmtacn derivatives.[6] The catalysts were prepared *in situ* by mixing manganese(II) acetate and chiral tmtacn ligands **L1** or **L2** (Figure 7.1; the synthesis of the ligands themselves had already been reported by Peacock and coworkers[7]). Using styrene as substrate, the corresponding epoxide was obtained in 43% *ee*, although the yield was low (15% after 5 h at 0 °C). Using longer reaction times, higher temperature, higher catalyst loading and larger excess of H_2O_2, the conversion could be increased, however, at the expense of the *ee*, which decreased. With *cis*-β-methylstyrene as substrate the *trans*-epoxide was obtained with 55%

---

[i] See section 1.2.1 (Chapter 1) for a short discussion on the Os-based catalysts for enantioselective *cis*-dihydroxylation.

[ii] Several chiral tmtacn ligands have indeed been reported for the enantioselective epoxidation of alkenes, albeit the highest *ee* values obtained are only moderate (see also section 7.1 for a more detailed discussion).

ee and the *cis*-epoxide with 13 % *ee* (*trans*:*cis* 7:1). The use of 2,2-dimethylchromene as substrate yielded the corresponding epoxide with 40 % *ee*. In a subsequent report Bolm and coworkers described the use of a chiral catalyst $[Mn^{III}_2(O)(CH_3CO_2)_2(tptacn)_2]^{2+}$, based on a reduced cyclic tris(proline) ligand tptacn (trispyrrolidine-1,4,7-triazacyclononane).[8] Again, *ee*'s were low (21-24%). Moreover, although a longer reaction time increased the conversion, the enantioselectivity decreased.

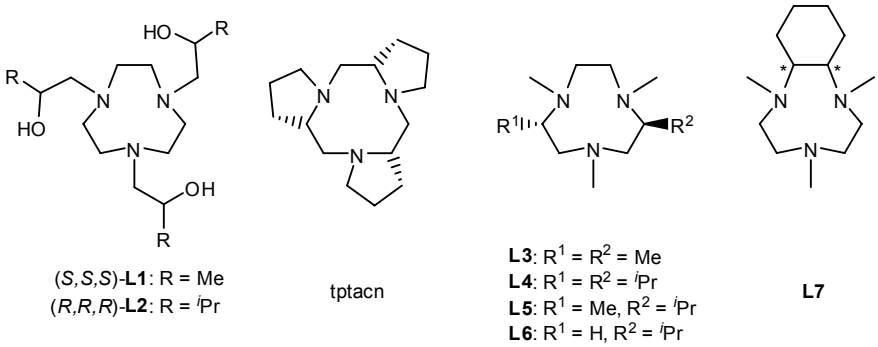

Figure 7.1 Chiral tmtacn derivatives used in the enantioselective epoxidation of alkenes.

Table 7.1 Enantioselective epoxidation using chiral tmtacn derivatives.

Substrate	Catalyst/additive	*ee* (%)	Yield (%)	Ref.
Styrene	$Mn^{II}(CH_3CO_2)_2$ + **L1** / -	43 (*R*)	15[a]	[6]
Styrene	$Mn^{II}(CH_3CO_2)_2$ + **L2** / -	38 (*S*)	n.d.	[6]
Cis-β-Me-styrene	$Mn^{II}(CH_3CO_2)_2$ + **L1** / -	55[b] (1*R*,2*R*) 13[c]	100[a]	[6]
Chromene	$Mn^{II}(CH_3CO_2)_2$ + **L1** / -	40 (3*R*,4*R*)	50[a]	[6]
Chromene	$Mn^{II}(CH_3CO_2)_2$ + **L2** / -	38 (3*S*,4*S*)	50[a]	[6]
Styrene	$[Mn^{III}_2(O)(CH_3CO_2)_2(tptacn)_2]^{2+}$ / -	24 (*S*)	28[a,d]	[8a]
Styrene	$[Mn^{III}_2(O)(CH_3CO_2)_2(tptacn)_2]^{2+}$ / -	15 (*S*)	88[a,e]	[8a]
3-Nitrostyrene	$[Mn^{III}_2(O)(CH_3CO_2)_2(tptacn)_2]^{2+}$ / -	26	n.d.	[8a]
4-Chlorostyrene	$[Mn^{III}_2(O)(CH_3CO_2)_2(tptacn)_2]^{2+}$ / -	21	n.d.	[8a]
Styrene	$Mn^{II}(CH_3CO_2)_2$ + **L3** / L-ascorbate buffer	-	0	[10a]
Styrene	$Mn^{II}(CH_3CO_2)_2$ + **L4**/ L-ascorbate buffer	16 (*R*)	31	[10a]
Styrene	$Mn^{II}(SO_4)$ + **L5** / -	23 (*R*)	15	[10a]
Dodecene	$Mn^{II}(CH_3CO_2)_2$ + **L6** / L-ascorbate buffer	0	36	[10b]
Dodecene	$Mn^{II}(CH_3CO_2)_2$ + **L6** / L-ascorbate buffer	16 (*R*)	31	[10b]
Chromene	$[Mn^{IV}_2(\mu\text{-}O)_3(\mathbf{L7})_2]^{2+}$	80	n.d.	[11a]
4-Methoxy-ethyl-phenyl-allylether	$[Mn^{IV}_2(\mu\text{-}O)_3(\mathbf{L7})_2]^{2+}$	94	n.d.	[11a]

a) Conversion of substrate. b) *Trans*-epoxide (*trans*-/*cis*-epoxide 7:1); note that the starting alkene is *cis*. c) *Cis*-epoxide. d) After 2 h. e) After 4 h.

A solid-phase synthesis protocol for the preparation of chiral tmtacn derivatives has been described by Hall and coworkers[9], but the use of these ligands for enantioselective epoxidation was not reported. The synthesis of several chiral tmtacn analogues was

reported by Gibson and coworkers (**L3-L6**, Figure 7.1).[10] The *ee*'s obtained for the epoxidation of styrene and dodecene were low (0-23%, Table 7.1). In a patent from 1996 by Hoechst[11], the enantioselective epoxidation of several alkenes was claimed with *ee*'s up to 94% using catalysts based on chiral tmtacn derivatives, most likely based on ligand **L7**. However, no reports on this system in the peer-reviewed literature could be found.

The examples discussed above constitute all enantioselective oxidations with chiral tmtacn derivatives reported in literature to date.[6-11] As is clear, the substrate scope tested thus far is very limited and the *ee*'s obtained are only low to moderate, except for the examples described in the patent from Hoechst where high enantioselectivity (80-94% *ee*) is reported for two substrates. Moreover, catalyst stability appears to be a major concern and for some examples where the conversion could be increased by extending the reaction time, the *ee* diminished. In most reports the emphasis is on the often difficult synthesis of the chiral triazacyclononane ligands and a systematic study on the optimisation of reaction conditions and/or substrate scope is not reported.

The studies described in Chapters 3-5, however, gave a detailed understanding of how to increase activity, catalyst stability, how to overcome the often observed lag period and how to limit overoxidation. With these results at hand a novel, Os-free enantioselective *cis*-dihydroxylation catalyst is a realistic, though challenging, goal.

7.2 2,2-Dimethylchromene as substrate

In order to develop an enantioselective *cis*-dihydroxylation catalyst based on Mn-tmtacn, a suitable substrate had to be identified for initial testing. Vinylarenes, such as styrene, are often used as substrates for enantioselective epoxidation reactions.[12] The Os-based enantioselective *cis*-dihydroxylation gives high to excellent *ee*'s for a wide variety of substrate classes. Although *cis*-alkenes are the most difficult substrate class for the Os-catalysed AD, *ee*'s of >95% have been obtained[13,14] (see Chapter 1 for a more detailed discussion).

From the substrate scope of the catalytic system **1**/carboxylic acid (see also Chapter 3) it is apparent that the highest selectivities towards *cis*-dihydroxylation are obtained with electron-rich *cis*-alkenes. Therefore, the choice for the initial substrate to be tested for potential enantioselective *cis*-dihydroxylation was the prochiral *cis*-alkene 2,2-dimethylchromene **7.1** (Scheme 7.1), which is an electron-rich *cis*-alkene and allylic oxidation is blocked by the two methyl substituents.

2,2-Dimethylchromene **7.1** was prepared by a condensation reaction between phenol and 3-methyl-2-butenal in the presence of phenylboronic acid and propionic acid in refluxing xylenes (Scheme 7.1).15 Azeotropic removal of water, as decribed in the original paper, provided the product in low yield (22%). Alternatively, the use of molecular sieves (3 Å) gave higher yields (40%). Despite this improvement, the yield was still only modest and, moreover, scale up of the reaction, resulted in decreased yields. Alternatively, 2,2-dimethylchromene was prepared in good yield (66%) via addition of excess MeMgBr to 1-benzopyran-2-one (**7.2**) at 0 °C and subsequent ring-closure in refluxing toluene (Scheme 7.1).[16]

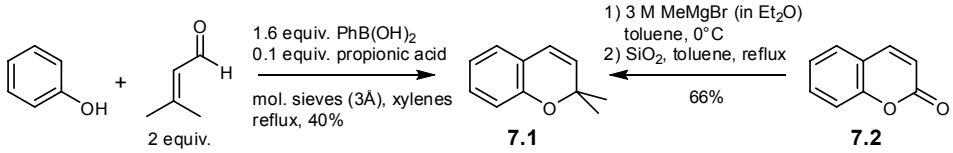

Scheme 7.1 Synthesis of 2,2-dimethylchromene (**7.1**).

In order to find and validate GC or HPLC separations, the racemate of both expected products, *i.e.* *cis*-2,2-dimethylchromane-3,4-diol (**7.3**) and 3,4-epoxy-2,2-dimethylchromane (**7.4**), had to be prepared and isolated. Standard *m*CPBA epoxidation of 2,2-dimethylchromene failed and instead a mixture of compounds was obtained, including the corresponding *trans*- (**7.5**) and *cis*-diol (**7.3**) and a mixture of *m*-chlorobenzoato esters[iii] (**7.6**) (Scheme 7.2). A small amount of the pure epoxide could be isolated by preparative TLC after *m*CPBA epoxidation of 2,2-dimethylchromene in the presence of excess $NaHCO_3$ buffer (see Appendix A for experimental details).

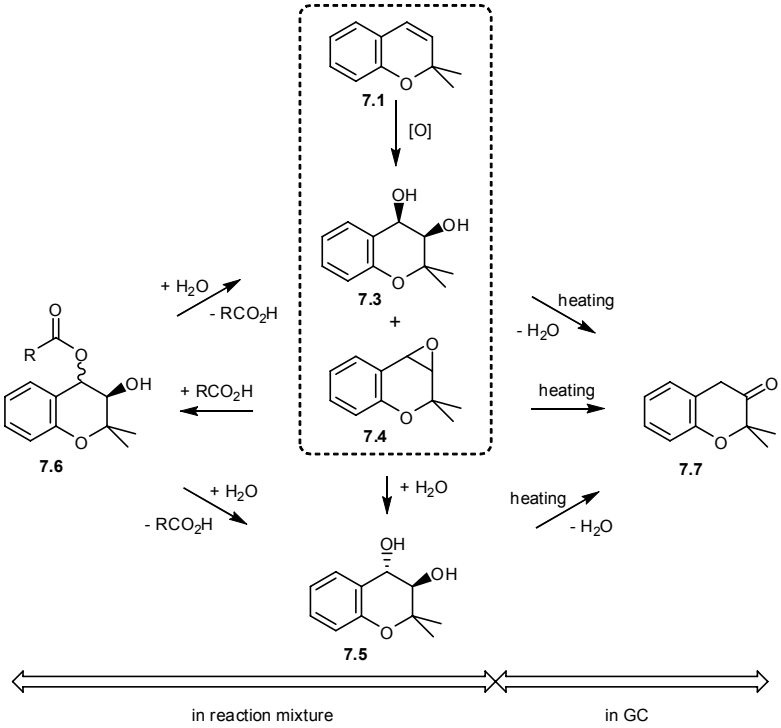

Figure 7.2 Processes occurring in the reaction mixture during the catalytic oxidation of 2,2-dimethylchromene and inside the GC injection port. The dehydration of both the *cis*- and *trans*-diol occurs only partially (ca. 20-35%).

[iii] The formation of a mixture of *m*-chlorobenzoato esters by the reaction between *m*-chlorobenzoic acid and the epoxide has been observed before (ref. [18]).

The stability of 3,4-epoxy-2,2-dimethylchromane (**7.4**) in CH_3CN in the presence of carboxylic acid and/or H_2O was tested. While in CH_3CN solution 3,4-epoxy-2,2-dimethylchromane is stable, in the presence of 2,6-dichlorobenzoic acid (10 mM) the 2,6-dichlorobenzoato ester is detected by CI-MS ($[M+NH_4]^+$ *m/z* 384); however, in the presence of H_2O (*i.e.* CH_3CN/H_2O 9:1) part of these esters are hydrolysed to the corresponding diols. Indeed, it is known that opening of 3,4-epoxy-2,2-dimethylchromane by a carboxylic acid gives both the *trans*- and *cis*-ester **7.6** in a 6:1 ratio.[18] Similarly, hydrolysis of the epoxide in aqueous dioxane buffer in the presence of $HClO_4$ (pH 2.5) yields the *trans*- (**7.5**) and *cis*-diol (**7.3**) in the same ratio (*trans*:*cis* 6:1).[17]

Isolation of the racemic *cis*-diol and epoxide product via catalytic oxidation of 2,2-dimethylchromene employing **2a**/CCl_3CO_2H was attemped; however, only the (racemic) *cis*- and *trans*-diols could be isolated. The intrinsic reactivity of the Mn^{III}_2 bis(carboxylato) complexes results in the formation of both the *cis*-diol and epoxide products. However, the epoxide formed is not stable under reaction conditions in the presence of a slight excess of carboxylic acid and ring-opening and hydrolysis gives both the corresponding *trans*- and *cis*-diol products (ratio *trans*/*cis* 6:1, as reported in the literature,[17,18] *vide supra*).

As a consequence, a minor part of the *cis*-diol is not formed directly by *cis*-dihydroxylation of the alkene, but originates either from hydrolysis of the epoxide or from hydrolysis of the *cis*-ester such as **7.6**, which in turn is the result from ring-opening by the carboxylic acid of the epoxide formed initially. The amount of *cis*-diol formed via these 'indirect' pathways could in principle be estimated via the observed *cis*/*trans*-diol ratio. It should be noted however, that quantitative analysis of the effect of these alternative pathways for the formation of the *cis*-diol product and the effect on its observed *ee* is complicated, since it should take into account the nature of the carboxylic acid used. The reason is two-fold. First of all, an enantiopure carboxylic acid interacts with an (presumably) enantiomerically enriched epoxide, which is then hydrolysed. While the first step of such a pathway constitutes a classic example of a kinetic resolution, in the second step two different diastereoisomers are involved, which each could have different hydrolysis rates. Secondly, direct hydrolysis of the epoxide intermediate yields the *cis*-diol also.

The occurrence of (partial) rearrangements of the epoxide and *cis*- and *trans*-diol products inside the gas chromatograph further complicates the analysis of the products formed during the catalytic oxidation of 2,2-dimethylchromene by **1**/carboxylic acid. While the GC trace of pure 3,4-epoxy-2,2-dimethylchromane (isolated by preparative TLC) showed a single compound, the same compound was observed in the GC trace of pure (>97% by ^{1}H NMR spectroscopy) *cis*-2,2-dimethylchromane-3,4-diol **7.3** and in the GC trace of pure (>97% by ^{1}H NMR spectroscopy) *trans*-2,2-dimethylchromane-3,4-diol **7.5** (Figure 7.3). That the epoxide, *cis*-diol and *trans*-diol showed a common species in their respective GC traces is judged from the identical retention times and mass spectra (obtained by GC-MS(EI), *m/z* 176) of this common species, which was identified to be 2,2-dimethylchroman-3-one **7.7**,[18,19] based on comparison with a sample synthesised

independently. This 3-ketone **7.7** is formed via rearrangement from the epoxide[iv] and via dehydration[18] of the diols inside the gas chromatograph.

Both conversion of the alkene and the turnover numbers for both *cis*-dihydroxylation and epoxidation for all substrates described in this thesis so far were determined by GC (using an internal standard, see also Chapter 3 and Appendix C). However, for the substrate 2,2-dimethylchromene the determination of the turnover numbers for the epoxide, *cis*-diol and *trans*-diol product was not possible with GC (the conversion of the alkene substrate, however, was determined by GC using an internal standard).

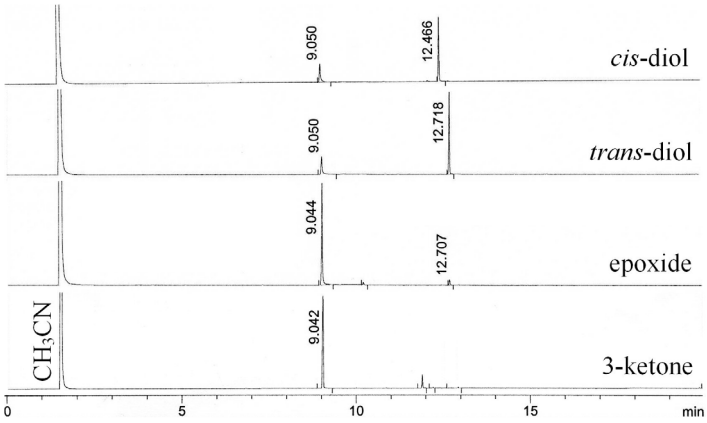

Figure 7.3 GC traces of *cis*-2,2-dimethylchromane-3,4-diol (**7.3**), *trans*-2,2-dimethylchromane-3,4-diol (**7.5**), 3,4-epoxy-2,2-dimethylchromane (**7.4**) and 2,2-dimethyl-chroman-3-one (**7.7**) (top to bottom). See Appendix C for conditions.

7.3 Chiral carboxylic acids

7.3.1 Synthesis of chiral Mn^{III}_2 bis(μ-carboxylato) complexes

Analogous to the methods described in Chapter 4, chiral Mn^{III}_2 bis(μ-carboxylato) complexes **31-35** were synthesised containing chiral carboxylato bridges derived from several *N*-protected α-amino acids (18-48% yield, Scheme 7.2, see Appendix B for experimental details and characterisation). These complexes behave similarly to the complexes described in detail in Chapter 4 and 5. Unfortunately, crystals suitable for single crystal X-ray diffraction were not obtained.

[iv] Similarly, phenylacetaldehyde has been observed in the GC traces of styrene oxide. These rearrangements of the epoxide take place inside the liner, which is part of the injection port of the GC. Using a deactivated liner, instead of a non-deactivated liner, and/or reduction of the temperature of the injection port suppresses this rearrangements partly, but not completely.

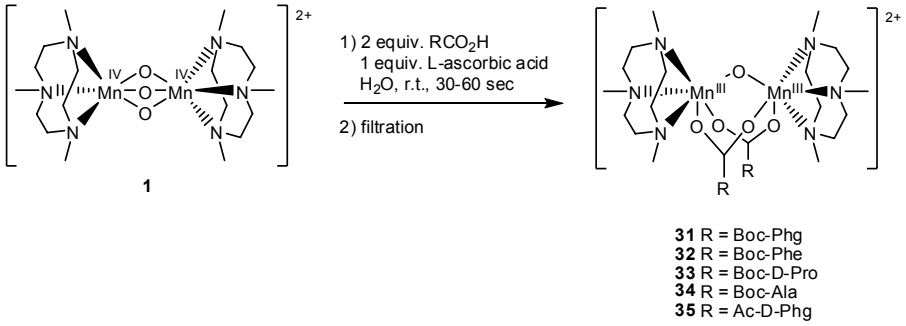

Scheme 7.2 Chiral $[Mn^{III}_2(\mu\text{-}O)(\mu\text{-}RCO_2)_2(tmtacn)_2]^{2+}$ complexes **31-35**.

7.3.2 Enantioselective *cis*-dihydroxylation

The standard conditions used for the catalytic oxidation of 2,2-dimethylchromene by the system **1**/carboxylic acid were modified slightly compared to the standard conditions used for cyclooctene. Because 2,2-dimethylchromene is available in only limited amounts, less substrate was used per experiment and as a consequence 0.4 mol% of manganese dimer and 4 mol% of (chiral) carboxylic acid was used (Scheme 7.3). It should be noted, however, that the alkene concentration was lowered (from 1 M to 0.25 M) and that the overall concentration of the manganese dimer (1 mM) was not altered compared with the standard conditions described in the previous chapters. The reactions were performed typically at 0 °C in CH_3CN containing 10% H_2O, since from mechanistic investigations it is known that the presence of H_2O promotes activity due to formation of species analoguous to **2d** (see also Chapter 5, scheme 5.2). Moreover, the presence of H_2O helps to hydrolyse the benzoato esters that are formed *in situ* (see also Scheme 7.2) and thus assures the presence of excess carboxylic acid in solution, which in turn stabilizes the Mn^{III}_2-dimers. H_2O_2 (50 % aq.) was added by syringe pump addition over 4 h and both final conversion and *ee* were determined one hour after the addition of H_2O_2 was completed.

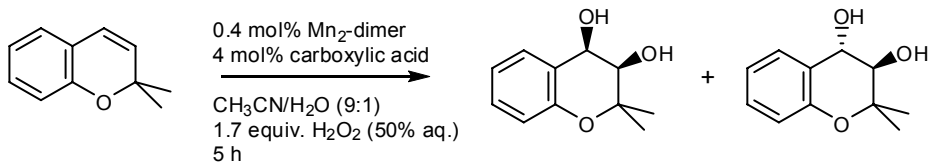

Scheme 7.3 Dihydroxylation of 2,2-dimethylchromene.

Initial results with the *Boc*-phenylglycine[v] (Boc-Phg-OH) derived complex $[Mn^{III}_2(\mu\text{-}O)(\mu\text{-Boc-Phg})_2(tmtacn)_2]^{2+}$ **31** in the presence of 25 mol% (62.5 mM) Boc-Phg-OH resulted in almost complete conversion of 2,2-dimethylchromene and the corresponding *cis*-diol was obtained with 37 % *ee* (Table 7.2, entry 1).[vi] The *ee* is constant over time (Figure 7.4). Decreasing the amount of Boc-Phg-OH from 25 to 4 mol% (*i.e.* from 62.5 to 10 mM) resulted in somewhat lower yield; however the *ee* was similar (entry 2). When the complex $[Mn^{III}_2(\mu\text{-}O)(\mu\text{-Boc-Phg})_2(tmtacn)_2]^{2+}$ **31** was formed *in situ* from **1**/Boc-Phg-OH by pretreatment with H_2O_2 (entry 5) almost similar results were obtained.

When the reaction was performed in CH_3CN (*i.e.* extra H_2O was not added, except that present in 50 w/w% H_2O_2 itself) the *ee* was similar; however, the conversion decreased (compare entries 2 and 3). When complex **31** is used as catalyst in the absence of additional Boc-Phg-OH, the *ee* is not affected; however, a decrease in conversion is again observed (entry 4). The combination of $Mn^{II}(ClO_4)_2.6H_2O$ and Boc-Phg-OH (thus in the absence of tmtacn ligand) results in an inactive system and conversion is not observed (entry 9).

The use of the Boc-phenylalanine (Boc-Phe-OH), Boc-D-proline (Boc-D-Pro-OH) and Boc-alanine (Boc-Ala-OH) derived complexes **32-34** in the presence of the respective Boc-protected amino acid resulted in *cis*-dihydroxylation of 2,2-dimethylchromene also, albeit with low *ee* (Table 7.2, entries 6-8).

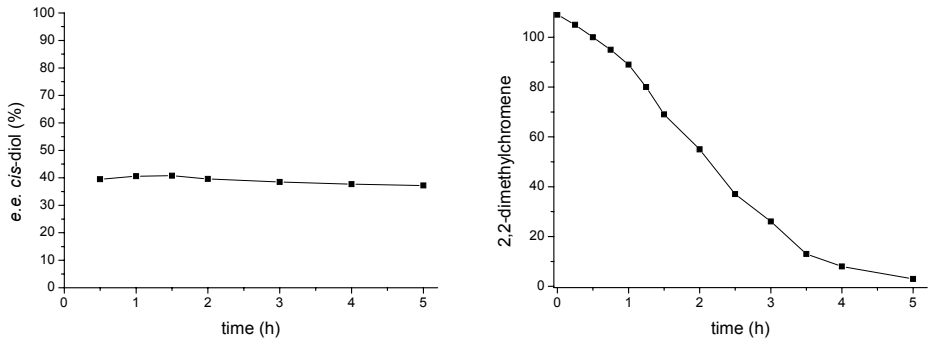

Figure 7.4 Enantioselective *cis*-dihydroxylation of 2,2-dimethylchromene by **31** (1 mM, 0.4 mol%) and Boc-Phg-OH (62.5 mM, 25 mol%) in CH_3CN/H_2O (9:1) at 0 °C. a) *Ee* of the *cis*-diol as function of time. b) Conversion of substrate as function of time.

[v] Initial screening by DSM (Geleen, The Netherlands) indicated that the combination of **1**/Boc-Phg-OH can result in enantioselective *epoxidation* of styrene, giving an *ee* for styrene oxide of 25% (Dr. P. L. Alsters, *personal communication*).

[vi] The *trans*-diol was obtained with low *ee*. This can be attributed to the different pathways by which it can be formed, see also section 7.2.

The combination of **1** and a chiral carboxylic acid such as Boc-Phg-OH affords an effective catalytic system for the enantioselective *cis*-dihydroxylation employing H_2O_2 as oxidant. In agreement with the use of achiral carboxylic acid additives in combination with **1** (Chapters 3 and 5) the formation of Mn^{III}_2 bis(carboxylato) complexes is a prerequisite for catalytic activity. Furthermore, the presence of H_2O is required to attain good conversion, since it is needed for both the formation of the $\{Mn^{III}_2(OH)_2\}$ 'open' species (see also Scheme 5.2, Chapter 5) as well as for the hydrolysis of the carboxylato esters formed *in situ* (from the epoxide and free carboxylic acid, Scheme 7.2), thus assuring catalyst stability by maintaining a slight excess of free carboxylic acid w.r.t. to the catalyst.

Table 7.2 Enantioselective oxidation of 2,2-dimethylchromene at 0 °C in CH_3CN/H_2O (9:1).[a]

Entry	Catalyst/carboxylic acid (mol%)	Conv. (%)	*ee* (%) *cis*-diol	*ee* (%) *trans*-diol	*cis*/*trans*-diol ratio
1	**31** / Boc-Phg-OH (25)	97	37	-8	4.1
2	**31** / Boc-Phg-OH (4)	85	36	-3	5.3
3	**31** / Boc-Phg-OH (4)[c]	41	44	-5	4.3
4	**31** / -	48	36	-2	7.7
5	**1** / Boc-Phg-OH (4)[b]	80	35	-3	1.8
6	**32** / Boc-Phe-OH (4)	80	3	1	1.2
7	**33** / Boc-D-Pro-OH (4)	50	-12	3	1.4
8	**34** / Boc-Ala-OH (4)	75	5	3	2.4
9	$Mn^{II}(ClO_4)_2.6H_2O$ / Boc-Phg-OH (25)	0	-	-	-

a) See procedure G (Appendix C). b) H_2O_2 pretreatment. c) Reaction performed in CH_3CN (without extra H_2O).

7.3.3 Screening chiral carboxylic acids

Screening a series of chiral carboxylic acids for the Mn-tmtacn catalysed *cis*-dihydroxylation of alkenes requires that a screening protocol to be developed and validated. For this screening, the catalytic oxidations were performed at r.t. in scintillation vials. The Mn^{III}_2-complexes were formed *in situ* from **1** and the respective chiral carboxylic acid by pretreatment with H_2O_2 prior to addition of the substrate. The oxidant, H_2O_2, was then added batchwise (1.7 equiv. in total, added in four portions) to the reaction mixture. The other conditions were identical to those described above for the 'standard' reaction, *i.e.* 0.4 mol% **1**, 25 mol% carboxylic acid in CH_3CN/H_2O (9:1). In Table 7.3 the results for four Boc-protected amino acids under these screening conditions are compared with the results obtained under 'standard' conditions employing the Mn^{III}_2 bis(μ-carboxylato) complexes. Although the *ee*'s are lower when using the screening conditions compared with the normal conditions, the results compare well under both conditions and the trends hold. That is, the combination **1**/Boc-Phg-OH gives good *ee*, while the combination of **1** and either Boc-Phe-OH or Boc-Ala-OH give very low *ee*, and Boc-Pro-OH gives an intermediate *ee*.

Subsequently, a series of 24 chiral carboxylic acids were screened. The major part of the acids of this series was selected to vary systematically around the general formula as depicted in Figure 7.5. The atom at the Y position was varied from O, N and C. The group (X) attached to this (hetero)atom was varied also: Boc-, Fmoc-, Z-, Ac- and H-. Finally,

variations were made in the nature of group Z: methyl-, *iso*-propyl-, *sec*-butyl, *iso*-butyl-, phenyl-, benzyl- and methoxy-naphthyl-. Furthermore, several other carboxylic acids (selected at random) were included. The structures of the complete series of chiral carboxylic acids tested are depicted in Figure 7.6.

Table 7.3 Comparison screening and 'standard' conditions.[a]

Entry	Carboxylic acid	Screening conditions		Standard conditions	
		Conv. (%)[b]	*ee* (%)	Conv. (%)[c]	*ee* (%)
1	Boc-Phg-OH	89	29	85	36
2	Boc-Phe-OH	82	2	80	3
3	Boc-Pro-OH	71	9	50[d]	-12[d]
4	Boc-Ala-OH	90	2	75	5

a) Enantioselective *cis*-dihydroxylation of 2,2-dimethylchromene in CH_3CN/H_2O (9:1). b) **1** (1 mM, 0.4 mol%) and chiral carboxylic acid (62.5 mM, 25 mol%) at r.t. and batchwise addition of H_2O_2, single run (see general procedure H, Appendix C). c) Mn^{III}_2 complex (1 mM, 0.4 mol%) and chiral carboxylic acid (10 mM, 4 mol%) at 0 °C and continuous addition of H_2O_2, *in duplo* (see general procedure G, Appendix C). d) Boc-D-Pro-OH used (instead of Boc-Pro-OH).

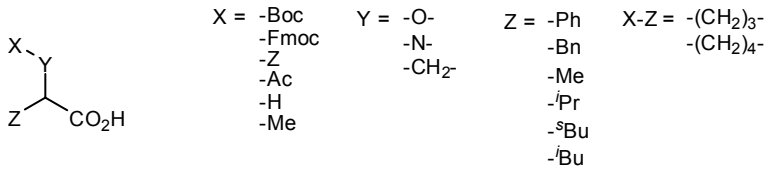

Figure 7.5 Chiral carboxylic acids used in screening.

The results of the catalytic oxidation of 2,2-dimethylchromene by the combination of **1** and this series of chiral carboxylic acids are summarised in Table 7.4. The combination of **1** and Ac-D-Phg-OH gave the highest *ee* (-38%) for the *cis*-diol (entry 2). Boc-, Fmoc- and Z-protected phenylglycine all result in similar *ee* for the *cis*-diol (28, -29 and 27%, respectively) and also their *cis*-/*trans*-diol ratios and conversions are very similar (entries 1, 4 and 5). The unprotected H-D-Phg-OH gives both very low conversion and low *ee* (entry 3). Chiral carboxylic acids which contain a phenyl or naphthyl group directly attached to the stereogenic carbon atom, *i.e.* the phenylglycine derivatives, (*R*)-(-)-2-phenylpropionic acid, (*S*)-(+)-naproxen, (*R*)-(+)-Mosher's acid, (*R*)-(-)-mandelic acid and (*R*)-(-)-α-acetoxyphenylacetic acid (entries 14, 15, 18, 20 and 21, respectively), all stand out as in giving a relatively good *ee* (13-20%). Interestingly, the *N*-protected dipeptide Boc-Pro-Pro-OH gives a substantially improved *ee* compared with Boc-Pro-OH (21 and 10%, respectively, entries 12 and 13). The combination of **1** and all other chiral carboxylic acids tested results in very low *ee* (<10%) for the *cis*-diol product.

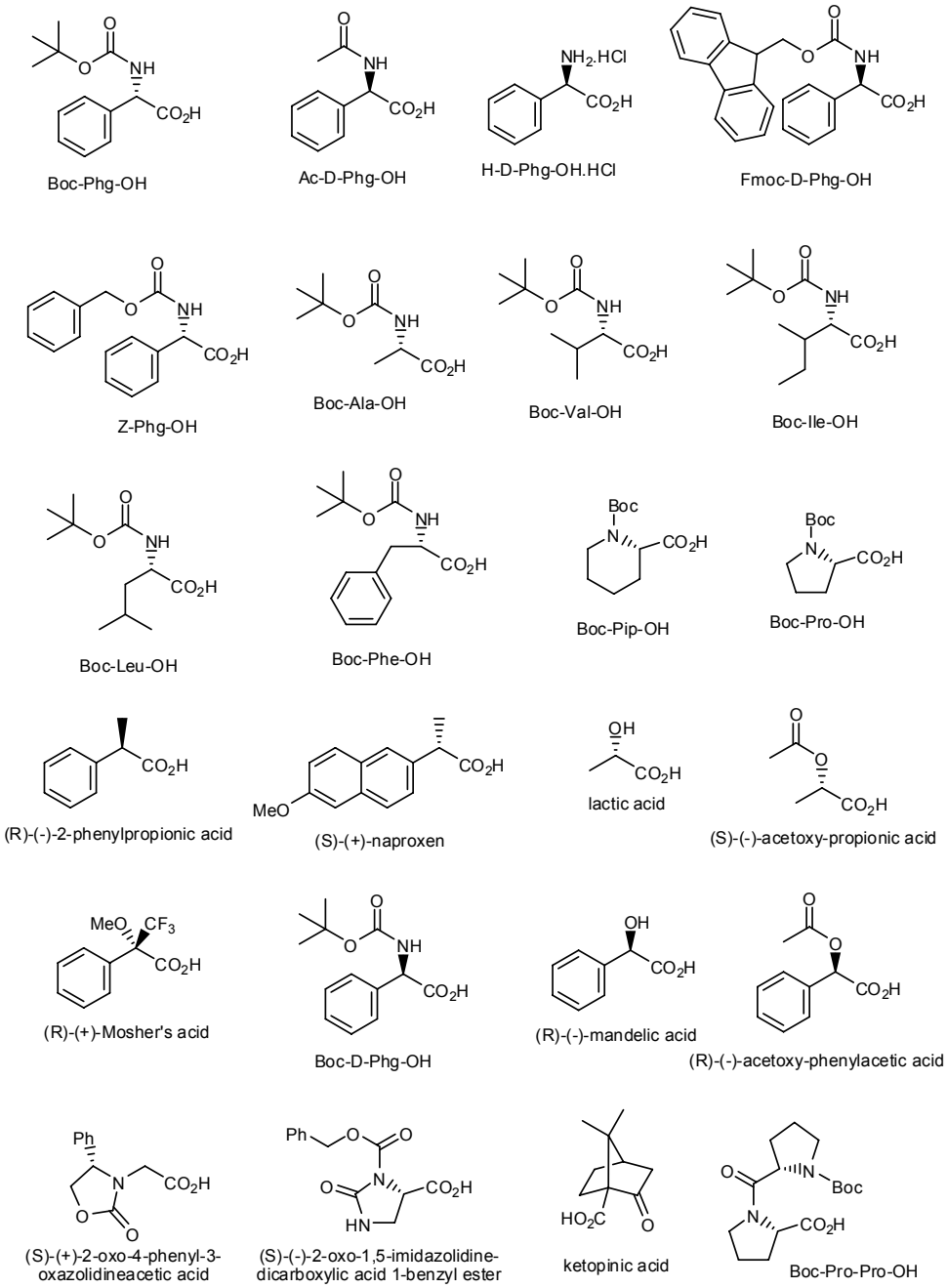

Figure 7.6 Chiral carboxylic acids employed in the screening for enantioselective *cis*-dihydroxylation of 2,2-dimethylchromene.

Table 7.4 Catalytic *cis*-dihydroxylation of 2,2-dimethylchromene.[a]

Entry	Acid	*ee*[b] *cis*-diol	*ee*[b] *trans*-diol	*cis*/*trans*-diol ratio[c]	Conv. (%)[d]
1	Boc-Phg-OH	28	-1	3,2	88
2	Ac-D-Phg-OH	-38	6	4,3	99
3	H-D-Phg-OH	-3	-1	1,2	13
4	Fmoc-D-Phg-OH	-29	3	3,7	92
5	Z-Phg-OH	27	-1	3,6	80
6	Boc-Ala-OH	3	2	3,6	86
7	Boc-Val-OH	5	3	3,6	73
8	Boc-Ile-OH.0,5H2O	5	7	4,0	69
9	Boc-Leu-OH.H2O	2	5	3,4	84
10	Boc-Phe-OH	3	3	3,3	81
11	(R)-(+)-Boc-Pip-OH	6	1	1,8	80
12	Boc-Pro-OH	10	-5	3,6	68
13	Boc-Pro-Pro-OH	21	-3	3,4	27
14	(R)-(-)-2-phenylpropionic acid	-13	-7	4,1	39
15	(S)-(+)-naproxen	16	3	4,6	31
16	lactic acid (>85% in water)	-1	5	1,2	61
17	(S)-(-)-acetoxypropionic acid	-0,4	10	2,7	77
18	(R)-(+)-Mosher's acid	-20	-6	3,8	73
19	Boc-D-Phg-OH	-28	4	3,3	88
20	(R)-(-)-mandelic acid	-15	-0,2	1,0	72
21	(R)-(-)-α-acetoxyphenylacetic acid	-20	-3	3,0	82
22	(S)-(+)-2-oxo-4-phenyl-3-oxazolidineacetic acid	3	-1	1,7	75
23	(S)-(-)-2-oxo-1,5-imidazolidine-dicarboxylic acid 1-benzyl ester	5	-2	3,5	86
24	(1S)-(+)-ketopinic acid	-9	-1	7,0	53

a) See procedure H (Appendix C). b) Determined by HPLC. c) Estimated from HPLC, assuming equal molar absorptivities for the *cis*- and *trans*-diol at 210 nm. d) Determined by GC after 4 h.

ee	< 2 %	2-10 %	11-25 %	25-35 %	>35 %
cis/*trans*-diol ratio	< 2	2-5	> 5		
conversion	< 50 %	50-75 %	> 75 %		

When Boc-D-Phg-OH is used instead of Boc-Phg-OH, the opposite enantiomer of the *cis*-diol is formed as major enantiomer (-28 and 28% *ee*, respectively, entries 19 and 1).[vii] When the absolute stereochemistry of the *cis*-diol product is compared with that of all the

[vii] Together with the good reproducibility with respect to the *duplo*'s, this underlines the validity of the screening protocol.

chiral carboxylic acids which show significant *ee* (thus above 2%), it is clear that there is perfect correlation between the both. That is, the configuration of the stereogenic carbon atom in the carboxylic acid determines which enantiomer of the *cis*-diol is formed in excess.

The *ee* of the *trans*-diol is low in all cases (<10%). The most likely explanation for this low *ee* is the presence of two distinct routes towards the formation of the *trans*-diol, *i.e.* via (enantioselective) epoxidation of the alkene followed by hydrolysis of the epoxide by H_2O directly and via opening of the epoxide by the chiral carboxylic acid followed by hydrolysis of the intermediate carboxylato ester (see also Figure 7.2 and section 7.2).

The *cis*-diol is formed as the major product in all cases and the *cis*-/*trans*-diol ratios are good: in the majority of the cases, the *cis*-/*trans*-diol ratio is between 2.7 and 4.3.[viii] The highest *cis*-/*trans*-diol ratio (7.0) is found for (1*S*)-(+)-ketopinic acid (Table 7.4, entry 24) and this is in line with the results reported in Chapter 3 and 5 for cyclooctene where it was shown that steric bulk close to the carboxylic acid functionality favors *cis*-dihydroxylation over epoxidation. Low *cis*-/*trans*-diol ratios (below 2) are encountered for H-D-Phg-OH, Boc-Pip-OH, lactic acid, mandelic acid and (S)-(+)-2-oxo-4-phenyl-3-oxazolidineacetic acid (entries 3, 11, 16, 20 and 22).

The conversion is good to excellent in most cases (53-99%) and the highest conversion is obtained with Ac-D-Phg-OH which gives 99% conversion. Exceptions are the unprotected H-D-Phg-OH (13% conversion, Table 7.4, entry 3), however, it should be noted that this compound was only slightly soluble under reaction conditions. Also Boc-Pro-Pro-OH, (*R*)-(-)-2-phenylpropionic acid and (*S*)-(+)-naproxen gave low conversion (27, 39 and 31%, respectively, entries 13-15).

Thus for enantioselective *cis*-dihydroxylation by **1**/carboxylic acid the carboxylic acid requires the presence of an aromatic group attached directly to the stereogenic carbon atom (group Z in figure 7.5). The other atom attached to the stereogenic carbon (group Y) is preferrently nitrogen. Furthermore, acetamide is preferred over the carbamate protecting groups (group X). The highest *ee* and highest conversion are obtained with Ac-D-Phg-OH.

7.3.4 Intrinsic *cis*-dihydroxylation

As noted in section 7.2 the *cis*-diol product can be formed via two different pathways: i) via direct *cis*-dihydroxylation of the alkene by the dinuclear manganese catalyst, or ii) via opening of the epoxide intermediate. Overall, it is apparent that the *cis*-diol product is enantiomerically enriched. However, the question remains whether this is due to direct enantioselective *cis*-dihydroxylation of the alkene by the manganese catalyst or whether the observed *ee* of the *cis*-diol is due to opening of the enantiomerically enriched epoxide and/or enantioselective opening of the epoxide intermediate.

[viii] The formation of the *trans*-diol is most likely to be due to ring-opening of the epoxide formed initially (see section 7.2).

The quantitative contributions of the indirect routes to the *cis*-diol product (*i.e.* via the epoxide intermediate) are complex. Especially since the *ee* of the epoxide intermediate and the relative contributions and enantioselectivities of these processes (*i.e.* opening of the epoxide by H_2O and epoxide opening by the chiral carboxylic acid with subsequent ester hydrolysis) are unknown. Furthermore, a detailed and complicated kinetic analysis of these parallel occuring processes would be required.

However, in order to answer the most pertinent question, whether the dinuclear manganese complexes engage in direct enantioselective *cis*-dihydroxylation of the alkene, it is sufficient to calculate the two extremes for the contribution to the observed *ee* of the portion of the *cis*-diol product formed indirectly via the epoxide intermediate. The *cis*-diol product ($cis\text{-diol}_{observed}$) is formed via direct *cis*-dihydroxylation of the alkene ($cis\text{-diol}_{direct}$) and via opening of the epoxide intermediate (either directly by H_2O or via hydrolysis of an ester intermediate, Figure 7.2). The latter are taken together as $cis\text{-diol}_{indirect}$.

$$cis\text{-diol}_{observed} = cis\text{-diol}_{direct} + cis\text{-diol}_{indirect}$$

As discussed in section 7.2, it has been reported previously that the acid-catalysed ring-opening of the epoxide results in formation of the *trans*- and *cis*-diol products with a ratio of 6:1. Ring-opening of the epoxide by a carboxylic acid yields the *trans*- and *cis*-esters with a *trans*/*cis* ratio of 6:1 also. It is thus fair to assume that $cis\text{-diol}_{indirect}$ can be calculated from the amout of *trans*-diol observed ($trans\text{-diol}_{observed}$) taking into consideration this *trans*/*cis*-ratio of 6:1, *i.e.*

$$cis\text{-diol}_{indirect} = 1/6 * trans\text{-diol}_{observed}$$

The *cis*-diol product observed ($cis\text{-diol}_{observed}$) consists of a mixture of its two enantiomers ($cis_{enantiomer1}$ and $cis_{enantiomer2}$). The *cis*-diol formed via the indirect pathways ($cis\text{-diol}_{indirect}$) can have a maximum *ee* of 100%. That is, it can in principle consists of only one of the two *cis*-diol enantiomers. In the one extreme case, $cis\text{-diol}_{indirect}$ consists of only a single $cis_{enantiomer1}$, in the other extreme case, $cis\text{-diol}_{indirect}$ consists of only $cis_{enantiomer2}$. Substracting these (extreme) contributions of the $cis\text{-diol}_{indirect}$ from $cis\text{-diol}_{observed}$ affords the mininum and maximum enantioselectivity achieved by direct formation of *cis*-diol by the dinuclear Mn^{III}_2 catalysts, respectively (Figure 7.7).

These two extreme cases have been calculated for all carboxylic acids used in the screening (Table 7.5). For Ac-D-Phg-OH, the carboxylic acid which affords the highest (observed) *ee* for the *cis*-diol product (-38%, entry 2), even in the worst case scenario, when all of the $cis\text{-diol}_{indirect}$ contributes positively to the *ee* of the $cis\text{-diol}_{observed}$, the intrinsic enantioselectivity of the direct *cis*-dihydroxylation of the alkene by the dinuclear Mn^{III}_2-catalyst is still -35%. In the other extreme case, *i.e.* when $cis\text{-diol}_{indirect}$ contributes negatively to the *ee* of the $cis\text{-diol}_{observed}$, the intrinsic enantioselectivity of the dinuclear Mn^{III}_2-catalyst would be -43%.

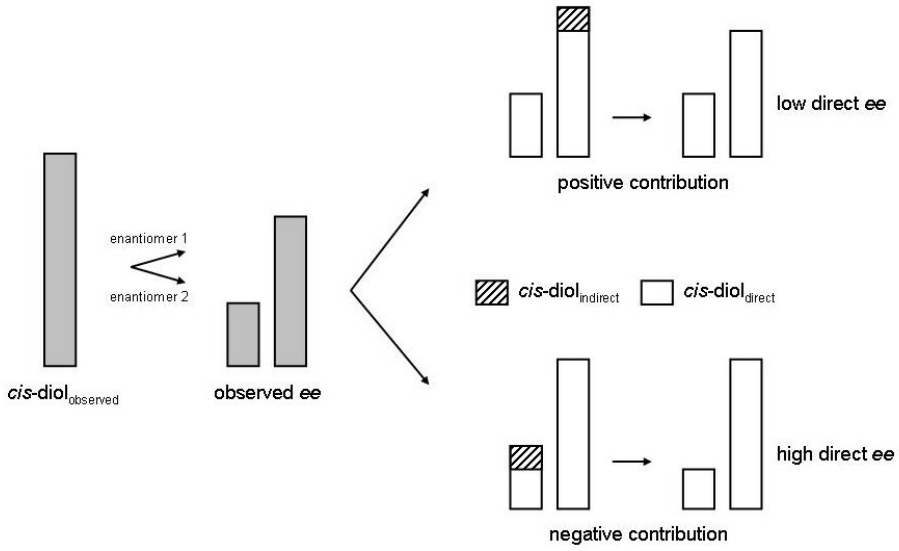

Figure 7.7 Effect of *ee* of the *cis*-diol formed indirectly on the enantioselecitivity of *cis*-dihydroxylation catalysed by the dinuclear Mn^{III}_2-complex.

It should be noted that even in these extreme cases the *ee* achieved by the catalyst is close to the *ee* observed. Furthermore, it is important to note that the assumption that the sum of the indirect pathways (*i.e.* formation of the *cis*-diol product via the epoxide intermediate) would afford 100% selectivity for only one of the *cis*-diol enantiomers is highly unlikely. In fact, the low *ee* observed for the *trans*-diol product, which is being formed via these 'indirect' pathways from epoxide intermediate also, suggests strongly that the *ee* of *cis*-$diol_{indirect}$ is low as well (0-10%, Table 7.4). The latter would mean that the intrinsic *ee* of the Mn-catalyst is even closer to the observed *ee* than suggested be the extreme values for the intrinsic enantioselectivity of the Mn^{III}_2-catalyst as summarized in Table 7.5. Thus it can be stated confirmatively that this catalytic system is truly a catalyst for enantioselective *cis*-dihydroxylation.

Table 7.5 Observed and maximum and minimum direct *ee*'s for the *cis*-dihydroxylation of 2,2-dimethylchromene.

Entry	Acid	Observed *ee*	Direct *ee* max.	Direct *ee* min.
1	Boc-Phg-OH	28	35	24
2	Ac-D-Phg-OH	-38	-43	-35
3	H-D-Phg-OH	-3	-20	14
4	Fmoc-D-Phg-OH	-29	-35	-25
5	Z-Phg-OH	27	33	24
6	Boc-Ala-OH	3	8	-2
7	Boc-Val-OH	5	10	1
8	Boc-Ile-OH.0,5H_2O	5	9	0
9	Boc-Leu-OH.H_2O	2	7	-3
10	Boc-Phe-OH	3	9	-2
11	(R)-(+)-Boc-Pip-OH	6	18	-5
12	Boc-Pro-OH	10	15	6
13	Boc-Pro-Pro-OH	21	27	17
14	(R)-(-)-2-phenylpropionic acid	-13	-18	-10
15	(S)-(+)-naproxen	16	20	12
16	lactic acid (>85% in water)	-1	-17	15
17	(S)-(-)-acetoxypropionic acid	-0,4	6	-7
18	(R)-(+)-Mosher's acid	-20	-25	-16
19	Boc-D-Phg-OH	-28	-35	-24
20	(R)-(-)-mandelic acid	-15	-38	2
21	(R)-(-)-α-acetoxyphenylacetic acid	-20	-27	-15
22	(S)-(+)-2-oxo-4-phenyl-3-oxazolidineacetic acid	3	15	-7
23	(S)-(-)-2-oxo-1,5-imidazolidine-dicarboxylic acid 1-benzyl ester	5	10	0
24	(1S)-(+)-ketopinic acid	-9	-12	-7

7.3.5 Temperature dependence

Although the procedure used for screening a series of chiral carboxylic acids is a simple and effective way to identify effective chiral acids quickly, the *ee*'s observed at room temperature are lower than those obtained at lower temperatures using the same carboxylic acid (see Table 7.3). When the temperature is reduced (20 °C, 0 °C and -17 °C, respectively) using the system **31**/Boc-Phg-OH the *ee* increased from 28% to 37% and finally 47%, respectively (Table 7.6, entries 1-3). Similarly, the *ee* increases from -38 to -42% when the temperature is lowered from 20 to 0 °C for the system **1**/Ac-D-Phg-OH (entries 4 and 5).

It is clear that higher enantioselectivities are obtained at lower temperatures, albeit with slightly lower yields. The yields could in principle be improved by employing increased reaction times since the catalytic performance is stable over prolonged reaction times (see for example Figure 3.5, Chapter 3). The limiting factor for lowering the temperature (and increasing *ee*), however, is the freezing point of water. At -17 °C, for example, the amount of water present is limited to 5% (in CH_3CN under reaction conditions, at 0 °C a water content of 10% is employed) since at higher concentrations the water freezes. Since water is

needed to attain catalytic activity (see section 7.3.2) this limits the improvement of *ee*, although further optimalisation of temperature, water content and reaction time might improve the enantioselectivity further.

Table 7.6 Temperature dependence of enantioselectivity.[a]

Entry	Catalyst/carboxylic acid (mol%)	temp. (°C)	*ee* (%) *cis*-diol	*ee* (%) *trans*-diol	*cis*/*trans*-diol ratio	conv. (%)
1	**1** / Boc-Phg-OH (25)[d]	20	28	-1	3.2	88
2	**31** / Boc-Phg-OH (25)	0	37	-8	4.1	97
3	**31** / Boc-Phg-OH (25)[c]	-17	47	-17	7.6	51
4	**1** / Ac-D-Phg-OH (25)[d]	20	-38	6	4.3	99
5	**1** / Ac-D-Phg-OH (4)[b]	0	-42	n.d.	n.d.	80

a) See procedure G (Appendix C). b) H_2O_2 pretreatment. c) Reaction performed at -17 °C in CH_3CN/H_2O (19:1). d) Screening conditions (procedure H, Appendix C).

7.4 Summary and conclusions

The understanding of both the solution chemistry of the substrate and products during the catalytic oxidation of 2,2-dimethylchromene and of the complexes involved in the catalysis itself, proved to be key to the development of this new protocol for the enantioselective *cis*-dihydroxylation of alkenes. Although the only substrate tested in the current study is 2,2-dimethylchromene, there is no reason to assume that the current system would be limited to this substrate. Future exploration should include the testing of a broader substrate scope. While one of the products formed initially, 3,4-epoxy-2,2-dimethylchromane (**7.4**), is not stable under the reaction conditions, the presence of H_2O helps to hydrolyse the esters formed initially from the epoxide and carboxylic acid. In this way, a small excess of free carboxylic acid is retained in solution, which is key to catalyst stability (and thus activity) over the full course of the reaction.

The use of Mn^{III}_2 complexes (0.4 mol%) containing two chiral carboxylato bridging ligands in combination with a slight excess of the corresponding carboxylic acid (4 mol%) proved to be effective for the enantioselective *cis*-dihydroxylation of 2,2-dimethylchromene and *ee*'s up to 47% were obtained. Furthermore, only 1.7 equiv. of H_2O_2 w.r.t. to substrate is employed. Although the enantioselectivity obtained thus far is still modest, this work constitutes the first manganese based catalyst for the enantioselective *cis*-dihydroxylation of alkenes and the *ee*'s are promising.

7.5 References

[1] Noyori, R. *Chem. Commun.* **2005**, 1807-1811.
[2] a) Beller, M. *Adv. Synth. Catal.* **2004**, *346*, 107-108. b) Chang, D.; Zhang, J.; Witholt, B.; Li, Z. *Biocatal. Biotransfor.* **2004**, *22*, 113-130.
[3] Costas, M.; Tipton, A. K.; Chen, K.; Jo, D.-H.; Que, Jr., L. *J. Am. Chem. Soc.* **2001**, *123*, 6722-6723.

[4] See for example: Hoen, R.; Boogers, J. A. F.; Bernsmann, H.; Minnaard, A. J.; Meetsma, A.; Tiemersma-Wegman, T. D.; de Vries, A. H. M.; de Vries, J. G.; Feringa, B. L. *Angew. Chem. Int. Ed.* **2005**, *44*, 4209-4212.
[5] For reviews, see also: a) Hage, R.; Lienke, A. *Angew. Chem. Int. Ed.* **2006**, *45*¸ 206-222. b) Hage, R.; Lienke, A. *J. Mol. Catal. A: Chem.* **2006**, *251*, 150-158. c) Sibbons, K. F.; Shastri, K.; Watkinson, M. *Dalton Trans.* **2006**, 645-661.
[6] Bolm, C.; Kadereit, D.; Valacchi, M. *Synlett.* **1997**, 687-688.
[7] a) Belal, A. A.; Farrugia, L. J.; Peacock, R. D.; Robb, J. *J. Chem. Soc., Dalton Trans.* **1989**, 931-935. b) Fallis, I. A.; Farrugia, L. J.; Macdonald, N. M.; Peacock, R. D. *J. Chem. Soc., Dalton Trans.* **1993**, 2759-2763.
[8] a) Bolm, C.; Meyer, N.; Raabe, G.; Weyhermüller, T.; Bothe, E. *Chem. Commun.* **2000**, 2435-2436. b) Meyer, N. C.; Bolm, C.; Raabe, G.; Kölle, U. *Tetrahedron* **2005**, 12371-12376.
[9] Kopac, D. S.; Hall, D. G. *J. Comb. Chem.* **2002**, *4*, 251-254.
[10] a) Argouarch, G.; Gibson, C. L.; Stones, G.; Sherrington, D. C. *Tetrahedron Lett.* **2002**, *43*, 3795-3798. b) Stones, G.; Argouarch, G.; Kennedy, A. R.; Sherrington, D. C.; Gibson, C. L. *Org. Biomol. Chem.* **2003**, *1*, 2357-2363. c) Argouarch, G.; Stones, G.; Gibson, C. L.; Kennedy, A. R.; Sherrington, D. C. *Org. Biomol. Chem.* **2003**, *1*, 4408-4417.
[11] a) Beller, M.; Tafesh, A.; Fischer, R. W.; Scharbert, B. (Hoechst AG, Germany) **1996**, DE 195 23 890. b) Beller, M.; Tafesh, A.; Fischer, R. W.; Scharbert, B. (Hoechst AG, Germany) **1996**, DE 195 23 891.
[12] See for example: a) Jacobsen, E. N.; Zhang, W.; Muci, A. R.; Ecker, J. R.; Deng, L. *J. Am. Chem. Soc.* **1991**, *113*, 7063-7064. b) Collman, J. P.; Zhang, X.; Lee, V. J.; Uffelman, E. S.; Brauman, J. I. *Science* **1993**, *261*, 1404-1411. c) Sasaki, H.; Irie, R.; Hamada, T.; Suzuki, K.; Katsuki, T. *Tetrahedron* **1994**, *50*, 11827-11838. d) Brinksma, J.; de Boer, J. W.; Hage, R.; Feringa, B. L.; Chapter 10 in: *Modern Oxidation Methods*, Bäckvall, J.-E. (ed.), **2004**, Wiley-VCH, 295-326, and references cited therein.
[13] Kolb, H. C.; VanNieuwenhze, M. S.; Sharpless, K. B. *Chem. Rev.* **1994**, *94*, 2483-2547.
[14] Wang, Z.-M.; Kakiuchi, K.; Sharpless, K. B. *J. Org. Chem.* **1994**, *59*, 6895-6897.
[15] The method for the synthesis of 2,2-dimethylchromene was adapted from the procedure as described for the synthesis of precocene I: Bissada, S.; Lau, C. K.; Bernstein, M. A.; Dufresne, C. *Can. J. Chem.* **1994**, *72*, 1866-1869. See also: North, J. T.; Kronenthal, D. R.; Pullockaran, A. J.; Real, S. D.; Chen, H. Y. *J. Org. Chem.* **1995**, *60*, 3397-3400.
[16] a) Livingstone, R.; Watson, R. B. *J. Chem. Soc.* **1957**, 1509-1512. b) Strunz, G. M.; Brillon, D.; Giguère, P. *Can. J. Chem.* **1983**, *61*, 1963-1964.
[17] Boyd, D. R.; Sharma, N. D.; Boyle, R.; Evans, T. A.; Malone, J. F.; McCombe, K. M.; Dalton, H.; Chima, J. *J. Chem. Soc., Perkin Trans. 1* **1996**, 1757-1765.
[18] Anastasis, P.; Brown, P. E. *J. Chem. Soc., Perkin Trans. 1* **1983**, 1431-1437.
[19] For NMR data for 2,2-dimethylchroman-4-one see: El-Essawy, F. A. G.; Yassin, S. M.; El-Sakka, I. A.; Khattab, A. F.; Søtofte, I.; Øgaard Madsen, J.; Senning, A. *J. Org. Chem.* **1998**, *63*, 9840-9845.

Chapter 8
General discussion and future prospects

The results of the research described in this thesis are discussed in relation to the requirements for new oxidation catalysts as stated in the preface. Focus is on the major issues encountered, solutions and possibilities for future developments.

As stated in the preface, the goal of the research described in this thesis was to develop new catalysts for the selective oxidation of alkenes. The requirements were not only to develop catalysts capable of activating environmentally benign terminal oxidants such as H_2O_2 or O_2 but that the catalysts themselves should be based on relatively non-toxic and cost-effective metals also; preferably first-row transition metals. In order to be synthetically useful, the catalysts should exhibit high activity, selectivity and robustness.

A problem with the combination of H_2O_2 and first-row transition metal (complexes) is often that catalase type activity occurs. That is, the metal salt or metal complex catalyses the disproportionation of the oxidant H_2O_2 into O_2 and H_2O. Depending upon the degree of the competing catalase-type activity with respect to oxidation catalysis a (large) excess of H_2O_2 is needed to attain full conversion of the substrate. Also with the complex $[Mn^{IV}_2(\mu\text{-}O)_3(tmtacn)_2]^{2+}$ **1** catalase-type activity occurs in addition to oxidation of (alkene) substrates.[1]

The complex $[Mn^{IV}_2(\mu\text{-}O)_3(tmtacn)_2]^{2+}$ is a versatile catalyst for oxidative transformations. It satisfies with the requirements mentioned above: manganese is a first-row transition metal and both the tmtacn ligand and the complex can be (and actually are) produced on large scale and are sufficiently cost-effective to see application in consumer products.[2] However, despite the activity of many groups using Mn-tmtacn based catalysts, mainly for the epoxidation of alkenes (and in many of those cases additives are used to suppress the catalase-type activity), a solid mechanistic insight into the mode of action of the Mn-tmtacn catalysts and into the mode of action of the additives used was much lacking at the outset of the research described in this thesis.

In our group electron-deficient aldehydes had been identified as useful additives for Mn-tmtacn catalysed oxidation of alkenes.[3] Not only did the presence of 25 mol% of aldehyde suppress the catalase type activity, it also induced *cis*-dihydroxylation in addition to epoxidation. However, the role of this additive was not understood.

At the start of the studies described in this thesis it became apparent that it is not the aldehyde which is the active additive. As discussed in Chapter 3, carboxylic acids are the actual additives responsible for the suppression of catalase-type activity and for the activity of the catalysts involved in the Mn-tmtacn catalysed *cis*-dihydroxylation and epoxidation of alkenes. By changing the carboxylic acid, both the activity and selectivity of the Mn-tmtacn catalysed oxidation of alkenes can be tuned. The activity of the catalytic system could be improved by employing electron-withdrawing substituents in the carboxylic acid. Furthermore, the use of salicylic acid as an additive results in preferential epoxide formation, while the use of 2,6-dichlorobenzoic acid results in preferential *cis*-dihydroxylation under otherwise similar reaction conditions.

Although these results were promising, two phenomena showed that the catalytic performance was not yet optimal. First of all, towards the end of the reaction the *cis*-diol product formed initially was (partly) converted to another compound (*i.e.* the corresponding α-hydroxyketone). This overoxidation decreased the yield of the desired *cis*-diol product, but this overoxidation could be suppressed almost completely by maintaining a pseudo

steady-state concentration of the alkene substrate.[i] Secondly, a lag period was encountered where conversion of the substrate did not occur. In order to solve the latter problem, the solution chemistry of the Mn-tmtacn complexes had to be understood.

Thus, despite the identification of carboxylic acids as the active addititive and the ability to tune the selectivity of the catalyst by changing the carboxylic acid, the mode of action of these carboxylic acid additives was not understood. On first sight this might appear of purily intellectual interest. However, the understanding of the mode of action of the carboxylic acid additives and of the solution chemistry of the Mn-tmtacn complexes proved to be key to tackling important issues regarding catalytic performance.

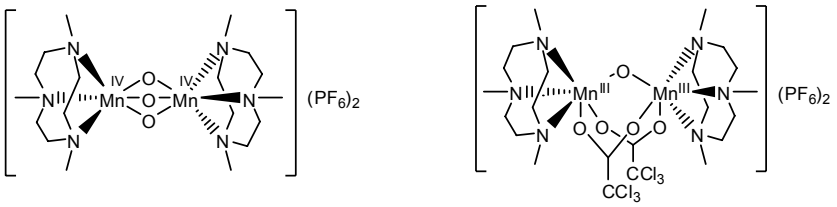

1 **2a**

Figure 8.1 $[Mn^{IV}_2(\mu\text{-}O)_3(tmtacn)_2]^{2+}$ **1** and $[Mn^{III}_2(\mu\text{-}O)(\mu\text{-}CCl_3CO_2)_2(tmtacn)_2]^{2+}$ **2a**.

Speciation analysis of the reaction mixture during the catalytic oxidation reaction showed that at the end of the lag period the complex $[Mn^{IV}_2(\mu\text{-}O)_3(tmtacn)_2]^{2+}$ **1** is no longer present and is converted mainly to the complex $[Mn^{III}_2(\mu\text{-}O)(\mu\text{-}RCO_2)_2(tmtacn)_2]^{2+}$ **2a** (Figure 8.1). The latter complex, containing two bridging carboxylato ligands, remains the major species in solution during the period over which catalytic activity is observed. The identification of these Mn^{III}_2-bis(carboxylato) complexes allowed for the rationalisation of the change in activity and selectivity observed when different carboxylic acid additives are used in combination with **1**. Actually the (bridging) ligands of the manganese dimers are being varied when using different carboxylic acid additives, thus tuning the activity and selectivity of the catalyst.

However, when this newly identified complex $[Mn^{III}_2(\mu\text{-}O)(\mu\text{-}RCO_2)_2(tmtacn)_2]^{2+}$ **2a** was used as catalyst, the lag period decreased only partially, and although the catalytic activity was initially similar to the system **1**/carboxylic acid, during the second half of the reaction, catalyst **2a** lost its activity gradually and eventually all catalytic activity ceased. Full stability of the catalyst throughout the full time course of the reaction could be attained by employing a slight excess of carboxylic acid in solution (Figure 8.2). In this way the equilibrium between the bound, bridging carboxylato ligand and free carboxylic acid is shifted towards the former, ensuring catalyst integrity and thus catalytic activity.

[i] This implies that the overoxidation is not an inherent problem of the catalyst selectivity and, moreover, that by immobilisation of the Mn-tmtacn catalyst on a solid support in a continuous flow reactor good selectivities would in principle be obtained.

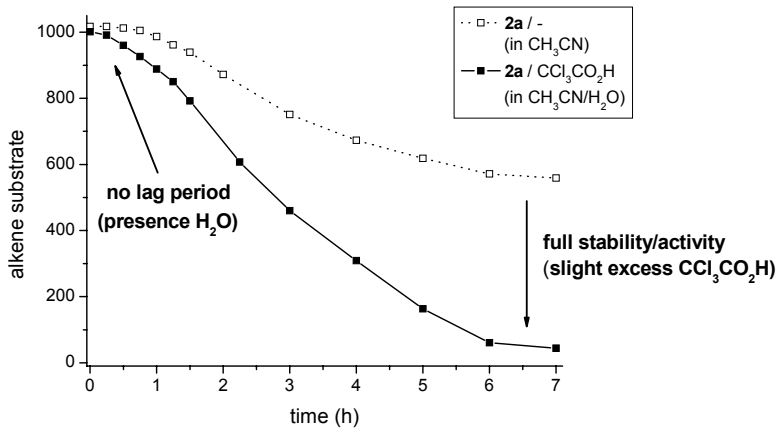

Figure 8.2 Catalytic oxidation of cyclooctene by **2a** (0.1 mol%) without H_2O pretreatment and in the absence of CCl_3CO_2H (dotted line) and with H_2O pretreatment and with CCl_3CO_2H (1 mol%) present (solid line).

The reason for the incomplete reduction of the lag period is more subtle. When the corresponding Mn^{II}_2-bis(carboxylato) complexes were used as the catalyst source, the lag period was suppressed completely and high activity was obtained during the full time course of the reaction. The selectivity during the initial period of the reaction on the other hand (*i.e.* the *cis*-diol/epoxide ratio) was different then during the remainder of the reaction. The differences in both activity and selectivity during the initial period of the reaction (*i.e.* during the 'lag period') are, however, not due to the differences in oxidation state of the manganese dimers (whenever catalytic activity is observed, Mn^{III}_2-bis(carboxylato) complexes are the major species in solution). The crucial factor for the differences in selectivity is the presence of water in the reaction mixture. Together with the oxidant H_2O_2, which is added slowly, water is added and its concentration thus increases over the time course of the reaction. When some water is added prior to starting the reaction, the selectivity observed is normal, together with full activity of the catalyst throughout the reaction, thus making use of the full potential of the catalytic system (Figure 8.2).

This effect of water can be understood in terms of the equilibrium between two Mn^{III}_2-bis(carboxylato) complexes with different non-carboxylato ligands: the 'closed' species **2a** contains a μ-oxo bridge, while the 'open' species **2d** contains two terminally bound hydroxo ligands (Figure 8.3). Since these are more labile then a μ-oxo bridge, ligand exchange with the oxidant H_2O_2 occurs more readily. The presence of water thus improves the activity of the catalyst.

The two important aspects about the proposed catalytic cycle are i) that dinuclear species are involved and ii) that a peroxo species, Mn^{III}_2-η^1-OOH, is proposed to be the catalytically active species that interacts with the alkene substrate to yield the *cis*-diol and

epoxide products.[ii] Coordination of H_2O_2 to the Mn^{III} center polarizes the O-O bond of the peroxide and this polarisation is further enhanced by intramolecular hydrogen bond formation with the hydroxo ligand on the adjacent Mn^{III} center. The present model would be a good starting point for DFT calculations to further explore its validity to the Mn-tmtacn catalysed oxidations and deepen the understanding of the factors governing the activity and the selectivity of the current catalytic system.

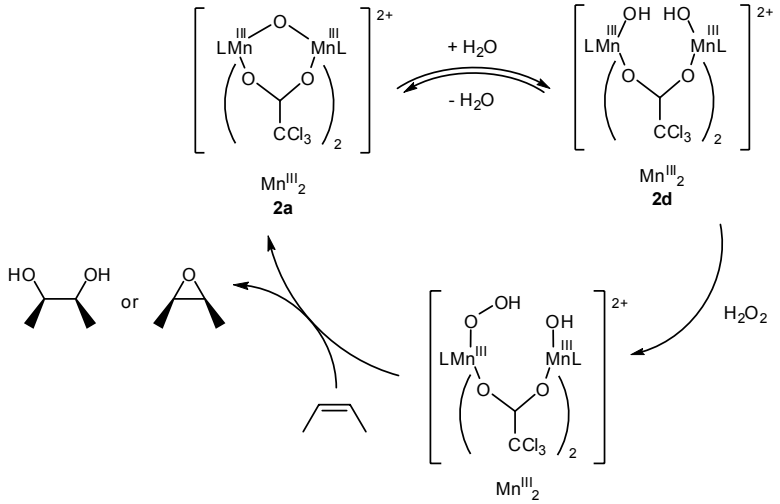

Figure 8.3 Catalytic cycle.

The role of the carboxylic acid additive is threefold: i) it acts as a proton source to protonate one of the μ-oxo bridges of **1**, thus enabling reduction and subsequent ligand exchange, ii) it acts as ligand in the dinuclear Mn^{III}_2 bis(carboxylato) species, thus tuning the activity and selectivity of the catalyst, and iii) slight excess of carboxylic acid in solution improves catalyst stability by suppressing the dissociation of the carboxylato ligands from the Mn^{III}_2 complexes. This, together with the observation that water is needed in the reaction mixture to improve the activity of the system, highlights the need to consider the whole system, instead of just the starting complexes, to improve catalytic performance. Moreover, it is important to consider that one component or parameter can have more than a single role to play. By taking an integrated approach between ('macroscopic') catalytic studies (systematically varying reaction conditions and monitoring changes in reactivity and product distribution in time) and by investigation of the solution chemistry of the manganese complexes involved, the activity and selectivity of the catalytic system could be enhanced and the mechanistic framework for the mode of action of the Mn-tmtacn catalysed oxidation of alkenes could be improved substantially.

[ii] Prior to the start of the studies reported in this thesis, mononuclear, high-valent Mn-oxo species were proposed to be responsible for the catalytic activity observed, despite the, at best, very limited experimental data to support these proposals (for a more detailed discussion of the previously proposed catalytically active species see section 5.4.2.1, Chapter 5 and references cited herein). However, the occurrence of high-valent Mn-oxo intermediates does not fit with the observed ^{18}O-labelling studies and mononuclear complexes have not been observed.

The research described in this thesis provides for the first time detailed experimental evidence for the role of (carboxylic acid) additives in Mn-tmtacn catalysed oxidation reactions. However, analysis of the literature clearly shows that carboxylato/carboxylic acid is present in most experimental procedures described for Mn-tmtacn catalysed oxidation reactions, strongly suggesting that the investigations and phenoma described and the mechanism proposed in this thesis hold direct relevance for Mn-tmtacn catalysed oxidations in general. In particular the importance of (two) bridging carboxylato ligands between two manganese centers as a structural motif and design requirement for manganese based oxidation catalysts is warranted.[4]

The importance of carboxylato ligands/carboxylic acids in Mn-tmtacn catalysed oxidative transformations is illustrated in the experimental procedures described in the referenced articles in a recent review.[iii] Of the 32 references cited concerning Mn-tmtacn catalysed oxidation employing H_2O_2, in 17 papers (53 %) carboxylic acids or carboxylato buffers are used as additive, 4 papers (13 %) report the use of either Mn^{II} or Mn^{III} acetato salts as manganese precursor, 7 papers (22 %) report acetone as solvent, 2 papers (6 %) report the use of a substrate which contains a carboxylic acid group itself and 1 paper (3 %) reports the use of a Mn^{III}_2 bis(carboxylato) complex. It is likely that the combination of H_2O_2 and acetone can result in the formation of acetic acid via Baeyer-Villiger[5] type reaction and thus, effectively, a carboxylic acid is also present when acetone is used as solvent and no carboxylic acid is added deliberately. Indeed, the formation of acetic acid was noted by De Vos and coworkers in a footnote in their report[6] on the Mn-tmtacn catalysed epoxidation of alkenes employing H_2O_2 in acetone.[iv]

Both the identification and the understanding of the role of carboxylic acid additives in Mn-tmtacn catalysed oxidation of alkenes paved the way for the development of the first Mn-based enantioselective *cis*-dihydroxylation catalyst.[v] Again, the understanding of the processes occurring in solution proved to be key to solving the initially low catalyst activity. The recognition that the presence of water liberates the carboxylic acid additive from the esters formed *in situ* was important to maintain the presence of a slight excess of carboxylic acid in solution with respect to Mn^{III}_2-dimer and thus ensures stability and activity of the catalyst.

The combination of **1** and achiral or chiral carboxylic acids, discovery and development of which are described in this thesis, hold considerable potential. Regarding epoxidation, the system **1**/salicylic acid is an attractive system compared with current systems because of its robustness and its ability to employ H_2O_2 as oxidant effectively, thus constituting a clean and environmentally benign method to synthesise epoxides. However, to find broad

---

[iii] Sibbons, K. F.; Shastri, K.; Watkinson, M. *Dalton Trans.* **2006**, 645-661. This review was chosen to provide an unbiased data set of the most relevant Mn-tmtacn literature.

[iv] Similarly, the formation of acetic acid from acetone and H_2O_2 in the presence of $[Fe^{II}(tpa)](OTf)_2$ was observed also: Mairata i Payeras, M.; Ho, R. Y. N.; Fujita, M.; Que, Jr., L *Chem. Eur. J.* **2004**, *10*, 4944-4953.

[v] Although one other Os-free system for the catalytic enantioselective *cis*-dihydroxylation of alkenes, based on Fe, is known [Costas, M.; Tipton, A. K.; Chen, K.; Jo, D.-H.; Que, Jr., L. *J. Am. Chem. Soc.* **2001**, *123*, 6722-6723], the current Mn-system exhibits much higher turnover numbers and catalyst stability.

applicability this system needs to be developed into a catalytic system which exhibits high enantioselectivity.

Of particular significance are the newly developed systems **1**/2,6-dichlorobenzoic acid and **1**/Ac-D-Phg-OH. The former is the most active Os-free *cis*-dihydroxylation catalyst know to date and, moreover, employs H_2O_2 as oxidant. With the latter catalytic system modest enantioselectivity has been obtained (up to 47% *ee*). Although this is far less then the *ee*'s typically obtained with Os-based catalysts and the enantioselectivity of this new system should be improved substantially, these results constitute a major breakthrough since this catalyst is based on a relatively non-toxic and cheap metal, employs H_2O_2 as oxidant and is more robust than the Fe-based systems availlable currently (see section 1.2.2, Chapter 1).

The studies presented in this work indicate that further work should focus on the development of several complementary catalytic systems to cover all substrate classes and the several types of oxidative transformation (*e.g. cis*-dihydroxylation, epoxidation, alcohol oxidation or C-H bond activation). Especially in light of the need to develop *selective* catalysts, it is perhaps naive to imagine that a single catalytic system 'can do it all', *i.e.* be capable of multiple oxidation reactions and be selective simultaneously.

The carboxylato-bridged dinuclear manganese structure should be considered as a potentially key structural motif for the design of new catalytic systems. In addition to the Mn-tmtacn family of catalysts, carboxylate salts or carboxylic acids are often present and their role has received little attention. Examples include compounds such as $[Mn^{III}_2(\mu\text{-}O)(\mu\text{-}CH_3CO_2)_2(tptn)]^{2+}$ [4a,b] and the dinuclear manganese complexes based on the ligand N2PyMePhOH[4c], where a remarkable shift between catalase activity and catalytic oxidation has been observed upon change of the bridging ligands. While the exact mechanism by which these catalysts operate is poorly understood, the similarities of these complexes with Mn-tmtacn in terms of core structure are obvious and the role of both the bridging carboxylato ligands and the other bridging units in these complexes deserves further exploration.

References

[1] Hage, R.; Iburg, J. E.; Kerschner, J.; Koek, J. H.; Lempers E. L. M.; Martens R. J.; Racherla, U. S.; Russell S. W.; Swarthoff, T.; van Vliet M. R. P.; Warnaar, J. B.; van der Wolf, L.; Krijnen, B. *Nature* **1994**, *369*, 637-639.
[2] Hage, R.; Lienke, A. *J. Mol. Catal. A.: Chem.* **2006**, *251*, 150-158.
[3] Brinksma, J.; Schmieder, L.; Van Vliet, G.; Boaron, R.; Hage, R.; De Vos, D. E.; Alsters, P. L.; Feringa, B. L. *Tetrahedron Lett.* **2002**, *43*, 2619-2622.
[4] a) Brinksma, J.; Hage, R.; Kerschner, J.; Feringa, B. L. *Chem. Commun.* **2000**, 537-538. b) Brinksma, J.; La Crois, R.; Feringa, B. L.; Donnoli, M. I.; Rosini, C. *Tetrahedron Lett.* **2001**, *42*, 4049-4052. c) La Crois, *R. M. Manganese Complexes as Catalysts in Epoxidation Reactions: a Ligand Approach*, Ph.D. thesis, University of Groningen, The Netherlands, **2000**. d) de Boer, J. W.; Browne, W. R.; Feringa, B. L.; Hage, R. *C. R. Chimie* **2007**, *10*, 341-354.
[5] March, J. *Advanced Organic Chemistry: Reactions, Mechanisms and Structure* (fourth edition), **1992**, Wiley, New York, pp. 1098-1099.
[6] De Vos, D. E.; Sels, B. F.; Reynaers, M.; Rao, Y. V. S.; Jacobs, P. A. *Tetrahedron Lett.* **1998**, *39*, 3221-3224.

Appendix A
Substrates and products

Suppliers of commercially availlable compounds. All reagents are of commercial grade (Aldrich, Acros, Fluka, Merck, NovaBiochem) and used as received unless stated otherwise. Hydrogen peroxide: 50 w/w % (Acros) or 30 v/v % (Merck, medical grade) solution in water. D_2O_2 (Icon Isotopes): 30 % solution in D_2O, 99 atom% D. D_2O (Aldrich): 99.9 atom% D. $H_2{}^{18}O_2$ (Icon Isotopes): 2 % solution in $H_2{}^{16}O$, 90 atom% ^{18}O. $H_2{}^{18}O$ (Icon Isotopes): 97 atom% ^{18}O. *m*CPBA (Acros): 70-75% in 3-chlorobenzoic acid and water. Peracetic acid (Fluka): 39% in acetic acid (45%) and contains up to 6% H_2O_2. ^{t}BuOOH (Aldrich): 70% in water. CH_3CN (Acros, extra pure). Cyclooctene: 95 % stabilized with 100-200 ppm irganox 1076 FD (Acros), or 95% (Aldrich) remainder cyclooctane; alternatively, cyclooctene (Acros) was triple distilled to remove the stabilizer. $Mn(OAc)_3.2H_2O$ (Aldrich). $Mn(ClO_4)_2.6H_2O$ (Acros).

TLC staining. UV-Vis: 254 and/or 366 nm. **Iodine:** A few crystals of iodine were mixed with silica (20 g). **Potassium permanganate:** $KMnO_4$ (6 g) and anhydrous Na_2CO_3 (6 g) were dissolved in H_2O (1 litre) and the solution was kept in the dark. **Cerium molybdate stain:** Phosphomolybdic acid (25 g) and cerium(IV) sulfate (7.5 g) were dissolved in H_2O (500 ml) and conc. H_2SO_4 (25 ml) was added. **Ninhydrin:** Ninhydrin (5 g) was dissolved in EtOH (100 ml). **Vanillin:** Vanillin (15 g) was dissolved in EtOH (250 ml) and conc. H_2SO_4 was added (2.5 ml).

Cis- and *trans*-2,3-epoxyheptane were prepared by stereospecific epoxidation of the corresponding alkene using *m*-chloroperoxybenzoic acid according to a modified literature procedure.[1]

***Cis*-2,3-epoxyheptane.** A solution of *m*-chloroperoxybenzoic acid (5.0 g, 20.3 mmol) in CH_2Cl_2 (50 ml) was added slowly to a cooled mixture of *cis*-2,3-heptene (2.00 g, 20.4 mmol) in CH_2Cl_2 (50 ml) maintaining the temperature below 5°C. The reaction mixture was allowed to reach room temperature and was stirred overnight. *m*-Chlorobenzoic acid was removed by filtration and the organic layer was washed with saturated $NaHCO_3$ (3x50 ml) and brine (1x50 ml), was dried over Na_2SO_4 and the solvent was evaporated *in vacuo*, yielding a colorless oil (1.58 g, 13.8 mmol, 68%). ^{1}H NMR (300 MHz, $CDCl_3$): δ 0.92 (t, J = 6.8 Hz, 3H), 1.26 (d, J = 5.5 Hz, 3H), 1.37-1.60 (m, 6H), 2.86-2.91 (m, 1H), 3.00-3.07 (m, 1H). ^{13}C NMR (75.4 MHz, $CDCl_3$): δ 13.2, 14.0, 22.6, 27.2, 28.6, 52.6, 57.1. Both ^{1}H and ^{13}C NMR spectra are in accordance with ref. [1].

***Trans*-2,3-epoxyheptane.** As for *cis*-2,3-epoxyheptane, except trans-2,3-heptene (4.00 g, 40.7 mmol) was used, yielding a colorless oil (3.38 g, 29.6 mmol, 73%). ^{1}H NMR (300 MHz, $CDCl_3$): δ 0.91 (t, J = 7.0 Hz, 3H), 1.29 (d, J = 5.1 Hz, 3H), 1.34-1.53 (m, 6H), 2.60-2.64 (m, 1H), 2.71-2.76 (m, 1H). ^{13}C NMR (75.4 MHz, $CDCl_3$): δ 14.0, 17.7, 22.5, 28.1, 31.7, 54.6, 59.8. Both ^{1}H and ^{13}C NMR spectra are in accordance with ref. [1].

Threo- and *erythro*-2,3-heptanediol were obtained by hydrolysis of the corresponding epoxide according to a modified literature procedure.[1b]

***Threo*-2,3-heptanediol.** A mixture of *cis*-2,3-epoxyheptane (2.00 g, 17.5 mmol), THF (24 ml) and 0.05 M $HClO_4$ (aq.) (16 ml) was stirred overnight at room temperature. Extraction with CH_2Cl_2 (3x20 ml), followed by drying of the combined organic layers with brine (30 ml) and Na_2SO_4, afforded the crude diol which was purified by column chromatography (silica, Et_2O/pentane 1:1), yielding a colorless oil (1.04 g, 7.9 mmol, 45%). ^{1}H NMR (300 MHz, $CDCl_3$): δ 0.91 (t, J = 6.6 Hz, 3H), 1.19 (d, J = 6.2 Hz, 3H), 1.32-1.50 (m, 6H), 2.17 (bs, 2H), 3.32-3.36 (m, 1H), 3.55-3.63 (m, 1H). ^{13}C NMR (75.4 MHz,

$CDCl_3$): δ 14.0, 19.5, 22.7, 27.7, 33.0, 70.9, 76.2. Both ^{1}H and ^{13}C NMR spectra are in accordance with ref. [1].

***Erythro*-2,3-heptanediol.** As for *threo*-2,3-heptanediol, except *trans*-2,3-epoxyheptane was used, yielding a colorless solid (1.49 g, 11.3 mmol, 64%). ^{1}H NMR (300 MHz, $CDCl_3$): δ 0.90 (t, J = 7.0 Hz, 3H), 1.12 (d, J = 6.6 Hz, 3H), 1.23-1.50 (m, 6H), 2.43 (bs, 2H), 3.57-3.62 (m, 1H), 3.73-3.81 (m, 1H). ^{13}C NMR (75.4 MHz, $CDCl_3$): δ 14.0, 16.5, 22.7, 28.2, 31.5, 70.4, 74.9. Both ^{1}H and ^{13}C NMR spectra are in accordance with that reported in ref. [1].

Dimethyl *cis*-2,3-oxiranedicarboxylate. *Cis*-epoxysuccinic acid was prepared according to the literature procedure,[2] except maleic acid (11.6 g, 100 mmol) was used, yielding the diacid as a colorless solid (8.42 g, 63.8 mmol, 64%). m.p. 145-148 °C (lit.[2]: 148-149 °C). ^{1}H NMR (400 MHz, D_2O): δ 3.94 (s, 2H). The dimethylester was prepared according to the literature procedure,[3] except using *cis*-epoxysuccinic acid (2.00 g, 15.1 mmol). Purification by columnchromatography (neutral alox, CH_2Cl_2/pentane 2:1) yielded the title compound as a colorless oil (0.35 g, 2.2 mmol, 15%). ^{1}H NMR (400 MHz, $CDCl_3$): δ 3.71 (s, 2H), 3.79 (s, 6H), in accordance with that reported in ref. [3]. ^{13}C NMR (50.3 MHz, $CDCl_3$): δ 52.5, 52.7, 166.1.

Dimethyl *trans*-2,3-oxiranedicarboxylate. *Trans*-epoxysuccinic acid was prepared according to the literature procedure,[2] except fumaric acid (11.6 g, 100 mmol) was used, yielding the diacid as a colorless solid (6.2 g, 47 mmol, 47%). ^{1}H NMR (400 MHz, D_2O) δ 3.72 (s, 2H). The dimethylester was prepared according to the literature procedure,[3] except using *trans*-epoxysuccinic acid (2.00 g, 15.1 mmol). Recrystalisation from CH_2Cl_2/pentane yielded a colorless solid (0.76 g, 4.7 mmol, 31%). m.p. 75.2-75.5 °C (lit.[4]: m.p. 75-76 °C). ^{1}H NMR (300 MHz, $CDCl_3$): δ 3.69 (s, 2H), 3.82 (s, 6H). ^{13}C NMR (50.3 MHz, $CDCl_3$): δ 51.9, 53.0, 167.0.

Dimethyl-*meso*-tartrate. Dimethyl-*meso*-tartrate was prepared by refluxing a mixture of *meso*-tartaric acid and excess $SOCl_2$ in MeOH according to the literature procedure[5] for the synthesis of dimethyl D-tartrate. Dimethyl-*meso*-tartrate was obtained as a colorless solid (0.49 g, 2.8 mmol, 21%). ^{1}H NMR (400 MHz, $CDCl_3$): δ 3.25 (d, J = 5.9 Hz, 2H), 3.81 (s, 6H), 4.58 (d, J = 5.9 Hz, 2H). ^{1}H NMR (300 MHz, acetone-d_6): δ 3.70 (s, 6H), 4.48 (s, 4H). ^{13}C NMR (50.3 MHz, $CDCl_3$): δ 53.0, 72.9, 171.4. Both ^{1}H and ^{13}C NMR spectra are in accordance with that reported in ref. [6].

Isolation of *cis*-cyclooctane diol from the reaction mixture (see Chaper 3, Table 3.8). The catalytic oxidation of cyclooctene (10 mmol) was performed according to general procedure C (see Appendix C). Subsequently, CH_2Cl_2 (10 ml) and saturated aq. $NaHCO_3$ (10 ml) were added and the organic layer was separated. The aqueous layer was extracted with CH_2Cl_2 (3x10 ml). The combined organic layers were washed with brine (15 ml) and dried on Na_2SO_4. The solvents were evaporated *in vacuo*. Pentane (5 ml) was added to the residue and the mixture was sonicated for a few minutes. The pentane was decanted and the resulting colorless precipitate was washed with pentane (2x5 ml) yielding *cis*-cyclooctane diol as a colorless solid (0.66 g, 4.6 mmol, 46%, average of 2 runs). ^{1}H NMR (400 MHz, $CDCl_3$) δ 1.48-1.56 (m, 6H), 1.64-1.69 (m, 4H), 1.86-1.96 (m, 2H), 2.06 (br s, 2H), 3.91 (d, 2H). ^{13}C NMR (100.6 MHz, $CDCl_3$) δ 23.72, 26.18, 30.09, 73.10.

Preparation and isolation of suberic acid using cis-1,2-cyclooctanediol as substrate. H_2O_2 (30 µl, 0.53 mmol) was added to a mixture of **1** (8.1 mg, 10 µmol) and 2,6-dichlorobenzoic acid (57.3 mg, 0.30 mmol) in CH_3CN (7 ml) at room temperature. The mixture was stirred for 20 min at room temperature followed by addition of *cis*-1,2-cyclooctanediol (0.72 g, 5 mmol) and CH_3CN (3 ml). The mixture was cooled to 0°C. H_2O_2 (50%, 1.13 ml, 20 mmol) was added *via* syringe pump (0.14 ml/h). The reaction mixture was stirred at 0°C for 1 h after the addition of H_2O_2 was completed. Water (10 ml) was added and the mixture was adjusted to pH 12 by adding 2 M aq. NaOH. The basic aqueous layer was washed with Et_2O (3x15 ml) and was subsequently acidified to pH 1 with 4 M aq. HCl. The acidic aqueous layer was extracted with Et_2O (5x15 ml) and the combined organic extracts were washed with brine (20 ml). After drying on anhydrous Na_2SO_4 the solvents were evaporated *in vacuo* yielding a colorless solid (367 mg, 42%). ^{1}H NMR (400 MHz, acetone-d_6) δ 1.31-1.35 (m, 4H), 1.55-1.58 (m, 4H), 2.25 (t, J = 7.3 Hz, 4H). CI-MS *m/z* 192 $[M+NH_4]^+$.

2,2-dimethylchromene (7.1). The synthesis was analogous to the preparation of precocene 1 as described in ref. [7]. Molecular sieves (3 Å) were heated at 160°C for 2 h under several vacuum/N_2 cycles. After cooling to room temperature, xylene (200 ml) was added, together with phenol (4.28 g, 45.5 mmol), phenylboronic acid (8.9 g, 73.0 mmol), 3-methyl-2-butenal (8.8 ml, 91.2 mmol) and propionic acid (2 ml, 27 mmol). The mixture was heated at reflux under Dean-Stark conditions for 3 days. After cooling to r.t., 20% NH_4OAc (150 ml) was added. The organic phase was separated and the aqueous layer was extracted with EtOAc (3x100 ml). The combined organic layers were washed with 0.5 M aq. $NaHCO_3$ (3x75 ml) and brine (100 ml). After drying on anhydrous Na_2SO_4 the solvents were evaporated *in vacuo* yielding a dark brown oil. Purification by column chromatography (silica, pentane) yielded **7.1** as a clear, pale yellow oil (2.95 g, 18.4 mmol, 40%). ^{1}H NMR (400 MHz, $CDCl_3$) δ 1.43 (s, 6H), 5.60 (d, J = 9.9 Hz, 1H), 6.32 (d, J = 9.9 Hz, 1H), 6.76-6.85 (m, 2H), 6.96-6.98 (m, 1H), 7.08-7.12 (m, 1H), in accordance with that reported in ref. [9]. ^{13}C NMR (50.3 MHz, $CDCl_3$) δ 27.97, 76.07, 116.27, 120.65, 121.23, 122.27, 126.24, 129.00, 130.67, 152.86. EI-MS *m/z* 160 $[M]^+$. HRMS (calc. for $C_{11}H_{12}O$: 160.089) found: 160.089.
Alternatively, this compound was prepared according to another modified literature procedure.[8] MeMgBr (68 ml, 205 mmol, 3 M in Et_2O) was added dropwise using a dropping funnel to a vigorously stirred solution of 1-benzopyran-2-one (10 g, 68.4 mmol) in toluene (500 ml) at 0°C. After the addition was complete, the reaction mixture was stirred for an additional 2 h at the same temperature. The reaction mixture was then poured onto a cold solution of 20% aq. NH_4Cl. The organic phase was concentrated *in vacuo* to remove Et_2O and MeOH. The residue (still containing toluene) was heated at reflux overnight under Dean-Stark conditions in the presence of 60 g of silica gel (activated immediately before use at 120°C). The hot reaction mixture was filtered and the residue of silica gel was washed several times with EtOAc. The combined filtrates were concentrated *in vacuo*. Purification by flash column chromatography (silica, pentane) yielded 2,2-dimethylchromene as a clear oil (7.2 g, 44.9 mmol, 66%).

***Cis*-2,2-dimethylchromane-3,4-diol (*cis*-7.3) and *trans*-2,2-dimethylchromane-3,4-diol (*trans*-7.5).** A mixture of **2a** (5.4 mg, 5 µmol), CCl_3CO_2H (500 µl of a 0.1 mM stock in CH_3CN, *i.e.* 50 µmol), H_2O (110 µl) and 2,2'-dimethylchromene (400 µl, 2.5 mmol) in CH_3CN (4.5 ml) was cooled to 0°C. H_2O_2 (50% aq., 240 µl, 4.2 mmol) was added *via*

syringe pump over 4 h (60 µl/h) and the reaction mixture was stirred for an additional 1 h after the addition of H_2O_2 was completed. CH_2Cl_2 (10 ml) and 0.5 M aq. $NaHCO_3$ (10 ml) were added. The organic layer was separated and the aqueous layer was extracted with CH_2Cl_2 (3x10 ml). The combined organic layers were washed with brine (15 ml). After drying on anhydrous Na_2SO_4 the solvents were evaporated *in vacuo*. Purification by column chromatography (silica, CH_2Cl_2/MeOH 97.5:2.5) afforded racemic *cis*-**7.3** (R_f 0.30) and racemic *trans*-**7.5** (R_f 0.27).
Cis-**7.3** (*rac*): 152 mg (0.78 mmol, 31%) of a very viscous, almost colorless oil which solidified upon standing. ^{1}H NMR (400 MHz, $CDCl_3$) δ 1.29 (s, 3H), 1.49 (s, 3H), 2.03 (d, *J* = 8.8 Hz, 1H), 2.61 (d, J = 9.9 Hz, 1H), 3.72 (dd, J = 8.4 and 4.4 Hz, 1H), 4.81 (dd, *J* = 9.5 and 4.0 Hz, 1H), 6.80-6.83 (m, 1H), 6.97-7.01 (m, 1H), 7.18-7.23 (m, 1H), 7.52-7.54 (m, 1H), in accordance with that reported in ref. [9]. ^{13}C NMR (50.3 MHz, $CDCl_3$) δ 23.30, 24.79, 65.24, 71.61, 77.70, 116.89, 121.29, 122.25, 128.83, 129.40, 151.93. EI-MS *m/z* 194 $[M]^+$. HRMS (calc. for $C_{11}H_{14}O_3$: 194.094) found: 194.094.
Trans-**7.5** (*rac*): 8 mg (0.04 mmol, 2%) of a very viscous, almost colorless oil which solidified upon standing. ^{1}H NMR (400 MHz, $CDCl_3$) δ 1.17 (s, 3H), 1.43 (s, 3H), 3.57 (d, *J* = 8.8 Hz, 1H), 3.84 (br s, 1H), 4.00 (br s, 1H), 4.54 (d, *J* = 8.8 Hz), 6.75-6.77 (m, 1H), 6.89-6.92 (m, 1H), 7.14-7.18 (m, 1H), 7.37-7.39 (m, 1H), in accordance with that reported in ref. [9]. ^{13}C NMR (50.3 MHz, $CDCl_3$) δ 18.64, 26.63, 69.61, 76.29, 78.38, 116.78, 120.69, 123.15, 127.34, 129.39, 152.16. EI-MS *m/z* 194 $[M]^+$. HRMS (calc. for $C_{11}H_{14}O_3$: 194.094) found: 194.094.

3,4-Epoxy-2,2-dimethylchromane (7.4). A mixture of 2,2-dimethylchromene (200 mg, 1.25 mmol) in CH_2Cl_2 (12 ml) and 0.5 M aq. $NaHCO_3$ (5 ml) was cooled to 0°C and *m*CPBA (242 mg, 1.05 mmol) was added in small portions. After the addition was complete, the reaction mixture was stirred for an additional 30 min at 0°C and was subsequently allowed to reach room temperature. The organic layer was separated and washed with 0.5 M $NaHCO_3$ (5x10 ml), H_2O (10 ml) and brine (10 ml). After drying on anhydrous Na_2SO_4, the solvents were evaporated *in vacuo*, yielding a mixture of unreacted alkene and epoxide (215 mg, epoxide/alkene ratio: 1.7 as judged from ^{1}H NMR). For spectroscopic data of the epoxide see *e.g.* ref. [9] and [10].

2,2-dimethylchroman-3-one (7.7). was prepared according to the literature procedure[11] by heating *cis*-2,2-dimethylchromane-3,4-diol at reflux in the presence of a catalytic amount of *p*-toluenesulfonic acid in benzene. ^{1}H NMR (400 MHz, $CDCl_3$) δ 1.41 (s, 6H), 3.60 (s, 2H), 6.98-7.24 (m, 4H), in accordance with that reported in ref. [11]. For the isomer 2,2-dimethylchroman-4-one, the signal due to the -C*H*$_2$- protons are observed at 2.72 ppm, as reported in ref. [12].

References

1 a) Kroutil, W.; Mischitz, M.; Faber, K. *J. Chem. Soc., Perkin Trans. 1* **1997**, 3629-3636.
b) Chiappe, C.; Cordoni, A.; Lo Moro, G.; Palese, C. D. *Tetrahedron: Asymmetry* **1998**, *9*, 341-350.
2 Payne, G. B.; Williams, P. H. *J. Org. Chem.* **1959**, *24*, 54-55.
3 Häbich, D.; Hartwig, W.; Born, L. *J. Heterocyclic Chem.* **1988**, *25*, 487-494.

4 Gawron, O.; Glaid, A. J.; LoMonte, A.; Gary, S. *J. Am. Chem. Soc.* **1958**, *80*, 5856-5860.
5 Kim, B. M.; Bae, S. J.; So, S. M.; Yoo, H. T.; Chang, S. K.; Lee, J. H.; Kang, J. *Org. Lett.* **2001**, *3*, 2349-2351.
6 Mohr, P.; Waespe-Šarčevic, N.; Tamm, C.; Gawronska, K.; Gawronski, J. K. *Helv. Chim. Acta* **1983**, *66*, 2501-2511.
7 Bissada, S.; Lau, C. K.; Bernstein, M. A.; Dufresne, C. *Can. J. Chem.* **1994**, *72*, 1866-1869.
8 a) Livingstone, R.; Watson, R. B. *J. Chem. Soc.* **1957**, 1509-1512. b) Strunz, G. M.; Brillon, D.; Giguère, P. *Can. J. Chem.* **1983**, *61*, 1963-1964.
9 Boyd, D. R.; Sharma, N. D.; Boyle, R.; Evans, T. A.; Malone, J. F.; McCombe, K. M.; Dalton, H.; Chima, J. *J. Chem. Soc., Perkin Trans. 1* **1996**, 1757-1765.
10 a) Sasaki, H.; Irie, R.; Hamada, T.; Suzuki, K.; Katsuki, T. *Tetrahedron* **1994**, *41*, 11827-11838. b) Wong, O. A.; Shi. Y. *J. Org. Chem.* **2006**, *71*, 3973-3976.
11 Anastasis, P.; Brown, P. E. *J. Chem. Soc., Perkin Trans. 1* **1983**, 1431-1437.
12 El-Essawy, F. A. G.; Yassin, S. M.; El-Sakka, I. A.; Khattab, A. F.; Søtofte, I.; Øgaard Madsen, J.; Senning, A. *J. Org. Chem.* **1998**, *63*, 9840-9845.

Appendix B
Ligands and complexes

All reagents are of commercial grade (Aldrich, Acros, Fluka, NovaBiochem, Bachem) and used as received unless stated otherwise. Unilever R&D (Vlaardingen, the Netherlands) is acknowledged for the generous gift of the complexes $[Mn^{IV}_2(\mu\text{-}O)_3(tmtacn)_2](PF_6)_2.H_2O$ **1**[1], $[Mn^{III}_2(\mu\text{-}O)(\mu\text{-}CH_3CO_2)_2(tmtacn\text{-}d_9)_2](PF_6)_2$ **3a**-d_{18},[2] $[Mn^{III,IV}_2(\mu\text{-}O)_2(Me_4dtne)](PF_6)_2$ [3] and the ligand tmtacn.[4] The synthesis and characterization of the complex $[Mn^{III}_2(\mu\text{-}O)(\mu\text{-}CH_3CO_2)_2(tmtacn)_2](PF_6)_2$ **3a** has been reported previously.[1]

Caution! Perchlorate salts of metal complexes incorporating organic ligands are potentially explosive. These compounds should be prepared in small quantities and handled with suitable protective safe guards.

B.1 Ligands

2,3,6-Trichlorobenzoic acid. This compound was prepared according to a reported procedure.[5] 2,3,6-Trichlorobenzaldehyde (2.00 g, 9.55 mmol) was added to a solution of $KMnO_4$ (1.58 g, 10.0 mmol) in H_2O (100 ml) and mixture was stirred at 90°C until the purple permanganate solution was decolorised and a brown suspension was obtained (1 h). The hot suspension was filtered on a glasfilter P4 and was rinsed with hot H_2O (3 x 40 ml). The filtrate was acidified with conc. HCl to pH 1 and a colorless precipitate formed. The solvent was evaporated *in vacuo* and the colorless solid was suspended in 0.1 M aq. HCl (25 ml). After filtration on a glasfilter P4, the colorless residue was dissolved in $CHCl_3$ (50 ml) and this solution was filtered to remove some insoluble material. The solvent was evaporated *in vacuo* and the title compound was obtained as a colorless solid (1.28 g, 5.68 mmol, 59%). ^{1}H NMR (300 MHz, $CDCl_3$) δ 7.32 (d, J = 8.6 Hz, 1H), 7.49 (d, J = 8.6 Hz, 1H), 10.13 (br s, 1 H). ^{13}C NMR (50.3 MHz, $CDCl_3$) δ 128.74, 129.72, 130.28, 130.35, 132.21, 134.06, 169.31. EI-MS *m/z* 224 $[M]^+$. HRMS (calc. for $C_7H_3O_2Cl_3$: 223.920) found: 223.921. m.p. 128.3-129.0 °C (lit.[5] 124-126°C). Elemental analysis (calc. for $C_7H_3O_2Cl_3$) C 37.3% (37.29%), H 1.20 (1.34%).

Ac-D-Phg-OH. Ac-D-Phg-OH was prepared according to a reported procedure.[6] D-(-)-α-phenylglycine (2.00 g, 13.2 mmol) was suspended in H_2O (30 ml) and the resulting suspension was cooled to 0-5°C with ice-water. Subsequently, NaOH (0.53 g, 13.2 mmol) was added and a clear solution was obtained. Acetic anhydride (2.5 ml, 26.4 mmol) was added, immediately followed by a solution of NaOH (1.59 g, 39.8 mmol) in H_2O (8 ml) (giving pH 5) and the mixture was stirred at 0-5°C for an additional 15 min. The reaction mixture was then acidified to pH 1 with conc. HCl (aq.). The colorless solid was collected on a glasfilter P4 and was subsequently washed with H_2O (3 x 20 ml). After recrystallisation from EtOH/H_2O (1:1) colorless needles were obtained (812 mg, 4.20 mmol, 32%). ^{1}H NMR (200 MHz, dmso-d_6) δ 1.89 (s, 3H), 5.32 (d, J = 7.7 Hz, 1H), 7.27-7.39 (m, 5H), 8.60 (d, J = 7.7 Hz, 1H), in accordance with literature[7]. ^{13}C NMR (50.3 MHz, dmso-d_6) δ 22.24, 56.24, 127.63, 127.89, 128.49, 137.22, 169.07, 171.99. EI-MS *m/z* 193 $[M]^+$. HRMS (calc. for $C_{10}H_{11}NO_3$: 193.074) found: 193.073.

Boc-Pro-Pro-OMe. Boc-Pro-OH (10.0 g, 46.4 mmol) was activated in CH_2Cl_2 (300 ml, freshly distilled from CaH_2) under N_2 with *N*-ethyl-*N'*-(3-dimethylaminopropyl)-carbodiimide (EDC) (9.76 g, 50.9 mmol) and 1-hydroxybenzotriazole hydrate (HOBt)

(6.88 g, 50.9 mmol) and this mixture was stirred at r.t. for 1 h giving a clear, colorless solution (solution A).
H-Pro-OMe.HCl (7.69 g, 46.4 mmol) and *N,N*-diisopropylethylamine (24.2 ml, 139 mmol) were dissolved in CH_2Cl_2 (400 ml, freshly distilled from CaH_2) under N_2 in a three-necked flask equipped with a dropping funnel, giving a clear, colorless solution (solution B).
Solution A was transferred (under N_2) to the dropping funnel and was subsequently added slowly to solution B (ca. 90 min.) at r.t. with the reaction mixture being cooled in a waterbath. When the addition was complete, the reaction mixture was heated at reflux overnight. After cooling to r.t. the organic layer was washed with brine (1x150 ml), 4 M $NaHCO_3$ (4x100 ml), 1 M $NaHSO_4$ (4x100 ml) and brine (1x200ml) and was dried over anhydrous Na_2SO_4. Evaporation of the solvents *in vacuo* yielded a very pale yellow oil. Purification by column chromatography (silica, CH_2Cl_2/MeOH 98:2; TLC visualised with ninhydrin dip) yielded Boc-Pro-Pro-OMe as a pale yellow oil (13.7 g, 42.0 mmol, 91%). ^{1}H NMR (400 MHz, $CDCl_3$) δ 1.39 and 1.44 (2 × s, (CH_3)$_3$, 9H), 1.81-2.23 (m, 8H), 3.35-3.80 (m, 7H), 4.37-4.60 (m, 2H), mixture of rotamers (the Boc-group shows coalescence at 60 °C in dmso-d_6). ^{13}C NMR (100.6 MHz, $CDCl_3$) δ 23.40, 23.89, 24.82, 24.88, 28.19, 28.35, 28.55, 28.67, 28.89, 29.83, 46.30, 46.34, 46.49, 46.68, 51.90, 51.96, 52.06, 57.53, 58.50, 79.23, 79.26, 153.56, 154.42, 170.95, 171.44, 172.49, 172.77, mixture of rotamers. EI-MS *m/z* 326 $[M]^+$. HRMS (calc. for $C_{16}H_{26}N_2O_5$: 326.184) found: 326.185.

Boc-Pro-Pro-OH. Boc-Pro-Pro-OMe (13.7 g, 42.0 mmol) was added to 2 M aq. NaOH (250 ml) and the resulting biphasic mixture was stirred at r.t. for 2 h until all oil had dissolved and TLC (silica, CH_2Cl_2/MeOH 98:2, ninhydrin-dip) showed complete conversion. The basic aqueous layer (pH 14) was washed with CH_2Cl_2 (3x100 ml) and was then acidified (to pH 1) with concentrated HCl (30% aq.). The resulting colorless suspension was extracted with EtOAc (5x75 ml). The combined EtOAc layers were washed with brine (1x100 ml) and dried on anhydrous Na_2SO_4. The solvents were evaporated *in vacuo* yielding a very sticky foam which was dissolved in a minimum amount of CH_2Cl_2 (40 ml). Pentane (200 ml) was added and the mixture was sonicated for a few minutes until a colorless suspension was obtained. Evaporation of the solvents *in vacuo* yielded Boc-Pro-Pro-OH as a white solid (10.2 g, 32.7 mmol, 78%). ^{1}H NMR (300 MHz, $CDCl_3$) δ 1.39 and 1.45 (2 × s, 9H), 1.85-2.41 (m, 8H), 3.38-3.80 (m, 4H), 4.37-4.68 (m, 2H), mixture of rotamers. ^{13}C NMR (50.3 MHz, $CDCl_3$) δ 23.65, 24.25, 25.04, 27.02, 27.24, 28.37, 28.44, 29.37, 30.20, 46.68, 46.92, 47.33, 57.57, 57.70, 59.91, 59.97, 79.79, 79.94, 153.48, 154.58, 172.16, 172.46, 174.38, 174.66, mixture of rotamers. EI-MS m/z 312 $[M]^+$. HRMS (calc. for $C_{15}H_{24}N_2O_5$: 312.168) found: 312.170.

B.2 Complexes

$[Mn^{III}_2(\mu\text{-}O)(\mu\text{-}CCl_3CO_2)_2(tmtacn)_2](PF_6)_2$ (2a). Complex **2a** was prepared by modification of the general procedure reported by Hage *et al.*[8]. L-Ascorbic acid (19 mg, 0.105 mmol) in H_2O (1 ml) was added to a solution of **1** (81 mg, 0.10 mmol) and CCl_3CO_2H (35 mg, 0.22 mmol) in H_2O (20 ml) with rapid stirring. The purple precipitate was isolated by filtration and rinsed with Et_2O (3x5 ml). Recrystallisation from CH_3CN by slow diffusion of Et_2O yielded purple crystals (75 mg, 0.07 mmol, 70%). ^{1}H NMR (400 MHz, CD_3CN) δ 66, 35, 32, 15, -74, -87, -108. ESI-MS *m/z* 935.0 $[\mathbf{2a}(PF6)]^+$, 395.0 $[\mathbf{2a}]^{2+}$,

isotope pattern in agreement with the predicted pattern for 6xCl. Elemental analysis (calc. for $Mn_2C_{22}H_{42}N_6Cl_6O_5P_2F_{12}$): C 24.8 % (24.4%), H 4.01% (3.87 %), N 7.76 % (7.76 %). FT-IR (in KBr powder): 1720, 1659 cm^{-1} (-CO_2-). X-band EPR silent, 10 mM in CH_3CN at 77 K. $[C_{22}H_{42}Cl_6Mn_2N_6O_5]^{2+}.2PF_6^-$ (CP929), M_r = 1083.13, monoclinic, $P2_1/n$, a = 12.2400(7), b = 15.5582(9), c = 21.494(1) Å, β = 97.405(1)°, V = 4059.0(4) $Å^3$, Z = 4, D_x = 1.772 gcm^{-3}, F(000) = 2184, μ = 11.93 cm^{-1}, $\lambda(MoK_\alpha)$ = 0.71073 Å, T = 100(1) K, 29469 reflections measured, $GooF$ = 1.030, $wR(F^2)$ = 0.0791 for 9313 unique reflections and 664 parameters and $R(F)$ = 0.0326 for 7837 reflections obeying $F_o \geq 4.0\ \sigma(F_o)$ criterion of observability. The asymmetric unit consists of three moieties: a cationic dinuclear Mn-complex and two PF_6^- anions.

$[Mn^{II}_2(\mu\text{-}OH)(\mu\text{-}CCl_3CO_2)_2(tmtacn)_2](ClO_4)$ (2b). Complex **2b** was prepared by modification of the general procedure reported by Wieghardt *et al.*[1a] $Mn(ClO_4)_2.6H_2O$ (250 mg, 0.69 mmol) was added to a N_2 purged solution of tmtacn (200 mg, 1.16 mmol). After 10 min, CCl_3CO_2Na (278 mg, 1.5 mmol) was added in one portion with rapid stirring. After 1 h, the volume was reduced (by N_2 flow) to half its volume and kept at 6°C to yield white crystals (175 mg, 0.195 mmol, 28%) suitable for single crystal X-ray analysis. ^1H NMR (400 MHz, CD_3CN) no signals observed between -120 and 100 ppm. ESI-MS *m/z* 791.0 $[\mathbf{2b}]^+$, isotope pattern in agreement with predicted pattern for 6xCl. Elemental analysis (calc. for $Mn_2C_{22}H_{43}N_6Cl_7O_9$) C 29.7 % (29.6 %), H 4.90% (4.81%), N 9.43 % (9.40%). FT-IR (in KBr powder): 1692 cm^{-1} (-CO_2-). $[C_{22}H_{43}Cl_6Mn_2N_6O_5]^+.[ClO_4]^-$ (CP921), M_r = 893.66, monoclinic, *Cm*, a = 15.695(3), b = 15.918(3), c = 15.594(3) Å, β = 104.801(3)°, V = 3766.6(12) $Å^3$, Z = 4, D_x = 1.576 gcm^{-3}, F(000) = 1832, μ = 12.19 cm^{-1}, $\lambda(MoK_\alpha)$ = 0.71073 Å, T = 100(1) K, 10049 reflections measured, $GooF$ = 1.052, $wR(F^2)$ = 0.1499 for 5496 unique reflections and 447 parameters, 2 restraints and $R(F)$ = 0.0567 for 4828 reflections obeying $F_o \geq 4.0\ \sigma(F_o)$ criterion of observability. The asymmetric unit consists of four half moieties: two cationic dinuclear Mn-complexes, and two disordered ClO_4^- anions; all moieties have a crystallographic imposed mirror plane.

$[Mn^{II}_2(\mu\text{-}O_2H_3)(\mu\text{-}CCl_3CO_2)_2(tmtacn)_2](PF_6)$ (2c). Hydrazine.hydrate (20 µl, 0.2 mmol) was added to a stirred solution of **1** (81 mg, 0.10 mmol) and CCl_3CO_2H (35 mg, 0.22 mmol) in CH_3CN (20 ml). The solution changed from red to light purple to colorless over 30 min. The solvent was evaporated to near dryness and the white precipitate washed with Et_2O yielding **2c** as a white solid (84 mg, 0.088 mmol, 88%). ESI-MS *m/z* 809.0 $[\mathbf{2c}]^+$; isotope pattern in agreement with predicted pattern for 6xCl. Elemental analysis (calc. for $Mn_2C_{22}H_{45}N_6Cl_6O_6PF_6$): C 26.5% (27.6%), H 4.23% (4.74%), N 8.79 % (8.78%). FT-IR (in KBr powder): 1695 cm^{-1} (-CO_2-).

$[Mn^{III}_2(\mu\text{-}O)(\mu\text{-}CD_3CO_2)_2(tmtacn)_2](PF_6)_2$ (3a-d$_6$). As for **2a** except CD_3CO_2D (13.5 mg, 0.21 mmol) was employed, yielding **3a**-d$_6$ (43 mg, 0.049 mmol, 49%). ^{1}H NMR (400 MHz, CD_3CN) δ 72, 68, 37, 22, -80, -93, -98, in accordance with that reported in ref. [2]. ESI-MS *m/z* 737.4 [**3a**-d$_6$(PF$_6$)]$^+$, 296.2 [**3a**-d$_6$]$^{2+}$. Elemental analysis (calc. for $Mn_2C_{22}H_{42}D_6N_6O_5P_2F_{12}$): C 30.07% (29.94%), H 4.47% (5.48%), N 9.47% (9.52%).[i]

$[Mn^{III}_2(\mu\text{-}O)(\mu\text{-benzoato})_2(tmtacn)_2](PF_6)_2$ (6). As for **2a** except benzoic acid (24 mg, 0.22 mmol) was employed, yielding **6** (75 mg, 0.075 mmol, 75%). ^{1}H NMR (400 MHz, CD3CN) δ 72, 35, 21, 14, 6, 0 -80, -92, -96. ESI-MS *m/z* 855.4 [**6**(PF$_6$)]$^+$, 355.2 [**6**]$^{2+}$. Elemental analysis (calc. for $Mn_2C_{32}H_{52}N_6O_5P_2F_{12}$): C 36.7% (38.41%), H 5.22% (5.24%), N 8.67% (8.40%). $[C_{32}H_{52}Mn_2N_6O_5]^{2+}.2(PF_6)^-.2(C_4H_8O_2)0.5$ (CP904), M_r = 1088.71, triclinic, *P*-1, a = 11.4974(5), b = 13.7430(6), c = 16.3508(7) Å, α = 76.826(1)°, β = 76.090(1)°, γ = 69.359(1)°, V = 2317.49(17) Å^3, Z = 2, D_x = 1.560 gcm^{-3}, F(000) = 1124, μ = 7.14 cm^{-1}, λ(MoK$_\alpha$) = 0.71073 Å, T = 100(1) K, 22101 reflections measured, $GooF$ = 1.025, $wR(F^2)$ = 0.1078 for 11061 unique reflections and 538 parameters and $R(F)$ = 0.0384 for 10023 reflections obeying $F_o \geq 4.0\ \sigma(F_o)$ criterion of observability. The asymmetric unit consists of five moieties: a cationic dinuclear Mn-complex, two PF_6^- anions and two disordered, half ethylacetate solvent molecules.

$[Mn^{III}_2(\mu\text{-}O)(\mu\text{-4-bromobenzoato})_2(tmtacn)_2](PF_6)_2$ (7). As for **9** except 4-bromobenzoic acid (44.2 mg, 0.22 mmol) was employed, yielding **7** (90 mg, 0.078 mmol, 78%). ^{1}H NMR (400 MHz, CD_3CN) δ 71, 34, 20, 14, 6, -81, -92, -98. ESI-MS *m/z* 1011.1 [**7**(PF$_6$)]$^+$, 433.2 [**7**]$^{2+}$, isotope pattern in agreement with predicted pattern for 2xBr. Elemental analysis (calc. for $Mn_2C_{32}H_{50}N_6O_5Br_2P_2F_{12}$): C 33.5% (33.22%), H 4.54% (4.36%), N 7.08% (7.27%). $[C_{32}H_{50}Br_2Mn_2N_6O_5]^{2+}.2[PF_6]^-$ (CP983), M_r = 1158.40, monoclinic, $P2_1/n$, a = 17.329(2), b = 19.586(2), c = 33.522(4) Å, β = 104.403(2)°, V = 11020(2) Å^3, Z = 8, D_x = 1.396 gcm^{-3}, F(000) = 4656, μ = 20.44 cm^{-1}, λ(MoK$_\alpha$) = 0.71073 Å, T = 100(1) K, 84406 reflections measured, $GooF$ = 1.067, $wR(F^2)$ = 0.2365 for 21538 unique reflections and 1111 parameters and $R(F)$ = 0.0803 for 12278 reflections obeying $F_o \geq 4.0\ \sigma(F_o)$ criterion of observability. The asymmetric unit consists of six moieties: two cationic dinuclear Mn-complexes and four disordered PF_6^- anions.

$[Mn^{III}_2(\mu\text{-}O)(\mu\text{-4-nitrobenzoato})_2(tmtacn)_2](PF_6)_2$ (8). As for **2a** except 4-nitrobenzoic acid (36.8 mg, 0.22 mmol) was employed, yielding **8** (30 mg, 0.028 mmol, 28%). ^{1}H NMR (400 MHz, CD_3CN) δ 71, 34, 19, 15, 7, -81, -92, -100. ESI-MS *m/z* 945.3 [**8**(PF$_6$)]$^+$, 400.2 [**8**]$^{2+}$. Elemental analysis (calc. for $Mn_2C_{32}H_{50}N_8O_9P_2F_{12}$): C 35.3% (35.22%), H 4.72% (4.62%), N 9.11 (10.28%). $[C_{32}H_{50}Mn_2N_8O_9]^{2+}.2[PF_6]^-$ (CP982), M^r = 1090.60, monoclinic, *C*2/*c*, a = 33.528(2), b = 20.104(1), c = 16.215(1) Å, β = 107.300(1)°, V = 10435.2(10) Å^3, Z = 8, Dx = 1.388 gcm^{-3}, F(000) = 4464, μ = 6.38 cm^{-1}, λ(MoK$_\alpha$) = 0.71073 Å, T = 100(1) K, 40157 reflections measured, $GooF$ = 1.074, $wR(F^2)$ = 0.1532 for 10248 unique

[i] The measured values for several elemental analyses are not close enough to the calculated values by acceptable standards (+/- 3%). This is due to the presence of fluor in these compounds (PF_6^- is used as anion in most cases) which makes the elemental analysis measured in our own laboratory too inaccurate. Elemental analyses of the same samples by Kolbe - Mikroanalytisches Laboratorium (Mülheim an der Ruhr, Germany) afforded values considerably closer to the calculated ones, indicating that the method used is the problem and not the purity of the samples. Due to cost considerations, however, not all samples were sent for analyses to Kolbe.

reflections and 592 parameters and $R(F)$ = 0.0545 for 7605 reflections obeying $F_o \geq 4.0\ \sigma(F_o)$ criterion of observability. The asymmetric unit consists of three moieties: a cationic dinuclear Mn-complex and two PF_6^- anions.

[Mn^{III}_2(μ-O)(μ-^{t}BuCO$_2$)$_2$(tmtacn)$_2$](PF$_6$)$_2$ (9). Hydrazine.hydrate (20 µl, 0.2 mmol) was added to a solution of **1** (81 mg, 0.10 mmol) and pivalic acid (22.5 mg, 0.22 mmol) in CH_3CN (20 ml) with stirring. The solution was evaporated to dryness, washed with Et_2O and recrystallised from CH_3CN by slow infusion of Et_2O. **9** was obtained as red/purple crystals (85 mg, 0.088 mmol, 88%). ^{1}H NMR (400 MHz, CD_3CN) δ 75, 68, 39, 21, 10, -82, -95, -102. ESI-MS *m/z* 815.3 [**9**(PF$_6$)]$^+$, 335.3 [**9**]$^{2+}$. Elemental analysis (calc. for $Mn_2C_{28}H_{60}N_6O_5P_2F_{12}$): C 35.0% (35.01%), H 6.79% (6.30%), N 8.66% (8.75%).

[Mn^{III}_2(μ-O)(μ-4-iodobenzoato)$_2$(tmtacn)$_2$](PF$_6$)$_2$ (10). As for **2a** except 4-iodobenzoic acid (54.6 mg, 0.22 mmol) was employed, yielding **10** (15 mg, 0.012 mmol, 12%). ^{1}H NMR (400 MHz, CD_3CN) δ 71, 34, 20, 14, 6, -81, -92, -98. ESI-MS *m/z* 1107.2 [**10**(PF$_6$)]$^+$, 481.2 [**10**]$^{2+}$. Elemental analysis (calc. for $Mn_2C_{32}H_{50}N_6O_5I_2P_2F_{12}$): C 30.8% (30.67%), H 4.33% (4.02%), N 6.84% (6.71%).

[Mn$_2$(μ-O)(μ-3-chlorobenzoato)$_2$(tmtacn)$_2$](PF$_6$)$_2$ (11). As for **2a** except 3-chlorobenzoic acid (34 mg, 0.22 mmol) was employed, yielding **11** (30 mg, 0.028 mmol, 25%). ^{1}H NMR (400 MHz, CD_3CN) δ 66, 35, 32, 15, -74, -87, -108. ESI-MS *m/z* 923.3 [**11**(PF$_6$)]$^+$, 389.3 [**11**]$^{2+}$, isotope pattern in agreement with predicted pattern for 2xCl. Elemental analysis (calc. for $Mn_2C_{32}H_{50}N_6Cl_2O_5P_2F_{12}$): C 36.0 % (35.9 %), H 4.98% (4.68 %), N 7.80 % (7.86 %).

[Mn^{III}_2(μ-O)(μ-4-chlorobenzoato)$_2$(tmtacn)$_2$](PF$_6$)$_2$ (12). As for **2a** except 4-chlorobenzoic acid (34.4 mg, 0.22 mmol) was employed, yielding **12** (10 mg, 9.4 µmol, 9%). ESI-MS *m/z* 923.2 [**12**(PF$_6$)]$^+$, 389.4 [**12**]$^{2+}$, isotope pattern in agreement with predicted pattern for 2xCl. Elemental analysis (calc. for $Mn_2C_{32}H_{50}N_6O_5Cl_2P_2F_{12}$): C 36.9% (35.95%), H 5.15% (4.72%), N 7.48% (7.87%).

[Mn^{III}_2(μ-O)(μ-2,6-dichlorobenzoato)$_2$(tmtacn)$_2$](PF$_6$)$_2$ (13). As for **2a** except 2,6-dichlorobenzoic acid (42 mg, 0.22 mmol) was employed, yielding **13** (50 mg, 0.044 mmol, 40%). ^{1}H NMR (400 MHz, CD_3CN) δ 65, 42, 36, 15, -80, -93, -100. ESI-MS *m/z* 991.3 [**13**(PF$_6$)]$^+$, 424 [**13**]$^{2+}$, isotope pattern in agreement with predicted pattern for 4xCl. Elemental analysis (calc. for $Mn_2C_{32}H_{48}N_6Cl_4O_5P_2F_{12}$): C 33.6 % (33.7 %), H 4.27% (4.22 %), N 7.30 % (7.38 %).

[Mn^{III}_2(μ-O)(μ-2,4-dichlorobenzoato)$_2$(tmtacn)$_2$](PF$_6$)$_2$ (14). As for **2a** except 2,4-dichlorobenzoic acid (42 mg, 0.22 mmol) was employed, yielding **14** (75 mg, 0.062 mmol, 62%). ^{1}H NMR (400 MHz, CD_3CN) δ 65, 42, 36, 15, -80, -93, -100. ESI-MS *m/z* 991.3 [**14**(PF$_6$)]$^+$, 424.3 [**14**]$^{2+}$, isotope pattern in agreement with predicted pattern for 4xCl. Elemental analysis (calc. for $Mn_2C_{32}H_{48}N_6Cl_4O_5P_2F_{12}$): C 33.6 % (33.7 %), H 4.47% (4.22 %), N 7.51 % (7.38 %).

[Mn$_2$(μ-O)(μ-2,4,6-trichlorobenzoato)$_2$(tmtacn)$_2$](PF$_6$)$_2$ (15). As for **2a** except 2,4,6-trichlorobenzoic acid (46 mg, 0.22 mmol) was employed, yielding **15** (75 mg, 0.062 mmol, 62 %). ^{1}H NMR (400 MHz, CD_3CN) δ 66, 35, 32, 15, -74, -87, -108. ESI-MS *m/z* 1059.0 [**15**(PF$_6$)]$^+$, 457.3 [**15**]$^{2+}$, isotope pattern in agreement with predicted pattern for

6xCl. Elemental analysis (calc. for $Mn_2C_{32}H_{46}N_6Cl_6O_5P_2F_{12}$) C 31.4 % (31.8 %), H 4.05% (3.81 %), N 7.08 % (6.96 %).

[Mn^{III}_2(μ-O)(μ-4-fluorobenzoato)$_2$(tmtacn)$_2$](PF_6)$_2$ (16). As for **2a** except 4-fluorobenzoic acid (29.4 mg, 0.21 mmol) was employed, yielding (54 mg, 0.052 mmol, 52%). ^{1}H NMR (400 MHz, CD_3CN) δ 72, 35, 20, 13, 6, -80, -92, -97. ESI-MS *m/z* 891.3 [**16**(PF_6)]$^+$, 373.2 [**16**]$^{2+}$. Elemental analysis (calc. for $Mn_2C_{32}H_{50}N_6O_5P_2F_{14}$): C 37.0% (37.06%), H 4.81% (4.86%), N 8.05% (8.11%).

[Mn^{III}_2(μ-O)(μ-2,4-difluorobenzoato)$_2$(tmtacn)$_2$](PF_6)$_2$ (17). As for **2a** except 2,4-difluorobenzoic acid (70 mg, 0.44 mmol) and **1** (162 mg, 0.20 mmol) were employed, yielding **17** (100 mg, 0.093 mmol, 47 %). ^{1}H NMR (400 MHz, CD_3CN) δ 66, 35, 32, 15, -74, -87, -108. ^{19}F NMR (121.5 MHz) δ -55, -84. ESI-MS *m/z* 927.3 [**17**(PF_6)]$^+$, 391.3 [**17**]$^{2+}$. Elemental analysis (calc. for $Mn_2C_{32}H_{48}N_6O_5P_2F_{16}$) C 35.9 % (35.8%), H 4.39% (4.48%), N 7.75 % (7.84 %).

[Mn^{III}_2(μ-O)(μ-2,6-difluorobenzoato)$_2$(tmtacn)$_2$](PF_6)$_2$ (18). As for **2a** except 2,6-difluorobenzoic acid (35 mg, 0.22 mmol) was employed, yielding **18** (85 mg, 0.079 mmol, 72 %). ^{1}H NMR (400 MHz, CD_3CN) δ 70, 34, 19, 7, -79, -90, -100. ^{19}F NMR (121.5 MHz) δ -58. ESI-MS *m/z* 927.3 [**18**(PF_6)]$^+$, 391.2 [**18**]$^{2+}$. Elemental analysis (calc. for $Mn_2C_{32}H_{48}N_6O_5P_2F_{16}$): C 37.3% (35.8%), H 5.27% (4.48%), N 7.10 % (7.84%).

[Mn^{III}_2(μ-O)(μ-3,4-difluorobenzoato)$_2$(tmtacn)$_2$](PF_6)$_2$ (19). As for **2a** except 3,4-difluorobenzoic acid (35 mg, 0.22 mmol) was employed, yielding **19** (75 mg, 0.07 mmol, 63%). ^{1}H NMR (400 MHz, CD_3CN) δ 70, 34, 19, 14.5, 13, 7, -79, -90, -98. ^{19}F NMR (121.5 MHz) δ -127.5, -104.5. ESI-MS *m/z* 927.3 [**19**(PF_6)]$^+$, 391.2 [**19**]$^{2+}$. Elemental analysis (calc. for $Mn_2C_{32}H_{48}N_6O_5P_2F_{16}$): C 36.3% (35.8%), H 5.35% (4.48%), N 7.50% (7.84%).

[Mn^{III}_2(μ-O)(μ-3,5-difluorobenzoato)$_2$(tmtacn)$_2$](PF_6)$_2$ (20). As for **2a** except 3,5-difluorobenzoic acid (70 mg, 0.44 mmol) and **1** (162 mg, 0.20 mmol) were employed, yielding **20** (125 mg, 0.12 mmol, 60%). ^{1}H NMR (400 MHz, CD_3CN) δ 70, 35, 34, 18, 7.5, 5.5, -79, -90, -96. ^{19}F NMR (121.5 MHz, CD_3CN) δ -99. ESI-MS *m/z* 927.3 [**20**(PF_6)]$^+$, 390.6 [**20**]$^{2+}$. Elemental analysis (calc. for $Mn_2C_{32}H_{48}N_6O_5P_2F_{16}$): C 36.0% (35.8%), H 4.52% (4.48%), N 7.95% (7.84%).

[Mn^{III}_2(μ-O)(μ-3-hydroxybenzoato)$_2$(tmtacn)$_2$](PF_6)$_2$ (21). As for **2a** except 3-hydroxybenzoic acid (31 mg, 0.22 mmol) was employed, yielding **21** (70 mg, 0.068 mmol, 68 %). ^{1}H NMR (400 MHz, CD_3CN) δ 72, 35, 20, 14, 7, 5, 3, -1, -80, -92, -96. ESI-MS *m/z* 887.3 [**21**(PF_6)]$^+$, 371.1 [**21**]$^{2+}$. Elemental analysis (calc. for $Mn_2C_{32}H_{52}N_6O_7P_2F_{12}$): C 37.31% (37.22%), H 5.14% (5.08%), N 8.06% (8.14%).

[Mn^{III}_2(μ-O)(μ-4-hydroxybenzoato)$_2$(tmtacn)$_2$](PF_6)$_2$ (22). As for **2a** except 4-hydroxybenzoic acid (31 mg, 0.22 mmol) was employed, yielding **22** (72 mg, 0.07 mmol, 63 %). ^{1}H NMR (400 MHz, CD_3CN) δ 72, 35, 19, 13.5, 8, -1, -80, -95. ESI-MS *m/z* 887.3 [**22**(PF_6)]$^+$, 371.3 [**22**]$^{2+}$. Elemental analysis (calc. for $Mn_2C_{32}H_{52}N_6O_7P_2F_{12}$): C 34.5% (37.2%), H 5.18% (5.04%), N 7.56 % (8.14%).

[Mn^{III}_2(μ-O)(μ-2-methoxybenzoato)$_2$(tmtacn)$_2$](PF_6)$_2$ (23). As for **9** except 2-methoxybenzoic acid (33.5 mg, 0.22 mmol) was employed, yielding **23** (75 mg,

0.071 mmol, 71%). ^{1}H NMR (400 MHz, CD_3CN) δ 71, 35, 21, 15, 13, 6, 0, -80, -94. ESI-MS *m/z* 915.4 [**23**(PF_6)]$^+$, 385.3 [**23**]$^{2+}$. Elemental analysis (calc. for $Mn_2C_{34}H_{56}N_6O_7P_2F_{12}$): C 38.8% (38.48%), H 5.49% (5.32%), N 8.06% (7.92%).

[Mn^{III}_2(μ-O)(μ-4-methoxybenzoato)$_2$(tmtacn)$_2$](PF_6)$_2$ (24). As for **2a** except 4-methoxybenzoic acid (33.5 mg, 0.22 mmol) was employed, yielding **24** (36 mg, 0.034 mmol, 34%). ^{1}H NMR (400 MHz, CD_3CN) δ 72, 36, 21, 13, 6, -80, -92, -95. ESI-MS *m/z* 915.4 [**24**(PF_6)]$^+$, 385.3 [**24**]$^{2+}$. Elemental analysis (calc. for $Mn_2C_{34}H_{56}N_6O_7P_2F_{12}$): C 38.8% (38.48%), H 5.64% (5.32%), N 7.84% (7.92%).

[Mn^{III}_2(μ-O)(μ-3-cyanobenzoato)$_2$(tmtacn)$_2$](PF_6)$_2$ (25). As for **2a** except 3-cyanobenzoic acid (32.4 mg, 0.22 mmol) was employed, yielding **25** (40 mg, 0.038 mmol, 38%). ^{1}H NMR (400 MHz, CD_3CN) δ 71, 35, 33, 18, 14, 7, -80, -92, -99. ESI-MS *m/z* 905.3 [**25**(PF_6)]$^+$, 380.3 [**25**]$^{2+}$. Elemental analysis (calc. for $Mn_2C_{34}H_{50}N_8O_5P_2F_{12}$): C 38.5% (38.85%), H 5.26% (4.80%), N 10.19% (10.67%).

[Mn^{III}_2(μ-O)(μ-2,4,6-trimethylbenzoato)$_2$(tmtacn)$_2$](PF_6)$_2$ (26). As for **2a** except 2,4,6-trimethylbenzoic acid (36.1 mg, 0.22 mmol) was employed, yielding **26** (80 mg, 0.074 mmol, 74%). ^{1}H NMR (400 MHz, CD_3CN) δ 73, 68, 34, 26, 20, 14, 11, -82, -87, -95. ESI-MS *m/z* 939.6 [**26**(PF_6)]$^+$, 397.4 [**26**]$^{2+}$. Elemental analysis (calc. for $Mn_2C_{38}H_{64}N_6O_5P_2F_{12}$): C 43.1% (42.05%), H 6.32% (5.95%), N 8.17% (7.75%).

[Mn^{III}_2(μ-O)(μ-$O_2C(CH_2)_3CO_2$)$_2$(tmtacn)$_2$](PF_6)$_2$ (27). As for **2a** except glutaric acid (14 mg, 0.106 mmol) was employed, yielding **27** (40 mg, 0.045 mmol, 45%). ^{1}H NMR (400 MHz, CD_3CN) δ 74, 70, 40, 19, 10, -76, -88, -102. ESI-MS *m/z* 743.5 [**27**(PF_6)]$^+$, 447.3 [**27**$_2$(PF_6)]$^{3+}$, 299.4 [**27**]$^{2+}$. Elemental analysis (calc. for $Mn_2C_{23}H_{48}N_6O_5P_2F_{12}$) Mn 12.35 % (12.32 %), C 31.2 % (31.0 %), H 5.54 % (5.39 %), N 9.35 % (9.44 %).

[Mn^{III}_2(μ-O)(μ-2-hydroxybenzoato)$_2$(tmtacn)$_2$](PF_6)$_2$ (28). As for **2a** except 2-hydroxybenzoic acid (31 mg, 0.22 mmol) was employed and the mauve precipitate was removed from water very quickly, yielding **28** (11 mg, 0.011 mmol, 11%). UV-Vis: 483 nm, 525 nm, 725 nm (shoulder) (see also Figure 6.4 and 6.5, Chapter 6). ESI-MS *m/z* 887.3 [**28**(PF_6)]$^+$, 371.2 [**28**]$^{2+}$, 362.2 [Mn^{III}(2-oxybenzoato)(tmtacn)]$^+$.

[Mn^{III}(2-oxybenzoato)(tmtacn)](PF_6) (29). 2-Hydroxybenzoic acid (16 mg, 0.116 mmol) was added to **3a** (50 mg, 0.058 mmol) in CH_3CN (20 ml). The solvent was evaporated and the precipitate dissolved in CH_3CN (20 ml) and $^iPr_2O$ (10 ml) was added. The green crystals were washed with Et_2O and air dried, yielding **29** (54 mg, 0.106 mmol, 91%). UV-Vis: 595 nm (see also Figure 6.4, Chapter 6). ^{1}H NMR (400 MHz, CD_3CN) δ -12, -20, -30. ESI-MS *m/z* 361.9 [**29**]$^+$, 403.0 [**29**+CH_3CN]$^+$. Elemental analysis (calc. for $MnC_{16}H_{26}N_3O_3PF_6$): Mn 10.72% (10.85%), C 37.7% (37.8%), H 5.23% (4.93%), N 8.22% (8.28%).

[Mn^{III}_2(μ-O)(μ-$BrCH_2CO_2$)$_2$(tmtacn)$_2$]PF_6 (30). As for **2a** except bromoacetic acid (30.6 mg, 0.22 mmol) was employed, yielding **30** (70 mg, 0.068 mmol, 68%). ^{1}H NMR (400 MHz, CD_3CN) δ 70, 68, 37, 35, 19, -79, -92, -104. ESI-MS *m/z* 887.0 [**30**(PF_6)]$^+$, 371.2 [**30**]$^{2+}$, isotope pattern in agreement with predicted pattern for 2xBr. Elemental analysis (calc. for $Mn_2C_{22}H_{46}N_6O_5Br_2P_2F_{12}$): C 25.8% (25.55%), H 4.43% (4.48%), N 8.14% (8.13%).

[Mn^{III}_2(μ-O)(μ-Boc-Phg)$_2$(tmtacn)$_2$](PF$_6$)$_2$ (31). As for **2a** except **1** (160 mg, 0.20 mmol) and Boc-Phg-OH (100.6 mg, 0.40 mmol) were employed, yielding **31** (86.1 mg, 0.068 mmol, 34%). ^{1}H NMR (400 MHz, CD_3CN) δ 75, 72, 68, 66, 61, 44, 40, 31, 24, 15, 10, 9, 7, -78, -80, -91, -93, -103. ESI-MS *m/z* 1113.6 [**31**(PF$_6$)]$^+$, 484.5 [**31**]$^{2+}$. Elemental analysis (calc. for $Mn_2C_{44}H_{74}N_8O_9P_2F_{12}$): C 41.64% (41.98%), H 6.05% (5.92%), N 8.80% (8.90%).

[Mn^{III}_2(μ-O)(μ-Boc-Phe)$_2$(tmtacn)$_2$](PF$_6$)$_2$ (32). As for **2a** except Boc-Phe-OH (106.1 mg, 0.40 mmol) and **1** (162 mg, 0.20 mmol) were employed, yielding **32** (64 mg, 0.050 mmol, 25%). ^{1}H NMR (400 MHz, CD_3CN) δ 81, 75, 69, 58, 41, 37, 33, 22, 20, 9, 8, 7.5, 7.3, 7.2, -73, -82, -90, -104. ESI-MS *m/z* 1141.6 [**32**(PF$_6$)]$^+$, 498.3 [**32**]$^{2+}$. Elemental analysis (calc. for $Mn_2C_{46}H_{78}N_8O_9P_2F_{12}$): C 43.41% (42.93%), H 6.01% (6.11%), N 8.45% (8.71%).

[Mn^{III}_2(μ-O)(μ-Boc-D-Pro)$_2$(tmtacn)$_2$](PF$_6$)$_2$ (33). As for **2a** except Boc-D-Pro-OH (86.1 mg, 0.40 mmol) and **1** (162 mg, 0.20 mmol) were employed, yielding **33** (98 mg, 0.084 mmol, 42%). ^{1}H NMR (400 MHz, CD_3CN) δ 88, 84, 76, 61, 50, 44, 29, 26, 12, 9, 6, 5, 4.2, 4.1, -80, -87, -98, -104. ESI-MS *m/z* 1041.6 [**33**(PF$_6$)]$^+$, 448.5 [**33**]$^{2+}$. Elemental analysis (calc. for $Mn_2C_{38}H_{74}N_8O_9P_2F_{12}$): C 36.99% (38.46%), H 6.34% (6.28%), N 9.47% (9.44%).

[Mn^{III}_2(μ-O)(μ-Boc-Ala)$_2$(tmtacn)$_2$](PF$_6$)$_2$ (34). As for **2a** except Boc-Ala-OH (75.7 mg, 0.40 mmol) and **1** (162 mg, 0.20 mmol) were employed, yielding **34** (41 mg, 0.036 mmol, 18%). ^{1}H NMR (400 MHz, CD_3CN) δ 79, 72, 61, 59, 44, 36, 22, 12, -72, -83, -87, -104. ESI-MS *m/z* 989.5 [**34**(PF$_6$)]$^+$, 422.5 [**34**]$^{2+}$. Elemental analysis (calc. for $Mn_2C_{34}H_{70}N_8O_9P_2F_{12}$): C 34.93% (35.99%), H 6.38% (6.22%), N 9.60% (9.87%).

[Mn^{III}_2(μ-O)(μ-Ac-D-Phg)$_2$(tmtacn)$_2$](PF$_6$)$_2$ (35). As for **2a** except **1** (160 mg, 0.20 mmol) and Ac-D-Phg-OH (77.3 mg, 0.40 mmol) were employed, yielding **35** (109.2 mg, 0.096 mmol, 48%). ^{1}H NMR (400 MHz, CD_3CN) δ 76, 68, 66, 45, 40, 32, 30, 23, 15, 11, 9, -79, -87, -96, -104. ESI-MS *m/z* 997.5 [**35**(PF$_6$)]$^+$, 426.4 [**35**]$^{2+}$. Elemental analysis (calc. for $Mn_2C_{38}H_{62}N_8O_7P_2F_{12}$): C 39.68% (39.94%), H 5.53% (5.47%), N 9.59% (9.81%).

B.3 References

[1] a) Wieghardt, K.; Bossek, U.; Nuber, B.; Weiss, J.; Bonvoisin J.; Corbella, M.; Vitols, S. E.; Girerd, J. J. *J. Am. Chem. Soc.* **1988**, *110*, 7398-7411. b) Koek, J. H.; Russell, S. W.; van der Wolf, L.; Hage, R.; Warnaar, J. B.; Spek, A. L.; Kerschner, J.; DelPizzo, L. *J. Chem. Soc., Dalton Trans.* **1996**, 353-362.

[2] Hage, R.; Gunnewegh, E. A.; Niël, J.; Tjan, F. S. B.; Weyhermüller, T.; Wieghardt, K. *Inorg. Chim. Acta* **1998**, *268*, 43-48.

[3] a) Hage, R.; Iburg, J. E.; Kerschner, J.; Koek, J. H.; Lempers, E. L. M.; Martens, R. J.; Racherla, U. S.; Russell, S. W.; Swarthoff, T.; van Vliet, M. R. P.; Warnaar, J. B.; van der Wolf, L.; Krijnen, B. *Nature* **1994**, *369*, 637-639. b) Schäfer, K.-O.; Bittl, R.; Zweygart, W.; Lendzian, F.; Haselhorst, G.; Weyhermüller, T.; Wieghardt, K. Lubitz, W. *J. Am. Chem. Soc.* **1998**, *120*, 13104-13120.

[4] a) Wieghardt, K.; Chaudhuri, P.; Nuber, B.; Weiss, J. *Inorg. Chem.* **1982**, *21*, 3086-3090. b) Wieghardt, K.; Schmidt, W.; Nuber, B.; Weiss, J. *Chem. Ber.* **1979**, *112*, 2220-2230. c) Atkins, T. J.; Richman, J. E.; Oettle, W. F. *Org. Synth.* **1978**, *58*, 86-98.
[5] Brimelow, H. C.; Jones, R. L.; Metcalfe, T. P. *J. Chem. Soc.* **1951**, 1208-1212.
[6] Holdrege, C. T. (Bristol-Meyers Company) **1969**, US Patent 3,479,339.
[7] Touet, J.; Faveriel, L.; Brown, E. *Tetrahedron* **1995**, *51*, 1709-1720.
[8] Hage, R.; Krijnen, B.; Warnaar, J. B.; Hartl, F.; Stufkens, D. J.; Snoeck, T. L. *Inorg. Chem.* **1995**, *34*, 4973-4978.

Appendix C
Measurements

Although the catalytic oxidation reactions were performed typically at 0 °C, spectroscopic investigations were performed typically at 20 °C for practical reasons. Several cross-checks and controls were performed to take this temperature difference into account. At higher temperatures (*i.e.* 20 °C) a decreased lag period is observed (30-45 min), however, overall conversion and turnover numbers are not affected significantly, although the amount of *cis*-diol is somewhat reduced due to increased overoxidation. Similar to the results obtained at 0 °C, the lag period for both initiation of the reaction and formation of, *e.g.*, **2a** coincide.

C.1 Catalysis experiments

All catalytic oxidation reactions were performed *in duplo*.

General procedure (A). The alkene (10 mmol), 1,2-dichlorobenzene (internal standard, 735 mg, 5.0 mmol), the appropiate Mn_2-dimer (10 µmol) and co-catalyst (typically 0.10 mmol) in CH_3CN (10 ml) was cooled to 0°C. H_2O_2 (50%, 0.74 ml, 13 mmol) was added *via* syringe pump over 6 h (0.12 ml/h). The reaction mixture was stirred at 0°C for 1 h after the addition of H_2O_2 was completed, prior to sampling by GC.

General procedure (B) for catalyst pretreatment (employing carboxylic acids in general). H_2O_2 (30 µl, 0.53 mmol) was added to a mixture of 1,2-dichlorobenzene (735 mg, 5.0 mmol), **1** (8.1 mg, 10 µmol) and carboxylic acid (0.10 mmol) in CH_3CN (7 ml) at room temperature. The mixture was stirred for 20 min, after which the alkene (10 mmol) was added together with CH_3CN (3 ml) and the mixture was cooled to 0°C. H_2O_2 (0.71 ml, 12.5 mmol) was added *via* syringe pump (0.12 ml/h). The reaction mixture was stirred at 0°C for 1 h after the addition of H_2O_2 was completed, prior to sampling by GC.

General procedure (C) for catalyst pretreatment (employing 2,6-dichlorobenzoic acid). H_2O_2 (30 µl, 0.53 mmol) was added to a mixture of 1,2-dichlorobenzene (735 mg, 5.0 mmol), **1** (8.1 mg, 10 µmol) and 2,6-dichlorobenzoic acid (0.30 mmol) in CH_3CN (7 ml) at room temperature. The mixture was stirred for 20 min at room temperature followed by addition of the alkene (10 mmol) and CH_3CN (3 ml). The mixture was cooled to 0°C. H_2O_2 (1.00 ml, 17.6 mmol) was added *via* syringe pump (0.14 ml/h). The reaction mixture was stirred at 0°C for 1 h after the addition of H_2O_2 was completed, prior to sampling by GC.

Procedure (D) for the catalytic oxidation of dimethylmaleate and dimethylfumarate. H_2O_2 (30 µl, 0.53 mmol) was added to a mixture of 1,2-dichlorobenzene (0.368 mg, 2.5 mmol), **1** (8.1 mg, 10 µmol) and co-catalyst (salicylic acid and trichloroacetic acid: 0.10 mmol; 2,6-dichlorobenzoic acid: 0.30 mmol) in CH_3CN (7 ml) at room temperature. The mixture was stirred for 20 min, after which the alkene (5 mmol) was added together with CH_3CN (3 ml). H_2O_2 (0.34 ml, 6.0 mmol) was added *via* syringe pump (0.06 ml/h) at room temperature. The reaction mixture was stirred at r.t. for 1 h after the addition of H_2O_2 was completed, prior to sampling by GC.
Under these conditions, using CCl_3CO_2H as additive, cyclooctene gives: 79% conversion, 122 t.o.n. epoxide, 166 t.o.n. *cis*-diol (mass-balance: 78%).

Procedure (E) for ^{18}O isotopic labelling studies. To CH_3CN (300 µl) was added 1,2-dichlorobenzene (100 µl of a 250 mM stock in CH_3CN, *i.e.* 25 µmol), the appropiate

Mn^{III}_2-complex (50 µl of a 10 mM stock solution in CH_3CN, *i.e.* 0.5 µmol), carboxylic acid (50 µl of a 100 mM stock solution in CH_3CN, *i.e.* 5 µmol) and cyclooctene (65 µl, 500 µmol) and the reaction mixture was cooled to 0°C. H_2O_2 (2% in H_2O, 4x45 µl, 106 µmol) was added at t = 0, 15, 30 and 45 min. Samples for both GC analysis (to determine t.o.n.) and GC-MS (CI) (to determine ^{18}O isotopic composition of the products) were taken at t = 60 min.

Procedure (F) for ^{18}O isotopic labelling studies (second phase 1/oxalic acid). To examine the ^{18}O isotopic labelling of the *cis*-diol and epoxide products during the second phase of the **1**/oxalic acid catalysed reaction, the reaction was first performed according to general procedure A employing *cis*-2-heptene (5 mmol) as substrate. H_2O_2 (50 w/w%, 4x30 µl, 2.1 mmol) was added every 15 min during one hour. The reaction mixture was then left overnight and the presence of a Mn^{III}_2 bis(carboxylato) complex was confirmed by UV-Vis spectroscopy. Part of this reaction volume (500 µl) was taken and subjected to procedure E using cyclooctene (250 µmol) as substrate.

Procedure (G) for the catalytic oxidation of 2,2-dimethylchromene. 2,2-Dimethylchromene (100 mg, 624 µmol), 1,2-dichlorobenzene (45.9 mg, 312 µmol), the appropiate Mn_2-dimer (2.5 µmol) and chiral carboxylic acid (typically 25 µmol) were dissolved in a mixture of CH_3CN (2.25 ml) and H_2O (0.25 ml). This mixture was cooled (typically) to 0°C. A solution of H_2O_2 (50 w/w%) in CH_3CN (250 µl of a 4.2 M solution, *i.e.* 1.7 equiv. H_2O_2 w.r.t. substrate) was added *via* syringe pump over 4 h (62.5 µl/h). The reaction mixture was stirred at 0°C for 1 h after the addition of H_2O_2 was completed, prior to sampling by GC and HPLC.

Procedure (H) for the screening of chiral carboxylic acids (in scintillation vials) for the enantioselective *cis*-dihydroxylation of 2,2-dimethylchromene. H_2O_2 (7.5 µl, 132 µmol) was added at room temperature to a mixture of 1,2-dichlorobenzene (1 ml of a 312 mM stock in CH_3CN, *i.e.* 312 µmol), **1** (1 ml of a 2.5 mM stock in CH_3CN, *i.e.* 2.5 µmol), CH_3CN (0.25 ml) and chiral carboxylic acid (156 µmol). The mixture was stirred for 20 min, followed by addition of 2,2-dimethylchromene (100 µl, 100 mg, 625 µmol) and H_2O (0.25 ml). H_2O_2 (50%, 4x15 µl, 1060 µmol) was added in four portions at t = 0, 1, 2 and 3 h at room temperature. The reaction mixture was stirred for 1 h after the addition of H_2O_2 was completed, prior to sampling by GC.
To determine the *ee* of both the *cis*- and *trans*-diol and the *cis/trans*-diol ratio by HPLC, a small sample of the diols was isolated via preparative TLC. A small sample of the reaction mixture (25 µl) was separated on a TLC plate (5x10 cm, silica, CH_2Cl_2/MeOH 97.5 : 2.5). After drying in the air (10-15 min), 0.5 cm of the TLC plate was cut off and stained with Ce/Mo-dip (the diols turn blue, R_f ~ 0.25-0.3). The area containing the diols was scraped off from the undeveloped TLC plate and this silica (containing the diols) was suspended in *n*-heptane/IPA (96:4). The resulting suspension was filtered on a plug of anhydrous Na_2SO_4 (1 cm) and the filtrate was collected in a sample vial (equipped with 0.3 ml glass insert) and subjected to HPLC analysis.

C.2 Gas chromatography

GC analyses were performed on an Agilent 6890 Gas Chromatograph equipped with a HP-1 dimethyl polysiloxane column (30 m × 0.25 mm × 0.25 µm). Peak identification and calibration were performed using independent samples (either purchased from a commercial supplier or independently synthesized, see Appendix A). Conversion and turnover numbers were determined *in duplo* employing 1,2-dichlorobenzene or bromobenzene as internal standard. Before and after each series of catalytic runs the calibrations were checked *in duplo* with two known, independent samples (the values found were +/- 10% of their expected values).

Benzylalcohol. Column: HP-1 (30 m × 0.25 mm × 0.25 µm), oven temp.: 5 min at 100°C, 10°C/min to 200°C, 5 min at 200°C, 25°C/min to 100°C (inlet: 250°C, detector: 250°C). Benzaldehyde (2.93 min), benzylalcohol (3.70 min), 1,2-dichlorobenzene (internal standard, 3.92 min), benzoic acid (6.59 min).

Cyclooctane. Column: HP-1 (30 m × 0.25 mm × 0.25 µm), oven temp.: 5 min at 100°C, 10°C/min to 200°C, 5 min at 200°C, 25°C/min to 100°C (inlet: 250°C, detector: 250°C). Cyclooctane (2.82 min), 1,2-dichlorobenzene (internal standard, 3.94 min), cyclooctanone (5.34 min), cyclooctanol (5.95 min).

Cyclooctene. Column: HP-1 (30 m × 0.25 mm × 0.25 µm), oven temp.: 5 min at 100°C, 10 °C/min to 200°C, 5 min at 200°C, 25 °C/min to 100°C (inlet: 250°C, detector: 250°C). Cyclooctene (2.64 min), 1,2-dichlorobenzene (internal standard, 3.94 min), cyclooctene oxide (5.21 min), α-hydroxycyclooctanone (not calibrated, 7.32 min), *trans*-1,2-cyclooctanediol (not calibrated, 9.11 min), *cis*-1,2-cyclooctanediol (9.28 min).

Cyclopentene. Column: HP-1 (30 m × 0.25 mm × 0.25 µm), oven temp.: 5 min at 40°C, 5 °C/min to 70°C, 2 min at 70°C, 25 °C/min to 200°C, 2 min at 200°C, 25 °C/min to 40°C (inlet: 250°C, detector: 250 °C). Cyclopentene (not calibrated, same retention time as solvent peak), cyclopentene oxide (4.30 min), 2-cyclopenten-1-one (not calibrated, 6.72 min), *cis*-1,2-cyclopentanediol (12.68 min), *trans*-1,2-cyclopentanediol (not calibrated, 13.20 min), 1,2-dichlorobenzene (internal standard, 14.40 min).

2,2-Dimethylchromene. Column: HP-1 (30 m × 0.25 mm × 0.25 µm), oven temp.: 5 min at 100°C, 10 °C/min to 250°C, 10 min at 250°C, 25 °C/min to 100°C (inlet: 250°C, detector: 250°C). 1,2-Dichlorobenzene (internal standard, 3.93 min), 2,2-dimethylchromene (7.33 min), 2,2-dimethylchroman-3-one (not calibrated, 9.04 min), *cis*-2,2-dimethylchromane-3,4-diol (not calibrated, 12.47 min, partially decomposes to 2,2-dimethylchroman-3-one), *trans*-2,2-dimethylchromane-3,4-diol (not calibrated, 12.72 min, partially decomposes to 2,2-dimethylchroman-3-one), 3,4-epoxy-2,2-dimethylchromane (completely decomposes to 2,2-dimethylchroman-3-one).

Dimethylmaleate and dimethylfumarate. Column: HP-1 (30 m × 0.25 mm × 0.25 µm), oven temp.: 5 min at 85°C, 5°C/min to 100°C, 25°C/min to 200°C, 2 min at 200°C, 25°C/min to 85°C (inlet: 250°C, detector: 250°C). Dimethylmaleate (4.92 min), dimethylfumarate (5.19 min), 1,2-dichlorobenzene (internal standard, 5.72 min), dimethyl-

cis-2,3-oxiranedicarboxylate (8.24 min), dimethyl-*trans*-2,3-oxiranedicarboxylate (8.49 min), dimethyl-*meso*-tartrate (9.49 min), dimethyl-*D,L*-tartrate (9.56 min).

***Cis*- and *trans*-2-heptene.** Column: HP-1 (30 m × 0.25 mm × 0.25 µm), oven temp.: 7.5 min at 35°C, 10°C/min to 130°C, 25°C/min to 250°C, 5 min at 250°C, 25°C/min to 35°C (inlet: 200°C, detector: 250°C). *Trans*-2-heptene (4.58 min), *cis*-2-heptene (4.81 min), racemic *trans*-2,3-epoxyheptane (10.17 min), racemic *cis*-2,3-epoxyheptane (10.92 min), 1,2-dichlorobenzene (internal standard, 14.39 min), racemic *threo*-2,3-heptanediol (15.03 min), racemic *erythro*-2,3-heptanediol (15.22 min).

***n*-Octane.** Column: HP-1 (30 m × 0.25 mm × 0.25 µm), oven temp.: 5 min at 100°C, 10°C/min to 200°C, 5 min at 200°C, 25°C/min to 100°C (inlet: 250°C, detector: 250°C). *n*-Octane (2.06 min), 1,2-dichlorobenzene (internal standard, 3.94 min).

1-Octene. Column: HP-1 (30 m × 0.25 mm × 0.25 µm), oven temp.: 7.5 min at 40°C, 10°C/min to 130°C, 2 min at 130°C, 25°C/min to 225°C, 5 min at 225°C, 25°C/min to 40°C (inlet: 250°C, detector: 250°C). 1-Octene (6.74 min), 1,2-epoxyoctane (13.41 min), 1,2-dichlorobenzene (internal standard, 13.75 min), 1,2-octanediol (17.39 min).

Styrene. Column: HP-1 (30 m × 0.25 mm × 0.25 µm), oven temp.: 5 min at 50°C, 10°C/min to 150°C, 20°C/min to 200°C, 5 min at 200°C, 20°C/min to 50°C (inlet: 150°C, detector: 150°C). Styrene (7.19 min), bromobenzene (internal standard, 8.07 min), benzaldehyde (8.53 min), phenylacetaldehyde (10.27 min), (±)-styrene oxide (10.82 min, partly decomposes to phenylacetaldehyde), 2-hydroxyacetophenone (not calibrated, 13.59 min), (±)-1-phenyl-1,2-ethanediol (14.50 min).

C.3 HPLC

HPLC analyses were performed on a Shimadzu LC10Advp.

2,2-dimethylchromene. Column: Chiralcel OD-H (4.6 mm × 250 mm, particle size 5 µm), *n*-heptane/^{i}PrOH (96:4) at 0.5 ml/min for 45 min. Monitored between 190-400 nm, *ee* determined at 210 nm. *Cis*-2,2-dimethylchromane-3,4-diol (27.6 and 33.5 min), *trans*-2,2-dimethylchromane-3,4-diol (25.8 and 30.0 min).

C.4 Electrochemistry

Recommended reading: ref. [1], [2], [3] and [4].

C.4.1 Cyclic voltammetry

Electrochemical measurements were carried out on a Model CHI630B or Model CHI760B electrochemical workstation (CH Instruments). Analyte concentrations were typically between 0.5 and 1.0 mM in anhydrous CH_3CN containing either 0.1 M tetrabutylammonium hexafluorophosphate ($TBAPF_6$) or 0.1 M KPF_6. Unless stated otherwise, a Teflon shrouded glassy carbon working electrode (CH Instruments, partnumber CHI104), a Pt-wire counter electrode (partnumber CHI115) and a SCE

reference electrode (partnumber CHI150) were employed (calibrated externally using a 0.1 mM solution of ferrocene in 0.1 M $TBAPF_6/CH_3CN$). Cyclic voltammograms were obtained at sweep rates of between 1 mV s^{-1} to 10 V s^{-1} (typically 0.1 V s^{-1}). For reversible processes the half-wave potential ($E_{½}$) values are reported. For irreversible processes either the cathodic or anodic peak potential ($E_{p,c}$ or $E_{p,a}$, respectively) is given. Redox potentials are reported +/- 10 mV.

The glassy carbon working electrode was always cleaned mechanically and by sonication: the electrode was polished on a polishing pad containing a slurry of alumina (0.05 micron) and water. After rinsing with water, the glassy carbon working electrode was sonicated in CH_3CN for 1-2 min. If needed, the glassy carbon working electrode was also cleaned electrochemically: 15 cycles in 0.2 M H_2SO_4 (aq.) between 1.1 and -0.3 V vs. SCE (at 0.1 V s^{-1}), followed by 30 sec at constant potential at 1.1, -0.3, 1.2 and finally 0.3 V, followed by rinsing thoroughly with water and then CH_3CN. The Pt-wire counter electrode was cleaned by rinsing with water, acetone and finally CH_3CN. The saturated calomel electrode (SCE) (Hg/Hg_2Cl_2) reference electrode was stored in sat. KCl (aq.). Before use, it was rinsed with water first, then with CH_3CN. After use, the SCE reference electrode was rinsed with CH_3CN, acetone and finally with water.

Before measurements, both the solvents, electrolyte and electrodes were checked for possible contaminants by scanning at 0.1 V s^{-1} (typically 5-7 cycles) between -0.4 and 1.8 V, starting cathodically from the open circuit potential (OCP).

Cyclic voltammetry was generally performed in 2 ml CH_3CN solutions containing $TBAPF_6$ electrolyte (0.1 M) and Mn_2 complex (1 mM), carboxylic acid (1-250 mM), cyclooctene (1 M) and/or 1,2-dichlorobenzene (0.5 M). Scans were always started at the OCP. Both positive and negative initial scan directions were run for all samples and at least 5 sweep segments were recorded in order to check reproducibility and/or the occurance of (electro)chemical changes/processes. Before each new experiment (*i.e.* before each scan with different scan rate, initial scan direction and/or potential window) the solution was shaken to allow for 'fresh' solution close to the working electrode surface. The electrodes were cleaned periodically as described above.

Table C.1 Relevant redox potentials in 0.1 M $TBAPF_6/CH_3CN$.

Compound	Potential (in V vs. SCE)	Remarks
$Fe^{II}(Cp)_2$ / $Fe^{III}(Cp)_2^+ + e^-$	$E_{1/2}$ +0.45 V	ref. [1a]
$O_2 + e^-$ / $O_2^{\cdot -}$	$E_{p,c}$ -0.7 V, $E_{p,a}$ -0.5 V	ref. [1a]
H_2O	$E_{p,a}$ +1.1 V	
SCE	+0.24 V vs. NHE	at 25°, ref. [1a]

C.4.2 Thin-layer electrochemistry

The setup for thin-layer electrochemistry is identical to that for standard (diffusion limited) cyclic voltammetry, except that the working electrode is placed directly on top of the (flat) base of the beaker containing the solution of interest, thus limiting diffusion of the species generated electrochemically (Figure C.1).

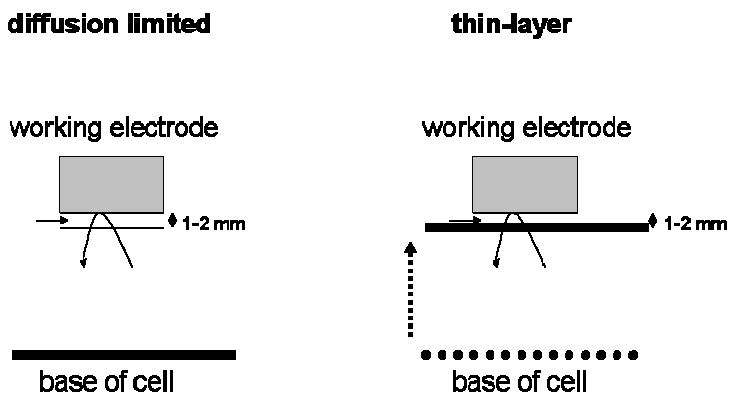

Figure C.1 Setup for standard (diffusion limited) cyclic voltammetry (left) and thin-layer electrochemistry (right).

C.4.3 Spectroelectrochemistry

UV-Vis spectroelectrochemistry was performed in a homemade Optically Transparent Thin Layer Electrochemical (OTTLE) cell, consisting of a 2 mm quartz cuvette, a Pt-guaze working electrode, Pt-wire counter electrode (separated from the main solution with a fritted glass tube) and a SCE reference electrode.

C.4.4 Bulk electrolysis

Bulk electrolysis was performed with a reticulated vitreous carbon working electrode, carbon rod counter electrode and a SCE reference electrode.

C.5 Electron paramagnetic resonance

Recommended reading: ref. [5].

EPR spectra (X-band, 9.46 GHz) were recorded in liquid nitrogen (77 K) on a Bruker ECS 106 instrument, equiped with a Bruker ECS 041 XK microwave bridge and a Bruker ECS 080 magnet. Samples for measurement (250 µl) were transferred from the reaction solution to an EPR tube, which was frozen in 77 K immediately.

Spectra were typically obtained with the following settings: conversion time (81 msec), time constant (81 msec), central field (3450 G), sweep width (6000 or 2000 G), number of scans (1), receiver gain (usually between $2x10^{+4}$ and $2x10^{+5}$).

C.6 Nuclear magnetic resonance

^{1}H (400, 300 or 200 MHz), ^{13}C (100.6 or 50.3 MHz) and ^{19}F NMR (376 MHz) spectra were recorded on a Varian Mercury Plus 400, Varian VXR-300, Varian Mercury Plus 200 or Varian Gemini-200. Chemical shifts are reported in ppm relative to the solvent residual peak[6]: ^{1}H NMR: $CDCl_3$ (7.26 ppm), dmso-d_6 (2.50 ppm), CD_3CN (1.94 ppm), acetone-d_6 (2.05 ppm), D_2O (4.79 ppm). ^{13}C NMR: $CDCl_3$ (77 ppm), dmso-d_6 (39.5 ppm), acetone-d_6 (29.8 ppm). ^{19}F NMR: PF_6^- (74.3 ppm, J_{PF} = 580 Hz). The splitting patterns are designated as follows: s (singlet), d (doublet), t (triplet), q (quartet), m (multiplet), br (broad).

^{1}H NMR spectra of the $[Mn^{III}_2(\mu\text{-}O)(\mu\text{-}RCO_2)_2(tmtacn)]^{2+}$ complexes were recorded on a Varian Mercury Plus (400 MHz) using the following settings: sw = 100000, alfa = 0 or -2, rof2 = 0. For processing of the data, to partly correct for 1st order phasing issues, the first 4 data points were recalculated using 32 prediction coefficients and 1024 data points (command blp) before setting line broading (lb = 2-10 Hz) and performing the weighted fourier transformation (wft).

C.7 UV-Vis

UV-Vis spectra were recorded on a Hewlett-Packard 8453 or Jasco V-570 UV/VIS/NIR spectrophotometer using either 2 or 10 mm pathlength quartz cuvettes. Unless noted otherwise, the concentrations used were the same as used for the standard catalysis experiments (section C.1).

C.8 FT-IR

FT-IR spectra were recorded (as intimate mixtures in KBr) in reflectance mode, using a Nicolet Nexus FT-IR spectrometer.

C.9 Mass spectrometry

ESI-MS. Electrospray ionization mass spectra were recorded on a Triple Quadrupole LC/MS/MS Mass spectrometer (API 3000, Perkin-Elmer Sciex Instruments) or API-365. Samples (2 µl) were taken from the reaction mixture at the indicated times and were diluted in CH_3CN (1 ml) before injection in the mass spectrometer (via syringe pump). Alternatively, spectra were recorded while injecting at standard catalytic concentrations of the analytes in the mass spectrometer, so without dilution (*i.e.* 1 mM Mn_2 complex in CH_3CN). Mass spectra were measured in positive mode (no manganese complexes were observed in negative mode) and in the range of *m*/*z* 100-1500. Typical settings: ion-spray voltage (5200 V), orfice (+15 V), ring (+150 V), Q0 (-10 V).

For kinetic measurements only a small portion of the spectrum was recorded to minimize measuring time between each subsequent data point, while monitoring the $[Mn^{III}_2(\mu\text{-}O)(\mu\text{-}RCO_2)_2(tmtacn)_2]^{2+}$ ion. The presence of cyclooctene (1 M) and/or

carboxylic acid did not result in significant interference of the mass spectra and neither cyclooctene nor the *cis*-diol and epoxide products gave rise to significant signals.

EI-MS. Electron impact ionisation mass spectrometry was performed on a Jeol JMS-600H mass spectrometer.

CI-MS. Chemical ionisation mass spectrometry was performed on a Jeol JMS-600H mass spectrometer using NH_3 as reacting gas.

GC-MS (CI). Samples to determine the isotopic composition of the products were taken at t = 60 min and were analyzed by GC-MS using chemical ionisation (CI) employing NH_3 as reacting gas. GC: Agilent 6890 Gas Chromatograph equipped with a HP-5 (5%-phenyl)-methyl polysiloxane column (30 m × 0.32 mm × 0.25 µm), oven temp.: 5 min at 100°C, 10 °C/min to 200°C, 5 min at 200°C, 25 °C/min to 100°C (inlet: 250°C). Cyclooctene oxide (3.5 min) and *cis*-cyclooctane diol (7.5 min) were detected as their $[M+NH_4]^+$ ions. MS: Jeol JMS-600H mass spectrometer.

C.10 References

1 Electrochemistry in general: a) Sawyer, D. T.; Sobkowiak, A.; Roberts, Jr., J. L. *Electrochemistry for Chemists* (second edition), John Wiley & Sons, New York, **1995**. b) Bond, A. M. *Electrochemistry: General Introduction*, in: Comprehensive Coordination Chemistry II, McCleverty, J. A. and Meyer, T. J. (eds.), Elsevier, Amsterdam, **2004**, pp. 197-234. c) Faulkner, L. R. *J. Chem. Ed.* **1983**, *60*, 262-264.
2 Cyclic voltammetry: a) Mabbott, G. A. *J. Chem. Ed.* **1983**, *60*, 697-702. b) Kissinger, P. T.; Heineman, W. R. *J. Chem. Ed.* **1983**, *60*, 702-706. c) Van Benschoten, J. J.; Lewis, J. Y.; Heineman, W. R.; Roston, D. A.; Kissinger, P. T. *J. Chem. Ed.* **1983**, *60*, 772-776.
3 Differential pulse voltammetry: Osteryoung, J. *J. Chem. Ed.* **1983**, *60*, 296-298.
4 Spectroelectrochemistry: Heineman, W. R. *J. Chem. Ed.* **1983**, *60*, 305-307.
5 Eaton, G. R.; Eaton, S. S. *Electron Paramagnetic Resonance Spectroscopy*, in: Comprehensive Coordination Chemistry II, McCleverty, J. A. and Meyer, T. J. (eds.), Elsevier, Amsterdam, **2004**, pp. 37-48.
6 Gottlieb, H. E.; Kotlyar, V.; Nudelman, A. *J. Org. Chem.* **1997**, *62*, 7512-7515.

Samenvatting

Cis-dihydroxylering en epoxidatie van alkenen met mangaan katalysatoren - selectiviteit, reactiviteit en mechanisme

(Oxidatie-)chemie

Scheikunde houdt zich bezig met de synthese (het maken) van verbindingen en het bestuderen van de eigenschappen hiervan. Om (nieuwe) verbindingen zoals medicijnen of plastics te kunnen maken heeft de chemicus een breed scala aan reagentia tot zijn beschikking om de ene stof in de andere om te zetten. Simpele uitgangstoffen zoals ruwe olie kunnen op deze manier, door het juist kiezen en op goede volgorde uitvoeren van een serie reacties, omgezet worden in ingewikkelde verbindingen zoals biologisch actieve stoffen (bijvoorbeeld medicijnen) of plastics (die bijvoorbeeld toegepast worden in tal van gebruiksvoorwerpen van tasjes tot televisies).

Oxidatiereacties behoren tot de meest fundamentele chemische reacties en zijn van essentieel belang in de biologie, chemische industrie en (synthetische organische) chemie. Verbranding is ook een voorbeeld van een oxidatie en is eigenlijk niets anders dan de volledige en ongecontroleerde oxidatie van koolwaterstoffen (bijvoorbeeld benzine) met zuurstof uit de atmosfeer. Volledige verbranding levert alleen koolstofdioxide (CO_2) en water (H_2O) als producten op. Echter, gedeeltelijke en selectieve oxidatie van koolwaterstoffen (zoals alkanen en alkenen) resulteert in het introduceren van functionele groepen en op deze manier kunnen bruikbare producten gevormd worden. Zelfs als het product van een dergelijke oxidatiereactie niet direct van belang is, vormt de nieuw geïntroduceerde groep vaak een handvat in het molecuul om weer andere functionele groepen te introduceren of om andere moleculen aan te bevestigen. Op deze manier kunnen dan ingewikkelde verbindingen gebouwd worden.

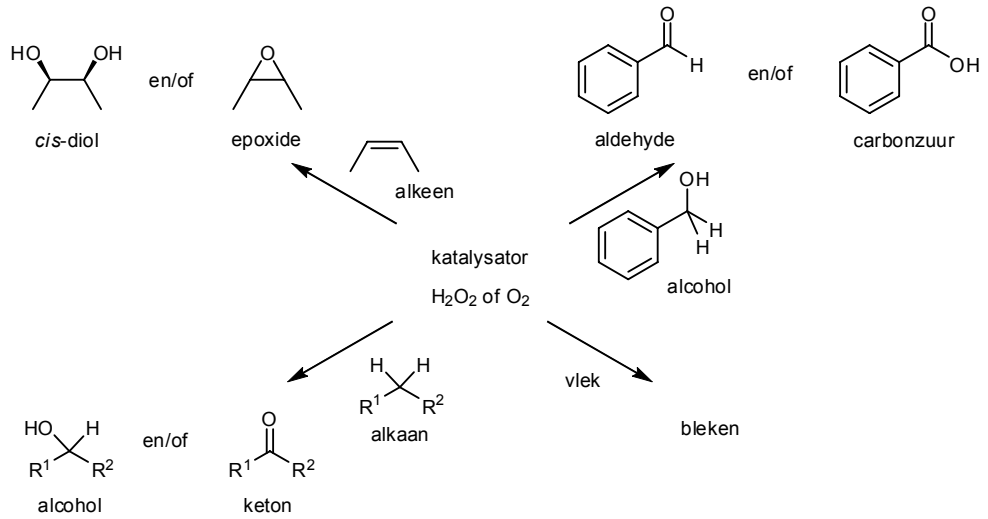

Figuur 1 Voorbeelden van oxidatie reacties.

Voorbeelden van oxidatiereacties zijn de omzetting van alkenen in epoxides of diolen (of in dicarbonyl verbindingen via het verbreken van de C=C binding), selectieve oxidatie van C-H bindingen in bijvoorbeeld alcoholen (C-OH) en de omzetting van alcoholen in

aldehyden, ketonen of carbonzuren (Figuur 1). Ook het bleken van vlekken in de was of het bleken van papierpulp zijn belangrijke processen gebaseerd op oxidatiechemie. Bleken is het proces waarbij gekleurde moleculen waaruit de vlek bestaat op een dusdanige manier worden geoxideerd dat deze moleculen geen zichtbaar licht meer absorberen en de vlek dus niet meer zichtbaar is.

De uitdaging

Ondanks de ontwikkelingen door de jaren heen, zijn er nog steeds grote uitdagingen binnen de oxidatiechemie. Ten eerste, methoden die gebruikmaken van traditionele oxidatoren leveren, naast het gewenste product, doorgaans ook grote hoeveelheden afval (bijproducten) op. Dit is duur, milieubelastend en niet efficiënt. Zowel uit het oogpunt van het milieu als van efficiëntie, is het veel beter om zuurstof (O_2) of waterstofperoxide (H_2O_2) te gebruiken. Bij het gebruik van waterstofperoxide wordt alleen water (H_2O) als bijproduct gevormd. Ten tweede is het van belang om de oxidatieve omzetting selectief uit te voeren; dat wil zeggen dat alleen of in grote mate het gewenste product gevormd wordt. Een nieuwe methode is namelijk alleen bruikbaar indien alleen het gewenste product gevormd wordt. Het gewenste product isoleren uit een mengsel van vele producten is niet alleen erg lastig, het is ook erg inefficiënt omdat alle niet gewenste producten als afval beschouwd moeten worden.

Hoewel katalysatoren (deeltjes die een bepaalde reactie faciliteren, zonder daarbij zelf verbruikt te worden) nodig zijn om zuurstof (O_2) of waterstofperoxide (H_2O_2) te activeren, zodat deze oxidatoren bij normale omstandigheden gebruikt kunnen worden voor de gewenste oxidatie reactie, is de rol van deze katalysatoren veel uitgebreider. De meest belangrijke rol van deze katalysatoren is namelijk om er voor te zorgen dat de oxidatoren op een dusdanige manier geactiveerd worden dat alleen de gewenste (oxidatie) reactie optreedt. Dit geldt voor de chemoselectiviteit (bv. oxidatie van een alkaan vs. alkeen), regioselectiviteit (bv. interne vs. externe alkenen) en enantioselectiviteit (de vorming van maar één van beide spiegelbeeldvormen van een molecuul, zie hieronder, Figuur 4). Andere belangrijke eisen aan de katalysator zijn dat deze goedkoop, robuust en niet giftig moet zijn.

Dit proefschrift

Het onderzoek, dat beschreven wordt in dit proefschrift, richtte zich op de ontwikkeling van nieuwe methoden voor de schone en selectieve *cis*-dihydroxylering en epoxidatie van alkenen (Figuur 2). Tevens is mechanistisch onderzoek verricht om beter inzicht te krijgen in deze nieuwe methoden.

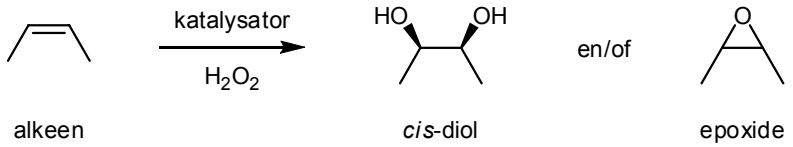

Figuur 2 *Cis*-dihydroxylering en epoxidatie van alkenen.

In hoofdstuk 1 wordt een overzicht gegeven van de diverse katalysatoren en systemen die reeds bekend zijn voor de *cis*-dihydroxylering en epoxidatie van alkenen. Tevens wordt hier kort ingegaan op de mogelijkheden en beperkingen van deze systemen.

Hoewel waterstofperoxide een milieuvriendelijke oxidator is, is de aanwezigheid van waterstofperoxide binnen in levende organismen erg schadelijk (en leidt onder andere tot de veroudering van cellen). Binnen in de cellen bevinden zich enzymen ('biologische katalysatoren') die ervoor zorgen dat het aanwezige waterstofperoxide wordt afgebroken. Een aantal van deze enzymen bevatten mangaan in het actieve centrum (het gedeelte van een enzym waar de reactie plaatsvindt). In hoofdstuk 2 worden modelsystemen voor deze enzymen besproken en worden deze vergeleken met oxidatie katalysatoren.

Een voorbeeld van een veelzijdige katalysator voor oxidatieve omzettingen is complex **1** dat afgebeeld staat in Figuur 3 (de verkorte naam van deze verbinding is $[Mn^{IV}_2(\mu\text{-}O)_3(tmtacn)_2]^{2+}$). Deze verbinding voldoet aan de eisen die hier boven besproken zijn voor een nieuwe oxidatiekatalysator (goedkoop, robuust en niet giftig).

Complex **1** is aan het eind van de jaren '80 in eerste instantie ontwikkeld als model systeem voor belangrijke enzymen (fotosysteem II en catalase enzymen). Begin jaren '90 is bij Unilever ontdekt dat deze verbinding zeer geschikt is voor het verwijderen van vlekken uit kleding (bleken van wit wasgoed). Deze katalysator is in het verleden dan ook gebruikt in een wasmiddel en wordt tegenwoordig gebruikt in een afwasmiddel voor de vaatwasmachine. Verder kan deze katalysator gebruikt worden voor de epoxidatie van alkenen (zie Figuur 2).

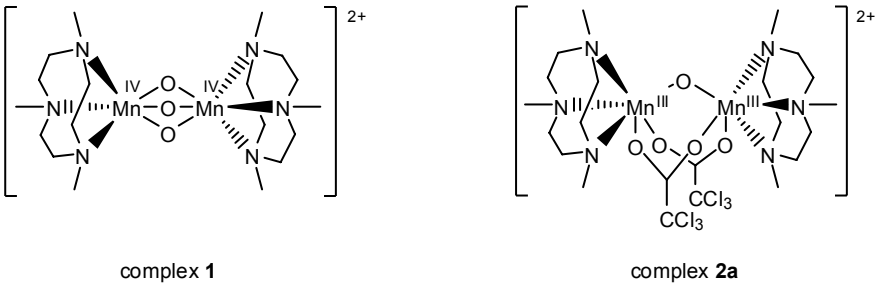

Figuur 3 Complex **1** en complex **2a**.

Een groot probleem met complex **1** is dat deze katalysator niet alleen activering van waterstofperoxide geeft (zodat bruikbare producten zoals epoxides gemaakt kunnen worden) maar dat dit complex ook de ontleding van waterstofperoxide (in zuurstof en water) katalyseert. Dit ontledingsproces staat bekend als catalase activiteit ($2\ H_2O_2 \rightarrow O_2 + 2\ H_2O$). Dit is problematisch aangezien op deze manier een groot gedeelte van het toegevoegde waterstofperoxide wordt vernietigd en dus verspild wordt.

Om deze nutteloze ontleding van de oxidator waterstofperoxide te onderdrukken, heeft een aantal onderzoeksgroepen zogenaamde additieven toegevoegd aan het reactiemengsel. Hoewel de toevoeging van deze additieven heeft geleid tot efficiënte epoxidatie van alkenen, was de precieze rol van deze additieven en het mechanisme waarmee ze opereren niet bekend.

Eerder onderzoek in Groningen heeft aangetoond dat ook aldehyden gebruikt kunnen worden voor het onderdrukken van de ontleding van waterstofperoxide. Tevens is toen gevonden dat deze aldehyde additieven, naast epoxidatie van alkenen, ook *cis*-dihydroxylering geven. Met name deze laatste reactie is zeer interessant aangezien het bestaande systeem om zeer selectief *cis*-diolen te maken uitgaat van een katalysator gebaseerd op het zeer giftige en dure metaal osmium.

Aan het begin van het onderzoek, dat beschreven wordt in dit proefschrift, werd echter gevonden dat het eigenlijk een vervuiling in het aldehyde is dat het actieve ingrediënt is. Carbonzuren bleken namelijk het eigenlijke actieve additief te zijn. Deze carbonzuren kunnen bij zeer lage concentraties gebruikt worden. Tevens kan door variatie in de structuur van het carbonzuur, zowel de activiteit als de selectiviteit van de katalytische oxidatie van alkenen gestuurd worden. Terwijl in de aanwezigheid van het ene carbonzuur voornamelijk *cis*-dihydroxylering plaatsvindt, wordt in de aanwezigheid van een ander carbonzuur voornamelijk het epoxide product gevormd. Deze vindingen staan beschreven in hoofdstuk 3.

In hoofdstuk 4 wordt het effect van verschillende reagentia (onder andere carbonzuren, water en waterstofperoxide) op de stabiliteit van complex **1** en een aantal andere dinucleaire mangaan complexen (complexen die twee mangaan ionen bevatten) bekeken. Hiertoe is gebruik gemaakt van een zo breed mogelijk scala aan meettechnieken. Dit leverde een goed begrip op van de veranderingen die optreden in deze complexen in oplossing onder invloed van deze andere reagentia.

In hoofdstuk 5 is gekeken naar welke mangaan complexen eigenlijk aanwezig zijn in oplossing tijdens de katalytische oxidatie van alkenen zoals beschreven in hoofdstuk 3. Hieruit is naar voren gekomen dat complex **1** eigenlijk niet de katalysator is. Complex **1** wordt in aanwezigheid van carbonzuren namelijk omgezet in zogenaamde Mn^{III}_2 bis(carboxylaat) complexen zoals complex **2a** (Figuur 3). De afkorting Mn^{III} geeft hier aan dat de oxidatie toestand van het mangaan ion '3' is (mangaan 'mist' 3 elektronen). Het getal $_2$ geeft aan dat er twee mangaanionen in het complex zitten. Bis(carboxylaat) wil zeggen dat er twee carboxylaat bruggen tussen beide mangaanionen zitten. Dit laatste is tevens het grote verschil met complex **1**, daar zorgen drie zuurstof ionen voor de verbinding tussen de twee mangaan ionen (zogenaamde μ-oxo bruggen).

Tevens wordt in dit hoofdstuk beschreven hoe de katalytische activiteit en selectiviteit veranderen ten gevolge van veranderingen in de reactiecondities. Samen met de analyse van welke complexen aanwezig zijn tijdens de verschillende fases van de katalytische oxidatie van een alkeen is een verbeterd inzicht verkregen in de precieze werking van deze katalysator.

In hoofdstuk 6 worden de vindingen en de algemeenheid van het mechanisme dat is voorgesteld in hoofdstuk 5 vergeleken met vergelijkbare systemen (ook gebaseerd op complex **1)** die ontwikkeld zijn door andere groepen. De resultaten tonen aan dat waarschijnlijk ook in de systemen beschreven door andere groepen Mn^{III}_2 bis(carboxylaat) complexen een belangrijke rol spelen.

Een ander belangrijk aspect binnen de chemie is het begrip chiraliteit. Dit woord is afkomstig van het Griekse woord voor hand (χειρ). Veel chemische verbindingen komen in twee 'vormen' voor. Hoewel de bouw van beide vormen van deze zogenaamde chirale verbindingen nagenoeg hetzelfde is, verschillen ze op een belangrijk punt: ze zijn niet gelijk aan hun spiegelbeeld (Figuur 4). Een linker- en een rechterhand zijn ook opgebouwd uit dezelfde elementen: beiden bevatten ze een duim en vier vingers. Echter, een linkerhand past niet in een rechterhandschoen. Een vergelijkbaar effect treedt op bij biologisch actieve verbindingen zoals medicijnen. Terwijl één vorm (enantiomeer) van een verbinding bijvoorbeeld een effectief medicijn is (en effectief kan binden aan een receptor molecuul in het lichaam), kan de andere vorm (de andere enantiomeer) bijvoorbeeld of niet werkzaam of erg schadelijk zijn.

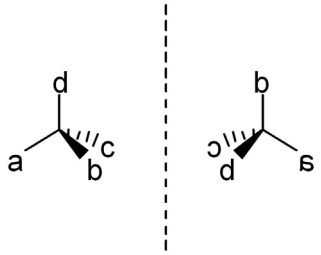

Figuur 4 Chiraliteit: het linker en rechter molecuul zijn elkaars spiegelbeeld en kunnen niet passend over elkaar heen gelegd worden.

Een belangrijk doel is dan ook om tijdens de synthese van moleculen maar één van beide spiegelbeeldvormen (enantiomeren) te maken in plaats van het statistisch te verwachten 50:50 mengsel. Ook hiervoor kunnen katalysatoren worden ingezet.

In hoofdstuk 7 wordt de ontwikkeling van een enantioselectieve versie van de eerder beschreven methode voor *cis*-dihydroxylering besproken. Hoewel de enantioselectiviteit (een maat voor de verhouding van de hoeveelheid van de ene enantiomere vorm ten op zichte van de andere) nog niet ideaal is, is het principe aangetoond en dit biedt mogelijkheden voor de verdere ontwikkeling van deze belangrijke reactie.

In hoofdstuk 8 worden de belangrijkste resultaten van het onderzoek zoals beschreven in dit proefschrift samengevat. Tevens wordt hierbij gekeken in hoeverre de nieuw ontwikkelde katalysatoren en de daarbij behorende methoden voor *cis*-dihydroxylering en epoxidatie van alkenen voldoen aan de eisen zoals robuustheid, activiteit en selectiviteit en worden enkele suggesties gedaan welke aspecten nog verdere aandacht verdienen.

Dankwoord

Hoewel het boekje bijna is volgeschreven, is het belangrijkste onderdeel van de promotie periode nog niet aan bod gekomen. Een beetje experimenteren en meten is één ding, maar alleen kom je niet ver. Dit geldt niet alleen voor de bijdragen die velen hebben geleverd aan het onderzoek, maar tevens zo belangrijk zijn de mensen die de afgelopen jaren op en buiten het lab tot een fantastische en onvergetelijke tijd hebben gemaakt.

Allereerst wil ik mijn promotor Prof. Dr. Ben Feringa bedanken voor de steun en alle mogelijkheden die je me hebt geboden om onderzoek te mogen doen in je groep. Zowel de gevarieerde groep als de uitgebreide faciliteiten, die je door de jaren heen hebt opgebouwd, vormen de ideale speelplaats om op een plezierige en uitdagende manier onderzoek te verrichten. Je kritische blik heeft altijd gezorgd voor uitdaging en stimulans om het onderzoek naar een hoger plan te tillen en dat heb ik zeer gewaardeerd.

Mijn copromotor Dr. Ronald Hage, bedankt voor de zeer plezierige samenwerking en begeleiding door de jaren heen. Je encyclopedische kennis van de vele ongrijpbare eigenaardigheden van de mangaan-chemie is ongeëvenaard. De (on)regelmatige discussies in Groningen en elders waar het ook maar uit kwam, alsmede het overleg via e-mail en telefoon heb ik altijd als zeer nuttig, maar vooral als zeer prettig ervaren.

I thank the members of the reading committee, Prof. Dr. Engberts, Prof. Dr. Reedijk and Prof. Dr. Que, Jr., for your critical reading of the manuscript. Your comments and suggestions were thorough and are very much appreciated.

Wes, aangezien je Nederlands net zo goed is als mijn Engels, houd ik het hier voor de verandering een keer bij mijn moedertaal. Dr. Wesley Browne, hartelijk dank voor de prettige samenwerking en het doen van vele metingen en syntheses. Tevens omdat je mij geïntroduceerd hebt in de wondere wereld der fysische meettechnieken. Ik heb je ongetwijfeld vaak het bloed onder de nagels vandaan gehaald, maar dat alles was in dienst van de wetenschap. Zonder je bijdrage en inzet had het onderzoek het er nooit in zijn huidige vorm uitgezien.

Tieme, met jou als collega oxidatie-aio kan onderzoek alleen maar plezierig en succesvol verlopen. Uiteraard heb ik mij regelmatig afgevraagd waarom je nu uitgerekend mijn chemicaliën en ander lab-toebehoren moest ‘lenen’, maar in ieder ander opzicht was je altijd de ideale collega, mede door je vele interessante en zeker verrassende gezichtspunten, de discussies over van alles en nog wat en natuurlijk de gedeelde smart en andere ellende met niet-meewerkende apparatuur. Ik kijk vol verwachting uit naar je boekje!

Dr. Jelle Brinksma, dank voor het feit dat je me geïntroduceerd hebt in de wondere wereld van de oxidatie chemie met mangaan. Dr. Paul Alsters, hartelijk bedankt voor de prettige samenwerking, input en voor de regelmatige herinnering om de toepasbaarheid niet uit het oog te verliezen. Dr. Gerard Roelfes, hartelijk dank voor de prettige en nuttige discussies over van alles en nog wat op het lab en over oxidatie chemie in het bijzonder. Hierbij tevens nogmaals dank voor je input en voor het kritisch doornemen van de manuscripten van diverse publicaties.

Tijdens de bijeenkomsten van de oxidatie-subgroup waren er altijd voldoende senior researchers aanwezig om dat zooitje ongeregeld uit Dokkum (Tieme, Rik en ondergetekende) aan het werk te houden door wijze raad, goede suggesties en wilde ideeën.

Ik wil alle leden (Ben, Ronald, Gerard, Wes, Rob, Jelle, Tieme en Rik) dan ook hartelijk danken voor de input.

Prof. Dr. Jan Reedijk, Dr. Stefania Grecea-Tanase, Dr. Paul Alsters en alle overige deelnemers van het EcOx-project; ik dank jullie voor de prettige samenwerking tijdens de meetings en voor de vele enerverende discussies en nuttige suggesties.

Dr. Syuzi Harutyunyan, thank you for the help with the synthesis of several organic compounds. The threshold of 80% *ee* was not reached, so you owe me a crate of beer (or was it the other way around?). Dr. Rob Hoen, ik ben blij dat je hebt ingezien dat je met alkenen veel meer kunt dan reduceren en ik dank je dan ook voor de plezierige samenwerking tijdens de paar maanden dat je deel uitmaakte van de oxidatie subgroup. Dr. Stefania Grecea-Tanase, thanks a lot for the pleasant collaboration and for performing the magnetic susceptibility measurements as described in this thesis (although most of it will be published elsewhere). Theodora Tiemersma-Wegman, je onvermoeibare inzet om het chromatografie lab op zo'n fantastische en hoogstaande manier draaiende te houden is ongeëvenaard en vormt de solide basis van veler (en mijn) onderzoek, bedankt! Dr. Andries Bruins en Annie van Dam wil ik bedanken voor alle hulp die jullie geboden hebben bij de ESI-MS metingen en vooral voor jullie interesse en bereidheid voor het doen van de vele niet-standaard metingen. Ook Albert Kiewiet en Margot Jeronimus dank ik hierbij voor het doen van vele MS metingen. Hans van der Velde (voor de elementen analyses), Ebe Schudde en Evert Hoekzema (voor het onderhoud aan de lab apparatuur), Klaas Dijkstra en Wim Kruizinga (NMR), Dr. Scott Killeen (for the help with the ESR measurements) en Hilda Biemold (secretariële samenwerking), hartelijk dank voor jullie hulp en inzet.

Bjorn (geachte zaalassistent), Davide (grazie, ook voor de Italiaanse lessen), Jerome, Joost, Nataša, Niek (favoriete aio), Nicolas, Norbert (ik ben het helemaal eens met je visie op werktijden), Rob (maar niet voor Andre Hazes en Scooter), Simone en Wes jullie waren fantastische zaalgenoten en hebben het verblijf op 14.223N/PhOxy Vanish tot een mooie tijd gemaakt. Naast mijn zaalgenoten wil ik tevens Arianna, Arnold, Bas V., Bart, Bea, Chris, David, Dirk, Francesca, Gabriella, Jaap, Jetsuda, Johannes, Kjeld, Menno, Michel, Mike, Nathalie, Patrick, Pieter, Robert, Ruben, Syuzi, Tati, Tibor, Tieme, Tim, Toon en alle leden van de Feringa-groep en andere labbewoners door de jaren heen danken voor alle gezelligheid in en buiten het lab tijdens de borrels, diners, feestjes, lunches, rondje-lab, eind-bbq, workweek, congressen en natuurlijk de dagelijkse kopjes thee tijdens de koffiepauze.

Ook de lotgenoten in de schrijfkamer: Bas V. (mocht de tour ook dit jaar geplaagd worden door doping perikelen, dan gaan gaan we toch gewoon zelf weer een eindje fietsen?), Francesca (you walked into the office, wrote and left us all amazed that writing up could be so quick and easy), Gabriella, Joost (jou zucht klinkt mij altijd als muziek in de oren: dan weet ik dat de computerproblemen veroorzaakt worden door mijn gebrekkige kennis en jij het in een handomdraai weer gefixed hebt), Norbert, Rob en Tieme, bedankt voor de tips, discussies en gezelligheid tijdens de vele uren achter het beeldscherm.

Lichting 96^{+}, te weten Agnes, Anja, Annet, Bas S., Bas V., Boelo, Chris, Danny, Dorothee, Edje, Floris, Hester, Jaap, Jan-Willem, Joep, Joost, Koetsier, Maaike H., Maaike M., Marc, Mark, Marta, Michel (Rh), Michel (2M), Mirjam, Norbert, Philana, Renske, Ronald, Ronny, Ruben, Sepp, sNiek, Suzan, Tieme, Werner en Wes (en diegenen die ik hier

vergeten ben te noemen) bedankt voor alle biertjes en gezelligheid tijdens borrels, feestjes, voetbal kijken, fitness, whisky proeven, etc.

Afke, Anton, Eelco, Jeroen, Leendert, Linda, Nynke, Pieter, Roelien, Werner en de andere oud-tjassers bedankt voor al het afzien en natuurlijk het appelgebak. Hoewel het aantal trainingsuren gedurende de laatste paar jaar steeds minder is geworden (in ieder geval voor mij tot een bedenkelijk niveau is gedaald) steekt het tjas-gevoel (ooit onovertroffen omschreven door Pieter) meteen weer de kop op tijdens het ardennenweekend en andere gelegenheden.

Albert, Asia, Danka, Ilja, Jornt, Nynke en Wiep Klaas bedankt voor de vele onvergetelijke momenten, onder andere tijdens de sneak en in de kroeg.

Mijn familie, en met name mijn ouders, zus en grootouders, bedankt voor jullie steun. Hoewel het wel eens lastig was om uit te leggen, waren jullie altijd geïnteresseerd in wat ik nu eigenlijk aan het doen was in het lab.

De laatste letters staan op papier, het boekje is klaar!